

**Asymmetric Organocatalysis with
bis-Silyl Ketene Acetals**

Inaugural-Dissertation

Zur

Erlangung des Doktorgrades

der Mathematisch-Naturwissenschaftlichen Fakultät

der Universität zu Köln

vorgelegt von

Francesca Mandrelli

aus Sansepolcro (Italien)

Köln 2019

Berichterstatter: Prof. Dr. Benjamin List

Prof. Dr. Hans-Günther Schmalz

Tag der mündlichen Prüfung:

29.11.2019

*“Most people say that
it is intellect which makes a great scientist.*

They are wrong: it is character”

Albert Einstein

Acknowledgments

The accomplishment of this thesis has been possible thanks to the efforts and the help of many people, which have taken part and assisted me during the last four years.

Special thanks go to Prof. Dr. Benjamin List:

Ben gave me a chance. His bet on me to become a Ph.D. in organic chemistry, despite my medicinal chemistry/pharmacy education, motivated me throughout the four years. He never gave up on me, despite ups and downs; he kept motivating me scientifically and personally. I feel that his inspiring motivation and passion for science have been highly contagious. He gave me the freedom to tackle my tasks and challenges in my own way. He trusted me with many tasks and responsibilities and I always accepted them as unique chances to grow. He gave me a new perspective on chemistry and the way of doing science. Thank you for all, Ben.

Defense committee:

I would also like to thank Prof. Dr. Hans-Günther Schmalz for accepting to review this thesis and Prof. Dr. Axel Klein and Dr. Monika Lindner for serving on my defense committee.

Cooperation partners and friends:

A special thank you goes out to Grischa, Benni, David, Manuel, Mathias and Miles for careful proofreading this thesis. They did an amazing job.

Thanks to Dr. Chendan Zhu for accepting to work with me in the aminomethylation project, for accepting my suggestions even when they were guided by feelings and for sharing the same great motivation to complete the project.

Thanks to Dr. Aurélie Blond for trusting me with the solving and completion of the protonation project.

Thanks to Dr. Desislava Petkova: first and best friend, since the first day of my PhD. She shared with me daily her positive attitude, wise thinking, brave and loving soul, merged with a very responsible and motivated attitude. She is an inspiring example for my life.

Thanks to Dr. Grigory Shevchenko: for the support during these four years, which was crucial for my development, the careful and meaningful corrections of my reports, the critical view on each matter (even when it doesn't matter), the scientific suggestions and for always caring.

Thanks to Dr. Markus Leutzsch: for being an amazing first lab mate in my earliest months, for coming back to Mülheim, for being a sincere friend, for his help with customized NMR experiments.

Thanks to my current and former PhD mates that I keep close to my heart: Jenni, Oleg, Sebastian, David, Tim, Mathias, Benni, Manuel, Gabriele, Luping, Lucas, Nobuya and all the others, who directly or indirectly helped me through this time.

Thanks to the PostDocs and super-PostDocs of the group: Hui, Carla, Roberta, Gabriela, Diane, René, Hyejin, Sayantani, Vijay, Jie, Sunggi, Hanyong, Aurélien, Thomas and all the others for sharing their knowledge and time with me.

Thanks to the permanent staff of the group: to Dr. Chandra Kanta De and Dr. Monika Lindner, for managing the whole lab with professionalism and deep care for the scientific and personal value of the whole group. To Alexandra, for helping with each administrative concern with a sincere smile. To the technicians, Henk, Steffi, Alex, Natascha, Lina, Arno for being of endless help in every moment, especially when anyone needed help. To the analytical departments, especially HPLC department, for their help in separating chiral compounds. Finally, I thank Dr. Martin Klußmann for his teaching efforts in our POC seminars.

My family:

Luca, my spouse, partner and friend, for supporting me, motivating me to give my best, for being brave and moving to Germany with me to share this life-changing experience with me.

My parents, for cheering for me from over thousand kilometers away, their constant support throughout my education and their unconditional love. My brother Andrea and his wife Aida, and the family that they recently created. My friends Claudia, Alessandra, Dr. Francesco Venturoni and all the other friends spread all over the world. Shipi.

Table of Contents

Acknowledgments	III
Abstract.....	IX
KURZZUSAMMENFASSUNG	X
List of Abbreviations	XI
1 Introduction.....	3
1.1 Carboxylic Acids in Organic Synthesis.....	3
1.1.1 Asymmetric α -Functionalization of Carboxylic Acids	4
1.2 <i>Bis</i> -Silyl Ketene Acetals as Carboxylic Acid Equivalents	6
2 Background.....	9
2.1 Asymmetric Catalysis	9
2.2 Asymmetric Organocatalysis.....	12
2.2.1 Introduction	12
2.2.2 Chiral Acids for Asymmetric Synthesis.....	14
2.2.3 Asymmetric Counteranion-Directed Catalysis (ACDC).....	18
2.2.4 Chiral Brønsted Acids.....	19
2.2.5 Chiral Lewis Acids.....	28
2.3 <i>Bis</i> -Silyl Ketene Acetals	35
2.3.1 <i>Bis</i> -SKAs in the Synthesis of α -Functionalized Carboxylic Acids	36
2.4 Enantioselective Protonation of <i>bis</i> -SKAs	41
2.4.1 Introduction	41
2.4.2 Catalytic Asymmetric Protonation of Enolate Derivatives	42
2.4.3 Catalytic Asymmetric Protonation of <i>bis</i> -Silyl Ketene Acetals	47
2.5 Enantioselective α -Aminomethylation.....	53

2.5.1	Introduction	53
2.5.2	Asymmetric Synthesis of $\beta^{2,3}$ -Amino Acids	56
2.5.3	Asymmetric Synthesis of β^2 -Amino Acids	58
3	Objectives.....	63
4	Results and discussion	67
4.1	Asymmetric α -Protonation with H ₂ O and α -Deuteration with D ₂ O	67
4.1.1	Reaction Design and Optimization Studies	69
4.1.2	Preliminary Substrate Scope	74
4.1.3	Fine-Tuning of the Catalyst Design.....	75
4.1.4	Substrate Scope.....	79
4.1.5	Mechanistic Investigations.....	81
4.1.6	Enantioselective Deuteration of <i>bis</i> -SKAs	83
4.1.7	Deracemization Sequence	84
4.1.8	Conclusions	85
4.1.9	Conclusions	85
4.2	Asymmetric α -Aminomethylation for the Direct Synthesis of Unprotected β - Amino Acids.....	87
4.2.1	Reaction Design and Optimization.....	87
4.2.2	Examination of IDP <i>i</i> Catalysts.....	94
4.2.3	Mechanistic Insights Lead to a New Catalyst Design	104
4.2.4	Final Catalyst Optimization.....	106
4.2.5	Substrate Scope.....	108
4.2.6	Outlook and Conclusion.....	109
5	Summary.....	111
5.1	Catalytic Asymmetric α -Protonation with Water and α -Deuteration with D ₂ O	111

5.2	Catalytic Asymmetric α -Aminomethylation	113
6	Outlook.....	114
7	Experimental Section	117
7.1	General Information and Instrumentation	117
7.2	Asymmetric α -Protonation with H ₂ O and α -Deuteration with D ₂ O	123
7.2.1	Synthesis and Characterization of Racemic Carboxylic Acids.....	123
7.2.2	Synthesis and Characterization of <i>bis</i> -Silyl Ketene Acetals	125
7.2.3	General procedure for the asymmetric protonation of <i>bis</i> -SKAs.....	133
7.2.4	General Procedure for the Asymmetric Deuteration of <i>Bis</i> -SKAs.....	143
7.2.5	Gram Scale Reaction	146
7.2.6	Synthesis and Characterization of DSI Catalysts.....	147
7.3	Asymmetric α -Aminomethylation for the Direct Synthesis of Unprotected β - Amino Acids.....	169
7.3.1	Synthesis of Aminomethylating Reagents	169
7.3.2	Synthesis and Characterization of <i>bis</i> -Silyl Ketene Acetals	170
7.3.3	General procedure for the α -Aminomethylation of <i>bis</i> -SKAs.....	173
7.3.4	Synthesis and Characterization of IDP <i>i</i> Catalysts	176
8	Bibliography	187
9	Appendix.....	196
9.1	Erklärung/Declaration.....	196
9.2	Lebenslauf/CV	197

Abstract

Enantiomerically pure α -stereogenic carboxylic acids are encountered in a variety of natural products and pharmaceuticals and are useful substrates for various transformations. The direct synthesis of such motifs *via* catalytic asymmetric α -functionalization remains challenging in both metal- and organocatalysis. A general approach toward α -functionalization can be envisioned *via* formation of *bis*-silyl ketene acetal intermediates followed by functionalization with an electrophilic counterpart. This thesis focuses on the development of enantioselective transformations with *bis*-silyl ketene acetals, exploring the generality of this strategy within Brønsted and Lewis acid catalysis for a variety of enantioselective C–H and C–C bond forming reactions, using simple and unactivated substrates. This strategy was successfully applied to the deracemization of α -branched aryl carboxylic acids *via* catalytic asymmetric protonation of *bis*-silyl ketene acetals with water or methanol as a proton source, delivering valuable products with high enantiomeric purity and high yields, including non-steroidal anti-inflammatory arylpropionic acids, such as Ibuprofen. Furthermore, this strategy showed great potential under Lewis acidic conditions for a direct aminomethylation, allowing the first asymmetric organocatalytic synthesis of β^2 -amino acids from aliphatic and aromatic unactivated substrates, in very good enantioselectivities and excellent yields. This work opens the field of catalytic asymmetric transformations with *bis*-silyl ketene acetals for the direct access of enantioenriched α -branched carboxylic acids.

KURZZUSAMMENFASSUNG

Enantiomerenreine α -stereogene Carbonsäuren kommen in einer Vielzahl von Naturstoffen und Pharmazeutika vor und sind nützliche Substrate für verschiedene Transformationen. Die direkte Synthese solcher Motive durch katalytische asymmetrische α -Funktionalisierung der entsprechenden Carbonsäuren ist sowohl in der Metall- als auch in der Organokatalyse eine Herausforderung. Ein möglicher allgemeiner Ansatz zur α -Funktionalisierung kann über die Bildung von *bis*-Silylketenacetal-Intermediaten und anschließende Funktionalisierung mit einem Elektrophil erfolgen. Diese Dissertation befasst sich mit der Entwicklung enantioselektiver Transformationen mit *bis*-Silylketenacetalen und untersucht die Allgemeingültigkeit dieser Strategie unter Brønsted- und Lewis-sauren-Bedingungen in einer Vielzahl enantioselektiver C–H- und C–C-Bindungsbildungsreaktionen unter Verwendung einfacher und nicht aktivierter Substrate. Diese Strategie wurde erfolgreich auf die Deracemisierung von α -verzweigten Arylcarbonsäuren durch katalytische asymmetrische Protonierung von *bis*-Silylketenacetalen mit Wasser oder Methanol als Protonenquelle angewendet, wobei wertvolle Produkte mit hoher Enantiomerenreinheit und hohen Ausbeuten, einschließlich nichtsteroidaler entzündungshemmender Arylpropionsäuren wie beispielsweise Ibuprofen, erhalten wurden. Darüber hinaus ermöglichte diese Strategie, unter Lewis-sauren-Bedingungen, die erste asymmetrische organokatalytische Synthese von β^2 -Aminosäuren durch direkte Aminomethylierung aliphatischer und aromatischer Substrate in guten Enantioselektivitäten und ausgezeichneten Ausbeuten. Zusammenfassend eröffnet diese Arbeit das Gebiet der katalytischen asymmetrischen Transformationen mit *bis*-Silylketenacetalen für den direkten Zugang zu enantiomerenangereicherten α -verzweigten Carbonsäuren.

List of Abbreviations

*	designating chiral element
ACDC	asymmetric counteranion-directed catalysis
Alk	alkyl
Ar	aryl
aq.	aqueous
BINOL	1,1'-bi-2-naphthol
Boc	<i>tert</i> -butyloxycarbonyl
cat.	catalyst or catalytic
conv.	conversion
DBU	1,8-diazabicyclo[5.4.0]undec-7-ene
DCE	1,2-dichloroethane
DCM	dichloromethane
DMF	dimethylformamide
DMSO	dimethylsulfoxide
dr	diastereomeric ratio
DSI	disulfonimide
E	electrophile
EDG	electron donating group

er	enantiomeric ratio
equiv.	equivalents
et al.	<i>et alii / et aliae</i> – and others
EWG	electron withdrawing group
Fmoc	fluorenylmethyloxycarbonyl
h	hours
HPLC	high performance liquid chromatography
<i>i</i>	<i>iso</i>
IDP	imidodiphosphate
IDP <i>i</i>	imidodiphosphorimidate
<i>i</i> IDP	imino-imidodiphosphate
<i>m</i>	<i>meta</i>
M	molar
MS	mass spectrometry or molecular sieves
MTBE	methyl <i>tert</i> -butyl ether
MW	molecular weight
NMR	nuclear magnetic resonance (spectroscopy)
Nu/NuH	nucleophile
<i>o</i>	<i>ortho</i>
P	product

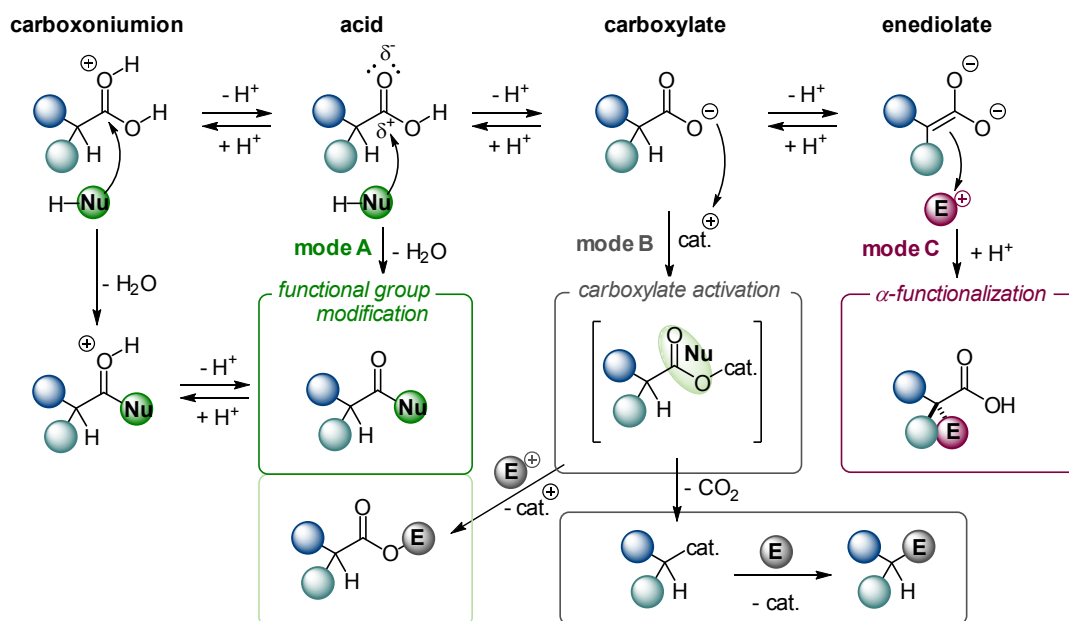
<i>p</i>	<i>para</i>
quant.	quantitative
<i>rac</i>	racemic
rt	room temperature
SKA	silyl ketene acetal
<i>t</i>	<i>tert</i> , tertiary
T	temperature
TBS	<i>tert</i> -butyldimethylsilyl
Tf	trifluoromethylsulfonyl
THF	tetrahydrofuran
TMS	trimethylsilyl
TRIP	3,3'- <i>bis</i> (2,4,6-triisopropylphenyl)-1,1'-binaphthyl-2,2'-diyl-hydrogen phosphate
TsOH	<i>para</i> -toluenesulfonic acid

Introduction

1 Introduction

1.1 Carboxylic Acids in Organic Synthesis

Carboxylic acids are ubiquitous structural motifs in biologically active compounds and are among the most common functionalities in organic chemistry.^[1] For organic synthesis, carboxylic acids are convenient raw materials and intermediates, as they are commercially available in a wide structural variety, easy to store and to handle, and preparatively accessible by a variety of established routes.^[2] The reactivity of the carboxylic group depends on its protonation state: (a) the protonated form as carboxonium ion, (b) neutral, in the acid form, (c) anionic, in the carboxylate form, and (d) di-anionic, in the form of the enediolate (Scheme 1.1). Addition of a nucleophile (NuH) at the partially positively charged carbon of the acid allows a variety of functional group modifications upon condensation, giving access to acyl chlorides, anhydrides, esters and amides (mode A). The same functional group modification can be envisioned *via* the initial formation of the carboxonium ion, followed by addition of a nucleophile, condensation and, ultimately, deprotonation to the corresponding acyl derivative. Carboxylates can be activated in a very similar way, however having a carboxylate–catalyst complex as the reactive intermediate. This can either still react as a carboxyl *O*-nucleophile, giving ester derivatives, or, on the other hand, it can undergo decarboxylation forming a highly nucleophilic organometallic intermediate; this latter reactive intermediate readily reacts with available electrophiles^[3] or with radicals^[4] (mode B). Lastly, the di-anionic form, accessed using an excess of a strong base, can react with a large variety of electrophiles, allowing the direct functionalization at the α -carbon (mode C).^[5] Noteworthy, the α -functionalization erases the stereochemical information of the starting carboxylic acid; hence the stereogenic information of the obtained product depends only on the nucleophilic attack onto the electrophile.

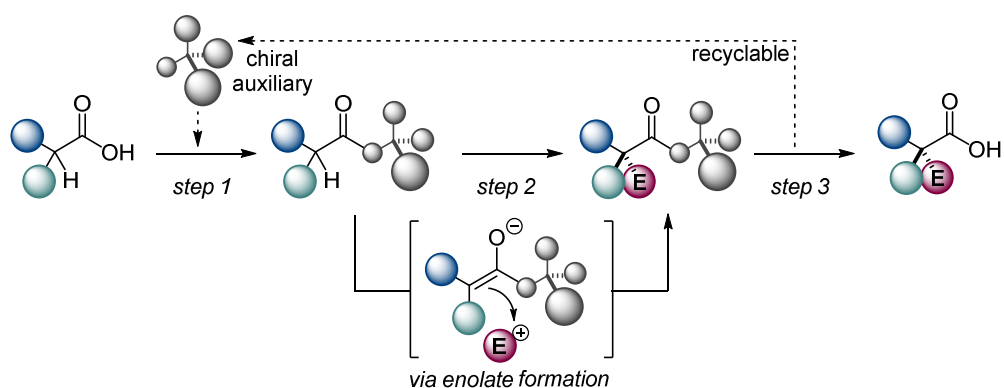


Scheme 1.1 Versatile reactivity of the carboxylic acid group.

Despite the importance and the versatility of carboxylic acids as synthetic intermediates, their application in catalytic transformations is rather limited. In recent years, progress in metal-catalysis has allowed the functionalization of unbiased and unprotected carboxylic acids.^[3] However, enantioselective transformations remain scarce and, more surprisingly, the direct and enantioselective α -functionalization is still elusive.

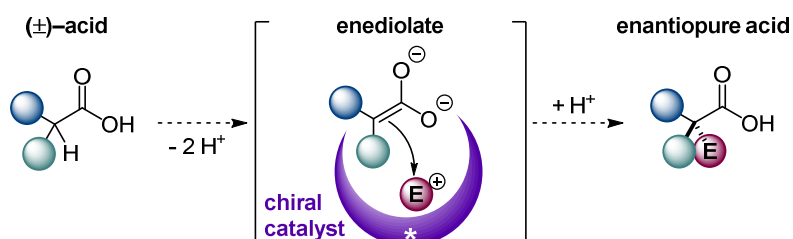
1.1.1 Asymmetric α -Functionalization of Carboxylic Acids

The most applied and reliable strategy to access α -functionalized carboxylic acids consists of multi-step procedures, taking advantage of chiral auxiliaries (Scheme 1.2). In such a sequence, the acid is first derivatized with an enantiopure auxiliary (step 1), followed by the desired, strong base-mediated functionalization in a diastereoselective fashion (step 2), and finally deprotected to furnish the desired enantioenriched product (step 3).^[6] The auxiliary can be recovered; however, this requires an additional purification step.



Scheme 1.2 Multi-step asymmetric α -functionalization using a chiral auxiliary.

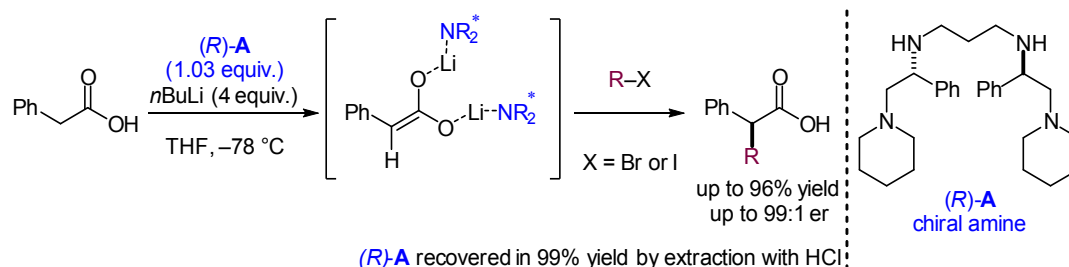
A possible direct α -functionalization, in an ideal case, would require a catalyst which is able to deprotonate the carboxylic acid twice, at the OH group and at its α -position, to afford the *bis*-enolate. Simultaneously, the catalyst would provide a chiral environment to control the enantioselectivity of the nucleophilic attack onto a given electrophile (Scheme 1.3). Such a transformation has not been reported so far, however a patent exists claiming the benzylation of glycine using (*R*)-2-amino-2'-hydroxy-1,1'-binaphthyl (NOBIN) as the catalyst.^[7]



Scheme 1.3 Direct asymmetric α -functionalization with a chiral catalyst.

In pioneering studies by Shioiri^[8] and Koga,^[9] and more recently further developed by Zakarian,^[10] the authors described an alternative solution to this challenge by using stoichiometric C_2 -symmetric diamine reagents as chiral ligands (Scheme 1.4). This strategy is based on the *in situ* coordination of the *bis*-lithium enolate to the chiral amine; this complex directly enables the enantioselective functionalization, furnishing the targeted free carboxylic acid upon acidic workup. Moreover, the

stoichiometric chiral amine as the non-covalent auxiliary can be quantitatively recovered upon extraction. Furthermore, the whole sequence does not require the isolation of covalently bonded chiral intermediates or subsequent deprotection steps.



Scheme 1.4 α -Functionalization with a traceless stoichiometric auxiliary.

The *in situ* formation of the *bis*-lithium enolate from the carboxylic acid requires at least two equivalents of a strong base ($pK_a > 30$) (Note: pK_a values of bases refer to the corresponding conjugate acid). Therefore, lithium diisopropylamide ($pK_a \cong 35$) or *n*-butyl lithium ($pK_a \cong 50$) are the most commonly used reagents. The highly reactive *bis*-lithium enolates have several disadvantages as they can undergo decomposition and cannot be isolated as stable intermediates. Furthermore, these harsh conditions are incompatible with a large variety of functional groups. Therefore, in order to develop a general asymmetric and catalytic strategy, a less reactive and more stable enediolate equivalent is required.

1.2 Bis-Silyl Ketene Acetals as Carboxylic Acid Equivalents

Silicon-based protecting groups are among the most frequently employed of all protecting groups.^[11] Furthermore, silyl enol ethers, silyl ketene acetals (SKAs), and *bis*-silyl ketene acetals (*bis*-SKAs) are the protagonists in a large variety of transformations since they represent stable and accessible enol and enolate equivalents of ketones, esters and carboxylic acids respectively (Figure 1.1). While a wide selection of catalytic asymmetric transformations has been developed using silyl enol ethers and SKAs,^[12] enantioselective transformations using *bis*-SKAs are

rare.^[13] The main advantage of *bis*-SKAs is that they allow direct access to carboxylic acids upon simple hydrolysis and, due to the absence of *E/Z*-diastereomers, their synthesis and purification is more facile compared to SKAs. However, *bis*-SKAs are challenging substrates as they are highly prone to hydrolysis and, in order to achieve high enantioselectivities, a chiral catalyst would have to differentiate the two relatively similar enantiotopic faces (Figure 1.1). Despite their challenges, *bis*-SKAs would be ideal substrates for accessing functionalized α -branched carboxylic acids.

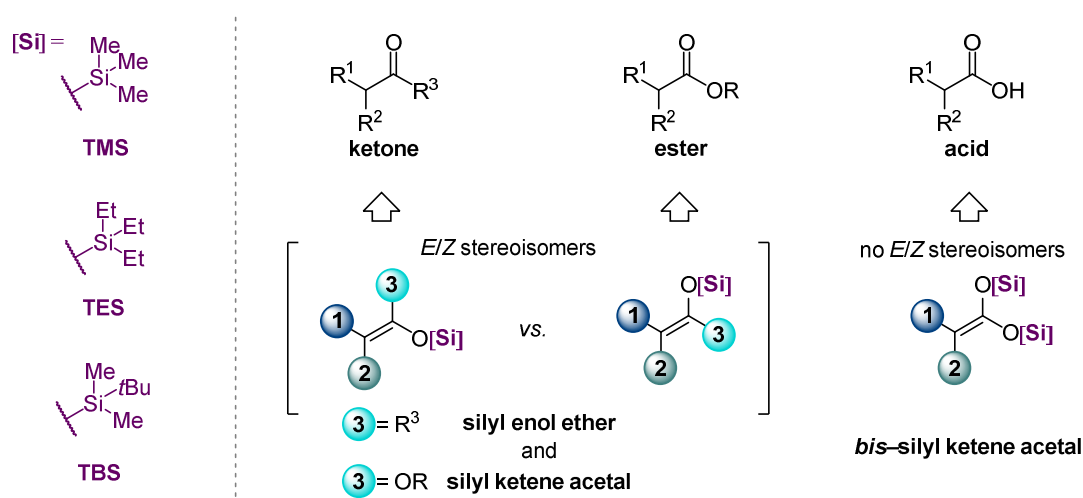


Figure 1.1 Stereochemical considerations of enolate equivalents and selected examples of silicon-based protecting groups.

In the following chapters, an overview of asymmetric catalytic reactions is presented, with particular focus on organocatalytic transformations under Brønsted and Lewis acidic conditions, followed by the discussion of the investigation conducted during these doctoral studies on the asymmetric transformations toward α -branched carboxylic acids.

Background

2 Background

2.1 Asymmetric Catalysis

A catalyst is a component of the reaction mixture which is not consumed during the reaction and is able to increase the reaction rate by lowering the activation energy of a chemical transformation. It does not modify the energy of the reagents or products, but interacts with reagents and reaction intermediates, allowing the same reaction to occur *via* a different and less energetic pathway (Figure 2.1). In the case of enantioselective transformations, stereogenic elements may assemble in a selective fashion through the action of a chiral catalyst and the two enantiomers are obtained through energetically non-equivalent diastereomeric reaction pathways.

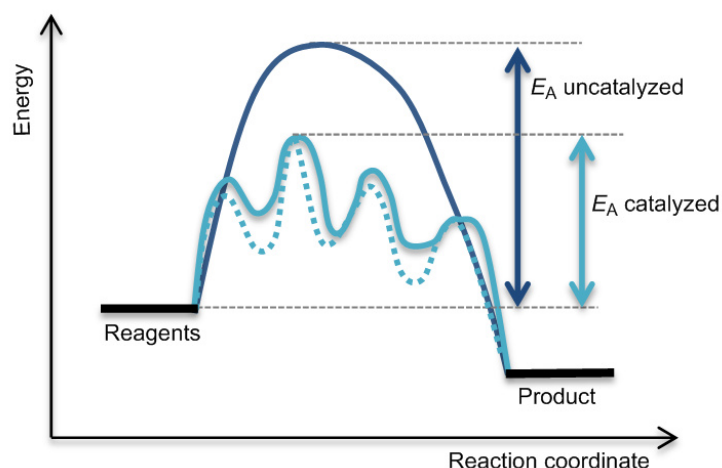
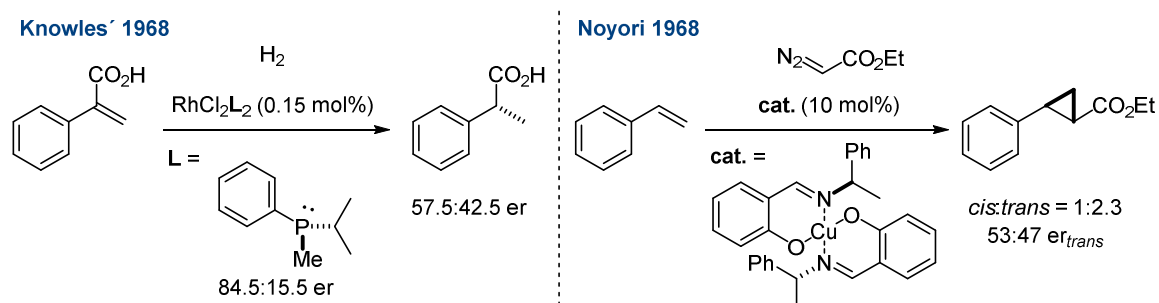


Figure 2.1 General energy diagram of non-catalyzed and catalyzed reactions.

The field of asymmetric transition metal catalysis was opened with the independent work of Horner,^[14] Knowles,^[15] Kagan,^[16] Noyori^[17] and Sharpless,^[18] in which the authors disclosed (transition) metal-catalyzed transformations in the presence of chiral ligands (Scheme 2.1). Despite the poor enantioselectivities achieved, these seminal discoveries were recognized by the scientific community as milestones for catalytic enantioselective synthesis and thus were awarded with the Nobel Prize in Chemistry in 2001. Soon after these first reports, chemical industries

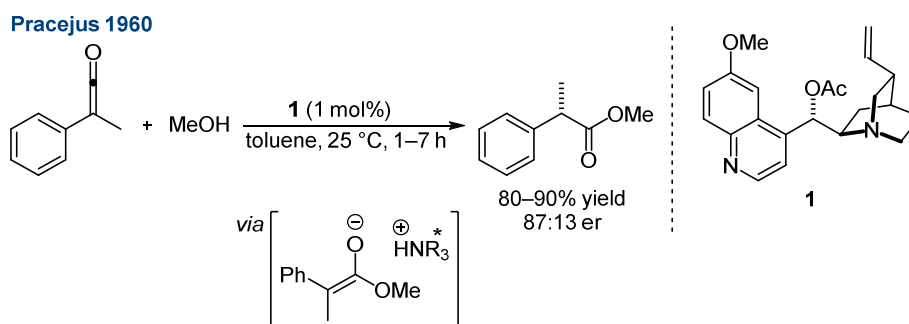
implemented the use of enantiopure ligands in catalytic processes underlining their importance.^[19]



Scheme 2.1 Knowles and Noyori's pioneering achievements in asymmetric catalysis.

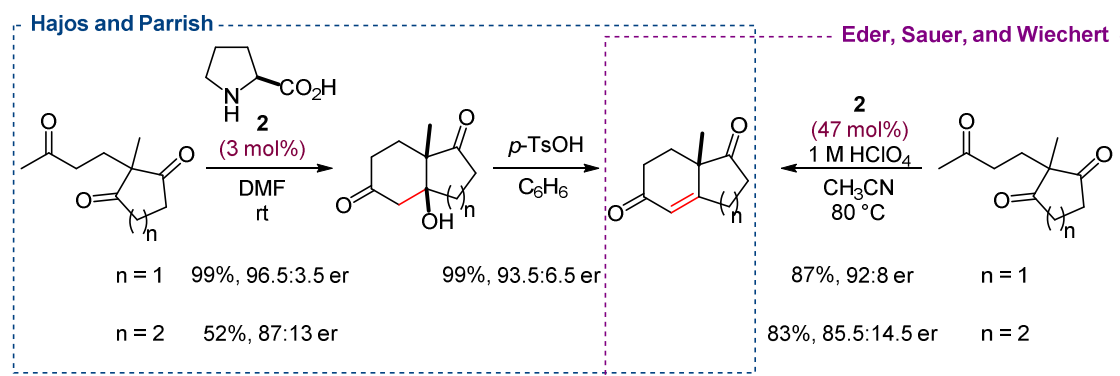
In the 1960s, bioengineering emerged as a parallel approach to overcome the challenge of controlling chemo- and enantioselectivity in chemical transformations.^[20] Today, the use of enzymes or even whole cells finds wide application across the chemical industries.^[21] Hence, by the beginning of the 21st century, the field of catalytic transformations was dominated by two independent approaches: metal- and biocatalysis.

However, few isolated examples were not fitting in either one of the two categories and have been considered for a long time as mere curiosities. Those examples had a small organic chiral molecule acting as the catalyst, inducing low^[22] to moderate enantioselectivities.^[23] For example, in 1960 Pracejus showed that *O*-acetylquinine **1** catalyzed the addition of methanol to ketenes and enabled chirality transfer in the protonation step, giving the targeted esters in moderate enantioselectivities (Scheme 2.2).^[23]



Scheme 2.2 Pracejus' pioneering achievement in asymmetric organocatalysis.

Another remarkable example was reported by Hajos and Parrish^[24] at Hoffmann-La Roche and Eder, Sauer, and Wiechert^[25] at Schering. In this case, using (S)-proline (**2**) as catalyst, the reported intramolecular aldol reaction afforded the cyclization products in good to excellent yields with moderate to very high enantioselectivities (Scheme 2.3).



Scheme 2.3 The Hajos–Parrish–Eder–Sauer–Wiechert reaction.

Only in the early 2000s, the rationalization of the basic concepts of organocatalysis allowed the establishment of this new research field (Figure 2.2). Nowadays, organocatalysis is widely accepted as the third pillar of catalysis, complementing metal- and biocatalysis.^[26] In fact, in terms of numbers of papers, organocatalysis is number one in asymmetric synthesis.

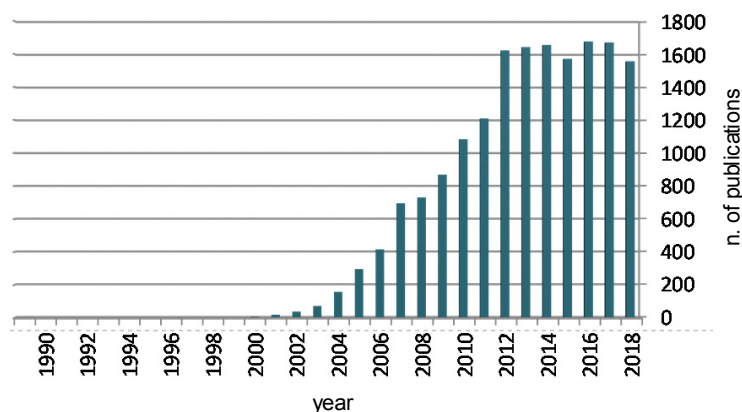
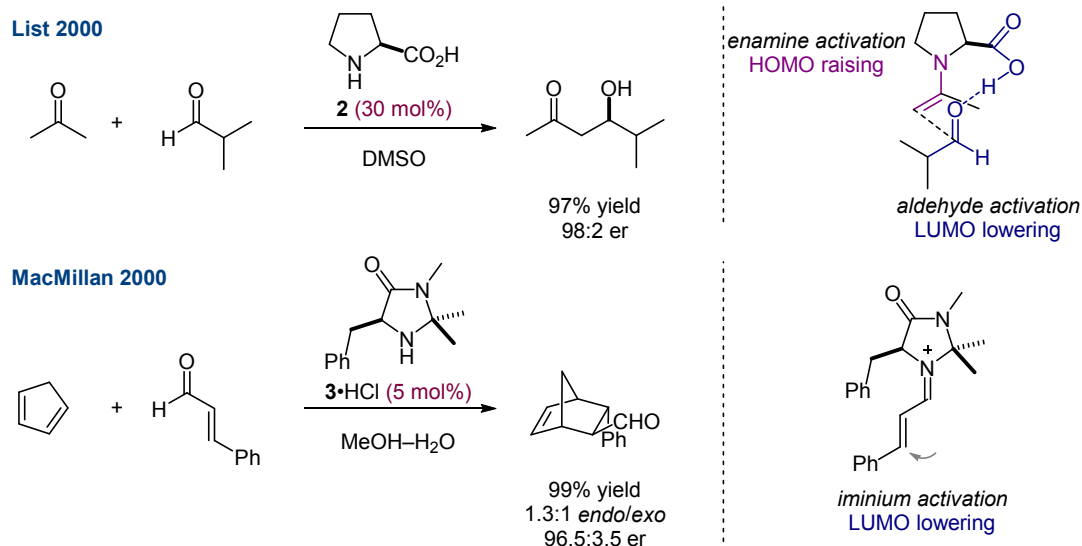


Figure 2.2 Chart exported from SciFinder on “organocatalysis” as “Research topic”, September 2019.

2.2 Asymmetric Organocatalysis

2.2.1 Introduction

The groundbreaking simultaneous reports of List^[27] and MacMillan^[28] opened the field of organocatalysis. They independently showed that small organic molecules without any metal in their active site are potent and general catalysts for asymmetric transformations. In particular, the former described the proline-catalyzed aldol reaction of acetone with different aldehydes *via* enamine catalysis (remarkably, elimination to the corresponding enone did not take place under these reaction conditions),^[29] while the latter reported an asymmetric Diels–Alder reaction of cyclopentadiene and unsaturated aldehydes *via* iminium ion catalysis (Scheme 2.4).



Scheme 2.4 Pioneering reports on secondary amine-catalyzed enantioselective reactions.

In the following years, the field was rationalized by well-defined interactions (covalent or non-covalent) and specific modes of action,^[30] thus allowing rational reaction design. A comprehensive classification was reported by Seayad and List,^[31] organizing the field based on the role of the catalyst and its mode of action: Brønsted acid, Brønsted base, Lewis acid and Lewis base (Figure 2.3).

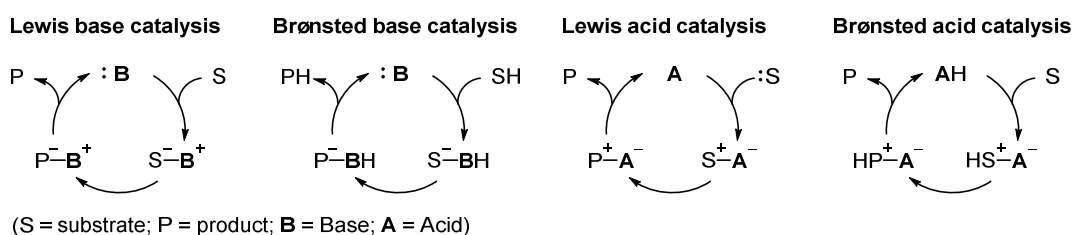


Figure 2.3 Classification of organocatalytic transformations based on the role of the catalyst.

Lewis base catalysis covers the majority of the reported transformations. Here, the catalyst promotes the reaction by donating one (or more) electrons to a substrate. Indeed, enamine^[32] and iminium ion catalysis,^[33] SOMO^[34] and carbene catalysis^[35] operate through this type of mechanism.

This classification should be considered flexible, as many of the reported catalysts exploit multiple activation modes. Those catalysts are defined as “bifunctional”, as their activation modes depend on different functionalities. For example, the above-mentioned proline-catalyzed aldol reaction is promoted both by a Lewis base (secondary amine) for the enamine formation and simultaneously by a Brønsted acid (carboxylic acid) for the activation of the aldehyde.

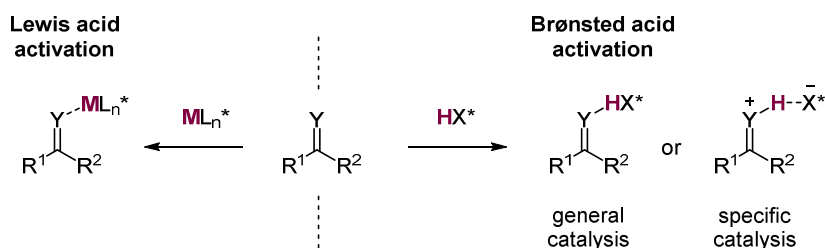
2.2.2 Chiral Acids for Asymmetric Synthesis

In 1923 Brønsted^[36] and Lowry^[37] independently published a theory in which bases are defined as proton acceptors and acids as proton donors. Accordingly, a Brønsted acid (HA) reacts by releasing a proton (H^+), thereby generating the corresponding anion, defined as the conjugated base (A^-). In the same year, Lewis gave a broader definition:

“It seems to me that with complete generality we may say that a basic substance is one which has a lone pair of electrons which may be used to complete the stable group of another atom, and that an acid substance is one which can employ a lone pair from another molecule in completing the stable group of one of its own atoms. In other words, the basic substance furnishes a pair of electrons for a chemical bond, the acid substance accepts such a pair.”^[38]

In contrast to the Brønsted–Lowry definition, the Lewis definition covers acid-base reactions in which no proton transfer is involved, and it concludes that a proton is the smallest possible Lewis acid.

In the context of asymmetric transformations, a close similarity can be envisioned between enantioselective Lewis- and Brønsted-acid activation. On one hand, Lewis acidic metals or metalloid centered atoms (**M**) are coordinated to enantiopure ligands (**L***) guiding asymmetric transformations; on the other hand, in the Brønsted acid activation, the proton can be envisioned as the smallest centered element and the backbone of an organic catalyst (**X***) may be the effective source of stereoselectivity (Scheme 2.5).



Scheme 2.5 Lewis acid and Brønsted acid electrophile activation.

Depending on the acidity of the Brønsted acid, a more specific differentiation can be made: general and specific catalysis. In the first case, the neutral or weakly acidic functionality activates the substrate by weak interactions. This category includes (thio)ureas, alcohols and phenols, and those functionalities are also referred to as hydrogen-bond donors. In the second case, the stronger acidic functionalities activate the substrate by direct protonation of the substrate. This class includes phosphoric acids and derivatives, carboxylic acids, sulfonamides, sulfonic acids, C–H acids, and phosphorimidate derivatives, which are generally referred to as Brønsted acid catalysts (Figure 2.4).

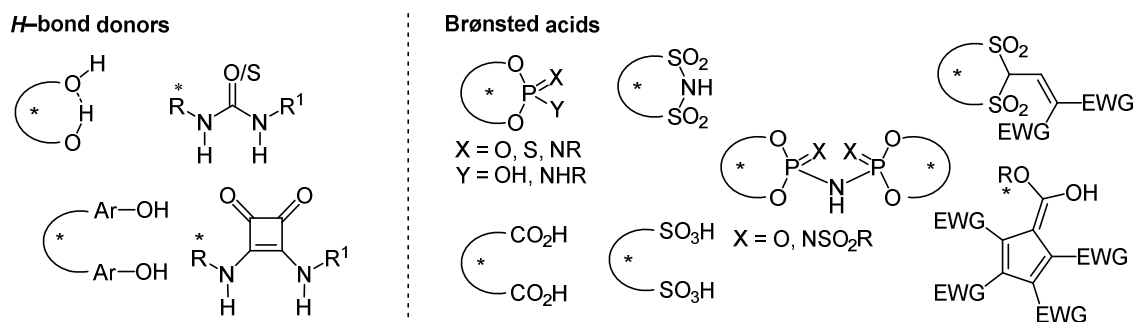
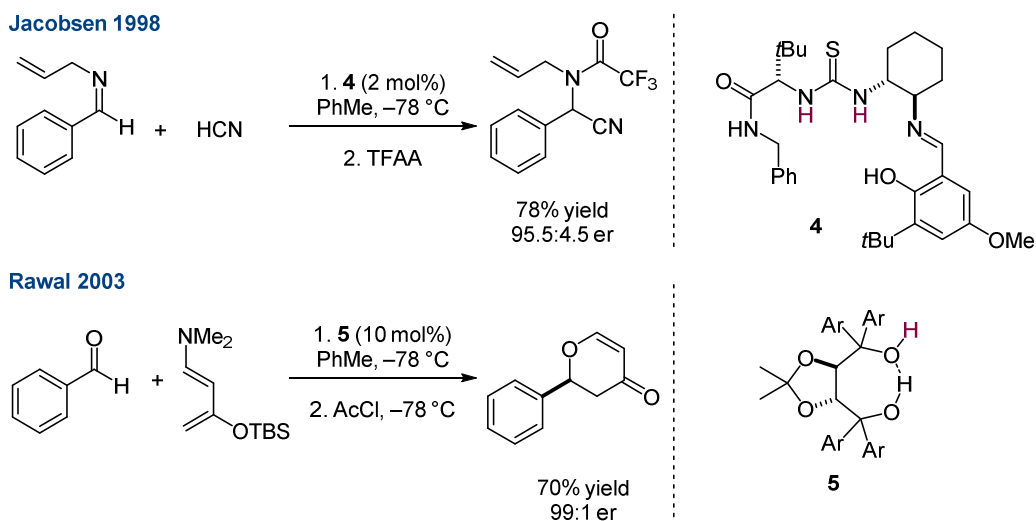


Figure 2.4 General and specific Brønsted acid catalysts.

The first application of chiral hydrogen bond donors as catalysts in an enantioselective transformation was serendipitously discovered by Sigman and Jacobsen while investigating a combinatorial approach to an enantioselective Strecker reaction.^[39] Surprisingly, among the many ligand-metal combinations tested, the control experiments using “ligand” **4** in absence of a transition-metal gave the highest enantioselectivity. Key interactions were identified in the hydrogen bonding

ability of the thiourea moiety. A few years later, Rawal and co-workers identified chiral TADDOL-derived diols **5** as effective catalysts for an asymmetric *hetero*-Diels–Alder reaction,^[40] proving that small molecules can control enantioselectivity solely by having hydrogen bond interactions with the corresponding substrate (Scheme 2.6).



Scheme 2.6 Strecker reaction catalyzed by chiral thiourea^[39] and *hetero*-Diels–Alder reaction catalyzed by chiral TADDOL.^[40]

Following these seminal works, the incorporation of various acidic functionalities (Figure 2.4) within different chiral scaffolds allowed the rapid development of enantioselective organocatalytic transformations.

Among the many possible sources of chirality, axially chiral molecules, for instance the binaphthyl structure **b1**, appear to be a privileged scaffold for organocatalysts. Many modifications have been explored on the naphthyl moiety, such as (a) modification of the 6,6'-position,^[41] (b) partial saturation of the backbone (**b2**),^[42] (c) addition and/or removal of benzene rings in either direction (**b3** and **b4**),^[43] or (d) formation of analogs such as 1,1'-spirobiindane (**b5**).^[44] The most recent development in this field includes the linkage of two binaphthyl units,^[45] in particular using highly acidic “linkers” (Figure 2.5).^[12a, 46]

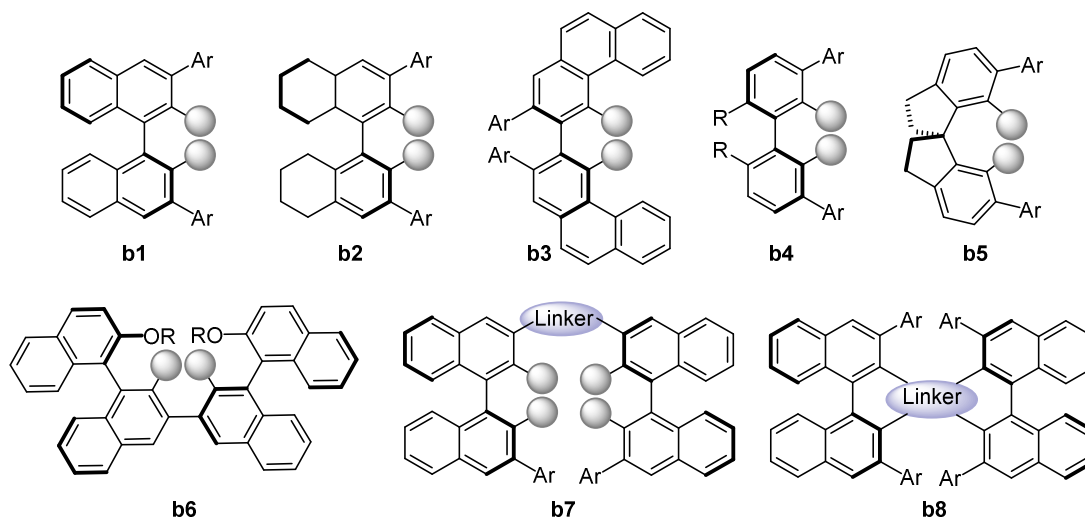


Figure 2.5 Examples of modifications of the chiral binaphthyl backbone.

An overview of the development of chiral Brønsted- and Lewis-acids for organocatalytic transformations is presented in the following sections, alongside with the discovery and the application of the concept of “asymmetric counteranion-directed catalysis” (ACDC).

2.2.3 Asymmetric Counteranion-Directed Catalysis (ACDC)

In general, the majority of asymmetric reactions proceed through partially charged or completely ionic intermediates. This feature is exploited and widely applied in the field of phase transfer catalysis (PTC), in which a negatively charged intermediate undertakes coulombic interaction with an enantiopure cationic catalyst.^[47] These ionic interactions are sufficient to create a chiral environment for the desired transformation. Asymmetric induction upon ion-pair formation may also proceed with a corresponding chiral anionic partner. In the concept of asymmetric counteranion-directed catalysis (ACDC), a cationic species, including but not being limited to a protonated intermediate from Brønsted acid activation, forms an ion pair with a chiral anion, determining the enantiodifferentiation of the desired transformation (Figure 2.6).^[48]

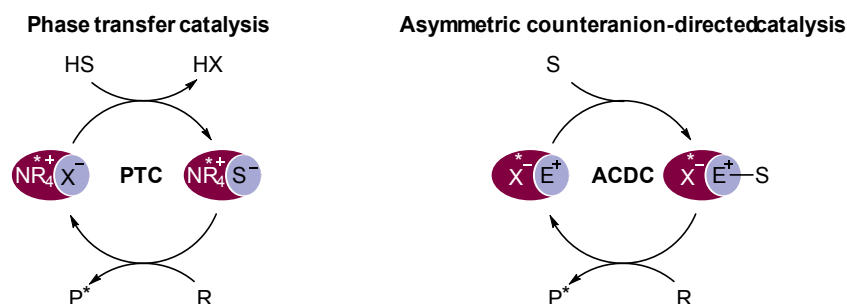
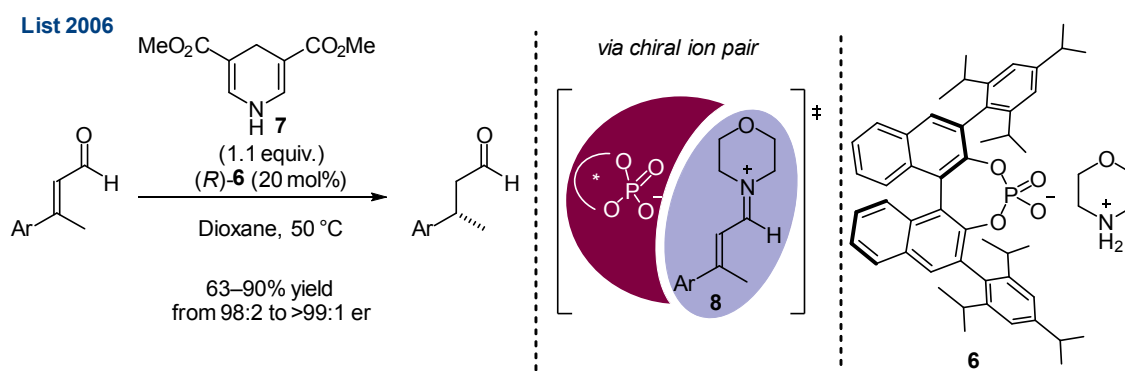


Figure 2.6 Schematic representation of PTC and ACDC. (S = substrate; X⁻ = anion; X⁻ = chiral anion; NR₄⁺ = chiral ammonium ion; R = reactant; P* = chiral product; E⁺ = achiral cation)

The term itself was introduced by Mayer and List, giving the proof of concept by developing the enantioselective amino-catalyzed transfer-hydrogenation of enals, using a Hantzsch ester as the reductant (Scheme 2.7).^[49] A general definition was given as:

“Asymmetric counteranion-directed catalysis refers to the induction of enantioselectivity in a reaction proceeding through a cationic intermediate by means of ion pairing with a chiral, enantiomerically pure anion provided by the catalyst.”^[48]

The authors showed the generality of this concept by employing the morpholinium salt of tri-isopropylphenyl phosphoric acid (TRIP) **6**. The BINOL-based phosphate anion was the only given source of chirality and, upon proposed coulombic interactions with the cationic iminium ion intermediate **8**, it directed the approach of the hydride source **7** with excellent stereoselection. The absence of additional “coordination” sites besides coulombic interactions, or assisting obvious hydrogen-bonding in the substrate, renders this example as a clear showcase of ACDC (Scheme 2.8).

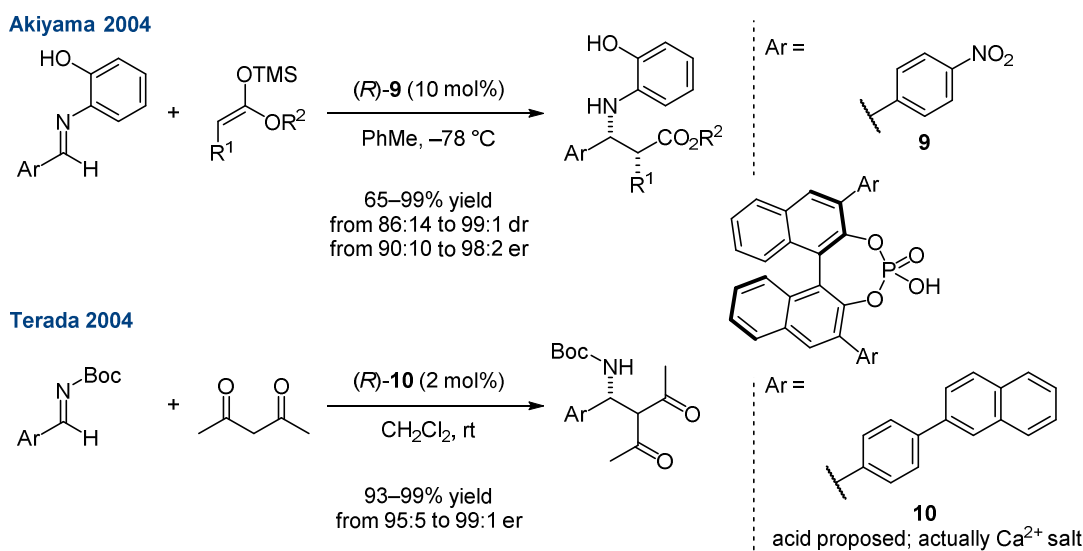


Scheme 2.7 Proof of concept of asymmetric counteranion-directed catalysis.^[49]

Since this groundbreaking publication, this concept has been extensively explored in context of chiral Lewis- and Brønsted-acid organocatalysis, as well as in metal-catalyzed transformations.^[50]

2.2.4 Chiral Brønsted Acids

In 2004, two groups independently reported the synthesis and application of axially chiral phosphoric acids derived from enantiopure 1,1'-bi-2-naphthol (BINOL) as chiral Brønsted acid catalysts. Akiyama and co-workers developed an enantioselective Mannich-type reaction of SKAs with imines,^[51] while Terada and co-workers reported an enantioselective addition of acetylacetone to imines^[52] (Scheme 2.8). However, Ishihara group later showed that the catalytic species in Terada's report was not the free acid, but the corresponding calcium salt formed during purification.^[53]



Scheme 2.8 Initial reports using BINOL-based Brønsted acid catalysts.^[51-52]

In the following years, several research groups focused their endeavors on the development of chiral phosphoric acid catalysts.^[54] The most prominent approach is the variation of the substituents at the 3,3'-positions of the binaphthyl backbone. These substituents create steric bulk around the active site and additionally, depending on their electron-donating or -withdrawing behavior, influence the electron density of the entire catalyst. The choice of the substituent has to be optimized for each individual enantioselective transformation. To date, the most successfully applied catalyst is the 2,4,6-triisopropylphenyl substituted phosphoric acid (TRIP) initially developed by List and co-workers.^[55]

Despite the success and generality of BINOL-derived phosphoric acids, two major challenges have to be considered: (a) the requirement for relatively (Lewis-)basic substrates to provide sufficient activation, and (b) the low stereinduction with small, unbiased substrates. In order to tackle these challenges, efforts within the scientific community have been devoted to develop (a) more acidic catalysts, able to protonate less reactive substrates and (b) catalysts able to provide a more confined chiral environment around the active site.

2.2.4.1 Toward More Acidic Catalysts

The acidity of BINOL-derived acids can be tuned by three individual approaches: (a) changing the electronics of the 3,3'-substituents, (b) introducing electron-withdrawing groups (EWGs) in the BINOL-backbone and (c), the most effective, changing the acidic functionality in the active site.^[56] Considering that high acidity implies particularly mild conjugated bases, improved charge delocalization in the conjugate base is expected to have the largest impact on acidity. Yagupolskii *et al.* showed that the substitution of oxygen atoms with N(H)Tf (trifluoromethylsulfonyl) in benzoic acid increases the acidity by several orders of magnitude (Figure 2.7).^[57]

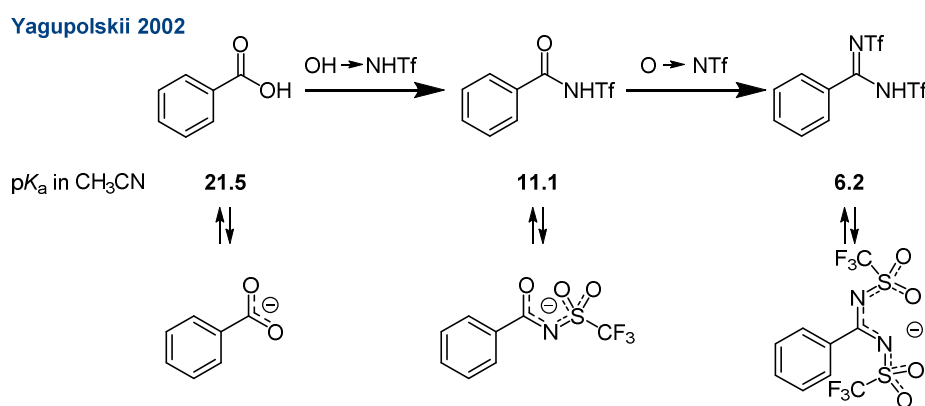
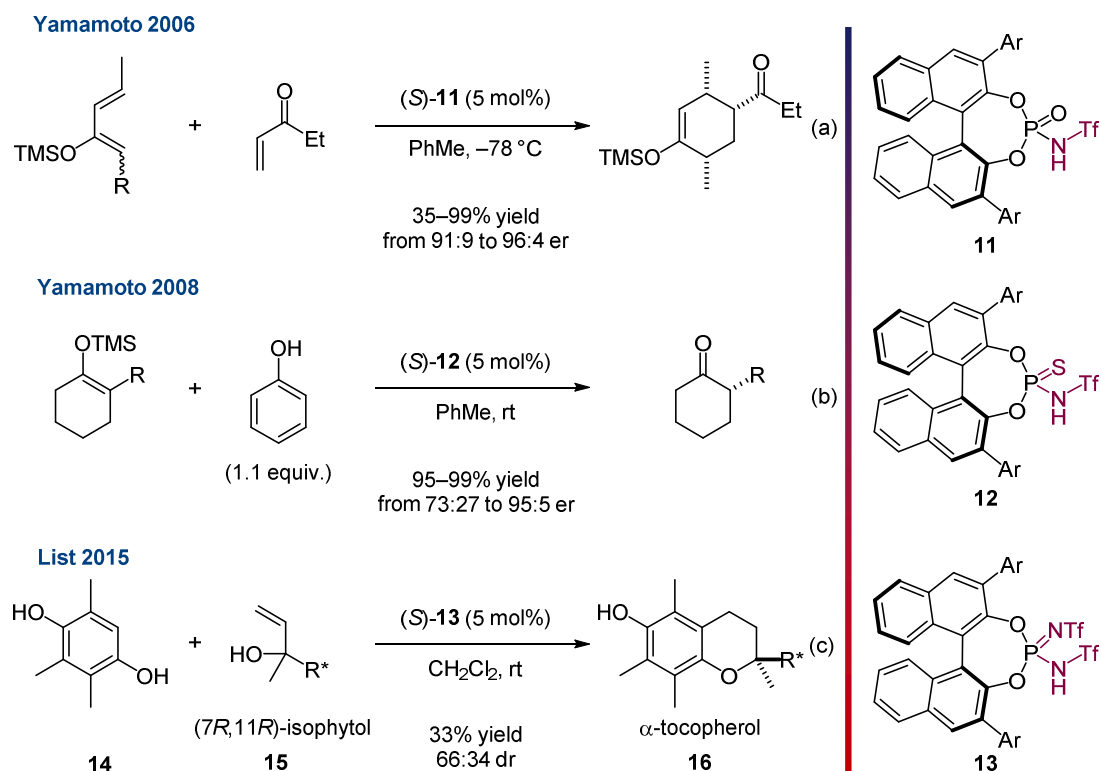


Figure 2.7 Yagupolskii's principle to increase acidity by substituting O with N(H)Tf.

Yamamoto and co-workers reported the expansion of this concept to BINOL-derived phosphates, introducing phosphoramidate **11**. The increased acidity allowed the development of a catalytic enantioselective Diels–Alder reaction of α,β -unsaturated ketones with silyloxydienes (Scheme 2.9, Eq. a).^[56c] The same authors could further increase the acidity by introduction of a sulfur atom, resulting in thiophosphoramidate catalyst **12**. This catalyst enabled the first organocatalytic enantioselective protonation of silyl enol ethers (Scheme 2.9, Eq. b). At the same time, List and co-workers reported several examples with BINOL-based thiophosphoramidate-derivatives.^[58] Almost a decade later, Kaib and List further expanded the application of Yagupolskii's principle to chiral phosphates, reporting the synthesis and synthetic application of highly acidic phosphoramidimidate **13**. The

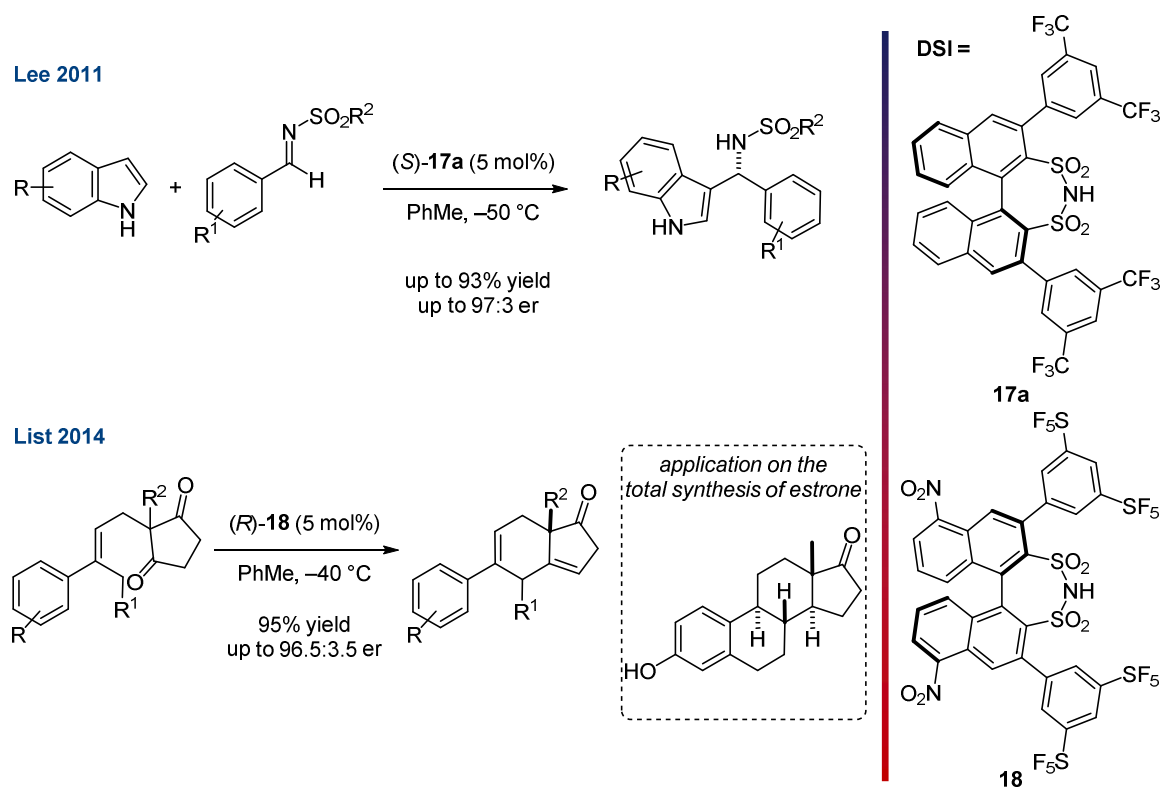
superior acidity enables more challenging reactions, such as the Friedel-Crafts alkylation of isophytol **15** and hydroquinone **14**, giving α -tocopherol (**16**).^[59] The outstanding acidity was not complemented by sufficient diastereodifferentiation, achieving only moderate diastereomeric ratios (Scheme 2.9, Eq. c).



Scheme 2.9 Synthetic application of BINOL-phosphoric acid derivatives with increased acidity achieved by applying Yagupolskii's principle.

An alternative approach to increase the acidity by changing the active site of the catalysts was reported by List.^[60] In these reports, a strong increase of acidity was achieved by substituting the phosphate moiety to the significantly more acidic disulfonimide (DSI). The main field of application of these structures is as highly potent precatalysts for silicon Lewis acid catalysis (*vide infra*). However, some reports exploiting their application as strong Brønsted acids also exist. In particular, Lee and co-workers applied DSI **17a** to the aminoalkylation of indoles.^[61] More recently, List and co-workers reported an asymmetric Torgov cyclization and applied

the method to the so far shortest reported total synthesis of (+)-estrone.^[62] In this case, an additional increase in acidity was achieved by introduction of strong EWGs on the 3,3'-substituents (SF₅ groups) and on the 5,5'-positions of the binaphthyl scaffold (NO₂ groups) (**18**) (Scheme 2.10).



Scheme 2.10 Application of chiral DSI as Brønsted acid catalysts.

Even higher acidities have been achieved when the disulfonimide unit was substituted with *bis*(sulfuryl)imides (JINGLE), introduced by Berkessel *et al.*,^[63] or with disulfonic acid (BINSAs), introduced by List *et al.*^[64] BINSAs could only be successfully applied in asymmetric transformations as either the pyridinium salt as reported by Ishihara *et al.*,^[65] or as ligands in the presence of Lewis acidic metals.^[66] However, the most acidic catalysts in this series have not found application in highly enantioselective catalysis,^[12b] as presumably the space around the active site is not confined enough to allow efficient enantiodifferentiation.

2.2.4.2 Toward More Confined Catalysts

In 2012, Čorić and List reported an innovative solution to increase the confinement around the catalytically active site.^[46a] The catalyst design included the expansion of the anion delocalization, by introducing the imidodiphosphate anion, and the restriction of the rotational freedom around the P–N bond, by introducing an additional BINOL unit. The combination of two identical BINOLs bearing 3,3'-substituents, which are large enough to block the rotation of the imidodiphosphate unit, maintains the C_2 -symmetry. This leads to a reduced amount of catalytically active conformations, which can stabilize only few and selected transition states, therefore resulting in higher selectivity (Figure 2.8).

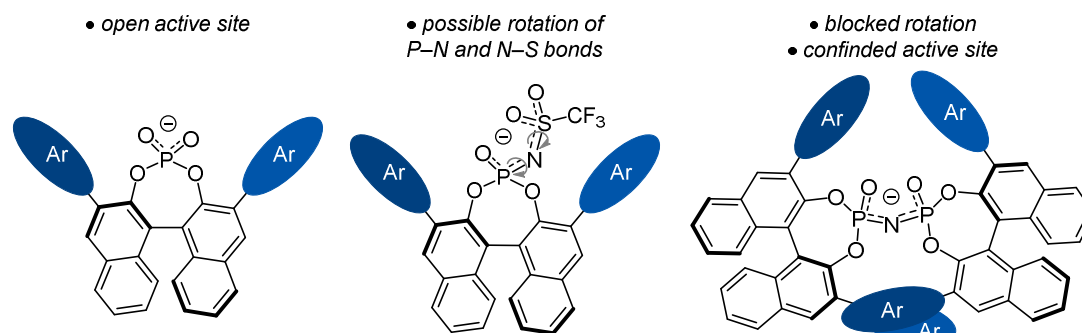
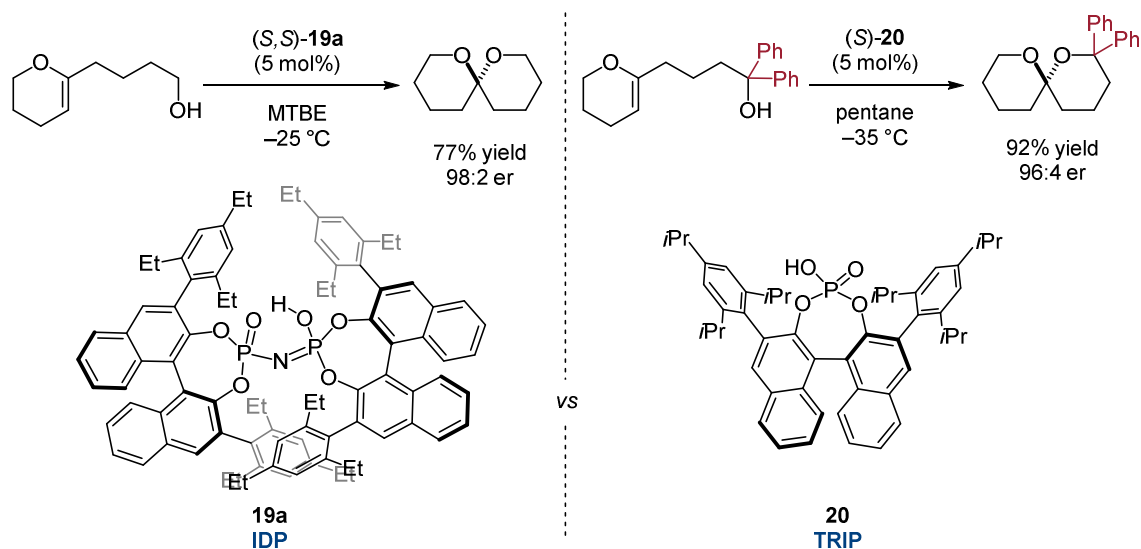


Figure 2.8 Design of conformationally locked imidodiphosphates with C_2 -symmetry.

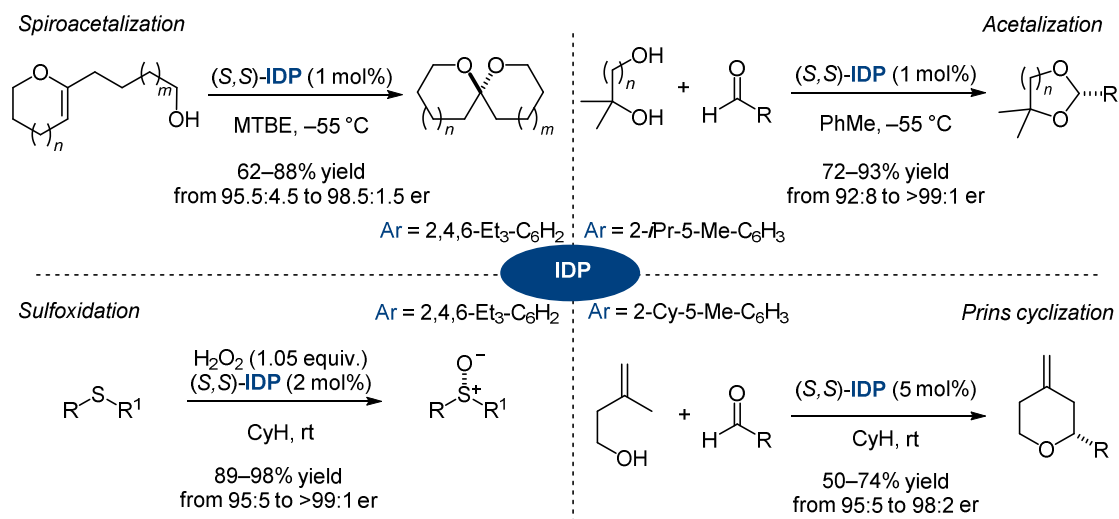
These newly designed confined imidodiphosphates (IDPs) allowed the spiroacetalization of electronically and sterically unbiased substrates, in high yields and very high enantioselectivities.^[46a] The power of the IDP scaffold can be highlighted by a direct comparison with the subsequently reported example of enantioselective spiroacetalization by Nagorny *et al.*^[67] In this case, specific modifications had to be added to the substrate in order to apply (S)-TRIP (**20**) as the chiral catalyst. In particular, the addition of two geminal phenyl groups (highlighted in red) were required in order to achieve good reactivity (Thorpe–Ingold effect) and high enantioselectivity (Scheme 2.11).

Background



Scheme 2.11 Comparison of IDP **19a** and TRIP (**20**) as chiral catalysts for the enantioselective spiroacetalization.

Furthermore, IDPs proved to be very efficient catalysts for a large selection of reactions (Scheme 2.12) and showed outstanding results also for unbiased, namely aliphatic, substrates.^[68] The main limitation of IDPs is their acidity ($\text{p}K_{\text{a}} \cong 11$), which is far lower than the phosphoramidates and dwells between phosphoric acids and DSIs.



Scheme 2.12 Initial reports using chiral IDPs as catalysts.

2.2.4.3 Toward More Acidic and Confined Catalysts

A higher acidity in the confined pocket of the IDPs was needed to activate and functionalize less reactive substrates. Increased reactivity was initially achieved by the incorporation of EWGs in the BINOL backbone,^[69] however the key to success was again the application of Yagupolskii's principle (Figure 2.7): the substitution of the P=O unit with P=NTf (iIDP and IDP_i).^[12a] These new classes of catalysts have complementary activation modes; iIDPs have moderate acidities (pK_a in CH₃CN \cong 7–9) and maintain a bifunctional character (whereas P=O is the basic site, and P=NTf is the acidic site), while IDP_is are exclusively strongly acidic (pK_a in CH₃CN \cong 2–5) (Figure 2.9).

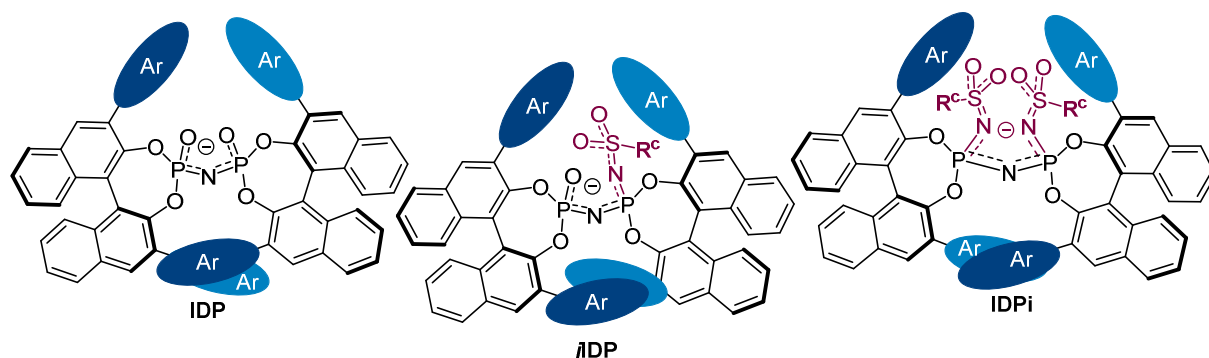
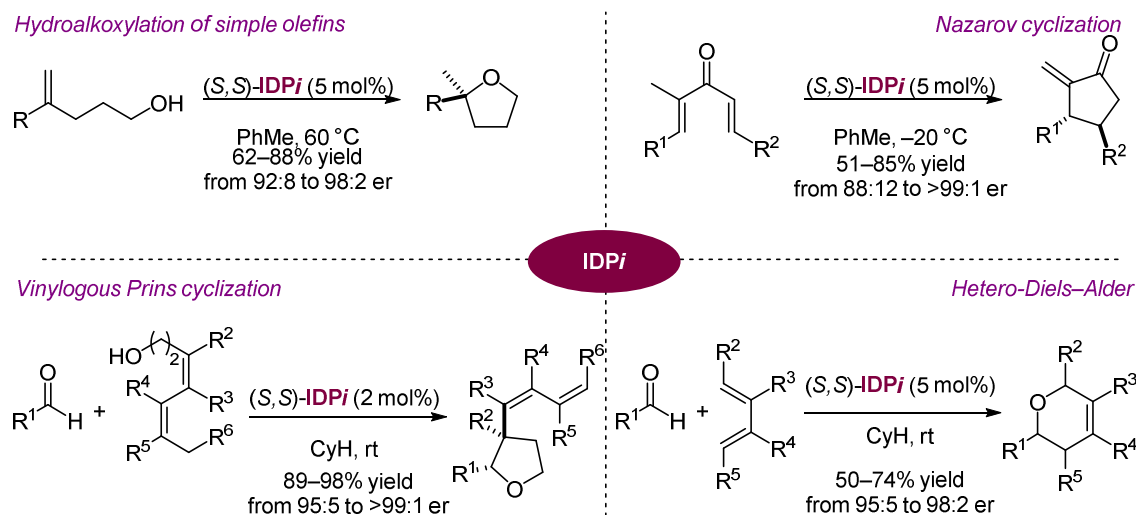


Figure 2.9 Evolution of the active site of the IDP, iIDP and IDP_i reported by List *et al.*

The significantly increased acidities attained with the IDP_is allowed the activation of unbiased and highly unreactive functionalities. Excellent enantioselectivities have been already shown in the *hetero*-Diels–Alder reactions,^[70] vinylogous Prins cyclizations^[71] and Nazarov cyclizations.^[72] Furthermore, the frontiers of asymmetric Brønsted acid catalysis have been expanded to the activation of simple and unbiased olefins^[73] (Scheme 2.13).

Background



Scheme 2.13 Transformations with IDPis as Brønsted acids.

Figure 2.10 gives a general overview of the historic development of the BINOL-based Brønsted-acid organocatalysts alongside with the experimental pK_a .

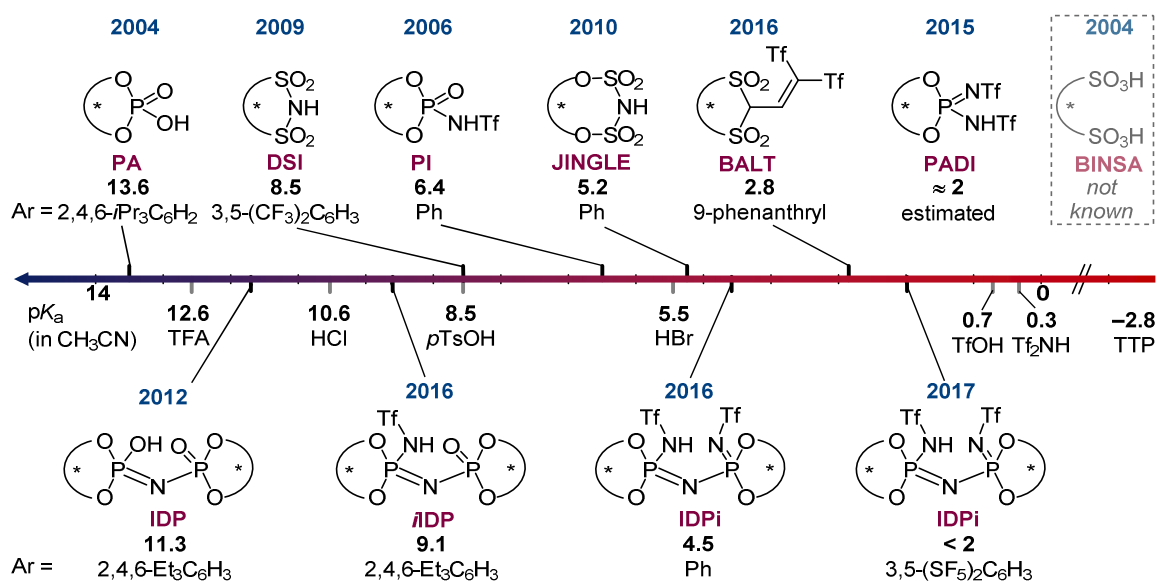


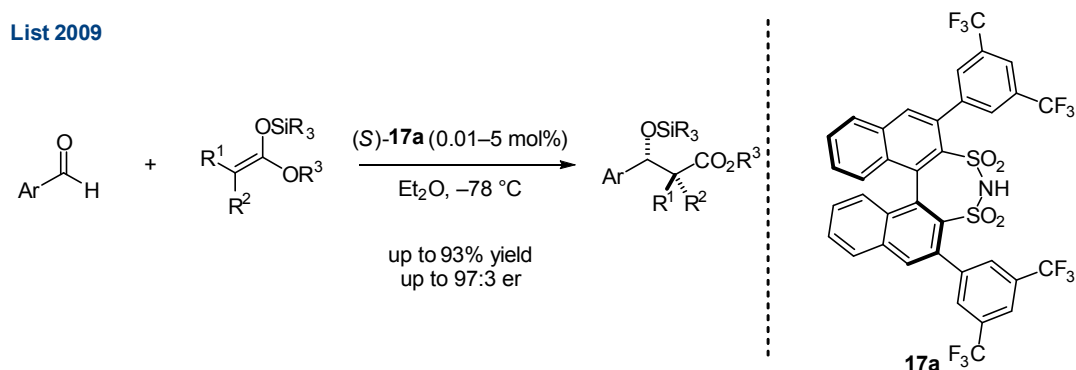
Figure 2.10 Development of BINOL-based Brønsted-acid organocatalysts and corresponding pK_a values (TTP = 1,1,3,3-Tetratriflylpropene).

2.2.5 Chiral Lewis Acids

Strong Brønsted acids can be converted into potent organic silylium Lewis acids^[74] upon treatment with a suitable silylating agent.^[75] The silylated forms of triflic acid (trimethylsilyl triflate, TMSOTf)^[76] and triflimide (trimethylsilyl *bis*-triflimide, TMSNTf₂),^[77] for instance, are well established highly reactive Lewis acid catalysts.^[78] Regarding asymmetric transformations involving silicon-protected enol equivalents, (transition-)metal-derived Lewis acid catalysts strongly suffer from the competition between the anticipated chiral Lewis acid itself and “silylium” background catalysis, a non-enantioselective off-cycle pathway.^[79]

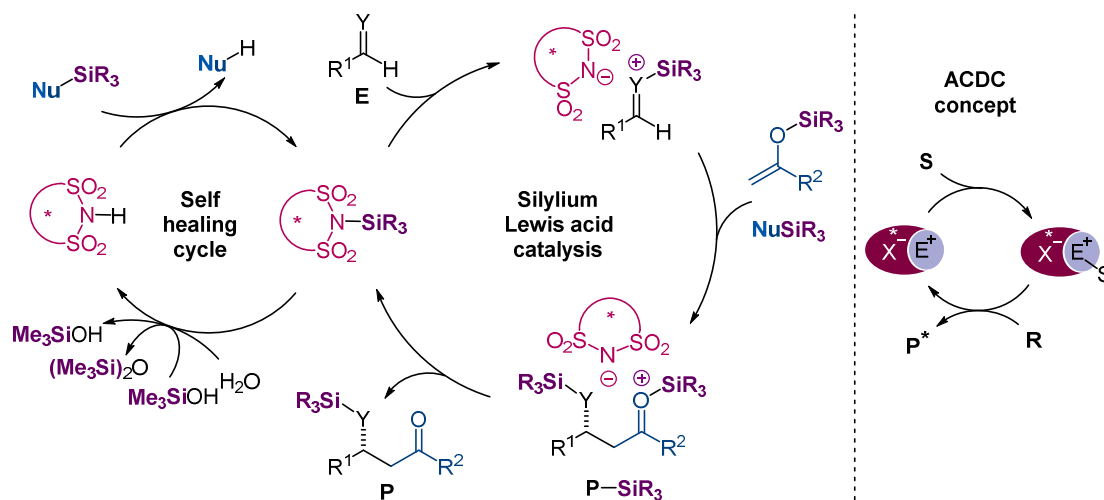
2.2.5.1 Disulfonimides as Lewis Acid Catalysts

The silylation of a suitable enantiopure strong organic Brønsted acid allows an asymmetric transformation through ACDC. Taking advantage of the silylium background catalysis, List and coworkers reported the first example of a catalytic enantioselective transformation exploiting “silylium” ions as potent Lewis acids in 2009. DSI **17** served as the precatalyst and, upon silylation, acted as the Lewis acid catalyst in the Mukaiyama–aldol reaction of aromatic aldehydes and SKAs (Scheme 2.14).^[60a]



Scheme 2.14 Chiral DSI-catalyzed Mukaiyama–aldol reaction.

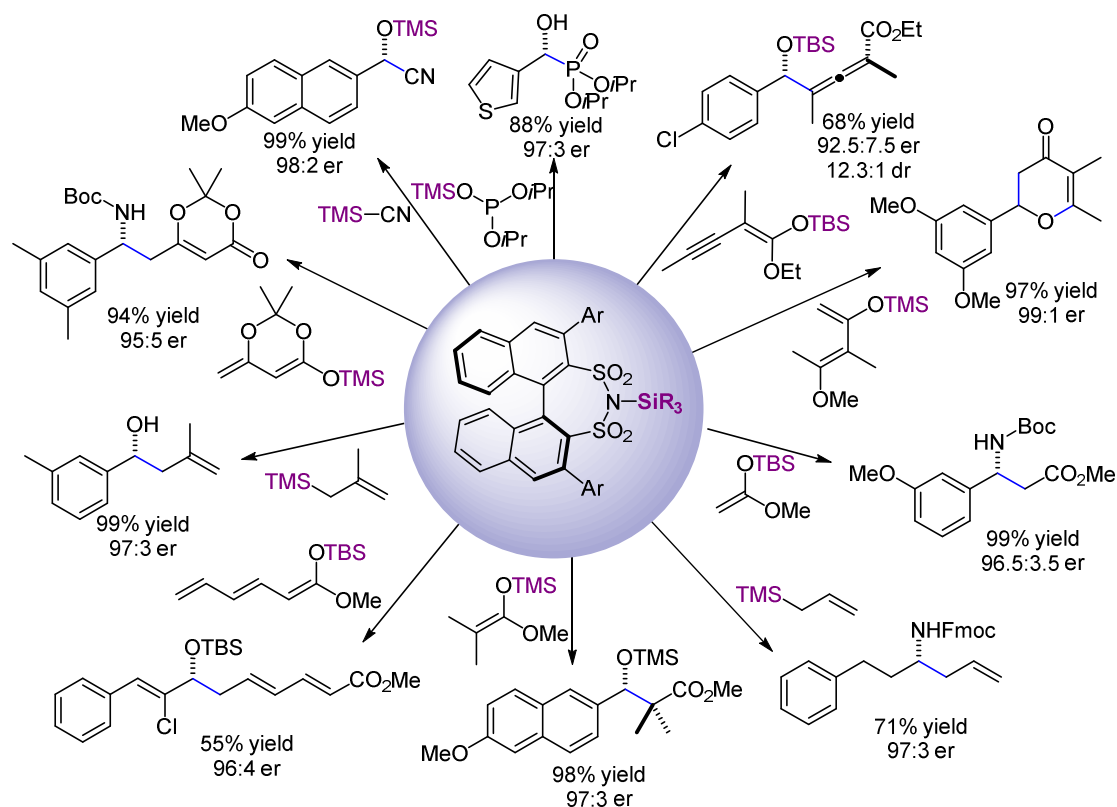
A generalized mechanism for disulfonimide-catalyzed reactions is depicted in Scheme 2.15. Initially, a Brønsted acid catalyst (pK_a usually < 11) is activated by a silylating agent to give the active Lewis acid catalyst. In case of residual water in the reaction mixture, the active catalyst is hydrolyzed and re-silylated until all the water is converted into the corresponding silyl ether (or hexamethyldisiloxane); even R_3SiOH substrates would still desilylate the catalyst, so that ultimately only $(R_3Si)_2O$ is formed. The ability of the catalyst to regenerate is referred to as *self-healing*. As no catalytic activity can be observed until the reaction solution is anhydrous, this period is referred to as the *dormant period*. The first step of the catalytic cycle consists of silylation of the electrophilic substrate (E), presumably forming a tight ion pair between the enantiopure anion (catalyst) and the cationic electrophile. In this induced asymmetric environment, the nucleophile (Nu) attacks onto the electrophile giving the silylated product. Finally, the lower affinity of the product (P) for the catalyst leads to silicon transfer back onto the catalyst releasing the desired product and completing the catalytic cycle (Scheme 2.15).



Scheme 2.15 General catalytic cycle for disulfonimide ACDC in silylium Lewis acid catalysis using SKAs.

Exploring the concept of ACDC, chiral DSIs were successfully applied as catalysts in numerous enantioselective transformations.^[12b] Aromatic aldehydes and imines were preferred substrates reacting with a variety of silylated nucleophiles. In

analogy to the Mukaiyama–aldol reaction (Scheme 2.14), the vinylogous,^[80] *bis*-vinylogous^[80] and alkynylogous^[81] variants were reported. Other examples include: the *hetero*-Diels–Alder reaction using Danishefsky-type dienes and their alkynylogous analogs,^[82] the Mukaiyama–Mannich reaction with SKA^[83] and its vinylogous variant to access α -amino- β -ketoesters in the presence of silyloxydienes,^[84] the cyanosilylation with TMSCN in the presence of 0.005 mol% (50 ppm) of catalyst,^[85] and the Abramov reaction with silylated phosphites to access α -hydroxy phosphonates.^[86] The asymmetric Hosomi–Sakurai allylation was achieved^[87] with highly nucleophilic (2-methylallyl)trimethylsilanes ($N = 4.41$),^[88] however, the use of allyltrimethylsilane ($N = 1.68$)^[89] proved to be challenging. This limitation was overcome using the *in situ* generated *N*-fluorenylmethoxycarbonyl (Fmoc) imines as electrophiles (Scheme 2.16).^[90]



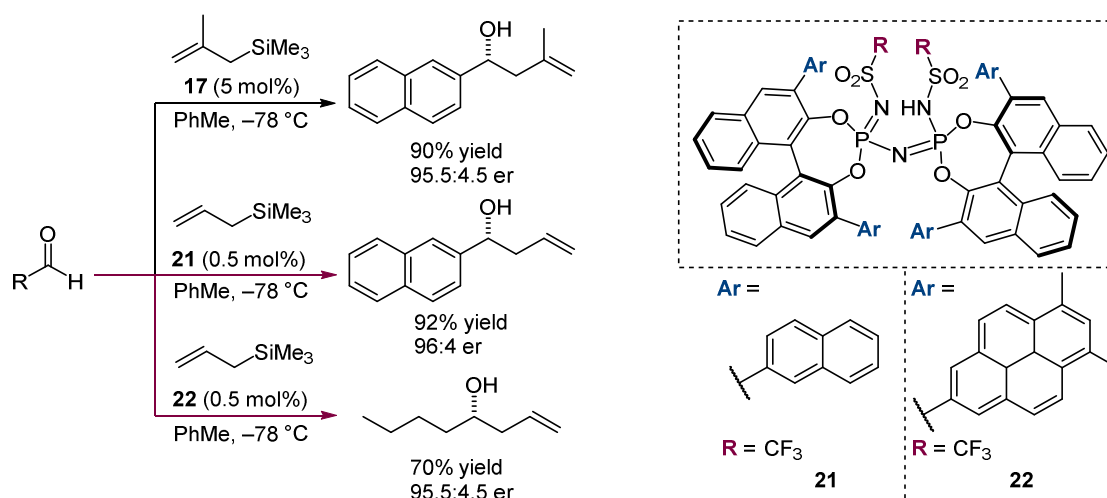
Scheme 2.16 Overview of DSI-catalyzed asymmetric transformations using aromatic aldehydes and imines reported so far.

In summary, the high acidity of the DSI motif enables a variety of enantioselective silylium-catalyzed transformations *via* ACDC. However, in order to achieve high levels of enantioinduction, the reported systems were limited to aromatic starting materials, presumably due to π/π -stacking between the 3,3'-substituents of the catalyst and the substrate. Therefore, the design of a more confined active site would be the next step toward generalizing silylium ACDC.

2.2.5.2 IDP*is* as Lewis Acid Catalysts

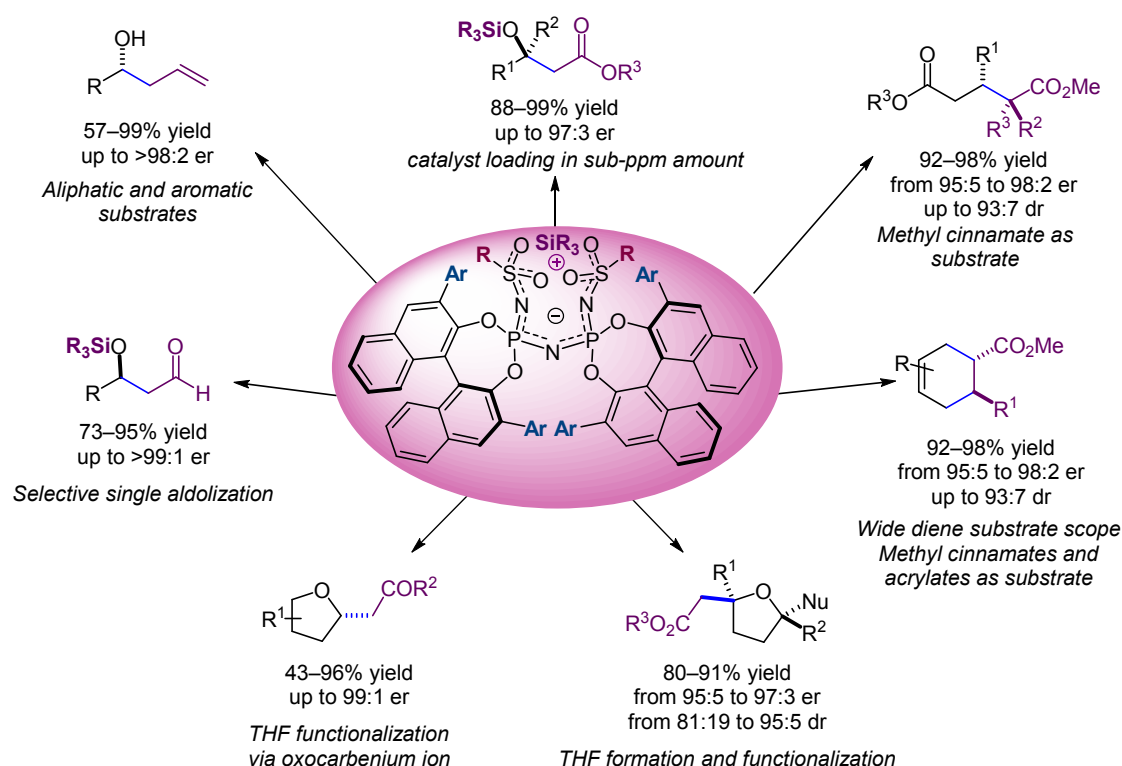
The transformation of small, unbiased aliphatic substrates is a major challenge in asymmetric Lewis acid organocatalysis, as a highly acidic functionality in a well-defined and confined environment is required. BINOL-based imidodiphosphates (IDPs) ensure a confined pocket; however, their reduced acidity ($pK_a \cong 11.5$) as compared to DSIs ($pK_a \cong 8.5$) renders them incompatible with “silylium” Lewis acid catalysis. The profoundly enhanced acidity of the IDP*is* ($pK_a < 4.5$) encapsulated inside the C_2 -symmetric BINOL dimer makes them promising candidates for the exploration of new reactivities in Lewis acid catalysis.

In 2016 the List group reported the development and application of IDP*is* in organic Lewis acid catalysis. A general Hosomi–Sakurai allylation of aromatic and aliphatic aldehydes with excellent enantioselectivities and yields was presented (Scheme 2.17).^[46b] Noteworthy, at even low catalyst loadings (down to 0.5 mol%) the less reactive allyltrimethylsilane ($N = 1.68$) readily reacted.



Scheme 2.17 Silylium Lewis acid-catalyzed Hosomi–Sakurai allylations using allyltrimethylsilane derivatives.

Following this groundbreaking work, the power of IDP*i* catalysts for the activation of small and unbiased substrates with high selectivity has been shown in several reports. Namely, the Mukaiyama–aldol reaction was made possible with catalyst loadings approaching the ppb levels;^[91] both the Mukaiyama–Michael reaction^[92] and the Diels–Alder reaction^[93] were performed exploiting a wide substrate scope. The latter allowed access to previously inaccessible cycloaddition products *via* Lewis acid catalysis. Furthermore, the synthesis and functionalization of the tetrahydrofuran moiety through stereoselective control of the corresponding oxocarbenium ion was reported.^[94] Last, the single addition of acetaldehyde derived silyl enol ethers to aldehydes^[95] proved that the chiral Lewis acid controls the chemo- and the enantioselectivity of the transformation, avoiding engineered substrates and undesired polymerization products (Scheme 2.18).



Scheme 2.18 Overview on applications of “silylium” IDPi-catalyzed asymmetric transformations.

The wide success of the IDP*i* scaffold can be attributed not only to the high acidity and the confinement of the catalytic active site, but also to the many structural diversifications achievable upon modification of the 3,3′-substituents (Ar) and the sulfonimidic residue (R). Indeed, in comparison the DSI motif offers limited possibilities of structural modifications; the explored ones are different 3,3′-substituents (electron-rich or electron-poor, aromatic and aliphatic substituents) which affects the enantioselectivity with its close proximity to the active site, or different positions in the backbone, with the introduction of EWG (e.g. nitro groups) or EDG (alkyl chains), usually influencing mainly the reactivity of the catalyst. IDP*i*s, on the other hand, in addition to all the above mentioned modifications, can be further modified in proximity to the catalytic active site, upon variation of the sulfonimidic residue (R) (Figure 2.11).

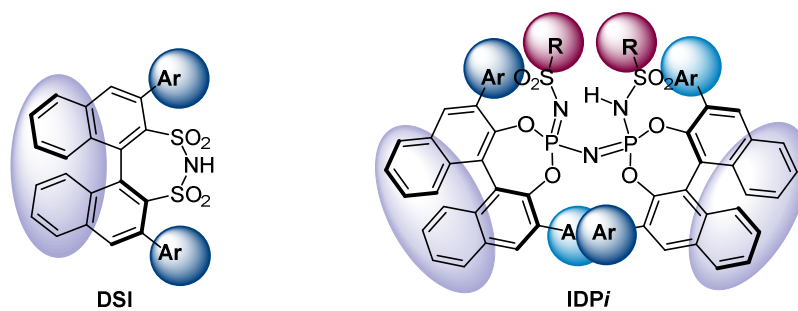


Figure 2.11 Structural diversity of DSI vs IDPi.

2.3 Bis-Silyl Ketene Acetals

The first reports on the synthesis and characterization of *bis*-SKAs appeared in the early 1970s.^[96] *Bis*-SKAs and silyl enol ethers differ both on electronic and structural properties. Moving from silyl enol ethers to SKAs, the nucleophilicity *N* at the α -position increases by several orders of magnitude.^[88] The presence of a second silicon group shifts *N* further toward higher nucleophilicity, implying a more facile reaction with an electrophilic partner.^[97] Structurally, *bis*-SKAs bearing the identical silyl groups do not exhibit *E/Z* stereoisomer isoforms; this reduces the amount of diastereomeric transition states when reacting with an electrophile in the presence of a chiral catalyst (Figure 2.12). Furthermore, the absence of *E/Z* stereoisomers enables facile synthesis and purification of the starting material.

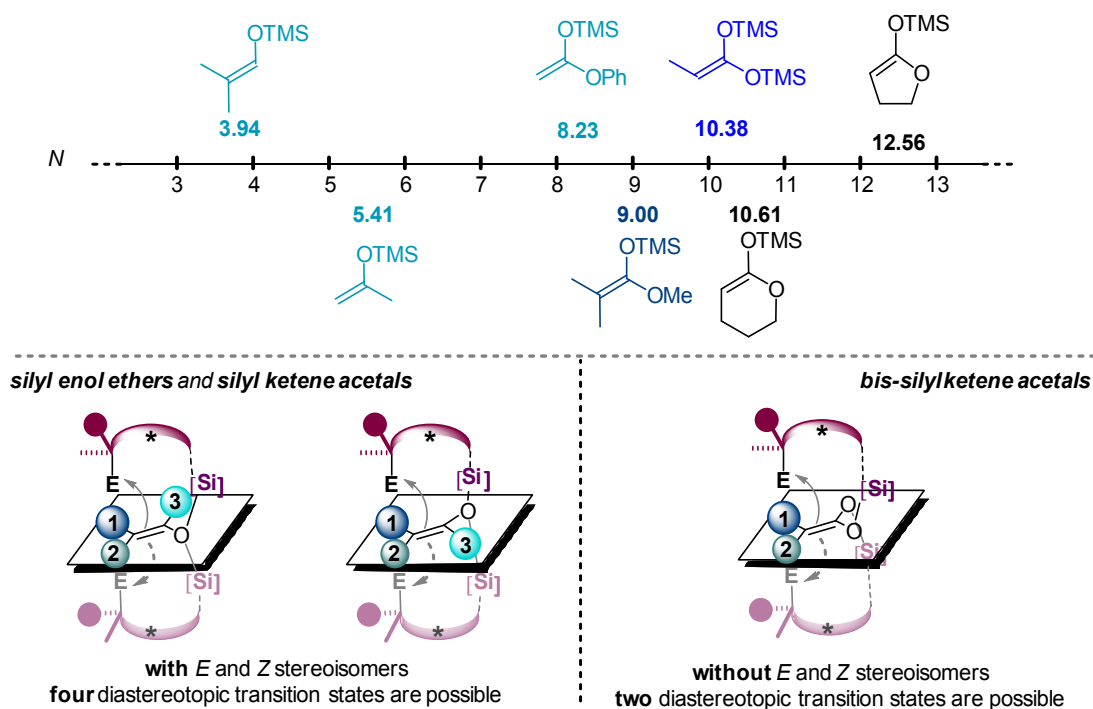
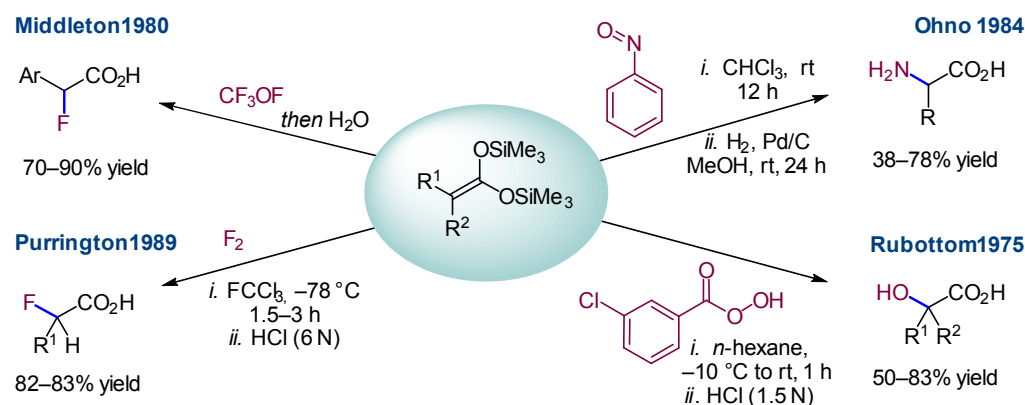


Figure 2.12 Comparison of electronic and structural properties of silyl enol ethers/SKAs and *bis*-SKAs.

2.3.1 Bis-SKAs in the Synthesis of α -Functionalized Carboxylic Acids

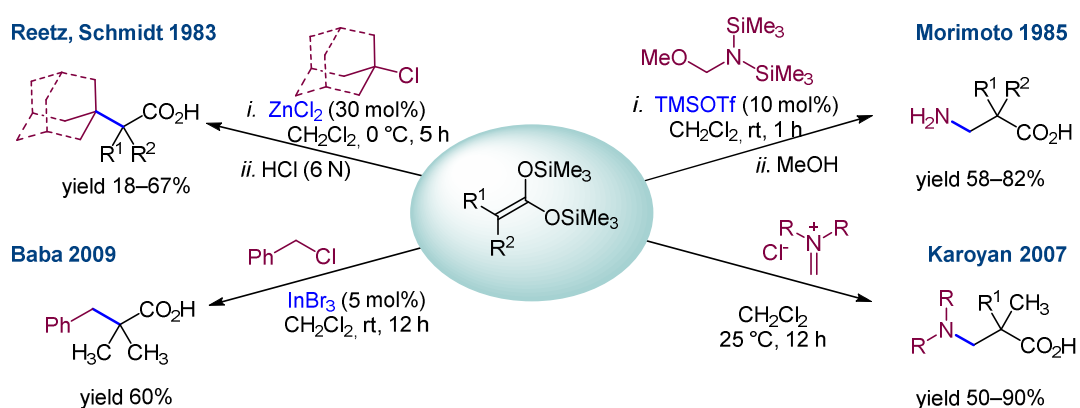
Significant attention has been devoted towards the exploration of the synthetic potential of *bis*-SKAs as surrogates of α -enolizable carboxylic acids. In this section, the different transformations so far developed with *bis*-SKAs are presented. Initial studies were performed with highly electrophilic reagents, such as trifluoromethyl hypofluorite,^[98] fluorine^[99] and nitrosobenzene^[100] or oxidants such as *m*-chloroperbenzoic acid.^[101] These reagents enabled the direct formation of C–F, C–N and C–O bonds, respectively, providing a formal α -functionalization of carboxylic acids (Scheme 2.19).



Scheme 2.19 *Bis*-SKAs in C–heteroatom bond forming reactions.

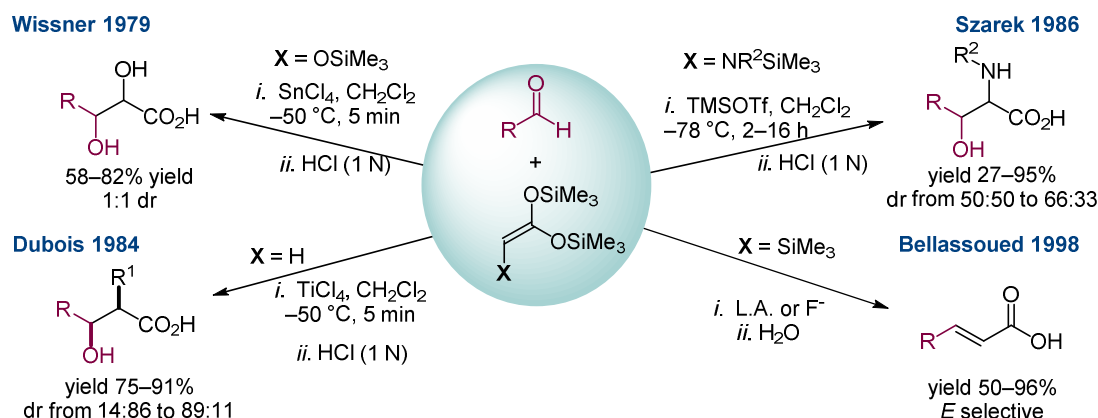
The pioneering work of Reetz *et al.* paved the way for several C–C bond forming reactions under Lewis acidic conditions.^[102] In this first example, an α -alkylation in the presence of catalytic ZnCl_2 and tertiary haloalkanes or tertiary acetates was reported. Recently, Baba *et al.* reported that InBr_3 was a competent Lewis acid for the α -alkylation of *bis*-SKAs in the presence of benzyl chloride.^[103] The first α -aminomethylation was reported by Morimoto *et al.* in 1985, where TMSOTf was chosen to catalyze the *in situ* formation of a reactive iminium ion, which is quantitatively trapped by the *bis*-SKA to afford the *tris*-silylated β^2 -amino ester. Upon protic workup, the free β^2 -amino acid is formed.^[100] An extension of this work was reported by Karoyan in 2007, in which various preformed iminium salts bearing

different protecting groups were used as reagents for the α -aminomethylation of *bis*-SKAs^[104] (Scheme 2.20).



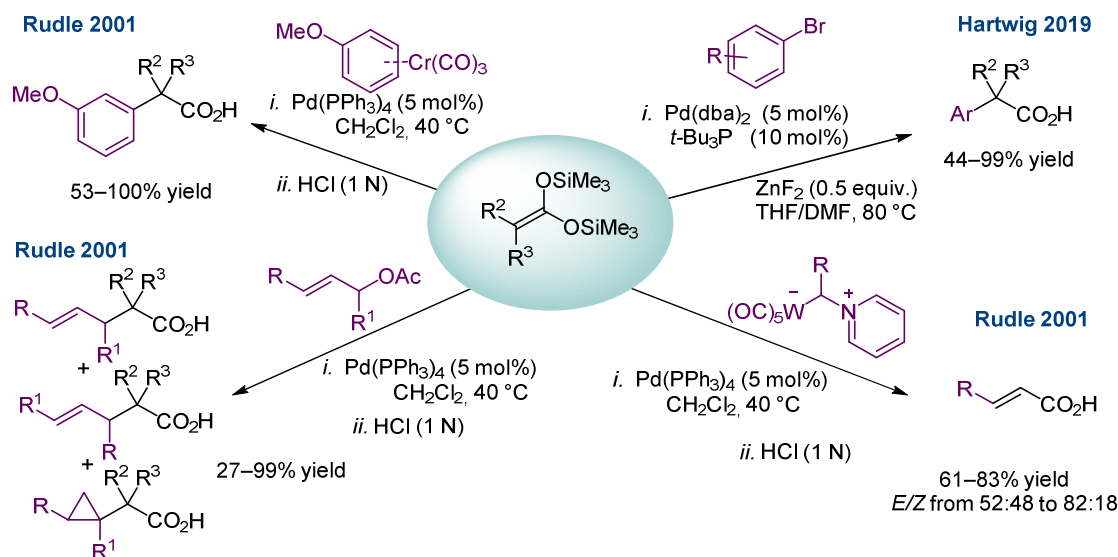
Scheme 2.20 C–C bond forming reactions: α -alkylation and α -aminomethylation of *bis*-SKAs.

One of the most explored reactions for this class of substrates is the Mukaiyama–aldol reaction in the presence of a Lewis acid. Wissner reported the first example in 1979 in the presence of SnCl_4 and *O*-trimethylsilyl *bis*-SKA affording 2,3-dihydroxy carboxylic acid.^[105] Dubois *et al.* showed a moderately diastereoselective example in the presence of α -monosubstituted *bis*-SKA and a catalytic amount of TiCl_4 .^[106] Skarek *et al.* used *N*-methyl-*N*-trimethylsilyl *bis*-SKA as a glycine surrogate and TMSOTf as the Lewis acidic catalyst, to obtain the α -functionalized β -hydroxy- α -amino acid, albeit with poor diastereoselectivities.^[107] More recently, Bellassoued showed that, when the *bis*-SKA has a TMS group in the α -position, the Mukaiyama–aldol product eliminates and selectively forms the (*E*)-cinnamic acid derivative (Scheme 2.21).^[108]



Scheme 2.21 Mukaiyama-aldol reactions with *bis*-SKA nucleophiles.

Rudle *et al.* reported several examples of α -arylations of *bis*-SKAs, catalyzed by $\text{Pd}(\text{PPh}_3)_4$. Successful coupling partners were tricarbonylchromium complexes of aryl ethers,^[109] tungsten(0) alkylidene complexes stabilized as pyridinium ylides^[110] and allylic acetates, albeit with poor regioselectivity. Recently, Hartwig *et al.* reported a general arylation of carboxylic acids and amides *via* the *in situ* formation of *bis*-SKA with a stoichiometric base (LiHMDS) and a catalytic amount of $\text{Pd}(\text{dba})_2$ and $t\text{-Bu}_3\text{P}$ (Scheme 2.22).^[111]



Scheme 2.22 Cross-coupling reactions with *bis*-SKAs.

The transformations shown above are summarized in the following timeline, giving a general overview for the transformations achieved so far with *bis*-SKAs as substrates for the α -functionalization of carboxylic acids (Figure 2.13). Until today, the only reported enantioselective transformation using *bis*-SKAs is their enantioselective protonation using stoichiometric quantities of an enantiopure BINOL–Sn complex, reported by Yamamoto *et al.*^[112] Recently, Ooi and co-workers expanded the portfolio of this reaction, reporting two catalytic examples using asymmetric phase-transfer catalysts.^[13b, 13c] A comprehensive overview on enantioselective protonation of *bis*-SKA is presented in the following section.

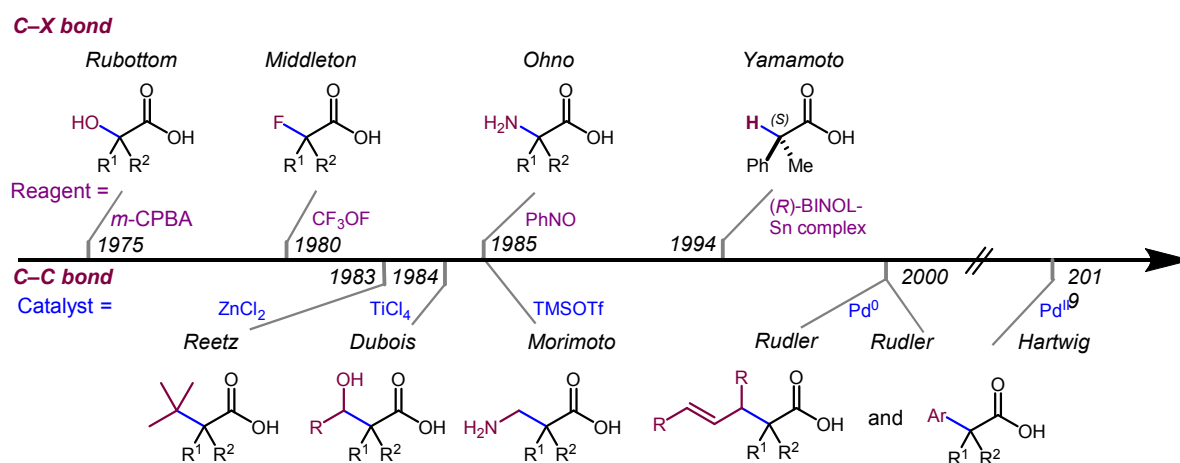


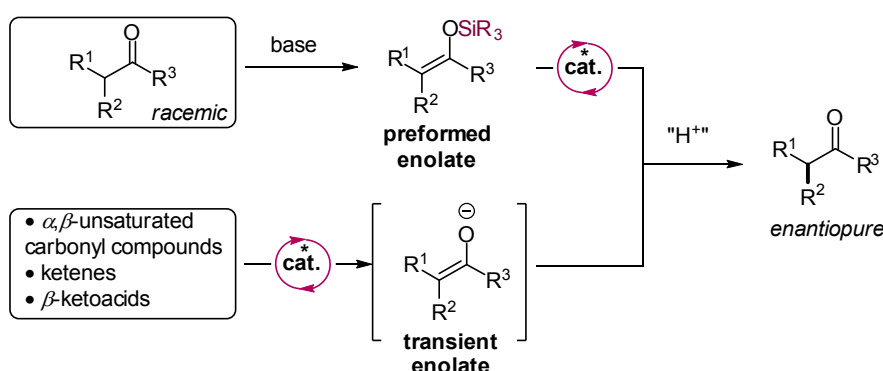
Figure 2.13 General overview of the transformations reported with *bis*-SKAs.

Background

2.4 Enantioselective Protonation of *bis*-SKAs

2.4.1 Introduction

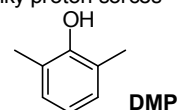
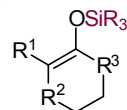
The abundance of tertiary carbon centers at the α -position of carbonyl compounds in biological and natural products encouraged many scientists to investigate enantioselective transformations to access the enantiopure α -chiral carbonyl motif in an efficient and highly selective manner. The asymmetric protonation of preformed or catalytically generated transient enol equivalents enables straightforward access to these valuable scaffolds (Scheme 2.23). As the high reactivity of the proton and the basicity of the enolate result in a fast reaction, control of the enantioselectivity is very challenging. Inhibition of the background reactivity is usually overcome by performing the reactions under cryogenic conditions, with slow addition of either reagent, and using bulky PSs as for instance DMP.^[113] The enantiocontrol of the proton transfer highly depends on the enolate geometry; therefore, many examples are reported using cyclic substrates, in which the geometry of the enolate is restricted to the *E*-form. In the case of metal-derived Lewis acid-catalyzed transformations, the stability of the catalyst can be affected by simple proton sources, such as water or methanol, due to their mild Lewis basic character (Scheme 2.23).



Challenges

Workaround solutions

- background reactivity
- control of *E/Z* geometry
- Lewis basic functionalities
- very low temperatures e.g. $-78\text{ }^\circ\text{C}$
- cyclic substrates
- bulky proton sources
- slow addition of reagents
- bulky proton sources



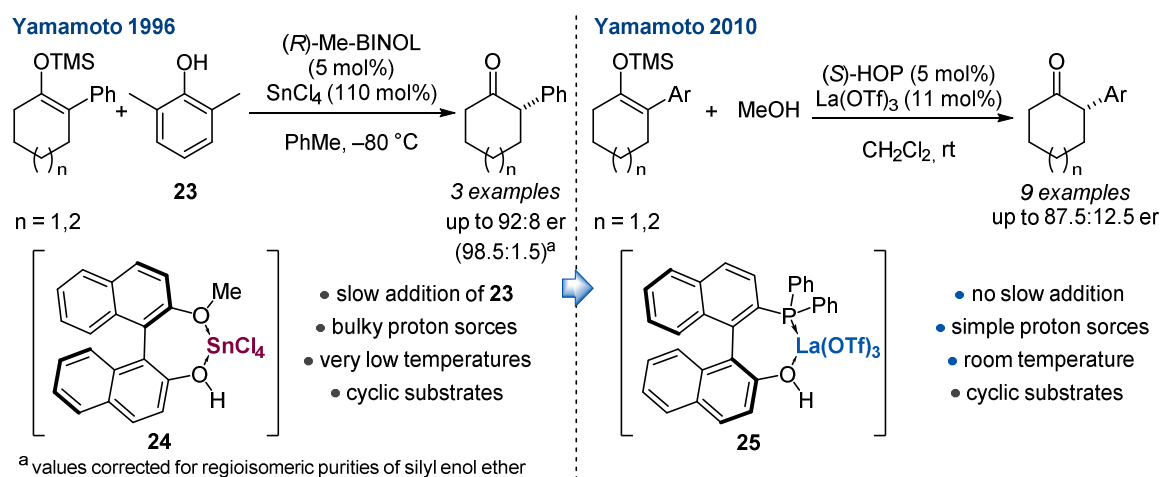
Scheme 2.23 Catalytic asymmetric protonation strategies and challenges.

The previously mentioned report from Pracejus (Scheme 2.2) represents an early example of a catalytic asymmetric protonation.^[23] Indeed, upon the nucleophilic addition of methanol to the ketene, the transient enolate is protonated to afford the corresponding enantioenriched ester. Despite this successful pioneering work, it was not until the late 1980s that significant developments for asymmetric protonation of metal enolates with the aid of stoichiometric chiral Brønsted acids began to emerge.^[114] Catalytic approaches started appearing in the early 1990s employing chiral catalysts for the protonation of lithium enolates by slow addition of an achiral PS.^[115] Since then, an increased interest in asymmetric protonation led to successful reports starting from silyl enolates,^[56d, 116] β -keto acids,^[117] ketenes,^[118] α,β -unsaturated carbonyl compounds,^[119] and many others.^[120] Furthermore, enzymes have also been employed in biocatalytic processes, including esterases^[121] and decarboxylases,^[122] for the protonation of enol esters or the decarboxylative protonation of malonic acid derivatives.

2.4.2 Catalytic Asymmetric Protonation of Enolate Derivatives

The first catalytic enantioselective protonation of silyl enolates was developed by Yamamoto *et al.*, exploiting Lewis acid-assisted Brønsted acid (LBA) catalysis.^[123] This concept is based on the association of an enantiopure BINOL-based Brønsted acid ((*R*)-Me-BINOL) and an achiral Lewis acid (e.g. SnCl₄), leading to an increased acidity of the BINOL proton.^[13a, 124] The transformation afforded the products in very high yields and enantioselectivities, however, a bulky PS (e.g. 2,6-dimethylphenol **23**, DMP) and very low temperatures (e.g. –80 °C) were required. Thus, the major drawbacks of LBA catalysis are the poor stability of the catalyst towards moisture and mild Lewis bases (e.g. simple alcohols), requiring strictly anhydrous conditions in order to perform efficiently.^[113a] The same author reported an improved LBA catalyst (**25**), which was formed by complexation of La(OTf)₃ with an (*S*)-HOP (2-hydroxy-2'-diphenylphosphino-1,1'-binaphthyl) scaffold, allowing methanol to be used as the stoichiometric achiral PS at room temperature, without the need of slow addition of

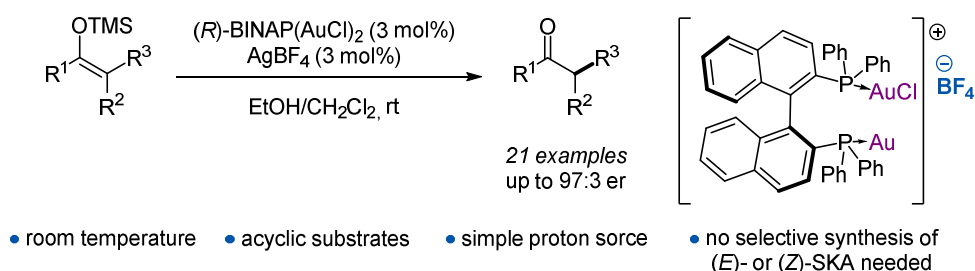
either reagent. Only cyclic substrates were tolerated attaining moderate enantioselectivities, thus, not exceeding the first generation of LBAs^[125] (Scheme 2.24).



Scheme 2.24 Development of LBA catalysis to Lewis base tolerant systems.

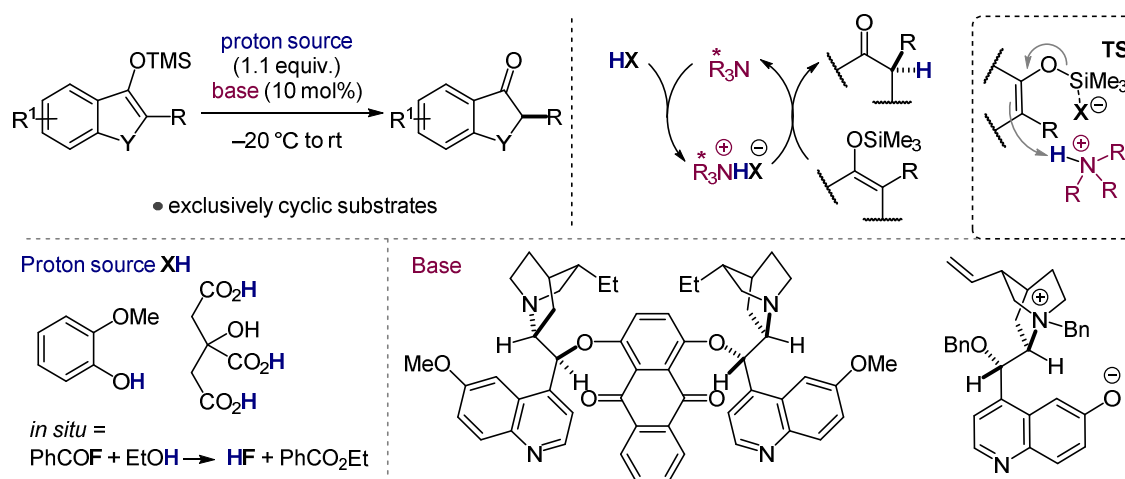
A major advance in the field of catalytic enantioselective protonation of silyl enol ethers and SKAs was achieved by Toste and co-workers, who further exploited the LBA catalysis concept.^[113b] The cationic (*R*)-BINAP (2,2'-bis-(diphenylphosphino)-1,1'-binaphthyl) gold(I) complex, combined with equimolar amount of AgBF₄, tolerates an excess of EtOH at room temperature, enabling very high enantioselectivities for a wide selection of cyclic and acyclic silyl enolates. The highlight of this system is the ability of the LBA catalyst to discriminate between the *Z*- and *E*-diastereomers approaching the silyl enol ether from the same enantiotopic face. This leads to a stereoconvergent asymmetric protonation, erasing the challenge of selective *Z* or *E* synthesis of the starting material (Scheme 2.25).

Background



Scheme 2.25 Gold(I) LBA catalysis for asymmetric protonation of acyclic silyl enolates.

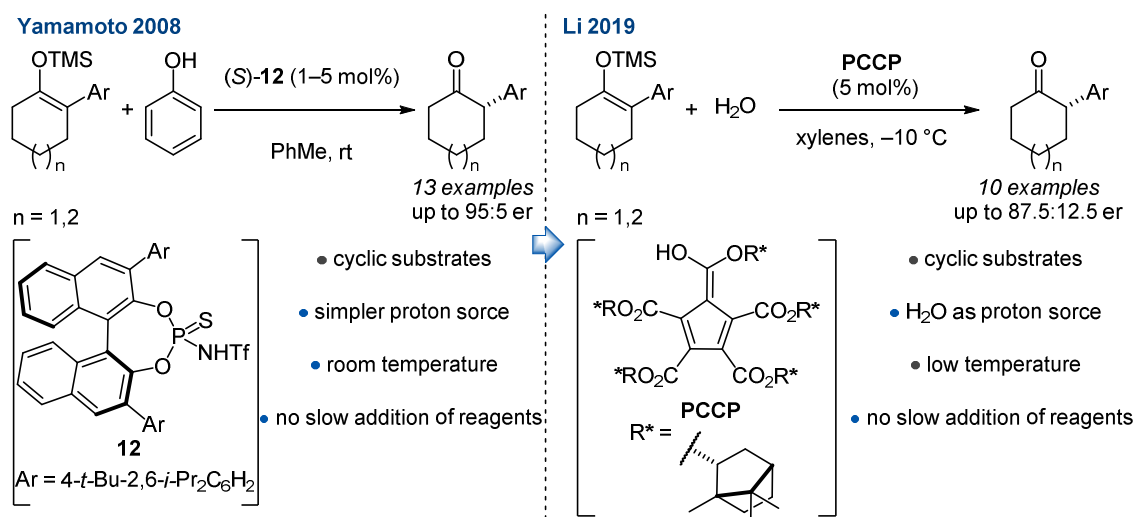
Many organometallic catalysts have been reported, providing excellent levels of enantioselectivity with wide substrate scopes. Metal-free solutions began to appear in 2007, with the first report from Levacher, in the presence of a chiral tertiary amine and a stoichiometric PS (**XH**).^[116a] In those systems, the Lewis basic anion (X^-) activates the silyl enol ether towards enantioselective protonation by the chiral ammonium salt (see **TS**, Scheme 2.26). Initially, only a limited substrate scope was reported, however, further developments included different PSs (bulky, highly acidic or generated *in situ*) and a variety of chiral bases (Scheme 2.26).^[126]



Scheme 2.26 Chiral ammonium salts for enantioselective protonation of silyl enol ethers.

The first organocatalytic Brønsted acid-catalyzed example was reported by Cheon and Yamamoto in 2008, using BINOL-based *N*-triflyl thiophosphoramidate **12** in the

presence of phenol as the achiral PS (Scheme 2.27).^[56d] This report represents an important achievement in the field of organocatalytic asymmetric protonations, even though only cyclic substrates with aromatic substituents were successfully employed. Recently, Li and co-workers aimed to use the simplest PS available, H₂O, in combination with pentacarboxycyclopentadiene (PCCP) as the chiral acid. Only cyclic substrates have been reported and only moderate enantioselectivities were achieved, thus showing the challenges associated with using water as the PS (Scheme 2.27).^[127]

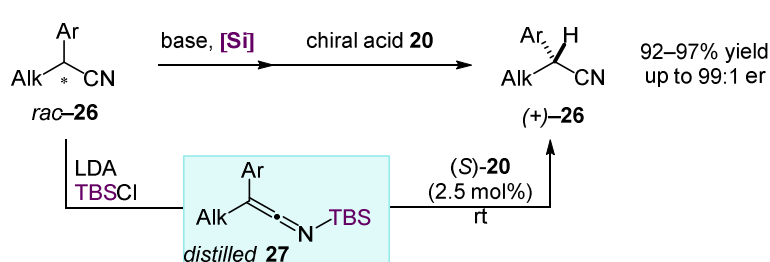


Scheme 2.27 Organocatalytic protonation of cyclic silyl enol ether with PhOH and H₂O.

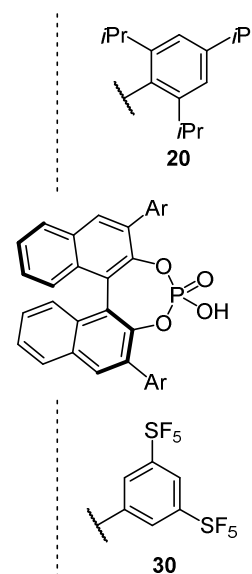
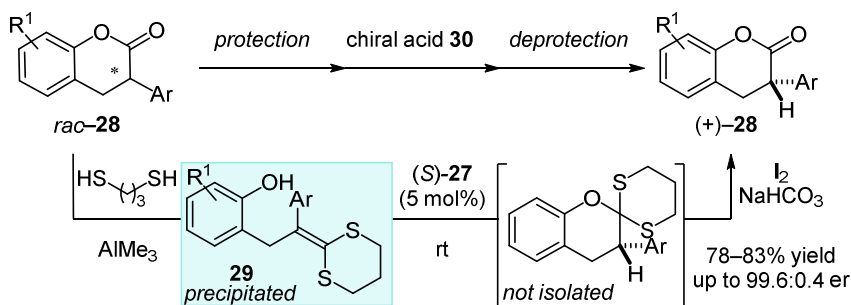
Additional examples of enantioselective organocatalytic protonations, enabled by chiral Brønsted acids, have been reported in the context of deracemization sequences of α -alkyl- α -arylnitriles (**26**) and α -aryl-substituted hydrocoumarins (**28**). In the first case, the protonation of silyl ketene imines occurred in the presence of MeOH and (*R*)-TRIP (**20**) as the catalyst,^[128] while in the second case, the enantioselective protonation of the intermediate ketene dithioacetals occurred with phosphoric acid **30** (Scheme 2.28).^[129] Both examples highlight the importance of this transformation, particularly when included in a deracemization sequence. Indeed, the racemic starting material was almost exclusively converted to a single enantiomer

without tedious purification of the intermediates. Stoichiometric reagents enabled the initial planarization of the stereogenic center to the protected ketene intermediates (**27** and **29**). A catalytic amount of chiral acid was sufficient to protonate the intermediate from only one enantiotopic face, reforming the sp^3 -configured carbon in high enantioselectivity.

List 2013



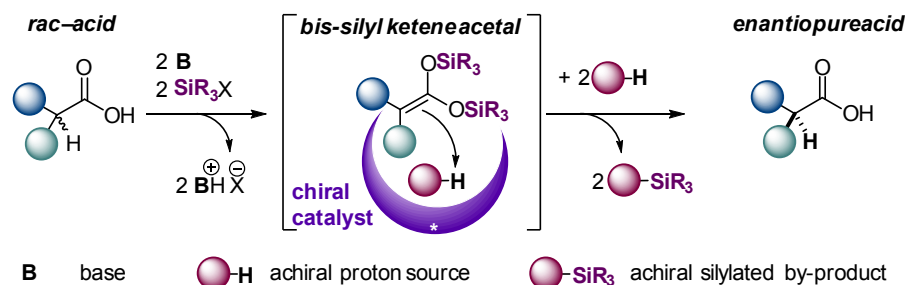
List 2012



Scheme 2.28 Examples of deracemization sequences *via* asymmetric protonation of the corresponding ketene intermediate.

2.4.3 Catalytic Asymmetric Protonation of *bis*-Silyl Ketene Acetals

The deracemization strategy of carboxylic acids *via* an intermediate (or catalytically formed) enolate has already been mentioned in the context of direct α -functionalizations (Chapter 1, Scheme 1.3). This strategy involves the transformation of racemic carboxylic acids into their corresponding enediolates. Subsequent asymmetric protonation can then afford the starting carboxylic acid as a single enantiomer. A similar sequence can be envisioned by stabilizing the intermediate enediolate with two silicon groups (Scheme 2.29).

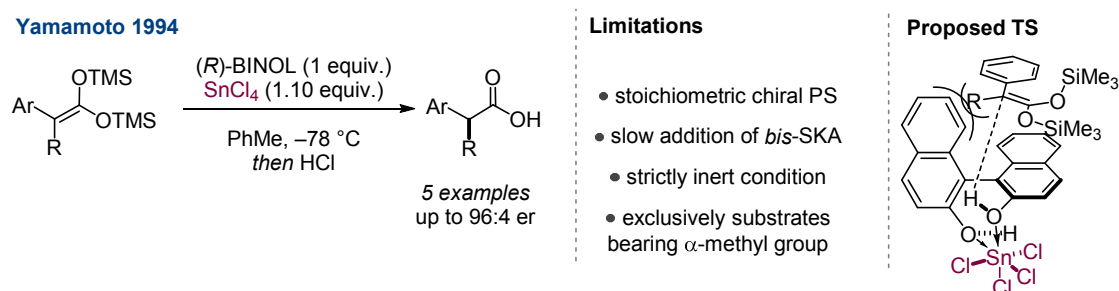


Scheme 2.29 Deracemization of carboxylic acids *via* a sequence of *bis*-SKA generation and subsequent enantioselective protonation.

Despite the similarity compared to SKAs, different considerations must be taken into account while envisioning catalytic enantioselective protonations of *bis*-SKAs. The higher nucleophilicity generally associated with *bis*-SKAs leads to faster background reactions with the achiral PS. Hence, the catalyst, in order to avoid high catalyst loadings, should be acidic enough to protonate the substrate faster than the stoichiometric reagent. Furthermore, the catalyst must deliver the proton with high selectivity, discriminating the two enantiotopic faces of the *bis*-SKA.

2.4.3.1 Stoichiometric Reagents

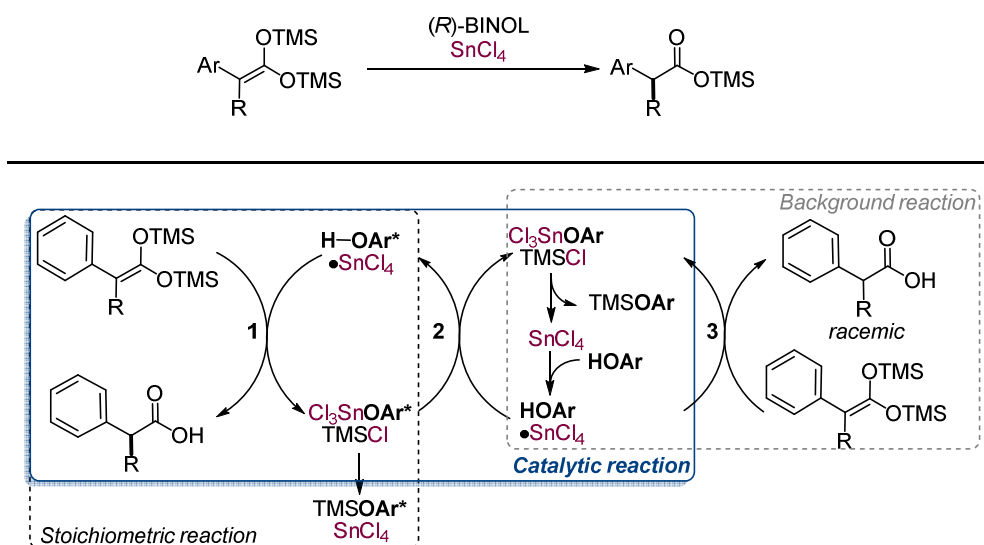
Significant effort has been dedicated to address the challenges encountered with the enantioselective protonation of *bis*-SKAs. The first example was reported in 1994 by Yamamoto *et al.* using stoichiometric amounts of a chiral complex generated *in situ* by reacting equimolar amounts of enantiopure BINOL and SnCl₄. Noteworthy, the acidity of the Brønsted acid was enhanced by the combination with a Lewis acid, thus named Lewis acid-assisted Brønsted acid (LBA). Although high levels of enantioselectivity were observed, the selection of substrates was limited only to β -methyl- β -aryl substituted *bis*-SKAs, as any alkyl group (R) other than methyl group resulted in low or moderate enantioselectivities. The authors derived a stereochemical model for the proposed transition state (Scheme 2.30), explaining the limitations in the substrate scope.^[112] Different ligands have been designed for the same transformation,^[130] however the limitations on the substrates scope tolerance remained.



Scheme 2.30 Enantioselective protonation with a stoichiometric chiral reagent.

2.4.3.2 Catalytic Asymmetric Protonation

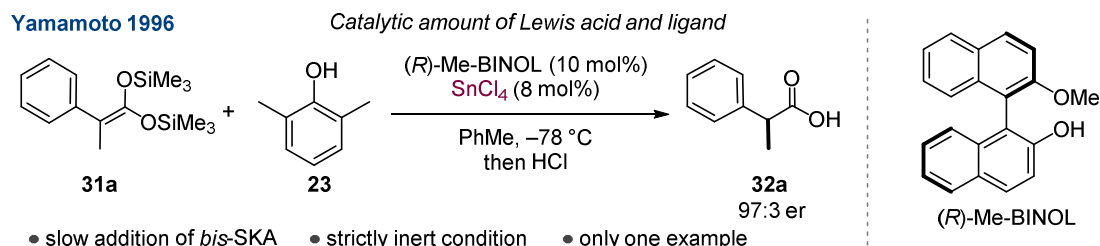
A proposed mechanism for the reaction described in the previous section is depicted in Scheme 2.31 (route 1) in which the chiral PS (**HOAr***), upon enantioselective protonation, is ultimately silylated ($\text{Me}_3\text{SiOAr}^*$) and the Lewis acid (e.g. SnCl_4) is regenerated. A catalytic version requires that **HOAr*** is regenerated from an achiral PS (**HOAr**). In this case, the SnCl_4 needs to be preferentially coordinated to **HOAr*** and the reactivity of **HOAr*** $\cdot\text{SnCl}_4$ has to be greater than of **HOAr** $\cdot\text{SnCl}_4$ in order to avoid the background reaction (Scheme 2.31). In fact, **HOAr** can react with two nucleophiles, the anion OAr^* and the *bis*-SKA, leading to the completion of the catalytic cycle (route 2) or to the undesired background reaction (route 3). A common strategy to minimize route 3 consists of keeping the ratio between the chiral and the achiral PS (**HOAr***/**HOAr**) as high as possible. This can be realized by slow addition of **HOAr** or by using biphasic systems (e.g. liquid/liquid or solid-liquid).^[131] Another strategy consists of designing an achiral PS which is less associated to the substrate, for example by reducing the accessibility of the transferred proton, as for example in the more strically hindered 2,6-dimethylphenol (DMP).



Scheme 2.31 Stoichiometric vs catalytic enantioselective protonation of *bis*-SKAs.

In summary, careful control of the reaction conditions is needed to avoid background reactivity, including a strictly inert atmosphere, very low temperatures and slow addition of the PS. Furthermore, tailored design of the PS is particularly crucial to avoid the undesired pathways. DMP appears to be particularly suitable to suppress background reactivity. In fact, the steric bulk of the methyl groups *ortho* to the phenol functionality disfavored both the formation of achiral Lewis acids and the direct protonation of silyl enol ether.

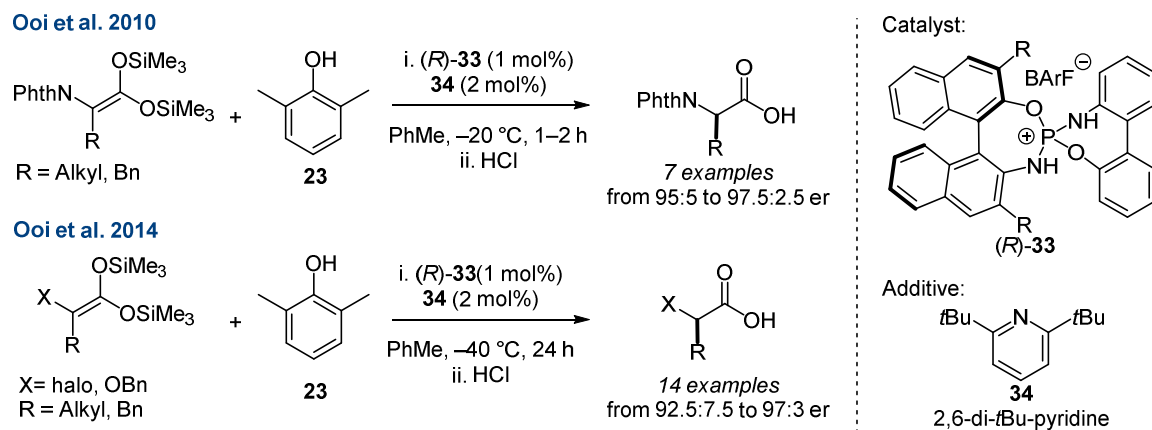
Yamamoto and co-workers showed that using (*R*)-Me-BINOL as the ligand, the above-mentioned transformation can be performed in the presence of a catalytic amount of Lewis acid (SnCl_4), maintaining the same high enantioselectivity (Scheme 2.32).^[113a] Unfortunately, the limitations of the system remained unsolved, such as slow addition of the *bis*-SKA, and the requirement for a sterically hindered PS (**23**) as well as strictly anhydrous conditions. Furthermore, only substrate **31a** was reported as single example.



Scheme 2.32 First catalytic asymmetric protonation of *bis*-SKA via LBA catalysis.

Ooi *et al.* reported two remarkable examples of catalytic enantioselective protonation of *bis*-SKA derivatives. The axially chiral Brønsted acid catalyst, *P*-spiro diaminodioxaphosphonium barfate **33**, showed high levels of enantioinduction for the protonation of α -amino acid-derived^[13b] and for α -halo and α -alkoxy acid-derived *bis*-SKAs.^[13c] However, it still required a bulky PS in order to inhibit both the background reaction with the substrate and the decomplexation of the catalytic system, leading to the formation of HBArF , which is itself a highly reactive achiral PS. This was prevented by addition of a scavenger (**34**) neutralizing this side reaction (Scheme 2.33). In this system, the enantiofacial discrimination depended predominantly on the

electronic bias of the substrate and was independent on the steric features of the substituents.



Scheme 2.33 Catalytic asymmetric protonation of *bis*-SKA via organic LBA catalysis; BARF = Tetrakis[3,5-*bis*(trifluoromethyl)phenyl]borate.

To date, a catalytic asymmetric protonation of *bis*-SKAs from electronically unbiased carboxylic acids in the presence of water as the simplest PS has not been reported.

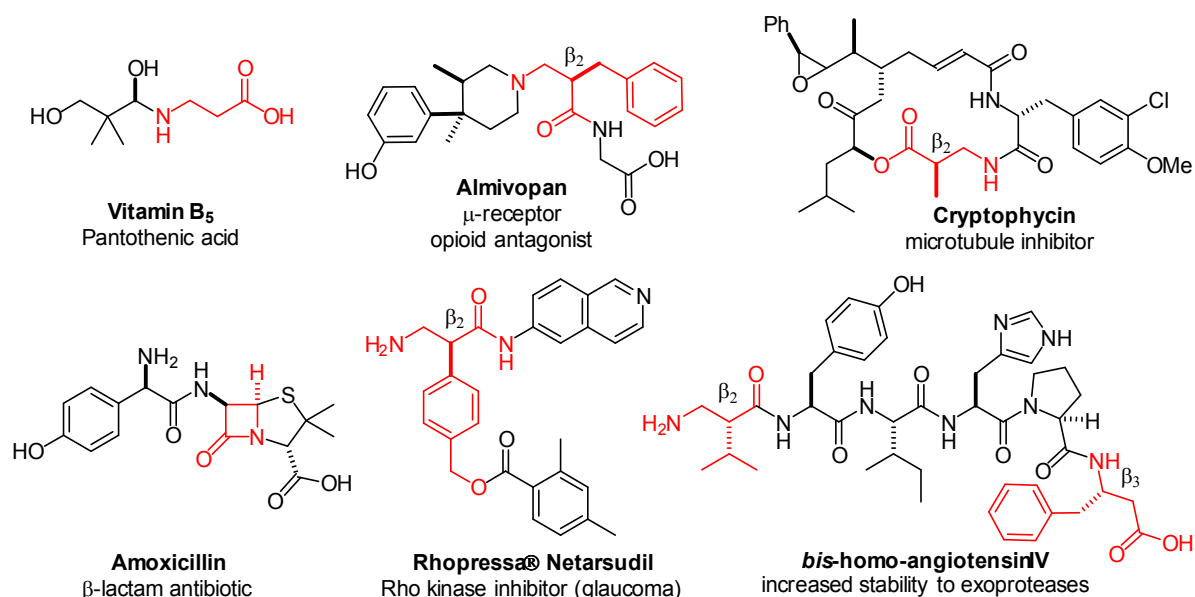
Background

2.5 Enantioselective α -Aminomethylation

2.5.1 Introduction

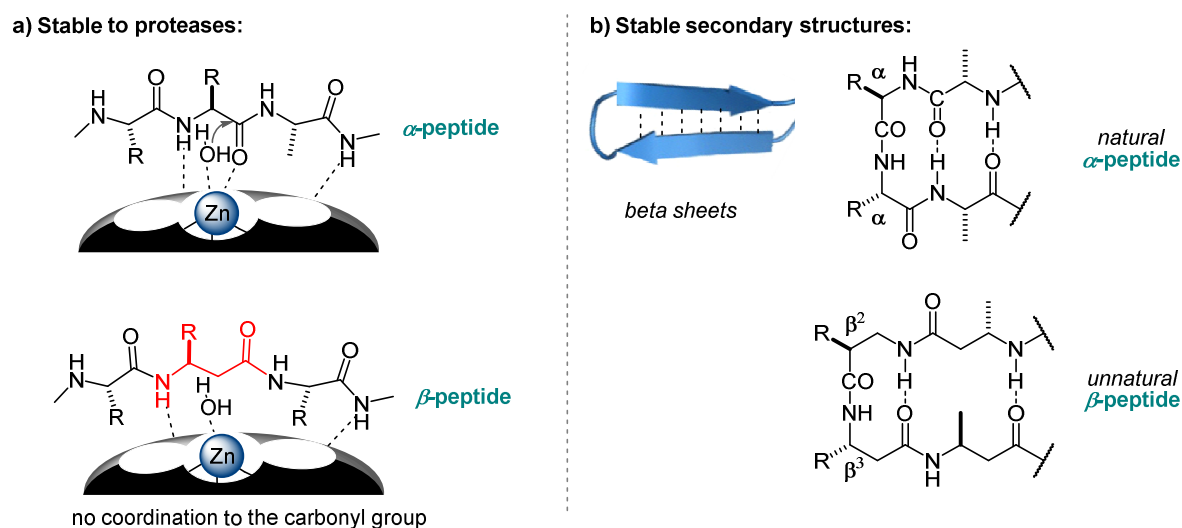
Over the last decades, catalytic and enantioselective C–C bond forming reactions at the α -position of carbonyl compounds have been an ambitious target, approached by many scientific groups. However, the direct, enantioselective α -functionalization of carboxylic acids still remains an unsolved challenge. The following chapter will give a concise overview of asymmetric α -functionalization reactions of carbonyl compounds in the context of direct aminomethylation reactions.

The high abundance of β -amino carbonyl compounds in biological and natural products (Scheme 2.34) drove the interest toward the investigation of enantioselective transformations to efficiently access this motif.^[132] β -Amino acids are naturally present in important co-factors, such as pantothenic acid (vitamin B₅), and β -lactam antibiotics. The key feature of this scaffold relies on the close structural similarity to the corresponding α -amino acid, maintaining their main functionality but increasing their metabolic stability by several orders of magnitude.^[133]



Scheme 2.34 Examples of biologically active compounds containing β -amino acid-derived functionalities.

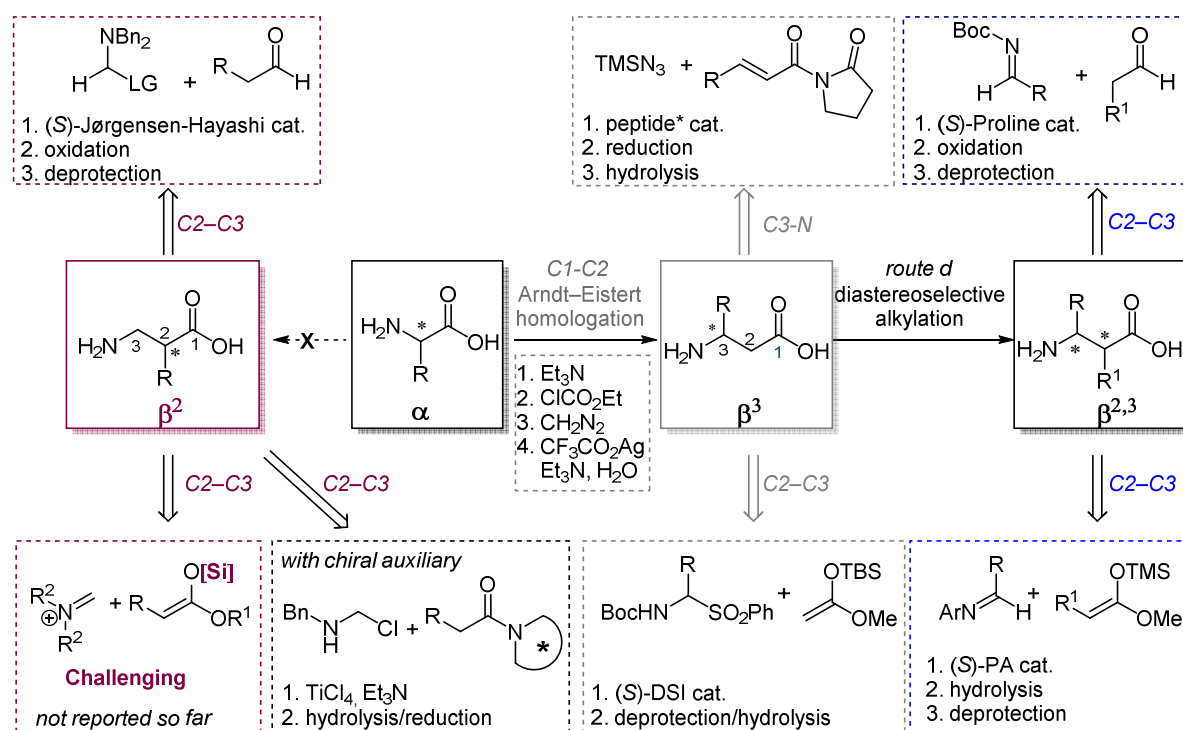
Peptide-containing molecules are highly unstable in the presence of proteases, which are ubiquitous enzymes designated for the digestion of proteins by hydrolyzing the peptide bond. The binding selectivity of the β -amino acid substrate to the active site of the proteases remains, but the catalytic activity is inhibited, rendering those substrates as metabolically stable (Scheme 2.35, a).^[134] The success of the β -amino acid functionality is also attributable to the ability of β -peptides (short sequence β -amino acids) to self-assemble into secondary structures such as α -helices or β -sheets, in close relationship to the analogous natural α -peptides (Scheme 2.35, b).^[135]



Scheme 2.35 a) Schematic representation of the binding of an α -peptide and a β -amino acid-containing peptide to the active site of a protease; b) structural similarity of a β -turn in natural occurring α -peptides and unnatural β -peptides.

The introduction of an aminomethyl group into small organic molecules has recently attracted a great deal of attention, particularly toward the synthesis of β -amino acids (Scheme 2.36). β^3 -Amino acids can be obtained by enantiospecific homologation of the natural α -amino acids, and the catalytic asymmetric synthesis of β^3 -amino acids, although not discussed in this section, has delivered remarkable progress in the last years.^[39, 83, 136] Few diastereoselective syntheses of $\beta^{2,3}$ -amino

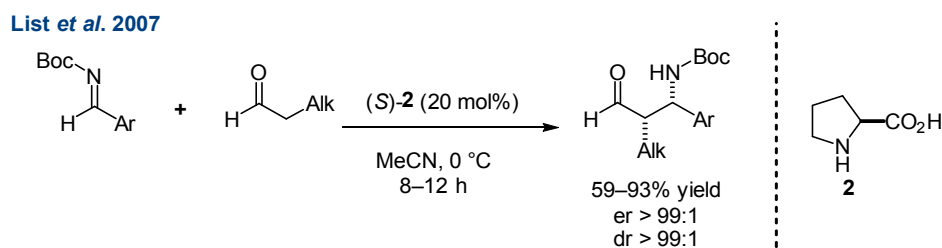
acid derivatives have recently been reported,^[52, 137] however, only in the presence of directing protecting groups or activated substrates. On the other side, β^2 -amino acids cannot be obtained through enantioselective transformations of the corresponding α -amino acids; currently, the use of chiral auxiliaries for a diastereoselective α -aminomethylation of the carboxylic acid derivative is a common and reliable synthetic alternative. The catalytic enantioselective synthesis of β^2 -amino acids *via* aminomethylation remains a challenge,^[138] particularly in protecting group-free approaches and using unbiased substrates.



Scheme 2.36 Retrosynthetic analysis of β -amino acids from the parent α -amino acid or *via* aminomethylation reaction.

2.5.2 Asymmetric Synthesis of $\beta^{2,3}$ -Amino Acids

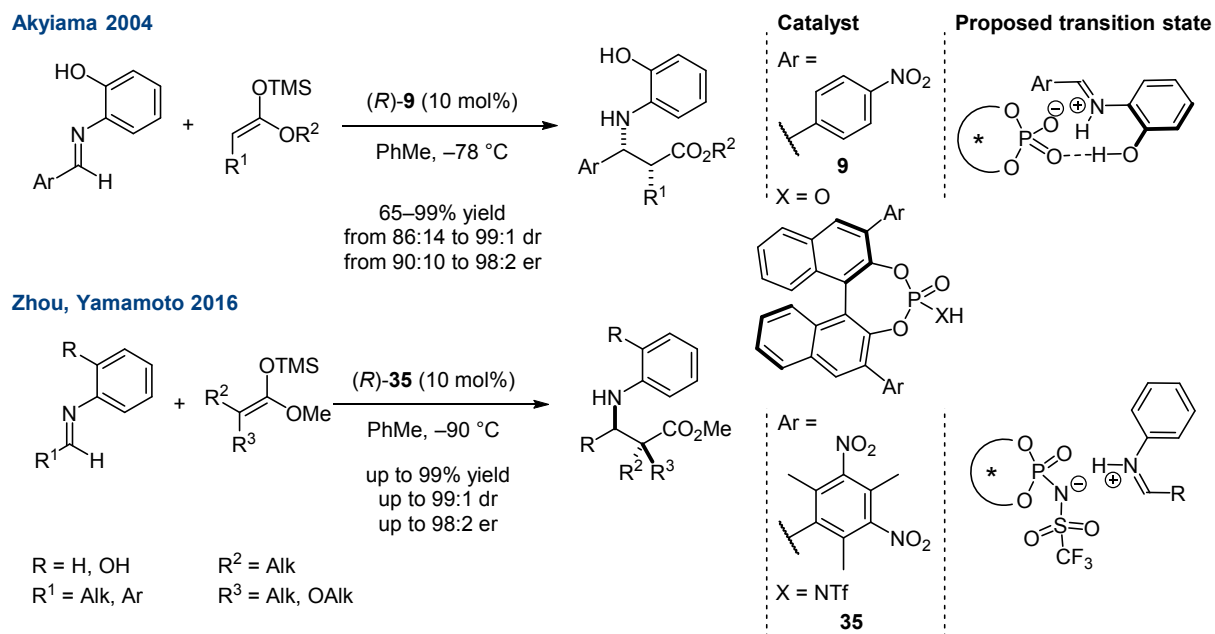
Organocatalytic asymmetric syntheses of $\beta^{2,3}$ -amino acids have been reported both in the field of Lewis base and Brønsted acid catalysis. Inspired by the pioneering discovery of a proline-catalyzed direct Mannich reaction by List in 2000,^[139] the combination of an enolizable aldehyde and an aromatic imine, bearing aromatic protecting groups, was reported by Barbas *et al.* in 2002 to give *syn* $\beta^{2,3}$ -amino aldehydes^[140] and, in 2006, to give *anti*- $\beta^{2,3}$ -amino aldehydes.^[141] In 2007, List *et al.* reported the Mannich reaction of simple alkyl aldehydes with *N*-Boc-protected aryl imines catalyzed by (*S*)-proline.^[137] The corresponding *syn*- $\beta^{2,3}$ -amino aldehydes were obtained in high yields as well as enantio- and diastereoselectivities. Finally, an additional oxidation step provided access to the desired enantioenriched β -amino acids (Scheme 2.37).



Scheme 2.37 Enantioselective synthesis of $\beta^{2,3}$ -amino aldehydes with (*S*)-Proline as catalyst.

An asymmetric synthesis of $\beta^{2,3}$ -amino acids in the field of Brønsted acid catalysis has been already mentioned in chapter 2.2.4 (Scheme 2.8): Akiyama *et al.* reported a Mannich-type reaction of SKAs with *N*-(2-hydroxyphenyl)-arylimines, affording the corresponding *syn*- β -amino esters in high yields, diastereo- and enantioselectivities.^[51] The 2-hydroxyphenyl substituent is crucial, as the *H*-bonding to the catalyst is a pre-requisite for the high selectivity of the reaction. However, the protecting group limits the utility of the transformation. Recently, Zhou, Yamamoto *et al.* reported an expansion of the substrate scope by applying the more acidic phosphoramidate **35** as the catalyst.^[142] The wider scope includes disubstituted SKAs and aliphatic imines, having either the same protecting group (2-hydroxyphenyl) or

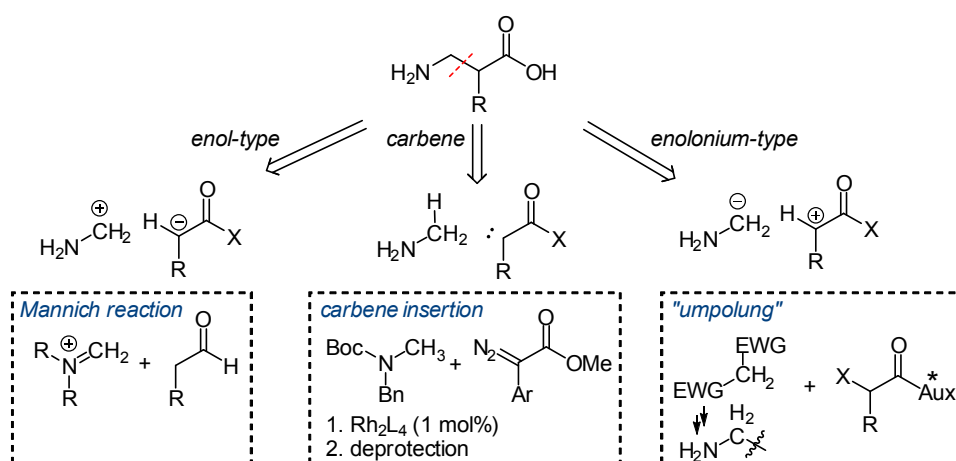
simply a phenyl group. However, additional steps are required to obtain the desired β -amino acids (Scheme 2.38).



Scheme 2.38 Asymmetric synthesis of $\beta^{2,3}$ -amino esters *via* Brønsted acid catalysis.

2.5.3 Asymmetric Synthesis of β^2 -Amino Acids

Several synthetically equivalent transformations can be envisioned for the synthesis of β^2 -amino acids, in which the $\text{NH}_2\text{-CH}_2$ synthon can act as electrophile,^[138] nucleophile^[143] or carbenophile.^[144] Among those, Mannich-type reactions are the most explored ones (Scheme 2.39).

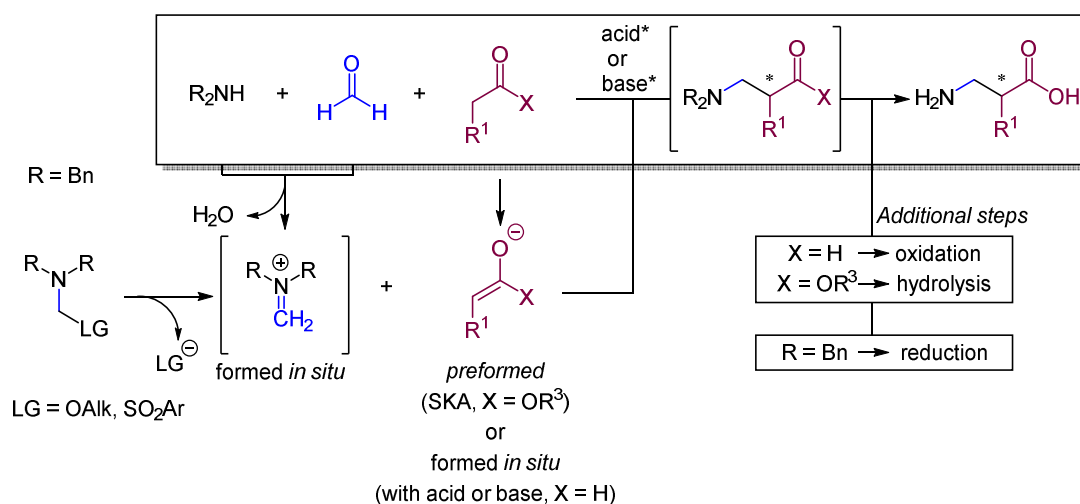


Scheme 2.39 Retrosynthetic analysis for the highlighted disconnection of β^2 -amino acids.

More than one century ago,^[145] Mannich found that β -amino acids could be formed by combining enolizable carboxylic acid derivatives, formaldehyde and ammonia.^[146] Despite the availability of these starting materials, asymmetric variants of this transformation have been developed only with more reactive substrates, such as enolizable aliphatic aldehydes,^[144] or preformed enolates,^[83, 147] such as SKAs. In the case of β^2 -amino acid derivatives, the three-component one-pot procedure would require formaldehyde, ammonia and an enolizable carboxylic acid derivative. The first two reagents are difficult to handle themselves, as they irreversibly form urotropine, the tetramer of the highly reactive unsubstituted iminium ion.

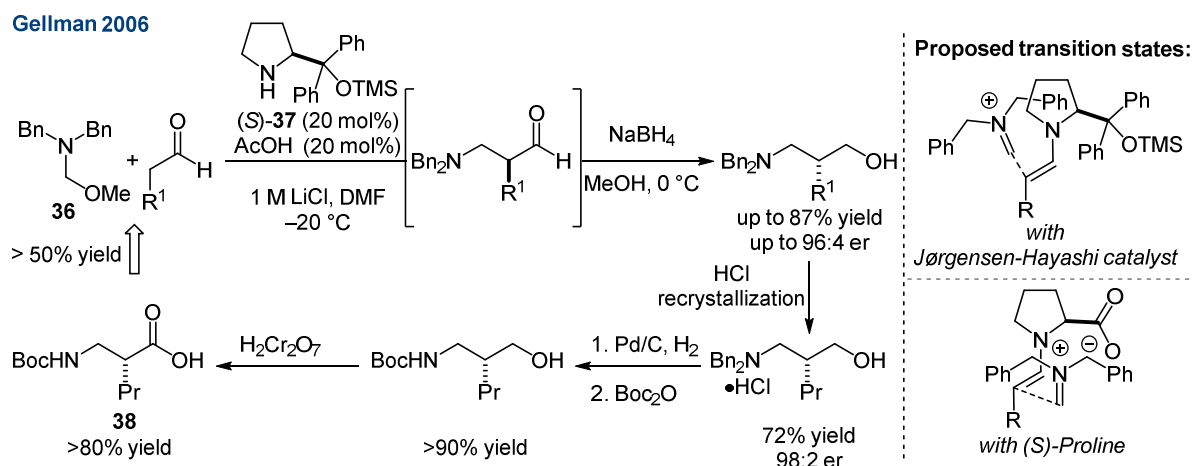
Therefore, this iminium ion can only be applied in protected form: A common precursor is *bis*-benzyl protected tertiary amine having a leaving group in the α -position.^[148] The protected methylene iminium ion is then liberated *in situ* under the

reaction conditions (Scheme 2.40). Protecting groups (e.g. benzyl groups) and activated substrates (aldehydes or SKAs) facilitate the design of asymmetric transformations; however, they imply additional steps (deprotection and functional group manipulation) before achieving the desired target β^2 -amino acid.



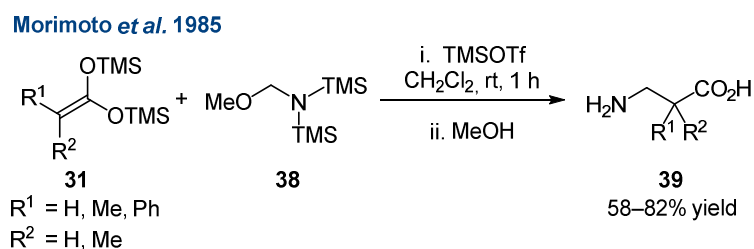
Scheme 2.40 Mannich reaction for the synthesis of β^2 -amino acids.

In 2006, Gellman *et al.* reported a remarkable example of a catalytic enantioselective transformation toward β^2 -amino acid precursors.^[138] In this case, the authors combined aliphatic aldehydes with *N,N*-dibenzyl-1-methoxymethanamine (**36**) as the iminium ion precursor and the Jørgensen–Hayashi catalyst (**37**). The hindered silyl ether prevents any hydrogen-bonding or ion-pairing interactions and, thus, directs the nucleophilic attack from the opposite face compared to (*S*)-Proline, however, the role of the additives remained unclear. The intermediate β^2 -amino aldehydes were immediately reduced to avoid epimerization. From the obtained enantioenriched β -amino alcohols, a recrystallization and three additional steps were required to obtain *N*-Boc- β^2 -homonorvaline (**38**) (Scheme 2.41).



Scheme 2.41 Enantioselective synthesis of β^2 -amino acids by Gellman.

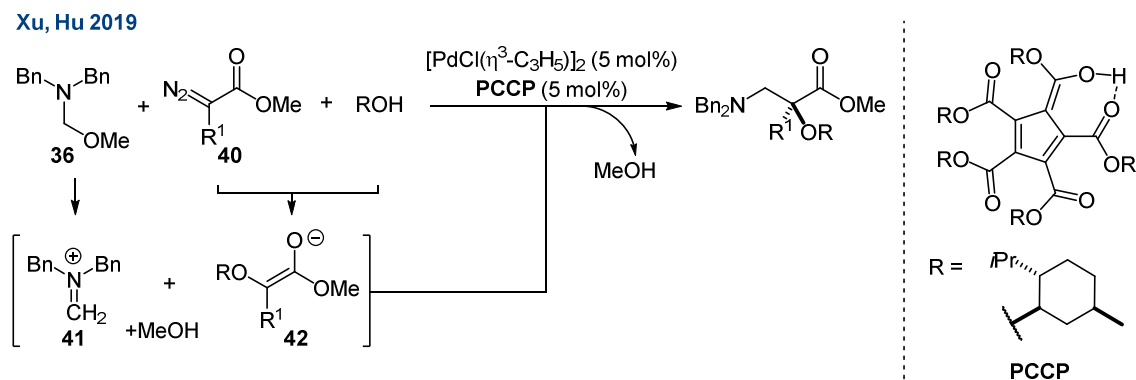
Enantioselective transformations directly affording the unprotected amino acids, hence containing the unprotected amine and acid functionalities, have not been reported to date. However, in 1985 Morimoto *et al.* demonstrated the principal feasibility of this transformation in a non-asymmetric fashion.^[100] Pre-activating a carboxylic acid as the corresponding *bis*-SKA in combination with the iminium ion precursor **38**, and a catalytic amount of Lewis acid yielded the targeted unprotected β^2 -amino acids, upon exposure to protic conditions (Scheme 2.42).



Scheme 2.42 Direct non-enantioselective synthesis of β^2 -amino acids.

Noteworthy, an enantioselective aminomethylation reaction exploiting a similar strategy was recently reported by Xu, Hu *et al.*^[127] The transformation was enabled by asymmetric counteranion-directed catalysis in the presence of a $[\text{PdCl}(\eta^3\text{-C}_3\text{H}_5)]_2$ catalyst and pentacarboxycyclopentadiene (PCCP) acid as the chiral counteranion. The metal-based catalyst promotes the *in situ* formation of reactive enolate **42** from

diazo compound **40** and an alcohol. PCCP activates the aminomethylating reagent **36**, forming the iminium ion **41**, and provides the chiral environment for the asymmetric Mannich-type reaction (Scheme 2.43). Despite the relevance of this transformation, the authors did not report a synthesis of β^2 -amino acids from the obtained $\beta^{2,2}$ -amino acids.



Scheme 2.43 Asymmetric Counter-Anion-Directed Aminomethylation to α -alkoxy- β -amino esters.

Objectives

3 Objectives

A direct enantioselective α -functionalization of carboxylic acids still remains elusive, both in metal-, bio- and organocatalysis. Only a few systems using *in situ* generated enediolates taking advantage of chiral auxiliaries have been reported.^[10a, 10d, 149] A highly attractive alternative for a versatile catalytic approach to the α -functionalization of carboxylic acids, circumventing the use of moisture-labile and highly reactive enediolates, could rely on the formation of *bis*-SKA intermediates followed by functionalization with an electrophilic partner (Figure 3.1).

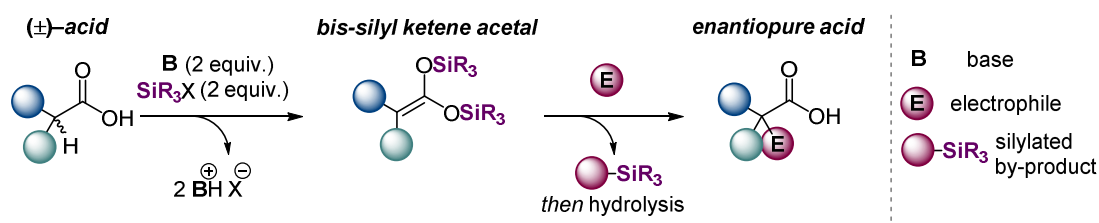


Figure 3.1 α -Functionalization of carboxylic acids *via* activation to the *bis*-SKA intermediate.

Despite the potential of this transformation, exclusively the catalytic asymmetric protonation of *bis*-SKAs has been reported so far, affording enantioenriched α -branched carboxylic acids by employing (Lewis acid-assisted) Brønsted acid catalysts. In order to achieve high enantioselectivities, the systems were limited to bulky proton sources^[113a] and electronically-biased *bis*-SKAs.^[13b, 13c] Furthermore, cryogenic conditions, inert atmosphere and slow addition of the reagents were needed, rendering these methods less practical. In this context we speculated if we could find a general solution for electronically-unbiased substrates, using a simple proton source, such as water (Figure 3.2). Furthermore, we envisioned the application of this method in a one-pot deracemization sequence of α -branched carboxylic acids-containing drugs, such as Ibuprofen[®].

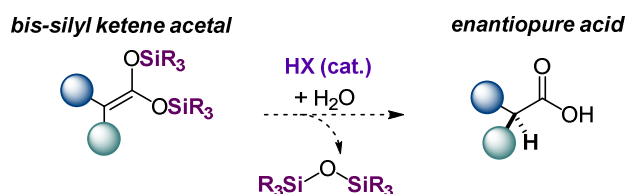


Figure 3.2 Envisioned enantioselective protonation of electronically-unbiased *bis*-SKAs using water as the proton source.

A catalytic enantioselective C–C bond formation for the α -functionalization of *bis*-SKAs has not been reported so far. Several reports have focused on the utilization of SKAs for the functionalization of various electrophilic species; in those systems, an enantiopure catalyst enables the nucleophilic attack selectively onto one of the enantiotopic faces of the electrophile, forming the stereogenic center in the β -position of the acid derivative.^[12b, 51] In this thesis, we aimed to reverse the roles: The employed catalyst should discriminate the enantiotopic faces of the nucleophile and install selectively the stereogenic center in the α -position of the carboxylic acid. With this aim in mind, we selected the α -aminomethylation of *bis*-SKAs as the targeted reaction, as this would lead to synthetically-valuable unprotected β^2 -amino acids, since those valuable motifs are not accessible *via* straightforward catalytic asymmetric transformations yet. This reaction was reported by Morimoto *et al.* under Lewis acidic conditions, using TMSOTf as the catalyst.^[100] We envisioned that we could exploit the ACDC concept and, after the *in situ* formation of the iminium ion, control the enantiotopic discrimination on the *bis*-SKA (Figure 3.3).

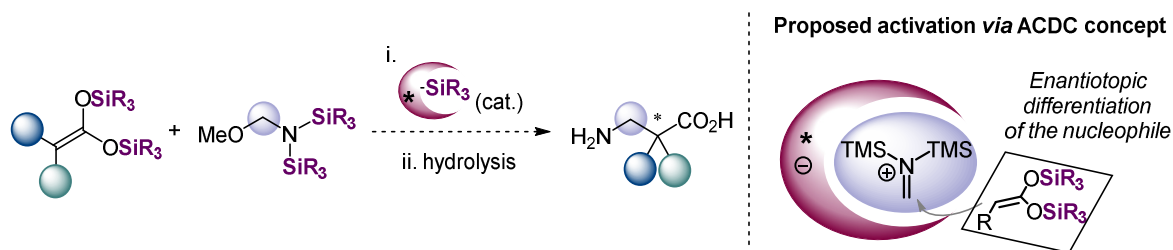


Figure 3.3 Proposed enantioselective aminomethylation of *bis*-SKAs *via* ACDC.

Objectives

In summary, the goal of this thesis is to explore the use of *bis*-SKAs as potent starting materials for the catalytic enantioselective synthesis of α -functionalized carboxylic acids under Brønsted or Lewis acidic conditions by developing conditions for an α -protonation and α -aminomethylation.

Objectives

4 Results and discussion

4.1 Asymmetric α -Protonation with H₂O and α -Deuteration with D₂O

The work presented in this section was performed in cooperation with Dr. Thomas James, Dr. Aurélie Blond and Dr. Hyejin Kim.

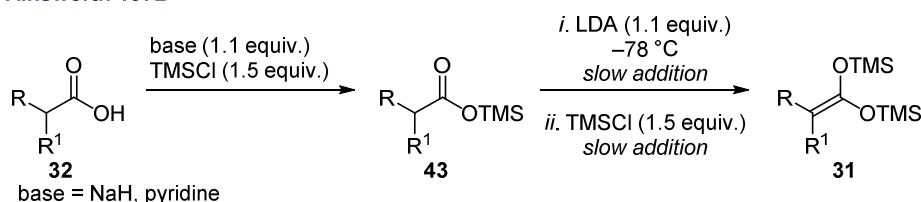
4.1.1.1 Synthesis and Handling of *bis*-SKAs

The purity of the employed *bis*-SKA, which has to be >99% as determined by ¹H NMR, is a crucial factor for the success of the targeted α -functionalizations. Traces of water are potent enough to protonate the starting material in the absence of an appropriate catalyst resulting in racemic product. Furthermore, after the protonation, one molecule of silanol (R₃SiOH) is released, which is itself a potent proton source reacting with the employed *bis*-SKA ultimately forming (R₃Si)₂O. Therefore, full conversion of the *bis*-SKA has to be ensured in order to determine the performance of a chiral catalyst, as partial conversion leads to background reactivity upon quench or exposure to the atmosphere. An additional crucial factor is the absence of bases, as they would react with the acidic catalyst forming very stable and unproductive salts. Moreover, low catalyst loadings (1 mol% or lower) are a crucial goal for the relevance of any catalytic transformation, thus the starting material has to be base-free (at least within the sensitivity of ¹H NMR). Due to these requirements, particular attention and effort had to be dedicated to synthesis, purification and storage of the *bis*-SKAs.

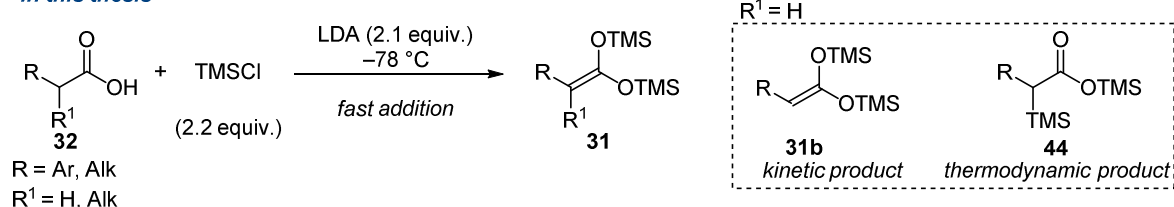
Commonly, *bis*-SKAs are synthesized by the original procedure reported by Ainsworth *et al.* in which the carboxylic acid is first reacted with base (usually NaH or pyridine) and TMSCl to the corresponding silyl ester. This is then subsequently treated with an additional base (e. g. LDA) and more TMSCl to give the desired products (Scheme 4.1).^[96] The speed of addition of the reagents is a crucial and tedious step influencing the yield of the reaction and consequently the efficiency of

the purification, particularly in the case of mono-substituted *bis*-SKAs ($R^2 = H$). However, during our studies we discovered a more facile and higher yielding single step procedure using an excess of LDA (2.1 equiv.) and TMSCl (2.2 equiv.). By premixing the carboxylic acid and the TMSCl at low temperatures, a faster addition of the base was the key to a cleaner reaction profile. This observation can be explained by the competition between kinetic and thermodynamic product: the *O,O*-*bis*-silylated ketene acetal (*bis*-SKA **31b**) is the kinetic product while the *C*-silylated trimethylsilyl ester **44** is the thermodynamic product and the main side reaction observed for mono-substituted *bis*-SKAs. The rapid “internal quench” of the *bis*-Li enolate by the constant high excess of TMSCl favored the kinetic product and thus resulted in a cleaner reaction profile and higher yield. A similar strategy was adopted by Corey *et al.* while developing *E*- or *Z*-selective synthesis of silyl enol ethers of SKAs.^[150] Interestingly, the migration of the TMS group from oxygen to carbon could be observed upon storage of *bis*-SKAs at ambient temperature. Noteworthy, additional precautions were required including the use of freshly distilled diisopropylamine, accurate butyl lithium titration, strict inert conditions and very low pressures for the purification *via* distillation.

Ainsworth 1972



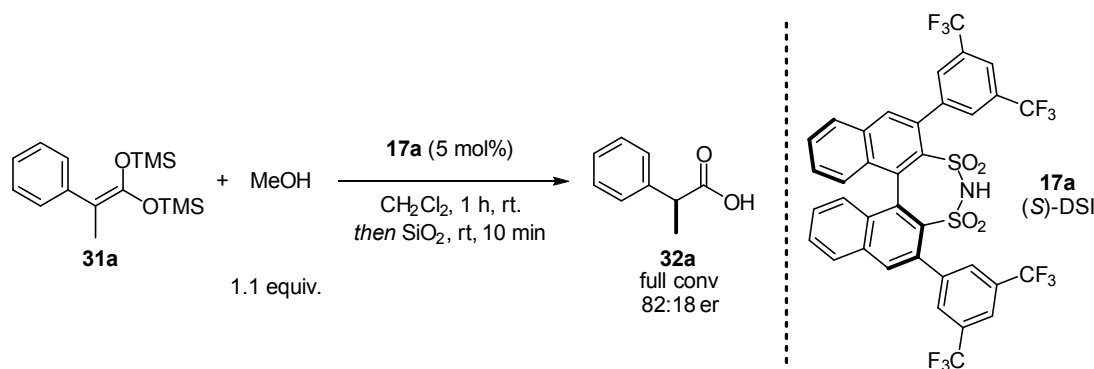
In this thesis



Scheme 4.1 Original and improved procedure for the preparation of *bis*-SKAs.

4.1.2 Reaction Design and Optimization Studies

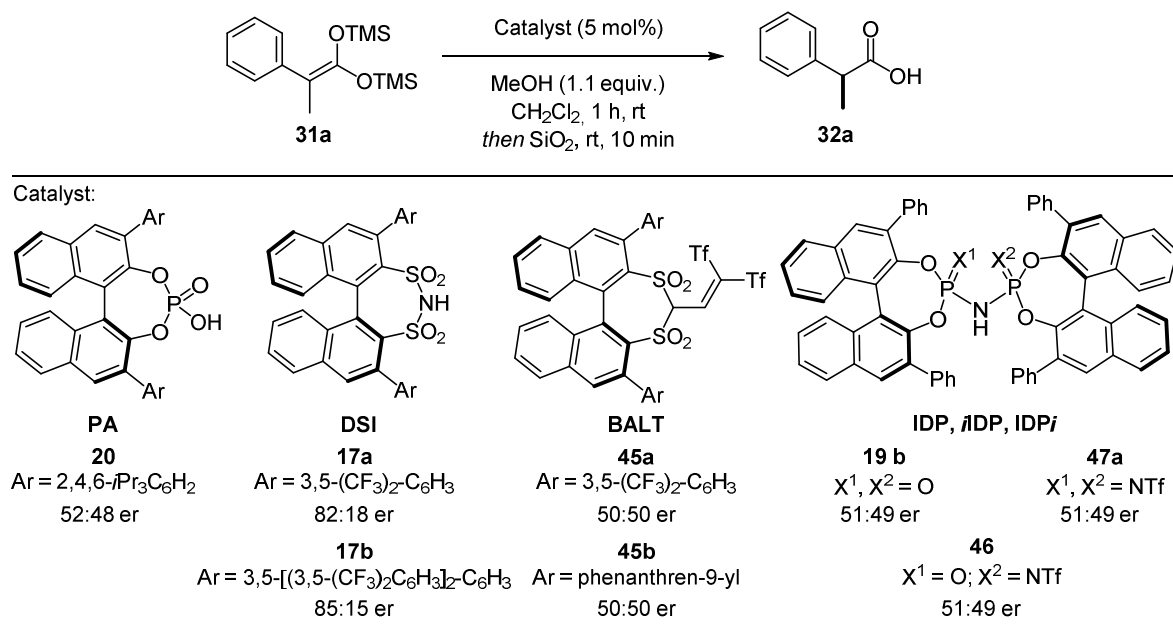
In an initial experiment, *bis*-SKA **31a** was added to a stoichiometric amount of methanol in dichloromethane with (*S*)-DSI (**17a**) as the catalyst. Gratifyingly, the desired product was obtained after full conversion in 82:18 er (Scheme 4.2) (Note: Conversion was monitored *via* ^1H NMR of the crude reaction mixture prior to treatment with SiO_2). Compared with previous results by Yamamoto *et al.* (95:5 er using 2,6-DMP as the PS),^[113a] this result indicated promising enantioselectivity in the presence of a non-bulky PS.



Scheme 4.2 Initial result for the asymmetric protonation of *bis*-SKA in the presence of methanol.

These results prompted us to evaluate the catalytic ability of different Brønsted acid catalysts, exploring different ranges of acidities and confinements (Scheme 4.3). Catalysts with lower acidities, such as (*S*)-TRIP **20** ($\text{p}K_{\text{a}}$ in CH_3CN = 13.6), (*S,S*)-IDP **19b** ($\text{p}K_{\text{a}}$ in CH_3CN = 11.3) and (*S,S*)-*i*IDP **46** ($\text{p}K_{\text{a}}$ in CH_3CN = 9.1), catalyzed the reaction with very low enantioselectivity (52:48 er; 51:49 er and 51:49 er respectively). Catalysts with higher acidities, such as the BALT catalysts **45a** and **45b** ($\text{p}K_{\text{a}}$ in CH_3CN = ~2.8), did not show any level of enantioselectivity (both 50:50 er). The combination of great acidity and confined active site as in IDP*i* **47a** ($\text{p}K_{\text{a}}$ in CH_3CN = 4.5) also did not show any level of enantioselectivity (51:49 er), presumably because *bis*-SKA (**31a**) may be too sterically congested and therefore not able to interact/to intercept the acidic proton of the IDP*i*. Exclusively, the intermediate

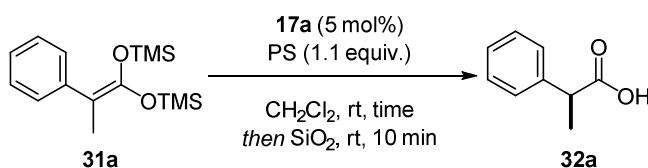
acidities of the DSIs **17a** ($pK_a = 8.5$) and **17b**, which have more open active sites, gave the desired products in improved enantioselectivities (82:18 er and 85:15 er respectively) (Scheme 4.3).



Scheme 4.3 Screening of catalysts.

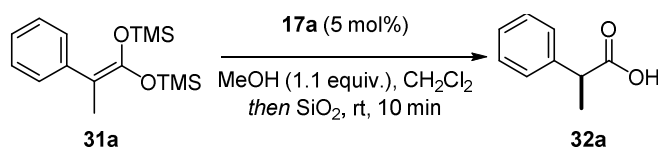
As DSIs were identified as the ideal class of Brønsted acids for this transformation, initial screenings were performed using catalyst **17a**. Remarkably, the use of different PSs had no influence on the enantioselectivity of the transformation (

Table 4.1). From the bulkiest PS in the series (Entry 5) to the smallest one (Entry 1), the enantioselectivity remained unchanged. These results indicate that the background reactivity is not a major concern under this condition and the catalyst is the exclusive proton source.

Table 4.1 Effect of the PS. ^aTime required to reach full conversion

Entry	PS	time ^a	er
1	H ₂ O	1 h	82:18
2	MeOH	1 h	82:18
3	<i>i</i> -PrOH	1 h	82:18
4	<i>t</i> -BuOH	1 h	82:18
5	DMP	4 h	82:18

Lowering the temperature to 0 °C did not improve the enantioselectivity and, interestingly, lower temperatures such as –20 °C and –40 °C were even detrimental. This result suggests that the activity of the catalyst is reduced, making the background reaction predominant (Table 4.2).

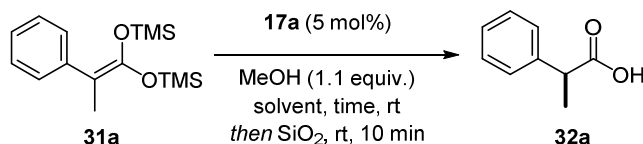
Table 4.2 Effect of temperature. ^aTime required to reach full conversion

Entry	T/°C	time ^a	er
1	rt	1 h	82:18
2	0	2 h	78:22
3	–20	16 h	51:49
4	–40	16 h	51:49

A solvent screening revealed that choice of solvent mainly affected the enantioselectivity, whereas reactivity remained similar (Table 4.3). Due to higher

enantioinduction obtained with it, dichloromethane was used as solvent for further studies.

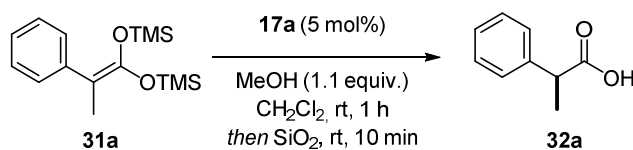
Table 4.3 Effect of solvent. ^aTime required to reach full conversion



Entry	solvent	time ^a	er
1	CH ₂ Cl ₂	1 h	82:18
2	PhMe	2 h	66:34
3	Et ₂ O	2 h	78:22
4	THF	2 h	56:44
5	<i>n</i> -pentane	1 h	78:22
6	MeOH	1 h	54:46

The optimal concentration was identified to be at 0.2 M (Table 4.5, Entry 3), since lower concentrations did not improve the enantioselectivity (Entries 1 and 2) and higher concentrations were detrimental (Entries 4 and 5).

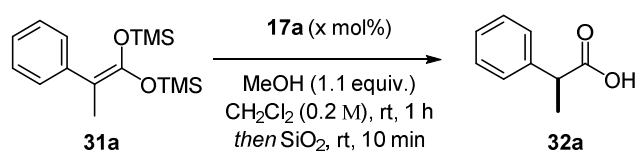
Table 4.4 Effect of the molarity on the DSI-catalyzed protonation of *bis*-SKA



Entry	Conc. (M)	er
1	0.05	82:18
2	0.1	82:18
3	0.2	82:18
4	0.5	76:14
5	neat	70:30

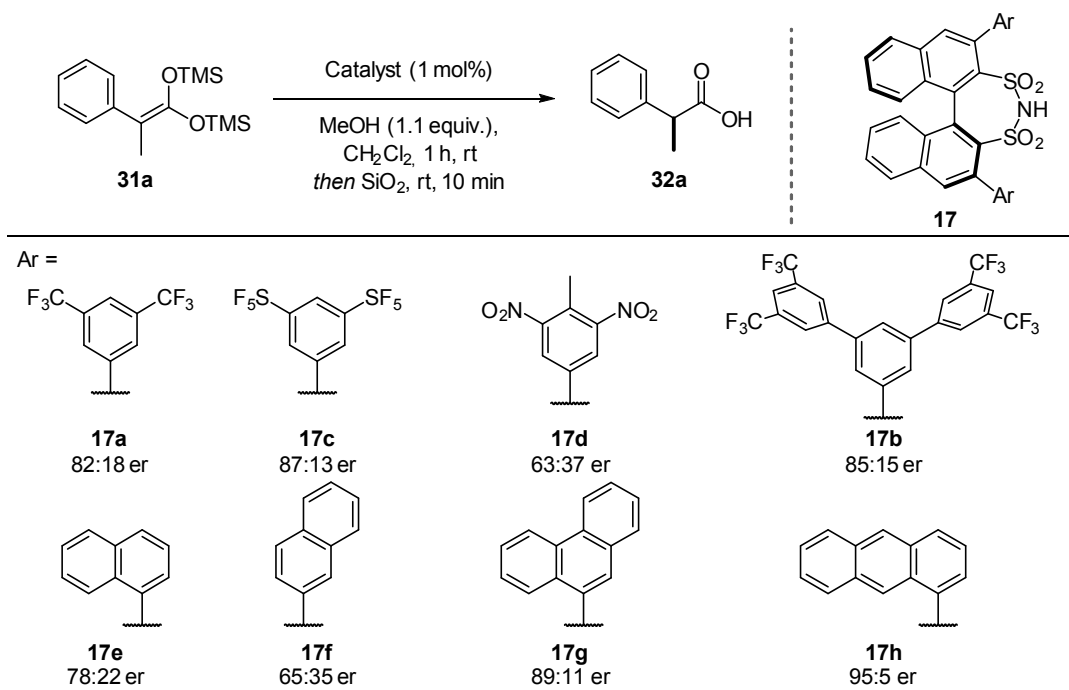
Using these optimized conditions, the catalyst loading could be reduced to 1 mol%, without deteriorating yield or enantioselectivity (Entries 1 and 2). Lower catalyst loadings however, gave worse and less reproducible results (Entries 4 and 5).

Table 4.5 Effect of the catalyst loading



Entry	mol% b	er
1	5	82:18
2	2	82:18
3	1	82:18
4	0.5	77:23
5	0.1	75:25

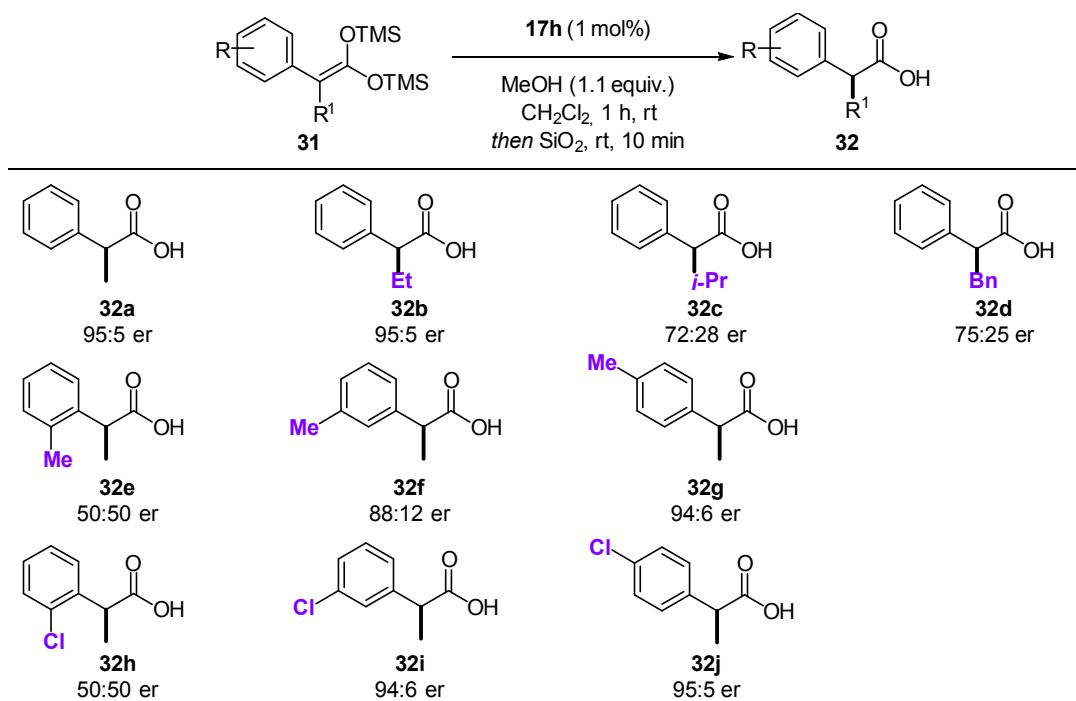
Taking the best reaction conditions, the catalytic activities of various DSI catalysts bearing different 3,3'-substituents were evaluated (Scheme 4.4). Modifications of the substituents in the *meta*-position slightly improved the enantioselectivity (**17b** 85:15 er and **17c** 87:13 er), however not to sufficient levels. The expansion of the aromatic surface to a naphthalene moiety was not sufficient (**17e** 78:22 er and **17f** 65:35 er). However, high enantioselectivity was achieved with the catalyst containing the phenanthrene (**17g**) and anthracene substituents (**17h**), which gave 89:11 er and 95:5 er respectively.



Scheme 4.4 Effect of the 3,3'-substituents of the DSI catalyst.

4.1.3 Preliminary Substrate Scope

Despite the promising result, a preliminary substrate scope showed that, in the presence of **17h** as the catalyst, the reaction scope lacked generality (Scheme 4.5). Whereas the model substrate **32a** could be obtained with very good enantioselectivities (95:5 er), modifications of the R¹ group from methyl to isopropyl (**32c**) or benzyl groups (**32d**) were detrimental for the enantioselectivity (72:28 er and 75:25 er). In particular, *ortho*-substituents at the aromatic group (**32e** and **32h**) of the substrate led to racemic products (both 50:50 er), and *meta*- (**32f** 88:12 er; **32i** 94:6 er) and *para*-substituents (**32g** 94:6 er) gave high but overall not sufficient enantioselectivities.



Scheme 4.5 Preliminary substrate scope.

4.1.4 Fine-Tuning of the Catalyst Design

In order to achieve a more general system, further catalyst development was required. Therefore, the synthetic focus on the catalysts structures was divided into two branches. Firstly, maintaining the anthracene unit and functionalizing possible positions (**17i-17k**), and secondly, reinvestigating the second best catalyst (**17g**) and modifying the present phenanthrene group (**17l-17p**) (Figure 4.1).

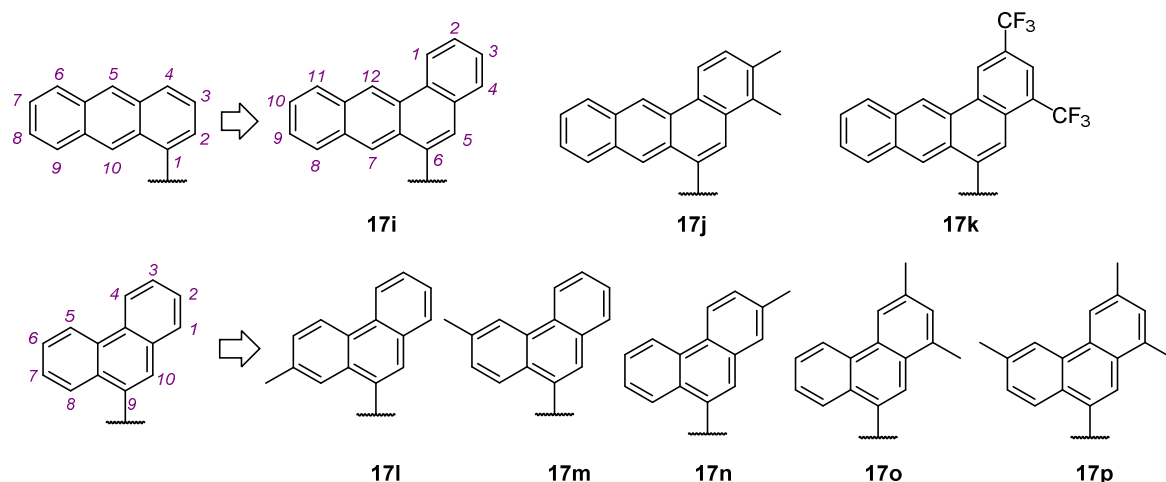
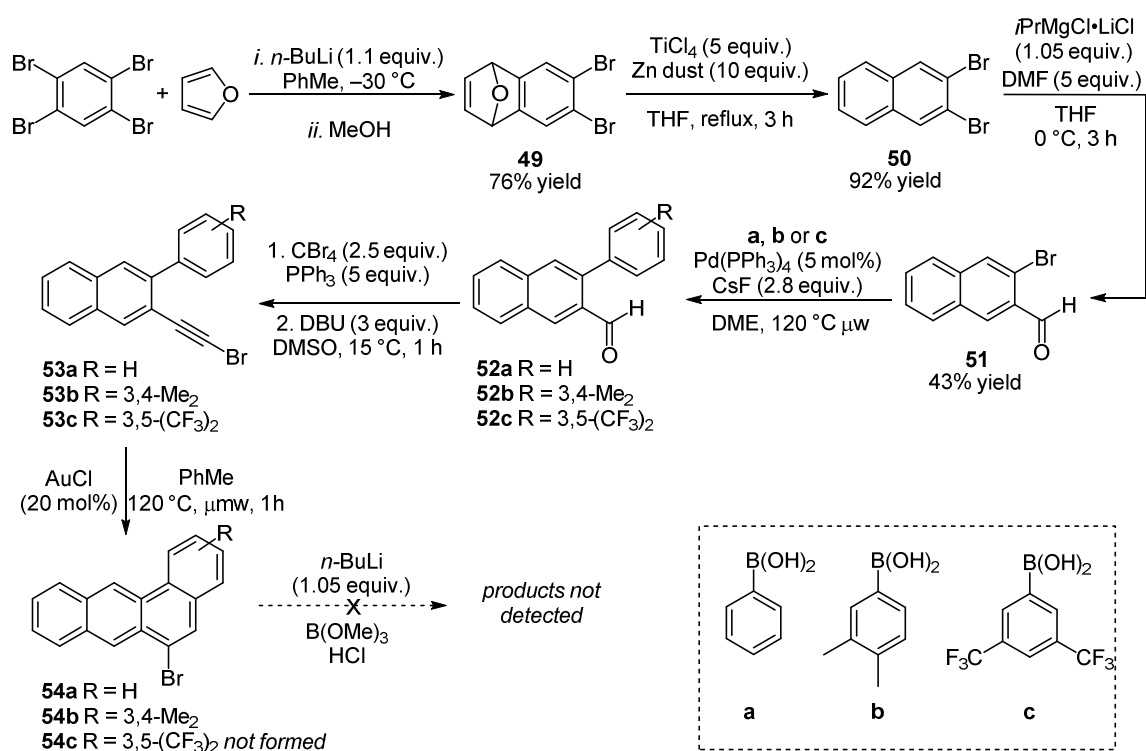


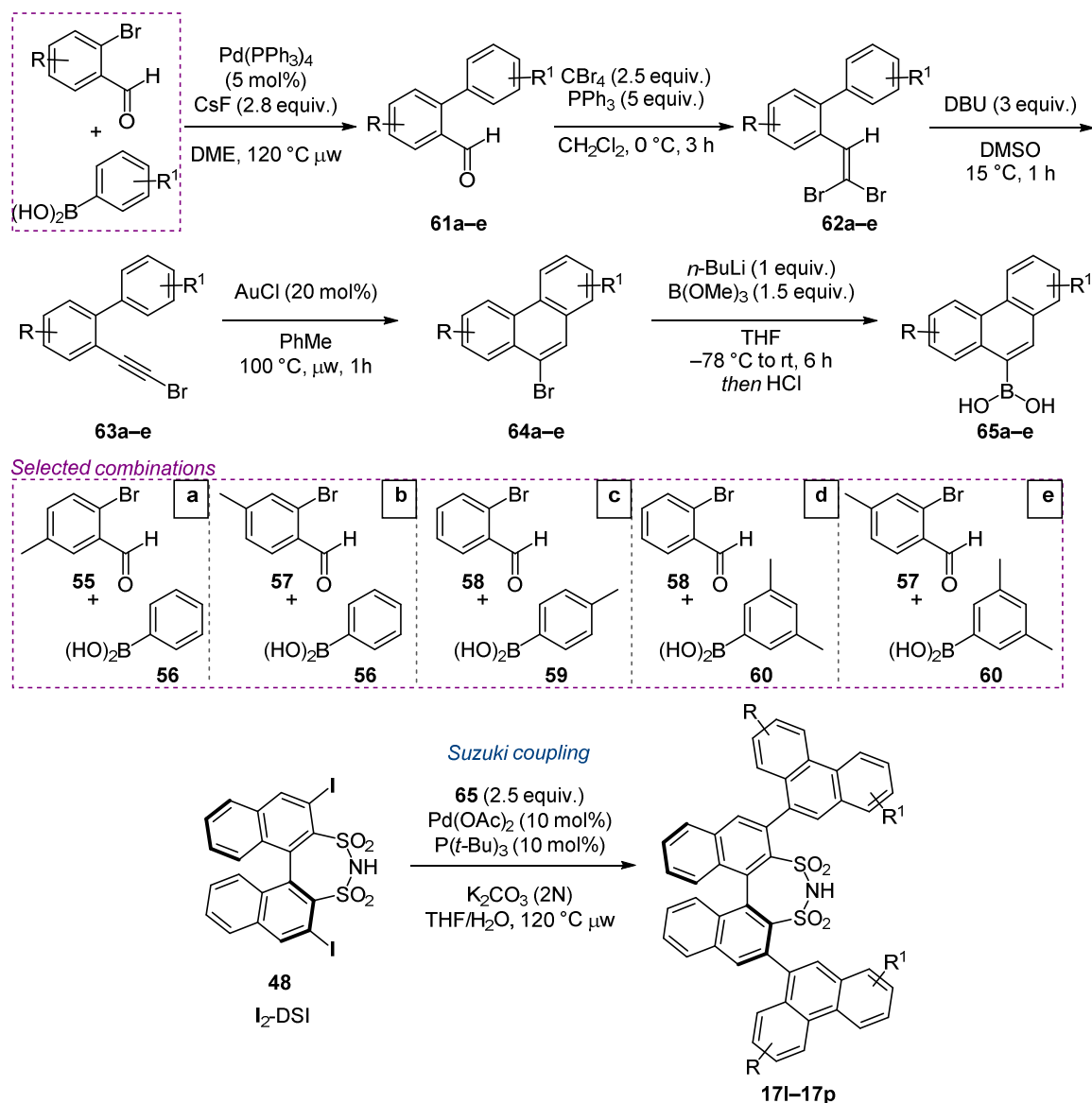
Figure 4.1 DSI 3,3'-substituents design: tetraphene derivatives and phenanthrenyl derivatives.

In the **17i-17k** series, the particular challenge was the functionalization of position 6 with a suitable boron reagent (acid or ester) in order to enable Suzuki cross coupling reactions with the corresponding 3,3'-I₂-DSI (**48**). Neither the envisioned boronic acids nor the corresponding bromides (**54a-c**) are commercially available or reported in literature, therefore a suitable synthetic sequence was designed (Scheme 4.6). The sequence consisted of an initial Diels–Alder reaction between an *in situ* formed benzyne and furane, followed by metal-catalyzed deoxygenation using TiCl₄ and Zn.^[151] After conversion of **50** to the bromo-aldehyde **51** with *i*PrMgCl•LiCl (turbo Grignard)^[152] and DMF,^[153] the Suzuki coupling with three different boronic acids afforded intermediates **54a**, **54b** and **54c**. The formyl group was used as a handle to install the required alkyne **53**, which was achieved by a Corey–Fuchs reaction.^[154] The newly introduced aryl group and the *ortho*-alkyne functionality underwent an Au(I)-catalyzed cycloisomerization in which a 1,2-halide shift occurred. This can be explained by assuming a metal vinylidene species as the reactive intermediate.^[155] Unfortunately, the desired boronic acids could not be synthesized, as intermediates **54a** and **54b** were extremely insoluble and additionally highly unstable in the presence of oxygen or light. Intermediate **54c** was not formed, as the Au(I)-catalyzed cyclization does not tolerate electron deficient ring systems.



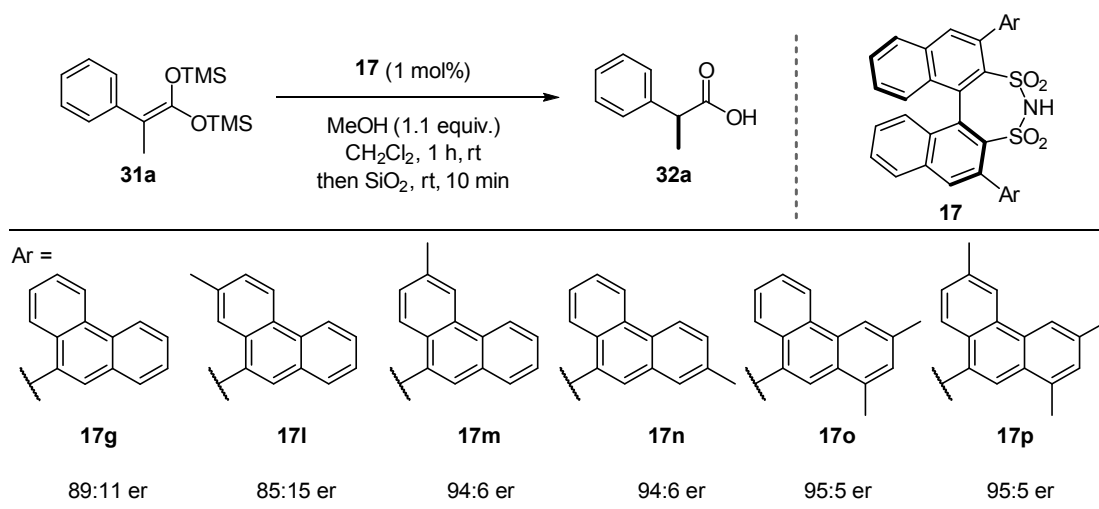
Scheme 4.6 Synthetic sequence toward tetraphene derivatives **54a**, **54b** and **54c**.

Further efforts were therefore dedicated toward the preparation of functionalized phenanthrene derivatives (Scheme 4.7). In this case, the same synthetic strategy was applied starting from the commercially available 2-bromo-arylaldehydes (**55**, **57**, **58**) in combination with different boronic acids (**56**, **59**, **60**). Finally, the obtained boronic acid intermediates (**65a–65e**) were reacted with **48** via a Suzuki cross-coupling reaction, affording the desired DSI catalysts (**17l–17p**).



Scheme 4.7 Synthesis of phenanthrene boronic acid derivatives **65a–65e**.

To our delight, the newly designed catalysts led to higher enantioselectivities when compared to the parent catalyst **17g** in the asymmetric protonation of the model substrate **31a** (Scheme 4.8). In particular, a significant increase of enantioselectivity was achieved when position 1, 3 and 6 were substituted with a methyl group (**17o** and **17p**, 96:4 er).

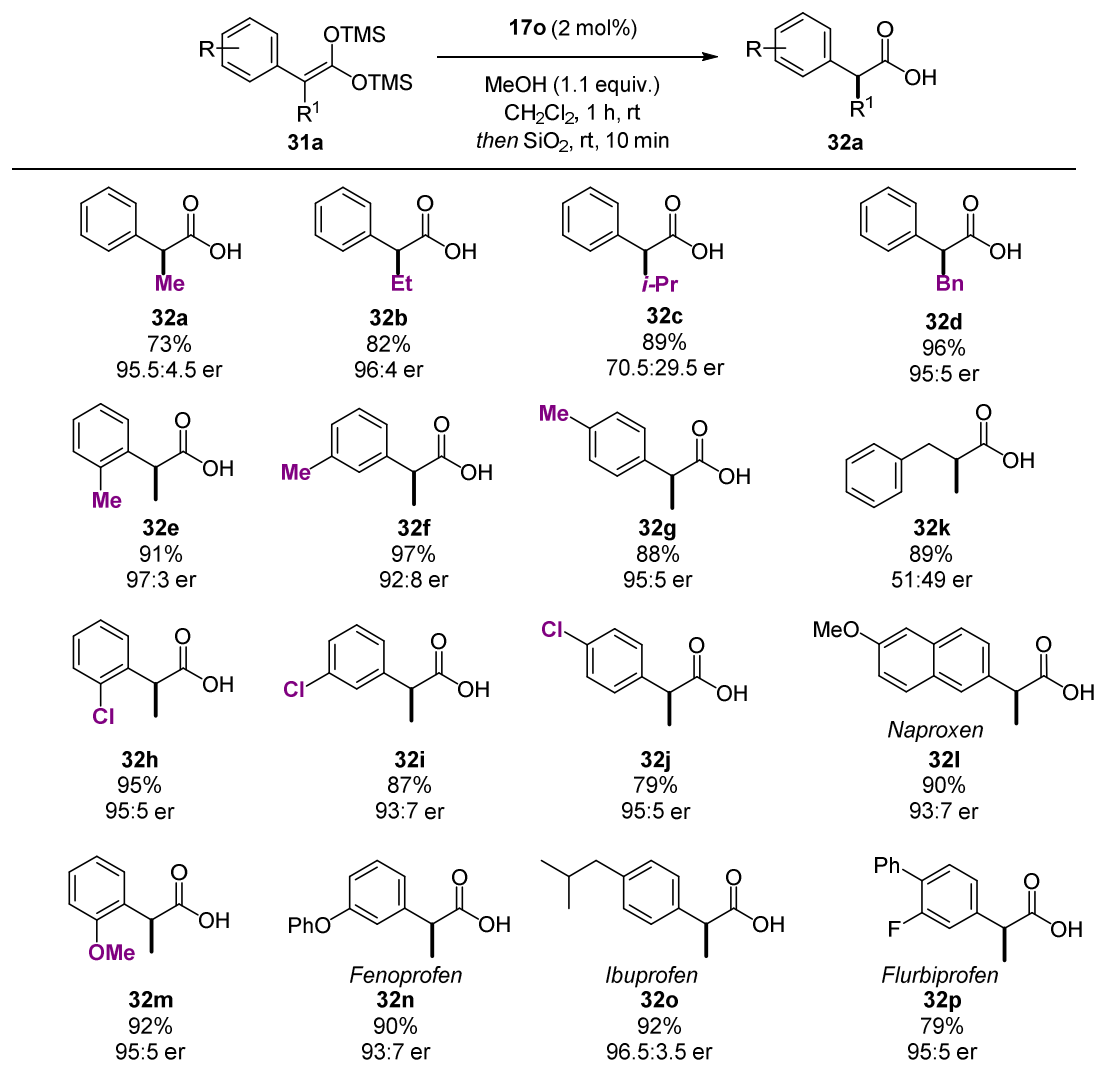


Scheme 4.8 Evaluation of differently substituted phenantrenes in the 3,3'-positions of the DSI.

4.1.5 Substrate Scope

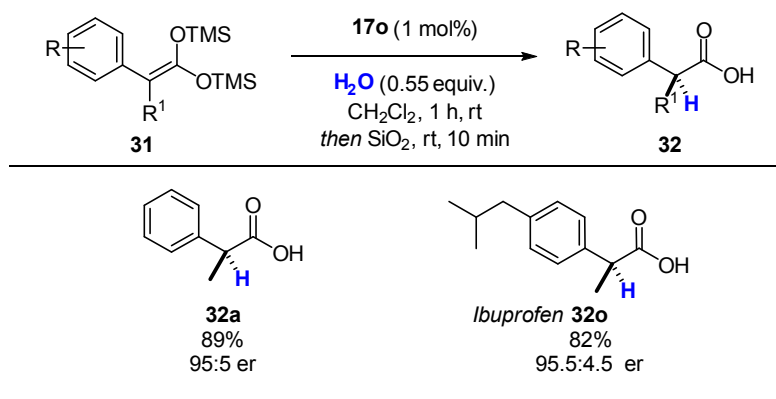
Encouraged by these promising results, we explored a variety of differentially-substituted *bis*-SKAs (Scheme 4.9). Various alkyl substituents were well tolerated in the asymmetric protonation, including a longer alkyl chain (**32b**, 96:4 er) and a benzyl group (**32d**, 95:5 er). However, substitution of the alkyl unit with an isopropyl group (**32c**) resulted in diminished enantioselectivity (70.5:29.5 er), suggesting that the enantioinduction of this catalytic system is extremely sensitive to the size of R¹ and R². *Ortho*- (**32e**, 97:3 er, and **32h**, 95:5 er) and *para*-substitution (**32g**, 95:5 er) on the aromatic unit proved to be superior to *meta*-substitution (**32f**, 92:8 er). Both electron-rich (**32e–32g**) and electron-deficient (**32h–32j**) aromatic substituents displayed a similar position-dependent selectivity pattern. Non-steroidal anti-inflammatory drugs (NSAIDs)-derived *bis*-SKAs showed an analogous trend, where *para*-substituted starting materials (**32o** and **32p**) gave slightly higher enantioselectivities than *meta*-substituted ones (**32l** and **32n**). As observed in previous DSI-catalyzed transformations, the enantioselectivity of this method is dependent on an α -aromatic- α -alkyl substitution pattern, as α,α -dialkyl substrates, such as carboxylic acid **32k**, were obtained in essentially racemic form.^[12b]

Results and Discussion



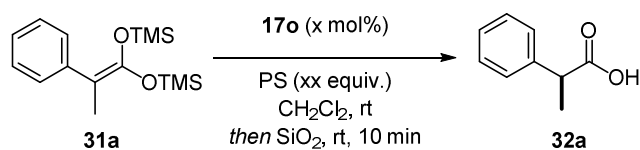
Scheme 4.9 Substrate scope of the enantioselective protonation of *bis*-SKAs.

As already mentioned in Table 4.1, consistent results were also obtained when using water as a PS (**3a**, 95:5 er, and **3m**, 95.5:4.5 er) (Table 4.6). However, initial results were non reproducible because the addition of 0.55 equiv. of water (6 μ L, in a 0.2 mmol scale of **31a**) in CH_2Cl_2 (1 mL) in a single portion resulted to a heterogeneous system (liquid/liquid). Therefore, the 0.55 equiv. of water were initially dissolved in CH_2Cl_2 reaching a saturated solution. The stock solution of water in CH_2Cl_2 was then added *via* syringe pump to the reaction mixture. Reproducible and consistent results could be obtained with this setup.

Table 4.6 Enantioselective protonation of *bis*-SKAs using water as the PS.

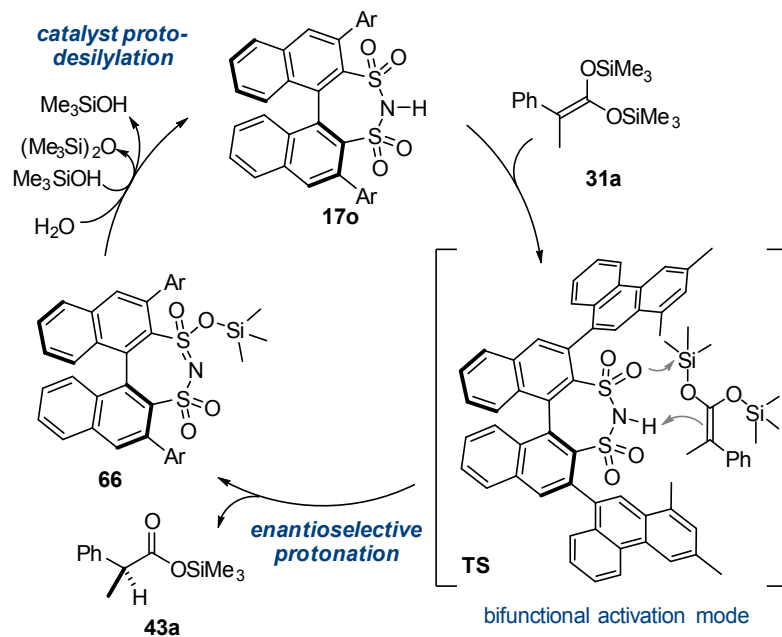
4.1.6 Mechanistic Investigations

To gain insight into the reaction mechanism, we studied the effect of the PS on the conversion and stereochemical outcome (Table 4.7). In the absence of a PS, a conversion equal to the catalyst loading was observed (Entries 1 and 2), suggesting that the substrate is only protonated by the catalyst. Turnover was only observed upon adding a stoichiometric amount of PS (Entries 3 and 4). Notably, enantioselectivities consistently proved to be independent of the PS (Entries 4-6), suggesting that the stoichiometric PS is not involved in the enantiodetermining step. Furthermore, a sub-stoichiometric amount of water also enabled full conversion (Entry 7), as the 0.5 equiv. of silanol, formed during the protodesilylation of the SKA, acts as an efficient PS, ultimately generating hexamethyldisiloxane.

Table 4.7 Reaction mechanism investigation

Entry	PS (equiv.)	mol% D	conv.	er
1	–	50	~50%	nd
2	–	100	full	95.5:4.5
3	MeOH (1.0)	50	full	95.5:4.5
4	MeOH (1.1)	1	full	95.5:4.5
5	DMP (1.1)	1	full	95.5:4.5
6	H ₂ O (1.1)	1	full	95:5
7	H ₂ O (0.55)	1	full	95:5

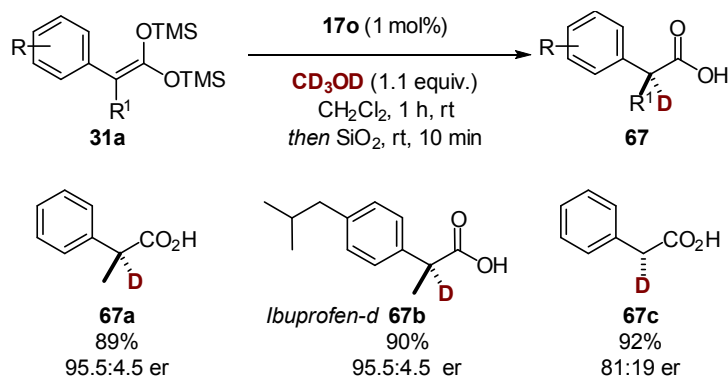
We speculate that the high efficiency of our catalytic system, compared to that of the racemic background reaction, is a result of a relatively fast protodesilylation event depicted in the proposed transition state (**TS**) (Scheme 4.10), which likely exploits the bifunctionality of the DSI with its high N–H acidity and concomitant Lewis basicity of the S=O bond, in combination with the oxophilicity of the silicon group. An analogous protodesilylation event can be envisioned for the re-protonation of **66** by the achiral PS, overall resulting in a fast and efficient enantioselective protonation. In this scenario, the background reaction between **31a** and the achiral PS is avoided by the high efficiency of the catalytic system without the need of a bulky PS, thereby improving the atom economy of the protonation step.



Scheme 4.10 Proposed catalytic cycle.

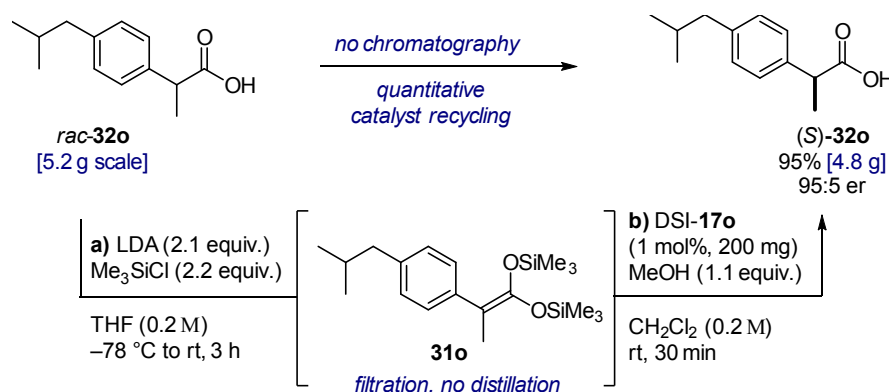
4.1.7 Enantioselective Deuteration of *bis*-SKAs

The robustness of this catalytic system to any PS also provided direct access also to the corresponding deuterated products (**67a**, 95.5:4.5 er, and **67b**, 95.5:4.5 er), achieving the first organocatalytic enantioselective deuteration of *bis*-SKAs with D_2O or CD_3OD (Scheme 4.11). Moderate enantioselectivity was obtained with a monosubstituted *bis*-SKA, furnishing enantioenriched α -deuterated phenylacetic acid **67c** with an er of 81:19.

Scheme 4.11 Enantioselective deuteration of *bis*-SKAs.

4.1.8 Deracemization Sequence

To illustrate the practicality of our method, a late stage deracemization of Ibuprofen[®] (**32o**) was performed on a multigram scale (Scheme 4.12). Starting from 5 g of (\pm)-**32o**, stoichiometric amounts of TMSCl and LDA were added. The resulting suspension was concentrated and LiCl was filtered, furnishing ketene acetal **31o** in >95% purity (determined by ¹H NMR), which was used without further purification. Subsequently, solvent and catalyst (1 mol%) were directly added to *bis*-SKA **31o** and 1.1 equiv. of MeOH was added over 30 min. Upon extraction, the final product was isolated in 95% yield and 95:5 er; furthermore, the catalyst could be recycled upon extraction, followed by acidification, in quantitative yield.

Scheme 4.12 Chromatography-free preparative deracemization of (\pm)-Ibuprofen[®] (**32o**).

4.1.9 Conclusions

In summary, we have developed a deracemization of α -branched aryl carboxylic acids based on the asymmetric Brønsted acid-catalyzed protonation of the corresponding *bis*-SKAs in the presence of methanol or water. The operationally simple protocol allows a facile transformation under mild reaction conditions and exclusively furnishes the enantioenriched products in almost quantitative yields starting from the corresponding racemic acids without the need for additional purification. We suggest that the bifunctional activation mode of the DSI catalyst enables a highly efficient catalytic cycle that in turn circumvents racemic background reactivity with the achiral, stoichiometric PS. The late stage deracemization of NSAIDs on gram scale and the simple direct enantioselective deuteration of *bis*-SKAs using CD₃OD or D₂O as deuterium source demonstrate the applicability of the developed system.

4.2 Asymmetric α -Aminomethylation for the Direct Synthesis of Unprotected β -Amino Acids

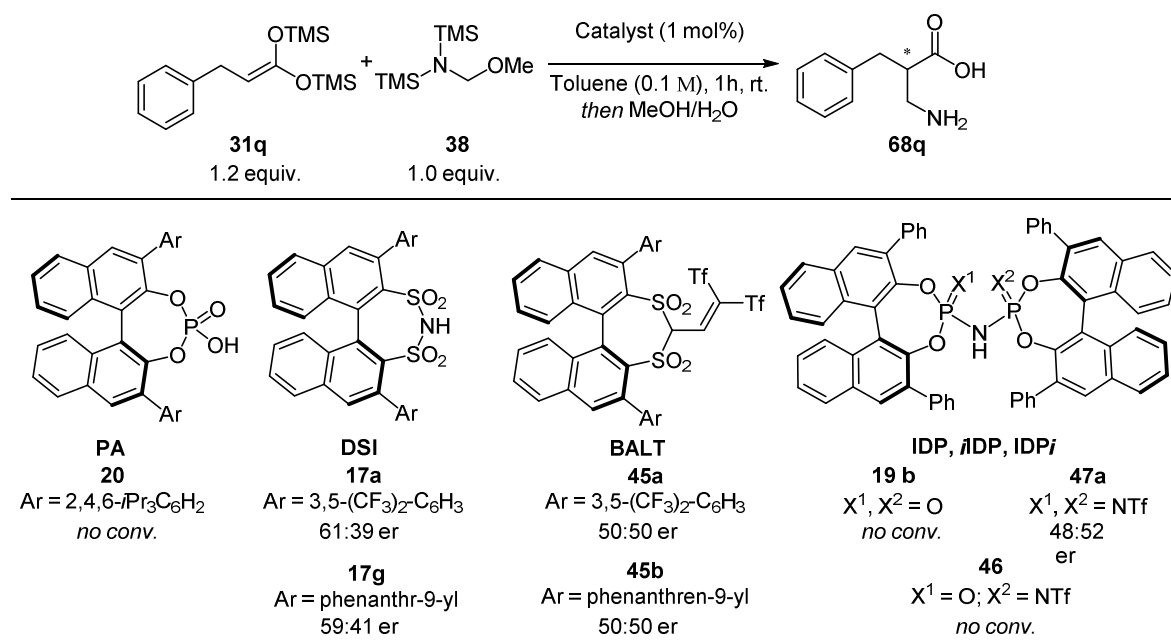
The work presented in this section was performed in collaboration with Dr. Chendan Zhu.

4.2.1 Reaction Design and Optimization

Inspired by the work of Morimoto *et al.*,^[100] an initial experiment was conducted using *bis*-SKA **31q** and *bis*-silylated hemiaminal **38** in the presence of a catalytic amount of (*S*)-DSI **17a** as the pre-catalyst. An apolar solvent (toluene) was chosen to enable the formation of a tight ion pair between the iminium ion formed *in situ* and the chiral counteranion, as proposed in an ACDC scenario. A small excess of the *bis*-SKA (1.2 equiv.) was added to a solution containing the catalyst **17a**, in order to (a) ensure the full activation of the catalyst by silylation and (b) convert each available source of protons to TMS₂O according to the *self-healing* cycle (see section 2.2.5.1). Subsequently, the electrophilic aminomethylating reagent was added. The targeted reaction (Scheme 4.13) proceeded within 1 hour in quantitative yield (Note: yield was determined by ¹H NMR analysis of the crude reaction mixture using mesitylene as an internal standard) and moderate yet promising enantioselectivity (61:39 er).

Scheme 4.13 Initial result for the asymmetric aminomethylation of *bis*-SKA **31q**; ^[a] NMR yield measured with mesitylene as internal standard. ^[b] The enantiomeric ratio of the product was determined by chiral phase HPLC analysis, without further derivatization using Chirobiotic T2 (for further details, see Experimental Part).

These results motivated us to explore the catalytic ability of different Brønsted acid pre-catalysts (Scheme 4.14). In the case of (*S*)-TRIP **20** (pK_a in CH_3CN = 13.6), IDP **19b** (pK_a in CH_3CN = 11.3) and *i*DP **46** (pK_a in CH_3CN = 9.1) no reaction occurred, as due to their low acidity presumably an irreversible silylation of the corresponding catalysts takes place. BALT catalysts **45a** and **45b** (pK_a in CH_3CN = ~2.8) and IDPi **47a** (pK_a in CH_3CN = 4.5) catalyzed the targeted reaction, however without any induction of enantioselectivity. Gratifyingly, DSIs **17a** (pK_a = 8.5) and **17g** gave the desired products in moderate enantioselectivities (61:39 er and 59:41 er respectively). We therefore decided to continue our investigations with the DSI motif (**17a**).



Scheme 4.14 Initial screening for the most suitable catalyst motif.

4.2.1.1 Exploration of DSI Catalysts

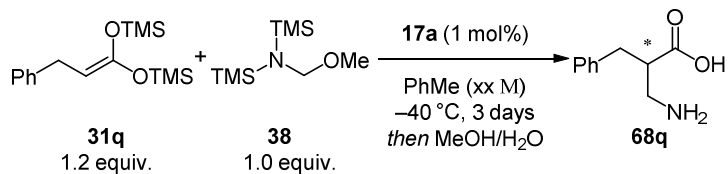
The initial screening of solvents and temperatures showed that apolar solvents were required and lowering the temperature down to -60 °C improved the enantioselectivity of the transformation. In particular, the targeted product was obtained in an enantioselectivity up to 78.5:21.5 er, in toluene at -60 °C. Using *n*-

hexane as the solvent resulted in comparable 76.5:23.5 er at $-40\text{ }^{\circ}\text{C}$. However, at $-60\text{ }^{\circ}\text{C}$, the enantioselectivity decreased to 69:31 er, probably due to the lower solubility and hence lower reactivity of the catalyst under these conditions (Table 4.8). In each case, the reaction profile was very clean and the substrates converted exclusively to the desired product. Therefore, yields will not be reported for all the initial screenings, unless they do not match with the conversion.

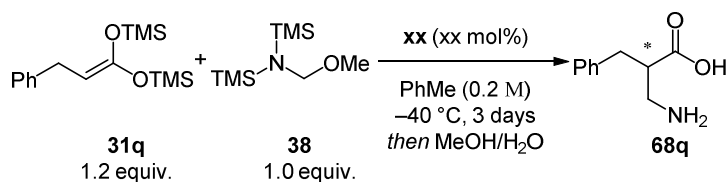
Table 4.8 Effect of temperature and solvent.

er	CH ₂ Cl ₂	EtOAc	Et ₂ O	PhMe	<i>n</i> -hexane
$-20\text{ }^{\circ}\text{C}$	52:48	62:38	68:32	71:29	72:28
$-40\text{ }^{\circ}\text{C}$	53:47	67:33	71:29	76:24	76.5:23.5
$-60\text{ }^{\circ}\text{C}$	53:47	61:39	68:32	78.5:21.5	69:31

Additional parameters were tested, including molarity (0.01, 0.05, 0.1, 0.5 and 1 M) (Table 4.9), catalyst loading (0.1, 0.5, 1, 2 and 5 mol%) (Table 4.10) and different stoichiometries of **31q** (2, 5 and 10 equivalents) (Table 4.11). However, these parameters had no particular effect on the enantioselectivity of the reaction.

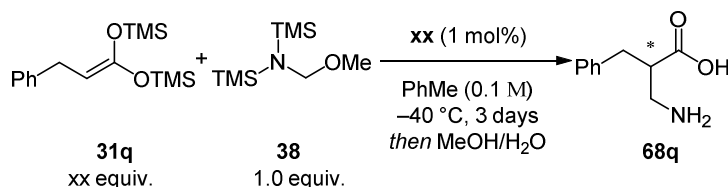
Table 4.9 Effect of molarity in toluene. ^[a] NMR yield measured with mesitylene as internal standard.

Entry	Conc. (M)	yield (%) ^[a]	er
1	0.01	73	77:23
2	0.05	>95	76:24
3	0.1	>95	76:24
4	0.5	93	75:25
5	1	81	74:26

Table 4.10 Effect of the catalyst loading. ^[a] NMR yield measured with mesitylene as internal standard.

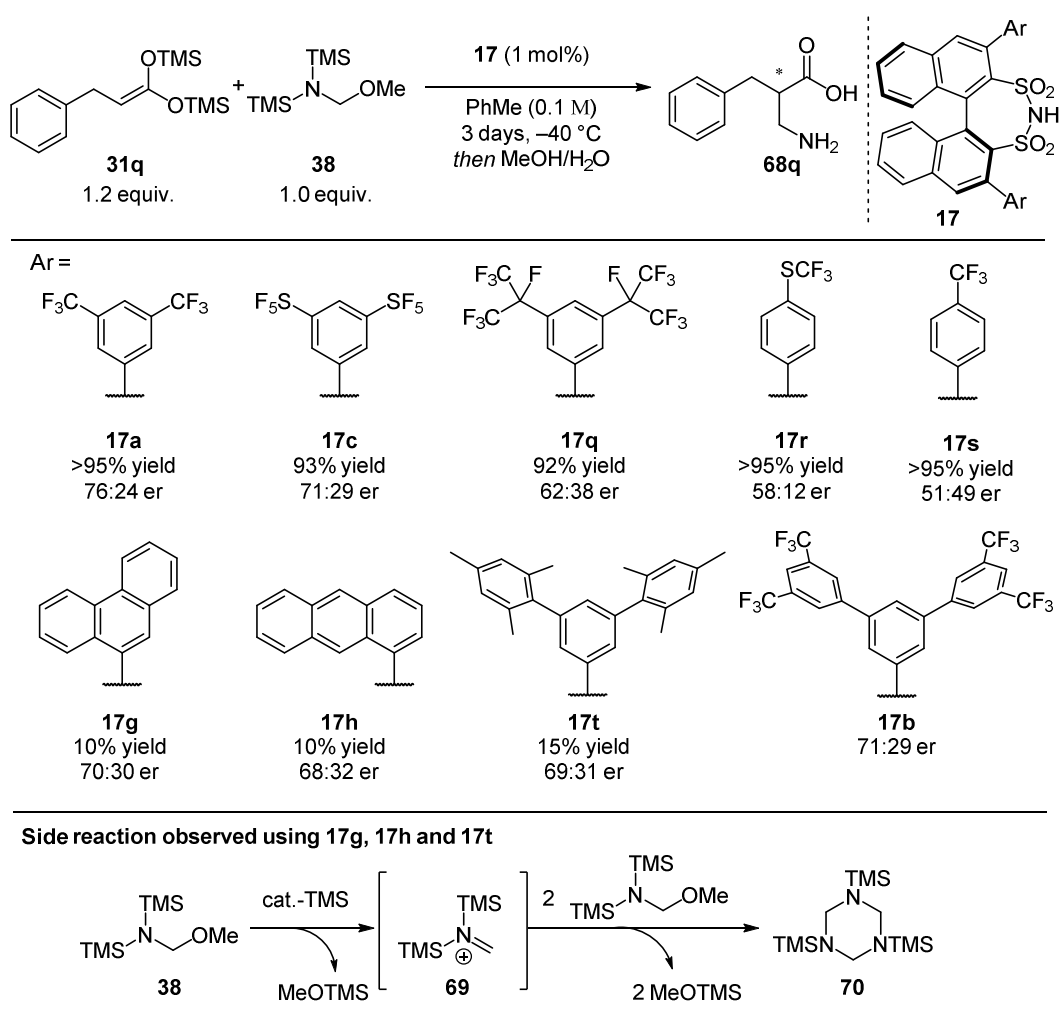
Entry	mol% xx	yield (%) ^[a]	er
1	0.1	6	70:30
2	0.5	30	75:25
3	1	>95	76:24
4	2	>95	76:24
5	5	86	76:24

Table 4.11 Effect of the stoichiometry of the *bis*-SKA. ^[a] NMR yield measured with mesitylene as internal standard.



Entry	xx (equiv.)	yield (%) ^[a]	er
1	1.2	95	76:24
2	2	>95	76:24
3	5	>95	76:24
4	10	>95	76:24

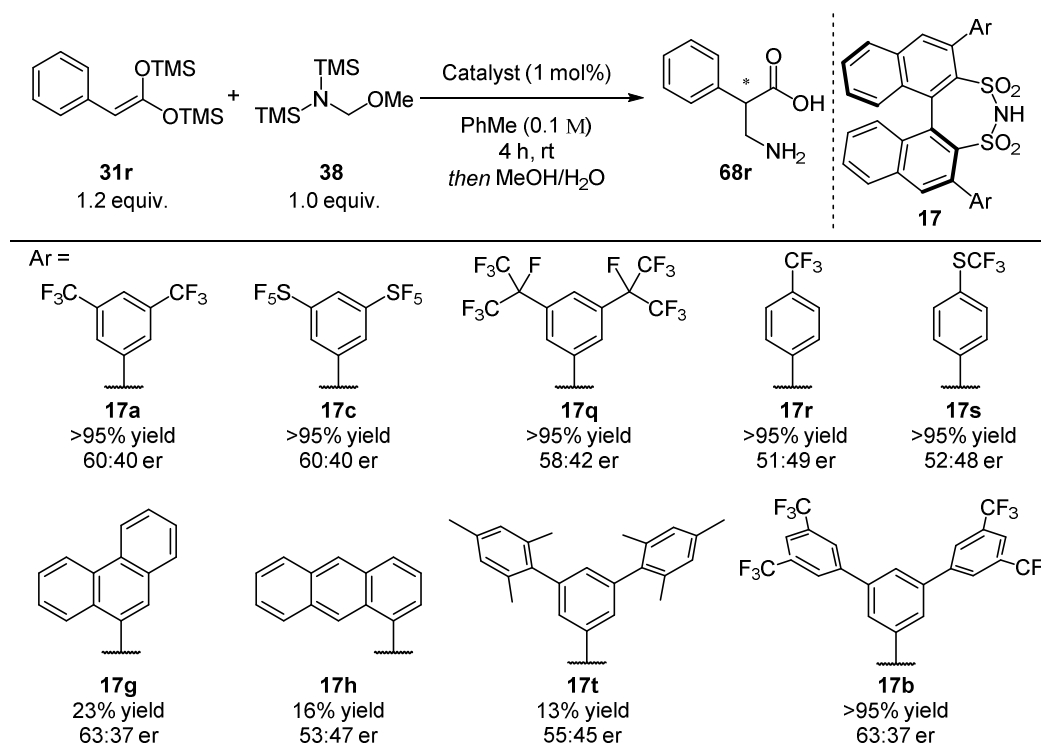
Thus, the same reaction conditions were maintained to evaluate the effects of the substituents in the 3,3'-positions of the DSI catalyst (Scheme 4.15). Modifications of the substituents in the *meta*-positions decreased the enantioselectivity (**17c** 71:29 er and **17q** 62:38 er) and any substituent in *para*-position resulted in either low enantioselectivity (**17r** 58:42 er) or racemic products (**17s** 51:49 er). Catalysts with lower acidities, such as the ones with extended aromatic substituents, gave lower enantioselectivities (**17g** 70:30 er, **17h** 68:32 er and **17t** 69:31 er) and yields (usually in the range of 10–15% NMR yield). In these cases the aminomethylating reagent was fully decomposed forming the *tris*-silylated 1,3,5-triazine **70** and unreacted *bis*-SKA **31q** remained in the reaction mixture. A possible explanation for the observed side-reaction could be that the nucleophilic attack of the *bis*-SKA is slowed down due to the decreased Lewis acidity, giving the *in situ* generated iminium ion **69** more time to react with itself. In agreement with this explanation, the presence of EWGs (**17b**) increased the acidity of the catalysts and resulted in quantitative yields, however without improving the enantioselectivity (71:29 er).



Scheme 4.15 Effects of the substituents in the 3,3'-positions of the DSI catalysts. NMR yield measured with mesitylene as internal standard.

The observed levels of enantioselectivity were only moderate to good at this point and there was no clear direction on how to improve them. On the other hand, the results were encouraging as the model substrate was aliphatic, and DSI catalysts have typically been only successful with aromatic substrates (as mentioned in section 2.2.5.1). However, when aromatic substrate **31r** was tested, lower reactivity but similar enantioselectivity was observed. The lower reactivity could be explained by the decreased nucleophilicity of the substrate, as the HOMO of **31r** is stabilized by conjugation. Higher temperatures were required as no conversion of the starting material could be observed below $-20\text{ }^{\circ}\text{C}$. Regarding the substituents on the catalyst,

a similar trend as for the previous substrate was observed: Whereas different *meta*-substituted aryl groups gave similar or lower enantioselectivities (**17c** 60:40 er and **17q** 58:42 er), *para*-substituted ones afforded only racemic product (**17r** and **17s**). The moderate enantioselectivity of **17g** was accompanied by mainly decomposition of **38** and thus low yield. Similar behavior could be observed for **17h** and **17t**. The best result in this series was obtained using **17b** (quantitative yield, 63:37 er), however, this result could not be improved by further optimizations (Scheme 4.16).



Scheme 4.16 Effect of substituents in the 3,3'-positions of the DSI catalysts. ^[a] NMR yield measured with mesitylene as internal standard.

As already pointed out in section 2.2.5.2, the DSI motif has structural limitations compared to the IDP*s*. Indeed, DSI can bear different 3,3'-substituents and modifications on 5,5'- and 6,6'-positions have been reported. In addition to all the previously mentioned possibilities of modification, IDP*s* can be further modified in proximity to the catalytically active site, by variation of the sulfonimide residue in the core of the catalyst. Based on our initial results, we concluded that IDP*s* were

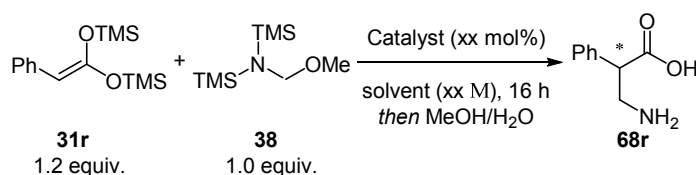
sterically too confined to incorporate the intermediate iminium-ion thus resulting in low or no enantioinduction in the targeted reaction. Reaching this point in our investigations, we questioned whether we discarded the IDP*i* motif too early, as it offers an additional possibility for modifications at the catalyst's core, allowing a more accurate design of the required key chiral counteranion. We therefore decided to reinvestigate and further explore the catalytic abilities of the IDP*i* motif by testing different combinations of substituents in the 3,3'-positions and sulfonimidic residues.

4.2.2 Examination of IDP*i* Catalysts

We began our investigations by comparing the reactivity of IDP*i* **47f** and DSI **17a** using **31r** as the starting material. A series of reaction parameters (e.g. solvent polarity, concentration, catalyst loading and reaction time) were evaluated for both catalysts in parallel (Table 4.12). When performed in toluene (0.5 M) at room temperature, a clean reaction profile was observed using 2 mol% of DSI **17a**, giving the targeted product in 91% yield and 60:40 er (Entry 1). Using IDP*i* **47f** under the same reaction conditions resulted in significant formation of by-products, mainly due to Claisen condensation. The desired product could be obtained in 75% yield, however in racemic form. Decreasing the temperature had different impact on the two catalytic systems: With **17a** no significant change in enantioselectivity was observed, however the reactivity decreased until no reaction could be obtained below -40 °C (Entries 2–4). Gratifyingly, with **47f**, the lower temperatures decreased the amount of side products, resulting in a cleaner reaction profile and the enantioselectivity increased to 60:40 er (Entries 3 and 4). Further modifications of the reaction parameters for DSI **17a**, such as the catalyst loading, molarity or solvent polarity did not improve the enantioselectivity (Entries 5–9). With IDP*i* **47f** on the other hand, increased catalyst loading lead to by-product formation (Entry 5, 93% yield instead of 99% yield of Entry 4), a higher concentration decreased the enantioselectivity (Entry 6, 56:44 er) and a lower concentration slowed down the reaction rate, yet with a cleaner reaction profile (Entry 7, 41% yield at 42%

conversion, 62:48 er). As already previously shown, the choice of the solvent was not a determining parameter for the enantioselectivity (Entries 4, 8 and 9).

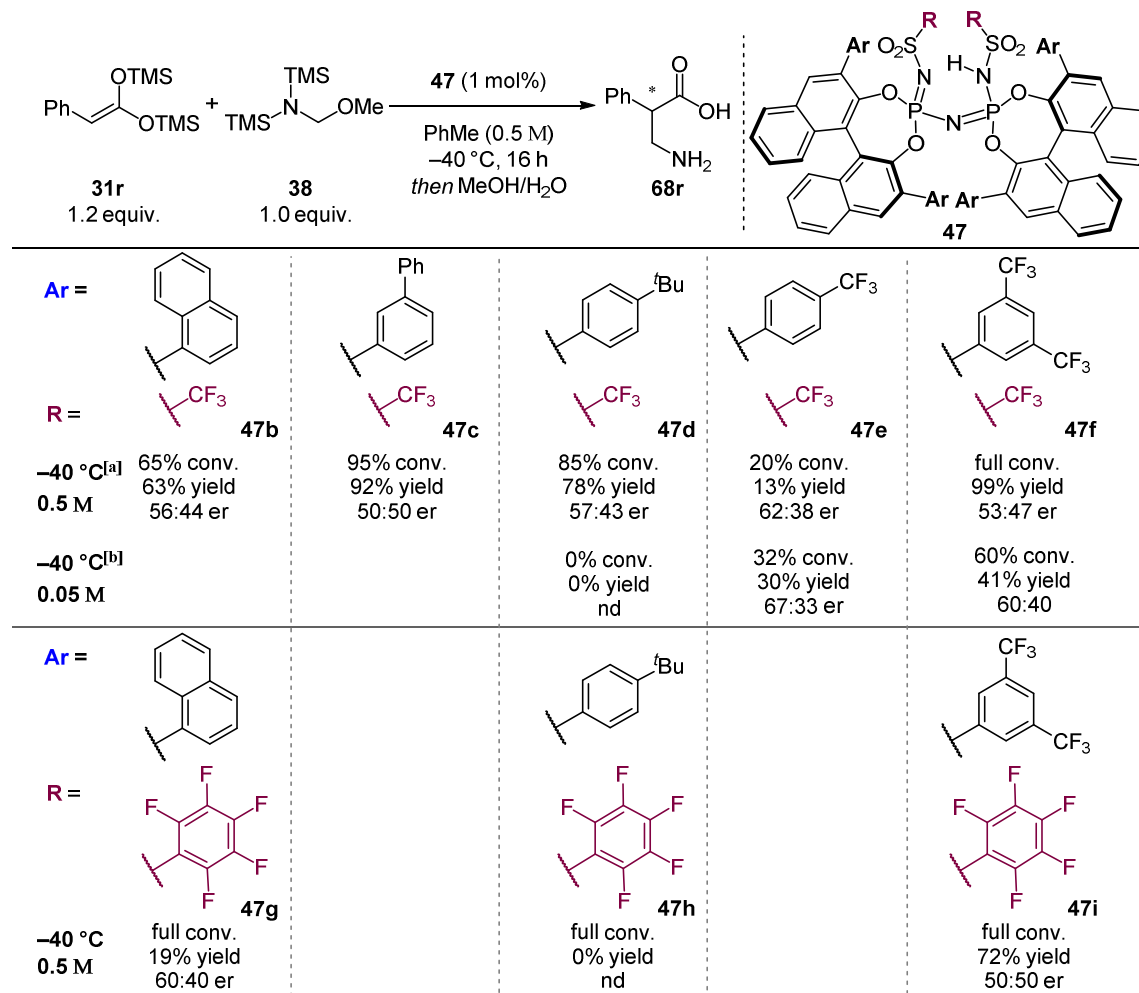
Table 4.12 Parallel screening of reaction conditions using DSI **17a** and IDPi **47f**;
[a] NMR yield measured with mesitylene as internal standard.



Entry	DSI 17a			IDPi 47f					
	mol%	Conc. (M)	solvent	T (°C)	yield (%) ^[a]	er	T (°C)	yield (%) ^[a]	er
1	2	0.5	PhMe	rt	91	60:40	rt	75	50:50
2	2	0.5	PhMe	0	69	60:40	0	86	50:50
3	2	0.5	PhMe	-20 °C	13	61:39	-20 °C	99	60:40
4	2	0.5	PhMe	-40 °C	nd	nd	-40 °C	99	60:40
5	5	0.5	PhMe	rt	70	61:39	-40 °C	93	61:39
6	2	1	PhMe	rt	64	58:42	-40 °C	99	56:44
7	2	0.05	PhMe	rt	26	61:39	-40 °C	41	62:38
8	2	0.5	CHCl ₃	rt	90	60:40	-40 °C	99	62:38
9	2	0.5	Et ₂ O	rt	86	60:40	-40 °C	86	62:38

With these reaction conditions in hand, a screening of IDPi catalysts employing a variety of aryl-substituents in the 3,3'-positions (Ar) and sulfonimidic residues in the core of the catalyst (R) (Scheme 4.17) was performed. In order to obtain a comprehensive overview of the electronic and steric effects of the substituents in the 3,3'-positions of the catalyst, aryl-groups having *ortho,meta*- (**47b** and **47g**), *mono-meta*- (**47c**), *para*-EDGs (**47d** and **47h**), and *para*-(**47e**) or *meta, meta*-EWGs (**47f** and **47i**) were tested in combination with CF₃- or C₆F₅- groups in the catalyst core. It could be shown that catalysts containing aromatic sulfonamide-derived cores afforded either lower yields (**47g**, 19% yield, full degradation of **38** to undefined

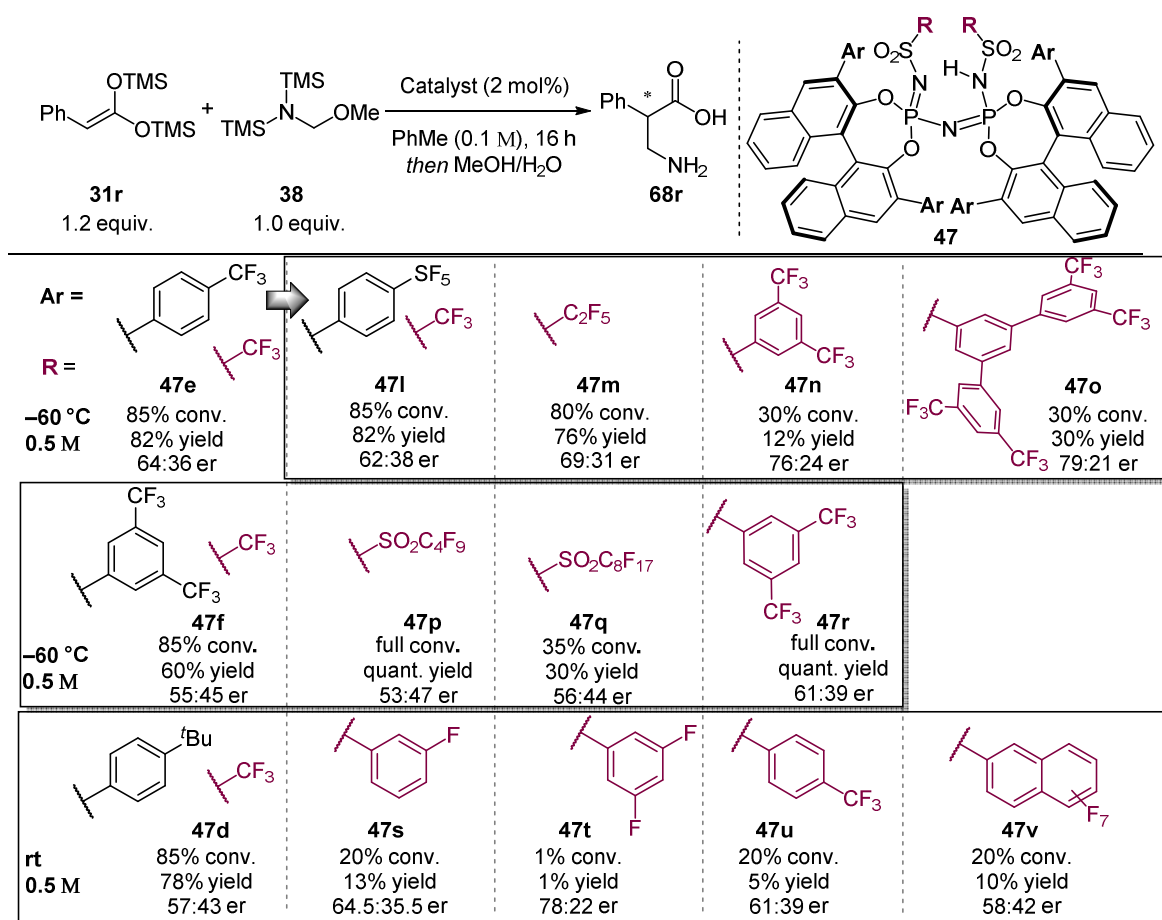
polymers according to ^1H NMR analysis of the crude reaction mixture) or lower enantioselectivity (**47i**, 50:50 er).



Scheme 4.17 Evaluation of different aromatic substituents in the 3,3'-positions (Ar) and cores (R). ^[a]Reactions quenched with Et₃N after 16 hours; ^[b]Reactions quenched with Et₃N after 3 days.

As no clear lead could not be identified due to the generally low obtained enantioselectivities, systematic investigations of each individual structural and electronic parameter were performed. Catalysts having electron-withdrawing *para*-substituents (**47e**), *meta,meta*-substituents (**47f**) and electron-donating *para*-substituents (**47d**) at the aryl-groups in the 3,3'-positions were combined with a variety of sulfonimidic substituents. Due to the high acidity and therefore increased

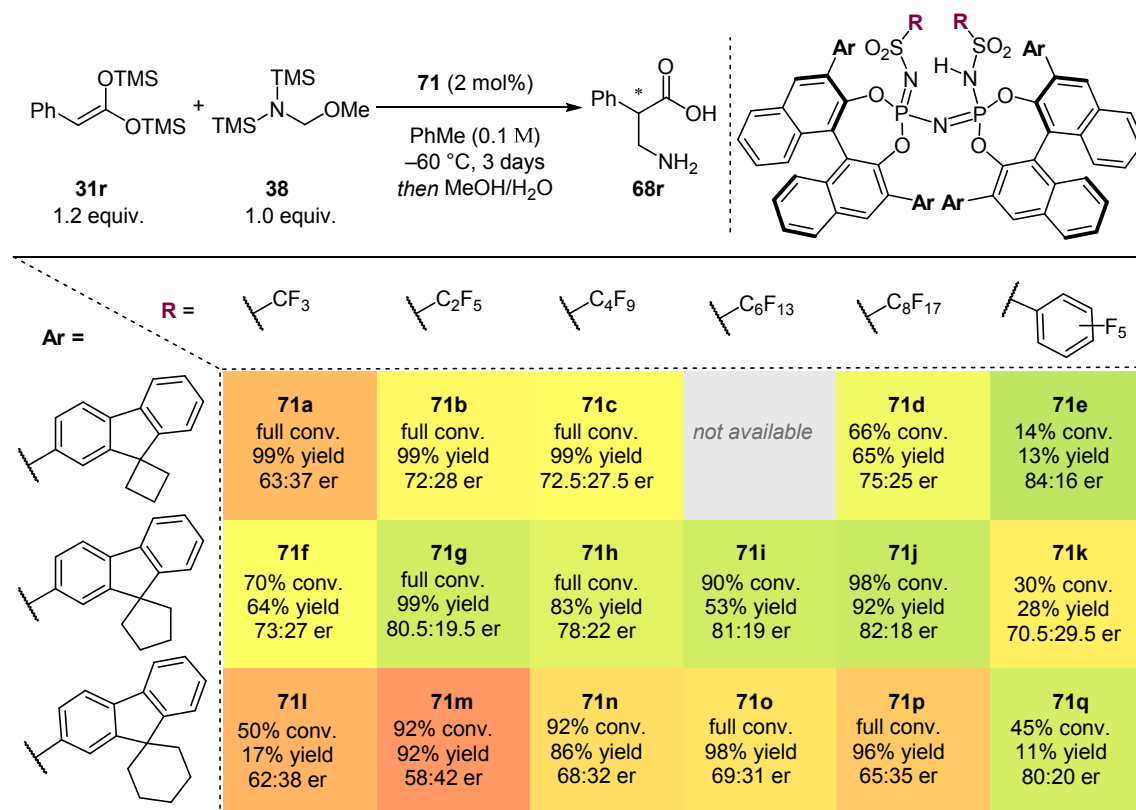
reactivity of the resulting IDP*s*, they were tested at $-60\text{ }^{\circ}\text{C}$, in contrast to catalysts (**47s–47v**) equipped with aromatic cores, which were tested at room temperature (Scheme 4.18). Changing the *p*-CF₃-substituent to a *p*-SF₅-group had no impact on the enantioselectivity (**47i**, 62:38 er). To our delight, modifications of the catalyst's core to a longer perfluorinated alkyl chain (**47m**, 69:31 er), to an electron-poor aryl group (**47n**, 76:24 er) or to an electron-poor terphenyl group (**47o**, 79:21 er) increased the enantiomeric excess of the desired product. Similar modifications of **47f** did not influence the enantioselectivity in the same amount (**47p**, 53:47 er and **47r**, 61:39 er), thus further catalysts in this series were not tested. The combination of *para-tert*-butyl-substituted aryl-groups in the 3,3'-positions and aromatic cores diminished the reactivity, however the enantioselectivity was increased (**47s**, 20% conv. and 64.5:35.5 er, **47t**, 1% conv. and 78:22 er, **47u**, 20% conv. and 61:39 er). Due to the low reactivity of the latter catalysts, the temperature had to be raised to room temperature in order to obtain some conversion of the starting material. IDP*i* **47s** in particular showed the same level of enantioselectivity under these reaction conditions as **47t** at $-60\text{ }^{\circ}\text{C}$, yet only with 1% yield. We therefore concluded that the catalyst should include electron-rich 3,3'-substituents; therefore, acidity and reactivity should be adjusted by suitable modification of the core. We envisioned that ideally we could identify a catalyst which would be reactive enough to allow us to improve enantioselectivity by decreasing the temperature.



Scheme 4.18 Evaluation of different cores for **47e**, **47f** and **47d**. NMR yield measured with mesitylene as internal standard.

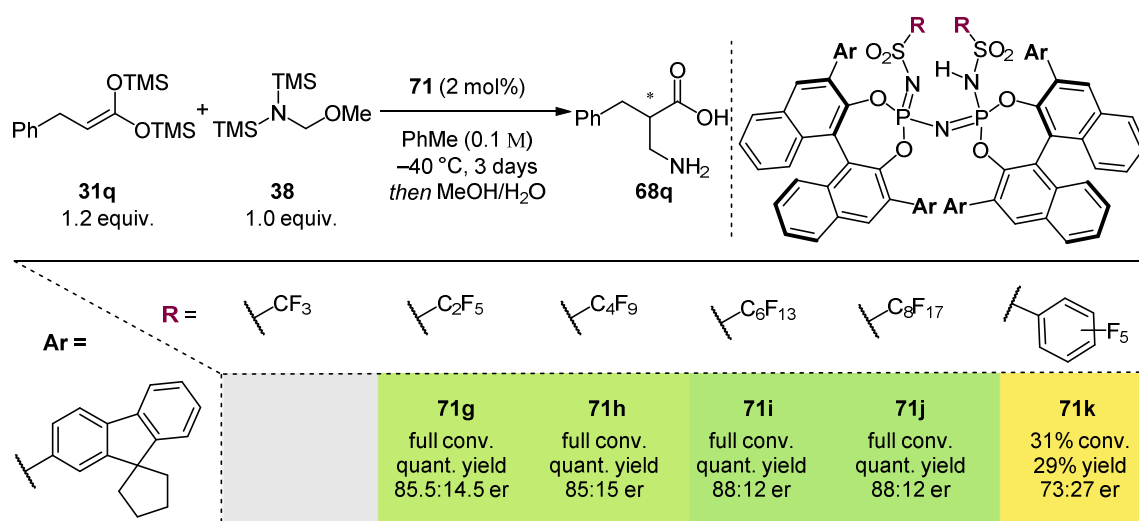
We identified 2-fluorenyl as a promising substituent at the 3,3'-positions of the IDP*i* catalyst (a selection of the tested catalysts is shown in Scheme 4.19). A library of catalysts consisting of (a) various perfluorinated alkyl-chains in the core and (b) fluorenyl-derived spiro-substituents were prepared and evaluated using *bis*-SKA **31r** as the starting material. Based on the obtained results, we concluded that an increased length of the perfluorinated alkyl chain leads to a slight increase in enantiomeric excess. When comparing different fluorenyl-substituents, the 5-membered ring-containing motif was consistently more selective than the other ones tested. Moreover, the majority of the catalysts afforded full conversion and quantitative yields within 3 days. The only catalysts that showed lower conversions were those containing a perfluorinated aromatic ring in the core (**48f**, **49f** and **50f**).

The best result within this series was obtained using the catalyst with the fluorenyl-3,3'-substituents **49** and $n\text{-C}_8\text{F}_{17}$ as perfluorinated alkyl chain in the core (**49e**), giving the desired product in 92% yield and 82:12 er.



Scheme 4.19 Screening of the fluorenyl-based IDPi library. NMR yield measured with mesitylene as internal standard given.

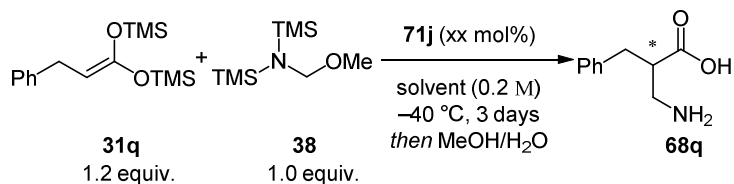
A similar series of screenings were performed using the aliphatic substrate **31q** (Scheme 4.20). To our delight, enantioselectivities obtained with this substrate were overall higher when compared with the aromatic *bis*-SKA **31a**. Nevertheless, this system follows the same trends as previously observed: Increased enantioselectivity was achieved upon elongation of the perfluorinated alkyl chain, reaching a maximum using $n\text{-C}_6\text{F}_{13}$ and $n\text{-C}_8\text{F}_{17}$ (88:12 er for both, **71i** and **71j**).



Scheme 4.20 Screening of 5-membered ring containing fluorenyl-derived IDPi catalysts with substrate **31q**. NMR yield measured with mesitylene as internal standard.

As the best catalyst (**71j**) strongly differs by means of sterics and electronics from the catalyst (**47f**) used for the initial optimization, we decided to reevaluate the reaction conditions by rescreening some crucial reaction parameters (Table 4.13). To our delight, using *n*-pentane (Entry 4) and *n*-hexane (Entry 5), the desired product was obtained in quantitative yield and improved enantioselectivity (93:7 er and 93.5:6.5 er respectively).

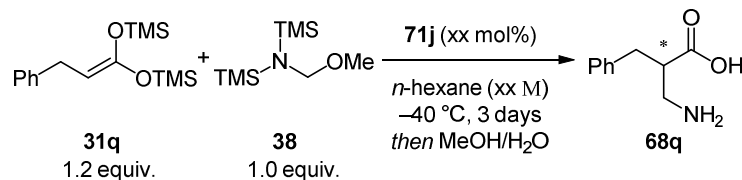
Table 4.13 Optimization of the reaction conditions using **71j**. ^[a] NMR yield measured with mesitylene as internal standard.



Entry	solvent	yield (%) ^[a]	er
1	PhMe	83	87:13
2	CyH	90	91.5:9.5
3	MeCy	99	93:7
4	<i>n</i> -pentane	99	93:7
5	<i>n</i> -hexane	90	93.5:6.5
6	<i>n</i> -heptane	97	93:7

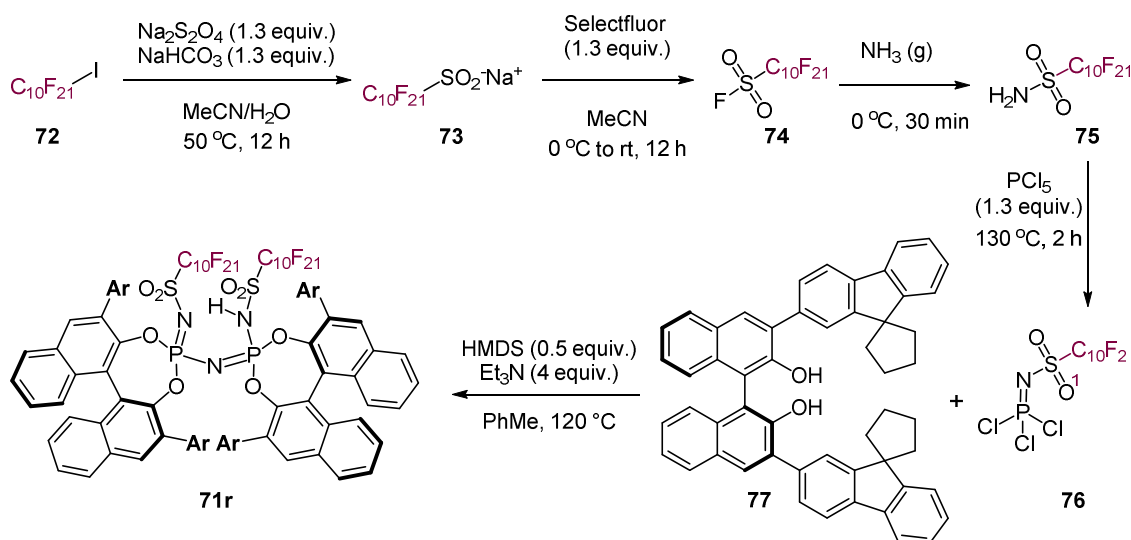
Regarding concentration and catalyst loading, we could confirm our previous findings with the catalytic system having an optimum at 0.2 M and 1 mol% of **71j** (Table 4.14, Entry 2). The use of lower catalyst loadings was possible without deterioration of the enantioselectivity; however, the reaction rate was reduced (Entry 6).

Table 4.14 Optimization of the reaction conditions using **71j**. ^[a] NMR yield measured with mesitylene as internal standard.



Entry	Conc. (M)	mol% 71j	yield (%) ^[a]	er
1	0.5	1	95	93:7
2	0.2	1	90	93.5:6.5
3	0.1	1	86	93.5:6.5
4	0.05	1	83	94:6
5	0.2	5	90	92:8
6	0.2	0.2	71	93.5:6.5

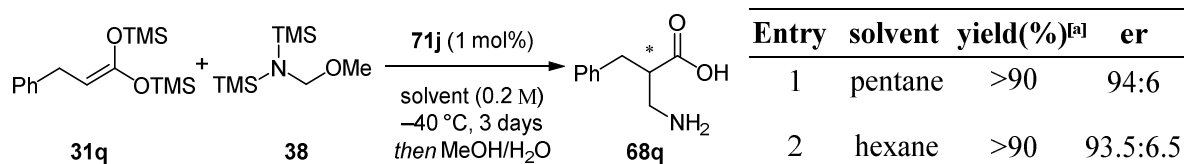
As the target level of enantioselectivity (> 95:5 er) could not be achieved by further optimization of the reaction conditions, we focused our attention back on optimizing the catalysts structure by further modification of core and/or the 3,3'-substituents. An easily accessible modification of the core was the extension of the length of the alkyl chain to *n*-C₁₀F₂₁ (Scheme 4.21). The required sulfonamide **75** was synthesized starting from the commercially available iodide **72** by first transforming it into the corresponding sulfinic acid **73**. Oxidation in the presence of an electrophilic fluorine source and subsequent treatment with ammonia gave **75**. Finally, catalyst **71r** could then be obtained using the established IDP*i* synthesis, by the reaction of phosphazene reagent **76**, resulting from the reaction of **75** and PCl₅, and BINOL-derivative **77**.



Scheme 4.21 Synthesis of $C_{10}F_{21}$ core-containing catalyst (**71r**).

Unfortunately, the newly designed core did not improve the enantioselectivity of the reaction (Table 4.15).

Table 4.15 Asymmetric aminomethylation using **71j**. ^[a] NMR yield measured with mesitylene as internal standard.



Due to low commercial availability of alternative precursors for synthesizing perfluorinated alkyl chains, we decided to focus on the modification of the fluorenyl substituents. However, before investing additional tedious efforts into multi-step synthesis of new catalysts, we initiated preliminary investigations of the reaction mechanism, aiming to identify strategic positions for modification.

4.2.3 Mechanistic Insights Lead to a New Catalyst Design

A proposed catalytic cycle is depicted in Figure 4.2, including a schematic representation of the catalyst in which the 3,3'-fluorenyl substituents are highlighted in black and the perfluoroalkyl chain on the sulfonimidic residue in purple. After the initial drying/self-healing cycle (introduced in Section 2.2.5.1), the key steps are (a) the activation of the electrophilic substrate (**38**), forming a tight ion pair between the anionic catalyst (**49f**) and the cationic electrophile (iminium ion **69**) and (b) the enantiodetermining step in which the *bis*-SKA **31q** attacks onto the electrophile, giving the silylated product (**79**) and the silylated catalyst (**78**).

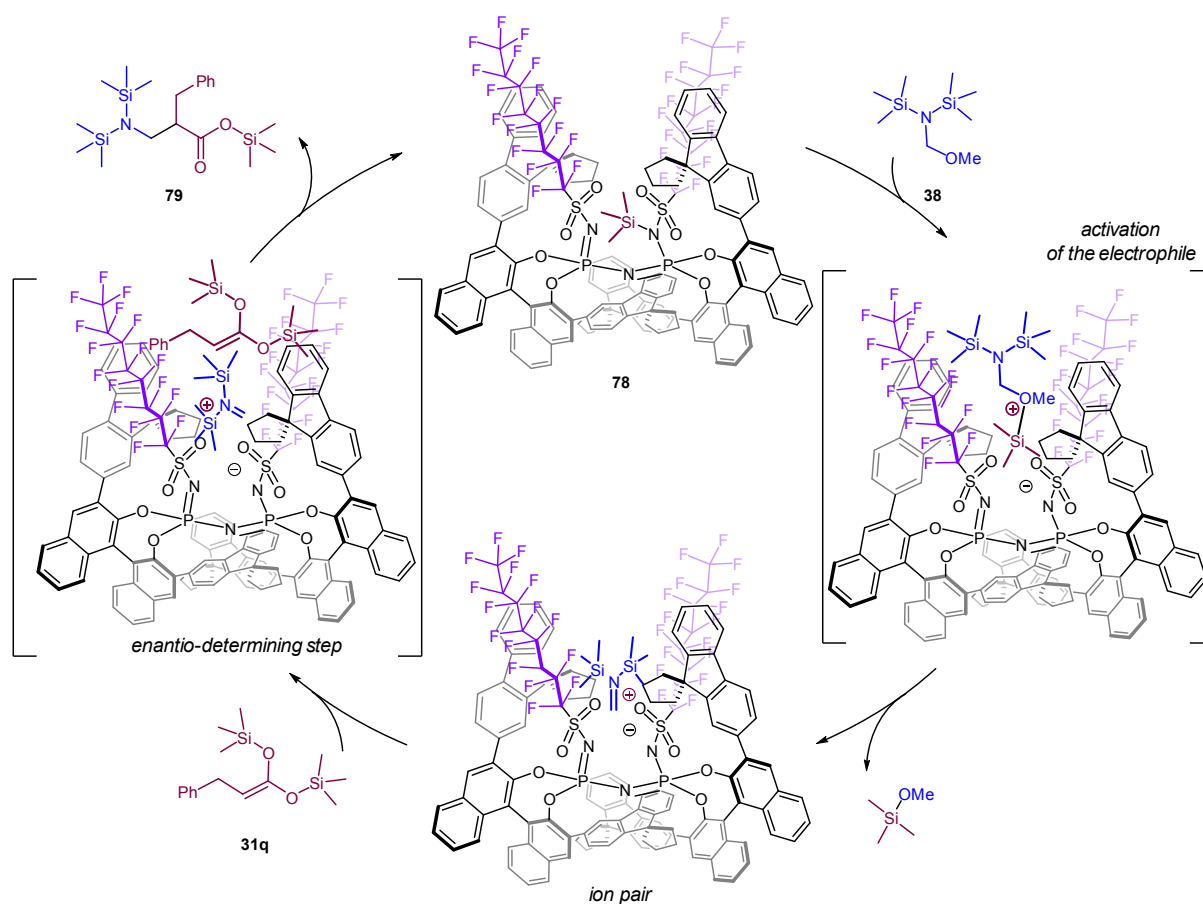
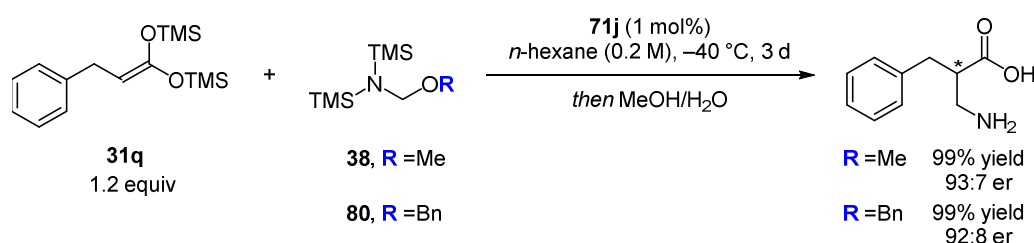


Figure 4.2 Proposed catalytic cycle.

In the first step, the silylium ion in the active site of the catalyst is attacked by the oxygen of the electrophile, and TMSOMe is liberated, leaving the *bis*-silylium iminium ion coordinated to the IDP*i*. In support of this mechanism, an additional aminomethylating reagent (**80**) was prepared and subjected to the reaction conditions. Following the proposed reaction mechanism, after the initial activation of **38** or **80**, the formed iminium ion (**69**) and the derived ion pair should be the same, and the enantioselectivity of the reaction should not be affected. Indeed, the use of **38** (R = Me) or **80** (R = Bn) afforded very similar enantioselectivities (93:7 er and 92:8 er, respectively) (Scheme 4.22).



Scheme 4.22 Preliminary mechanistic studies: use of **38** or **80** as aminomethylating reagent. NMR yields measured with mesitylene as internal standard given.

The proposed stereochemical model depicted in Figure 4.3 supports the observed trends in catalyst design, namely (a) a clear influence of the size of the spiro-cycle in the fluorenyl substituent (4, 5 or 6 membered ring) and (b) the influence of the perfluoroalkyl chain up to a certain length of the residue. Based on this model, we reasoned that introducing an additional EDG substituent in 7-position of the fluorenyl group might influence the enantioselectivity for two reasons: (1) an electron-rich aromatic unit could favor the stabilization of cation in the crucial ion pair, and (2) the additional steric bulk may remotely influence the access to the active site or the rearrangement of the neighboring groups.

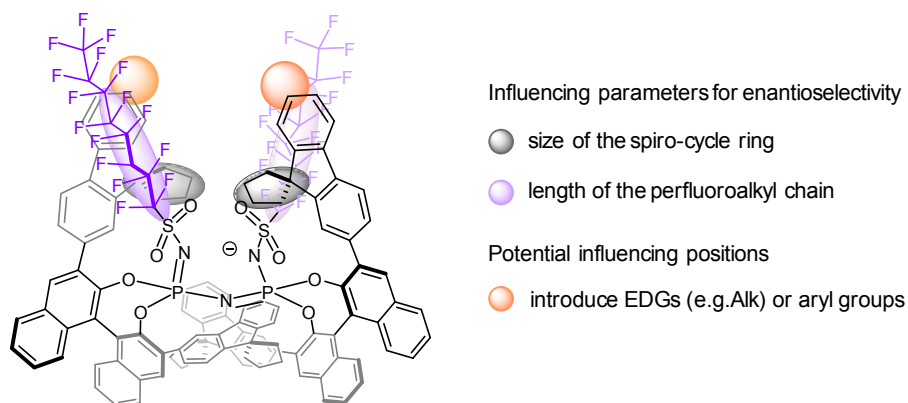
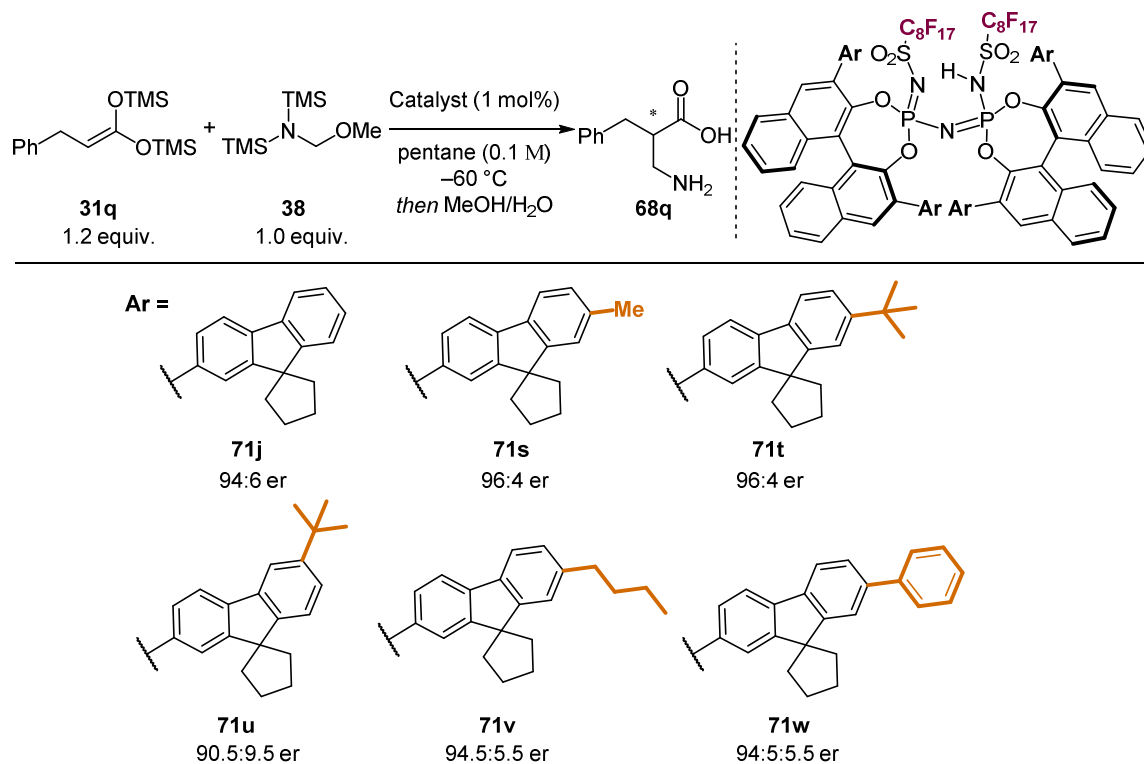


Figure 4.3 Proposed stereochemical model.

4.2.4 Final Catalyst Optimization

In order to validate these assumptions, a series of catalysts were prepared in which the fluorenyl-substituents were additionally substituted in either the 6- or 7-positions. C_8F_{17} were chosen as the substituents in the core (Scheme 4.23). To our delight, all the modifications performed in position 7 increased the enantioselectivity. A methyl group (**71s**) influenced the steric properties and the electron-density of the system enough giving the desired product in 96:4 er. The bulkier *tert*-butyl-substituted analogue resulted in the same enantiomeric excess (**71t**, 96:4 er) and a longer alkyl chain (**71v**) or a phenyl group (**71w**) did not afford the desired enantioselectivity (>95:5 er). Moreover, substitution in position 6 with a *tert*-butyl group even decreased the enantioselectivity to 90.5:9.5 er (**71u**).

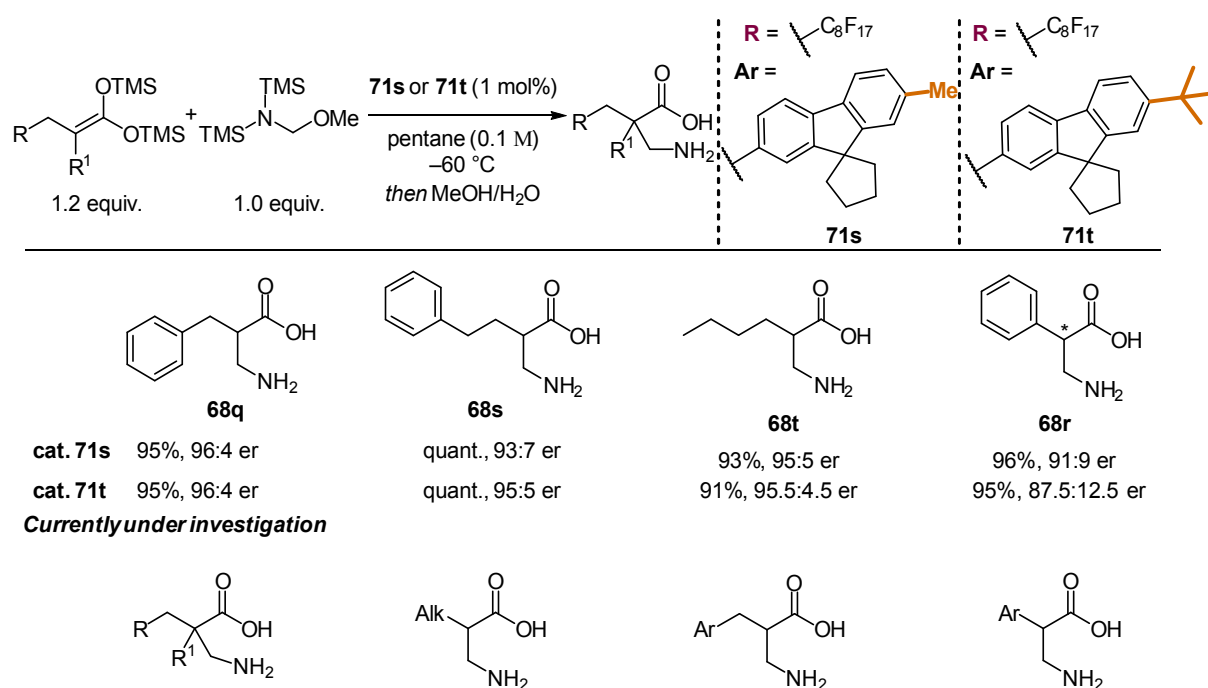
Results and Discussion



Scheme 4.23 Screening of 6- and 7-substituted fluorenyl derivatives.

4.2.5 Substrate Scope

Finally, with this set of catalysts in hand, we set out to explore the scope of this transformation. As this is currently under investigation in our laboratory, only preliminary results using IDPis **71s** and **71t** are depicted in Scheme 4.24. Both catalysts delivered the desired products in high yields (>90%), however their performances differ in selectivity. Whereas the *tert*-butyl-substituted catalyst **71t** delivered aliphatic substrates (R=Alk) in slightly higher enantioselectivities, the Me-substituted catalyst **71s** was better with the single tested aryl-substituted substrate **31a** (R=Ph).



Scheme 4.24 Preliminary substrate scope. NMR yields measured with mesitylene as internal standard given.

While this thesis is being written, experiments to fully investigate the discovered process are ongoing and are expected to lead to a successful completion of the project in due course.

4.2.6 Outlook and Conclusion

In summary, we have developed the first asymmetric organocatalytic α -aminomethylation of *bis*-SKAs, enabling direct access to unprotected β^2 -amino acids under Lewis acidic conditions. The newly designed catalyst, upon activation of the aminomethylating reagent, forms a tight ion pair with the *bis*-silylated iminium ion, formed *in situ*, and controls the enantiotopic differentiation of the nucleophilic *bis*-SKA. The enantioenriched silylated products are formed in quantitative yields and a mild acidic workup, or simply protic conditions, liberates the unprotected β^2 -amino acid. The final compounds can be isolated quantitatively upon precipitation and filtration, without additional purification steps. Currently, investigation of the generality of the developed method is under examination; the developed methodology will be applied in the synthesis of biologically active compounds, such as Alvimopan[®] and Rhopressa[®] (Figure 4.4).

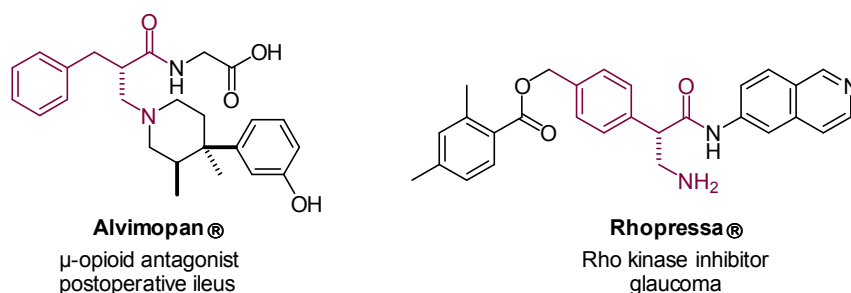
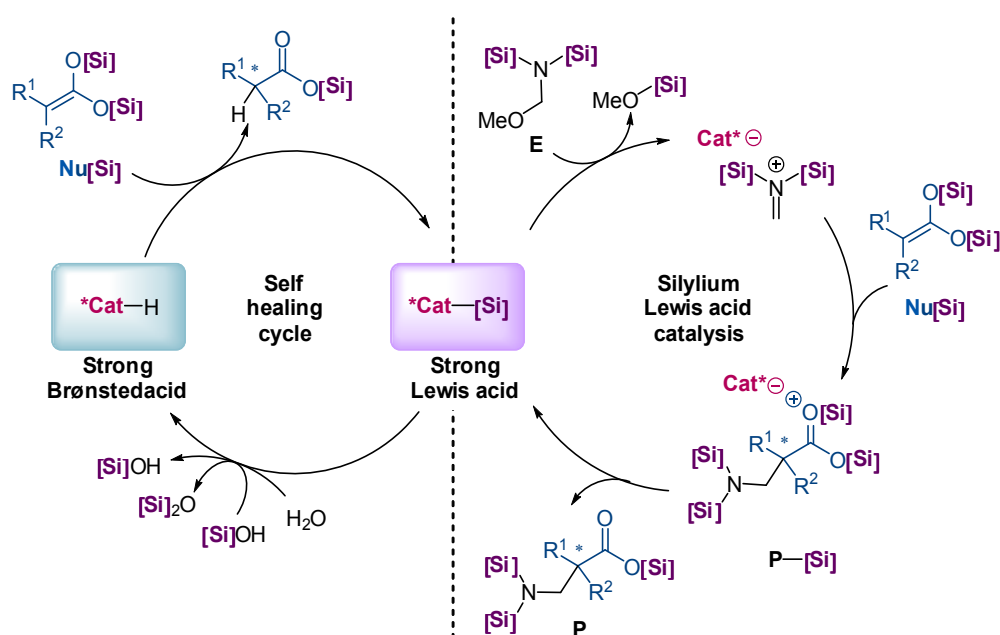


Figure 4.4 Candidates for the application of the developed enantioselective aminomethylation.

Summary

5 Summary

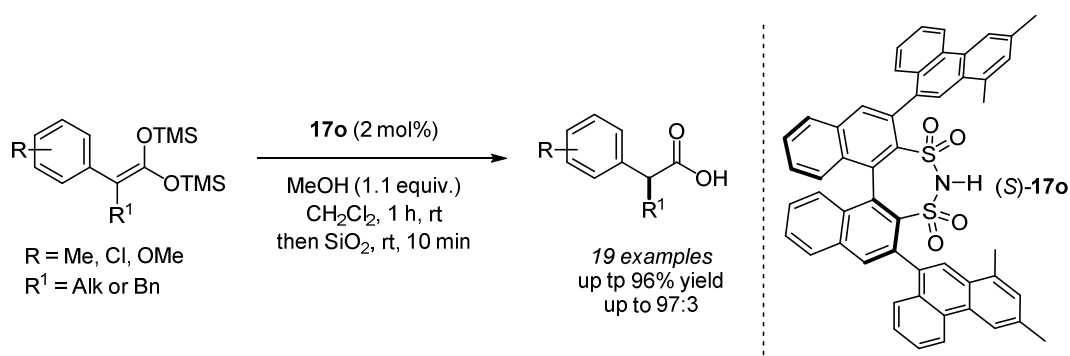
Strong Brønsted acids can be converted in strong Lewis acids upon silylation with a suitable reagent. This ambivalent feature was fully exploited in this thesis (Scheme 5.1).



Scheme 5.1 Enantioselective protonation and enantioselective aminomethylation of *bis*-SKAs.

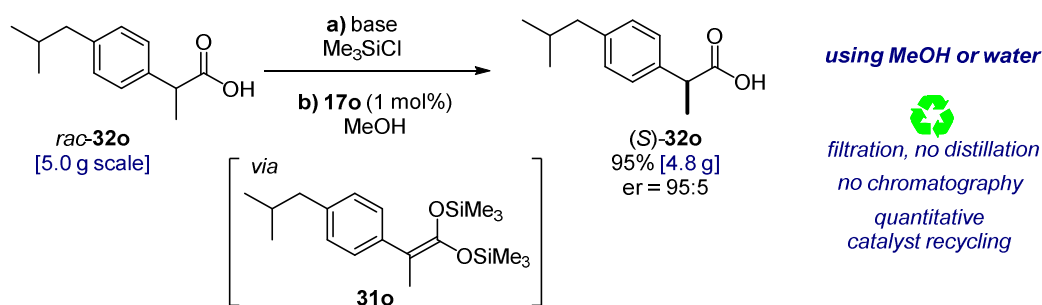
5.1 Catalytic Asymmetric α -Protonation with Water and α -Deuteration with D_2O

In the first part of this thesis, we exploited this cycle to protonate enantioselectively *bis*-SKAs using simple PSs (e.g. water). We showed that Brønsted acid DSI **17o** enabled the facial recognition of the *bis*-SKA and afforded the corresponding carboxylic acids in high yields and enantioselectivities (Scheme 5.2).



Scheme 5.2 Catalytic Asymmetric α -Protonation with a simple PS.

The application of this method in the late stage deracemization of Ibuprofen proved the potential and utility of this strategy (Scheme 5.3).



Scheme 5.3 Late stage deracemization of NSAIDs with DSI.

The greater advantage of this methodology relies on the possibility to use any PS; this enabled the use of D_2O or CD_3OD for the enantioselective deuteration of *bis*-SKAs and allowed an easier access to enantioenriched α -deuterated carboxylic acids. A particularly interesting substrate was **67c**, in which we introduced a stereogenic center upon deuteration (Figure 5.1). Further development of a highly enantioselective deuteration could open the access to this class of compounds, which is not particularly explored yet.

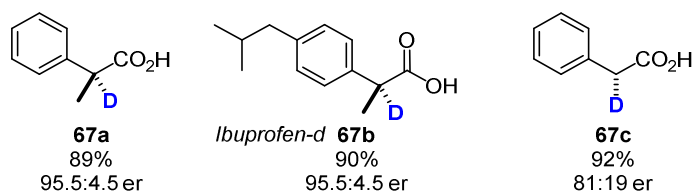


Figure 5.1 Enantioselective deuteration of *bis*-SKAs with CD_3OD .

5.2 Catalytic Asymmetric α -Aminomethylation

In the second part of this thesis, we exploited the Lewis acidity of the silylated IDPi **71s** for the *in situ* formation of a highly reactive protected iminium ion and subsequent reaction with a *bis*-SKA, affording unprotected β^2 -amino acids in an enantioselective fashion.

Until now, ACDC was widely applied in enantioselective transformations in which the activated electrophile would initially interact in a tight ion pair with the catalyst providing a chiral environment. Subsequently, the nucleophile preferentially attacks from one side onto the catalyst-electrophile complex, generating a stereogenic center on the former electrophile. However, this differs in the reported aminomethylation. While the activation of the electrophile follows the same logic, the stereogenic center formed by the attack of the nucleophile is located on the nucleophile itself (Figure 5.2). The targeted α -aminomethylation of *bis*-SKAs was achieved by using **71s** or **71t** as the Lewis acid catalyst. The unprotected β^2 -amino acids were obtained in quantitative yields and high enantioselectivities.

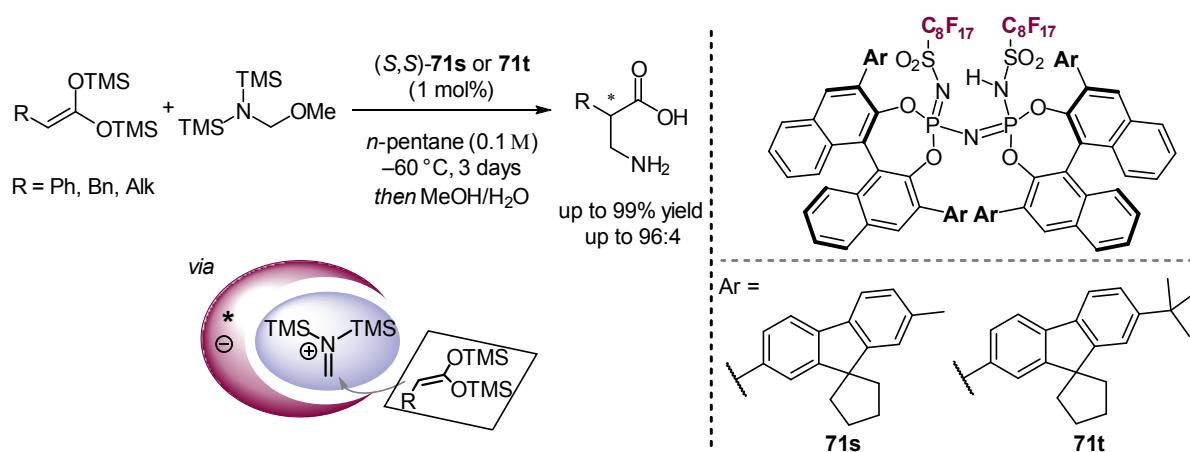


Figure 5.2 Enantioselective α -aminomethylation of *bis*-SKAs.

6 Outlook

We have demonstrated that *bis*-SKAs are valuable intermediates for the enantioselective α -functionalization of carboxylic acids. As mentioned in section 2.3.1, a wide selection of transformations have been reported in a non-asymmetric fashion. We believe that ACDC is a powerful concept that could enable access to their enantioselective equivalents. Among the many possible functionalizations, we envisioned a few interesting, yet very challenging, transformations:

(1) The α -amination of *bis*-SKAs, to access α -amino acids directly from the corresponding carboxylic acid. Unfortunately, a successful catalytic system has not been identified yet, since the selection of the electrophilic nitrogen source is crucial for the turnover of the catalyst. Particularly, under Lewis acidic conditions, any Lewis basic functionality (such as amines) forms stable salts with the catalyst and inhibits its reactivity.

(2) The α -trifluoromethylation of *bis*-SKAs, to directly access the enantioenriched α -trifluoromethylated carboxylic acids. In initial experiments we found that this transformation is possible under catalytic Lewis acidic conditions, however, only low enantioselectivity was observed. A highly Lewis acidic catalyst is required in order to outcompete the radical mechanism. Furthermore, the nature of the electrophilic trifluoromethylating reagent highly influences the reactivity and feasibility of the transformation.

This thesis opens the field of enantioselective Lewis acid-catalyzed α -functionalizations of carboxylic acids *via* the formation of *bis*-SKAs intermediates. Ideally, an enantioselective catalytic system could be envisioned for each of the transformations previously reported in Section 2.3.1, exploiting the ACDC concept (Figure 6.1), in which the enantiopure Lewis acidic catalyst could control the formation of the positively charged electrophilic reagent and the nucleophilic attack by the *bis*-SKA.

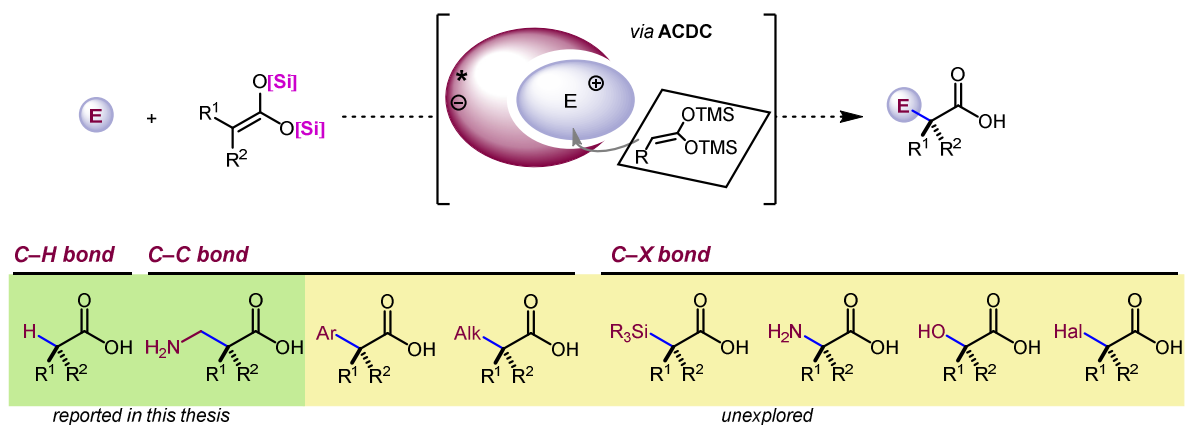


Figure 6.1 Potentially-accessible compounds from *bis*-SKAs upon asymmetric transformations.

Outlook

7 Experimental Section

7.1 General Information and Instrumentation

Chemicals

Chemicals (Abcr, Acros, Aldrich, Gelest, Fluka, Fluorochem, Strem, TCI) were purchased as reagent grade and used without further purification unless indicated otherwise. Commercially available carboxylic acids were purchased from Sigma-Aldrich, Alfa Aesar, Acros Organics, AK Scientific, Apollo Scientific, Key Organics and Aronis. *n*-Butyllithium was purchased from Sigma-Aldrich (2.5 M solution in hexanes) and used directly as received. The reagent was titrated before use.

Solvents

Solvents (CH₂Cl₂, CHCl₃, Et₂O, THF, PhMe) were dried by distillation from an appropriate drying agent in the technical department of the Max-Planck-Institut für Kohlenforschung and received in Schlenk flasks under argon. Other solvents (acetone, benzene, cyclohexane, chlorobenzene, 1,4-dioxane, DME, DMF, DMSO, EtOAc, EtOH, MeCN, MeOH, MTBE, NMP, *n*-Bu₂O, *n*-hexane, *n*-octane, *n*-pentane, pyridine, xylenes) were purchased from commercial suppliers and dried over molecular sieves.

Inert Gas

Dry argon was purchased from Air Liquide with >99.5% purity.

Glassware

All non-aqueous reactions were performed in oven-dried (85 °C) or flame-dried glassware under Argon. Solvents were removed under reduced pressure at 40 °C using a rotary evaporator and drying under high vacuum (10⁻³ mbar).

Thin Layer Chromatography

Thin layer chromatography (TLC) was performed using silica gel pre-coated plastic sheets (Polygram SIL G/UV254, 0.2 mm, with fluorescent indicator; Macherey-Nagel), which were visualized with a UV lamp (254 or 366 nm) and phosphomolybdic acid (PMA). PMA stain: PMA (20 g) in EtOH (200 mL). Preparative thin-layer chromatography was performed on silica gel pre-coated glass plates SIL G-25 UV254 and SIL G-100 UV254, with 0.25 mm and 1.0 mm SiO₂ layers, respectively (Macherey-Nagel).

Flash Column Chromatography

Flash column chromatography (FCC) was carried out using Merck silica gel (60 Å, 230–400 mesh, particle size 0.040–0.063 mm) using technical grade solvents. Elution was accelerated using compressed air. All reported yields, unless otherwise specified, refer to spectroscopically and chromatographically pure compounds.

Nomenclature

Nomenclature follows the suggestions proposed by the computer program ChemBioDraw (15.0.0.106) of CBD/Cambridgesoft.

Nuclear Magnetic Resonance Spectroscopy

¹H, ¹³C, ¹⁹F, ³¹P nuclear magnetic resonance (NMR) spectra were recorded on a Bruker AV-500, AV-400 or DPX-300 spectrometer in a suitable deuterated solvent. The employed solvent and respective measuring frequencies are indicated for each experiment. Chemical shifts are reported with tetramethylsilane (TMS) serving as a universal reference of all nuclides and with two or one digits after the marker. The resonance multiplicity is described as s (singlet), d (doublet), t (triplet), q (quadruplet), p (pentet), hept (heptet), m (multiplet), and br (broad). All spectra were recorded at 298 K unless otherwise noted, processed with Bruker TOPSPIN 2.1 or MestReNova 11.0.2 suite of programs, and coupling constants are reported as observed. The

residual deuterated solvent signals relative to tetramethylsilane were used as the internal reference in ^1H NMR spectra (e.g. $\text{CDCl}_3 = 7.26$ ppm), and are reported as follows: chemical shift δ in ppm (multiplicity, coupling constant J in Hz, number of protons). ^{13}C , ^{19}F , ^{31}P NMR spectra were referenced according to Ξ - values (IUPAC recommendations 2008) relative to the internal references set in ^1H NMR spectra (e.g. ^{13}C : Me_4Si , ^{19}F : CCl_3F , ^{31}P : H_3PO_4 ; each 0.00 ppm). All spectra are broadband decoupled unless otherwise noted.

Mass Spectrometry

Electron impact (EI) mass spectrometry (MS) was performed on a Finnigan MAT 8200 (70 eV) or MAT 8400 (70 eV) spectrometer. Electrospray ionization (ESI) mass spectrometry was conducted on a Bruker ESQ 3000 spectrometer. High resolution mass spectrometry (HRMS) was performed on a Finnigan MAT 95 (EI) or Bruker APEX III FTMS (7T magnet, ESI). The ionization method and mode of detection employed is indicated for the respective experiment and all masses are reported in atomic units per elementary charge (m/z) with an intensity normalized to the most intense peak.

Specific Rotations

Specific rotations were measured with a Rudolph RA Autopol IV Automatic Polarimeter at the indicated temperature with a sodium lamp (sodium D line, $\lambda = 589$ nm). Measurements were performed in an acid-resistant 1 mL cell (50 mm length) with concentrations ($\text{g}/(100 \text{ mL})$) reported in the corresponding solvent.

High Performance Liquid Chromatography

High performance liquid chromatography (HPLC) was performed on Shimadzu LC-20AD liquid chromatograph (SIL-20AC auto sampler, CMB-20A communication bus module, DGU-20A5 degasser, CTO-20AC column oven, SPD-M20A diode array detector), Shimadzu LC-20AB liquid chromatograph (SIL-20ACHT auto sampler, DGU-20A5 degasser, CTO-20AC column oven, SPD-M20A diode array detector), or

Shimadzu LC-20AB liquid chromatograph (reverse phase, SIL-20A auto sampler, CTO-20AC column oven, SPD-M20A diode array detector) using Daicel columns with a chiral stationary phase. All solvents used were HPLC-grade solvents purchased from Sigma-Aldrich. The column employed and respective solvent mixtures are indicated for each experiment.

Preparative High Performance Liquid Chromatography

Preparative high performance liquid chromatography (Prep-HPLC) was performed on a Shimadzu LC-8A/10A liquid chromatograph (FRC-10A fraction collector, SPD-10-AVP diode array detector). All solvents used were HPLC-grade solvents purchased from Sigma-Aldrich. The column employed and respective solvent mixtures are indicated for each experiment.

Gas Chromatography

Gas chromatography (GC) analyses on a chiral stationary phase were performed on HP 6890 and 5890 series instruments (split-mode capillary injection system, flame ionization detector (FID), hydrogen carrier gas). All the analyses were conducted in the GC department of the Max-Planck-Institut für Kohlenforschung. The conditions employed are described in detail in the individual experiments.

Gas Chromatography Mass Spectroscopy

Gas chromatography-mass spectrometry (GC-MS) analyses were recorded on an Agilent Technologies 6890N Network GC System equipped with a 5973 Mass Selective Detector, Gerstel Multi-Purpose Sampler MPS2, and a Macherey-Nagel Optima 5 column (30 m length, 0.25 mm i. D.), and an Agilent Technologies 7890A GC System equipped with a 5975C VL MSD mass selective detector, Gerstel Multi-Purpose Sampler MPS2, and a Macherey-Nagel Optima 5 column (30 m length, 0.25 mm i.D.).

Liquid Chromatography Mass Spectrometry

Liquid chromatography-mass spectrometry (LC-MS) was performed on a Shimadzu LC-MS 2020 liquid chromatograph. All solvents used were HPLC-grade solvents purchased from Sigma-Aldrich. The column employed, the respective solvent mixture, and the MS parameters are indicated for each experiment.

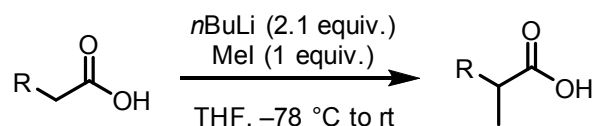
Experimental Section

7.2 Asymmetric α -Protonation with H_2O and α -Deuteration with D_2O

7.2.1 Synthesis and Characterization of Racemic Carboxylic Acids

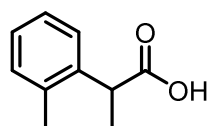
Non-commercially available carboxylic acids were prepared following a reported procedure.^[10a]

General Procedure A



n-BuLi (2.54 M in hexanes, 2.1 equiv.) was added dropwise to a solution of acid (1.0 equiv.) in THF (0.2 M) at $-78\text{ }^\circ\text{C}$ and the reaction mixture was allowed to stir at this temperature for 15 min. Methyl iodide (1.0 equiv., neat) was added to the reaction mixture dropwise over 10 min. The reaction was allowed to stir and warm to room temperature overnight. The reaction was quenched with sat. $\text{NH}_4\text{Cl}_{(\text{aq})}$ solution. After 5 min, the reaction mixture was diluted with diethyl ether. The aqueous layer was extracted with diethyl ether (x3). The combined organic layers were washed with sat. $\text{Na}_2\text{S}_2\text{O}_3_{(\text{aq})}$ solution until the organic phase turns to transparent, then washed with brine, dried with magnesium sulfate, concentrated under reduced pressure, and the solid residue was purified by flash column chromatography (SiO_2 , dichloromethane/methanol = 95:5).

2-(2-methylphenyl)propanoic acid (32e)



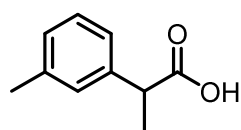
Prepared according to general procedure **A** using *o*-Tolylacetic acid (4.8 g, 32 mmol) and obtained as a colorless solid (4.95 g, 30.1 mmol, 93% yield).

^1H NMR (501 MHz, CDCl_3) δ = 7.29 (d, J = 7.2 Hz, 1H), 7.23–7.15 (m, 3H), 3.99 (q, J = 7.1 Hz, 1H), 2.38 (s, 3H), 1.50 ppm (d, J = 7.1 Hz, 3H), [acid proton not visible due to fast exchange].

^{13}C NMR (126 MHz, CDCl_3) δ = 179.69, 138.33, 135.89, 130.56, 127.21, 126.55, 126.47, 40.96, 19.63, 17.56 ppm.

HRMS (GC–EI) m/z calculated for $\text{C}_{10}\text{H}_{12}\text{O}_2$ [M–H]: 164.0832; found 164.0837.

2-(3-methylphenyl)propanoic acid (32f)



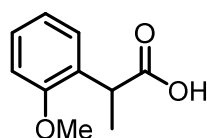
Prepared according to general procedure **A** using *m*-Tolylacetic acid (4.8 g, 32 mmol) and obtained as a colorless solid (4.75 g, 28.9 mmol, 89% yield).

^1H NMR (501 MHz, CDCl_3) δ = 7.26–7.14 (m, 1H), 7.16–7.02 (m, 3H), 3.71 (q, J = 7.2 Hz, 1H), 2.35 (s, 3H), 1.50 ppm (s, 3H), [acid proton not visible due to fast exchange].

^{13}C NMR (126 MHz, CDCl_3) δ = 167.33, 139.72, 138.38, 128.59, 128.28, 128.16, 124.58, 45.05, 21.41, 18.16 ppm.

HRMS (GC–EI) m/z calculated for $\text{C}_{10}\text{H}_{12}\text{O}_2$ [M–H]: 164.0832; found 164.0837.

2-(2-methoxyphenyl)propanoic acid (32m)



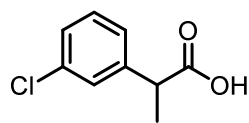
Prepared according to general procedure **A** from 2-methoxyphenylacetic acid (5.39 g, 32.4 mmol) and obtained as a colorless solid (5.31 g, 29.5 mmol, 90% yield).

^1H NMR (501 MHz, CDCl_3) δ = 7.37–7.15 (m, 2H), 6.96 (td, J = 7.5, 1.1 Hz, 1H), 6.89 (dd, J = 8.7, 1.1 Hz, 1H), 4.09 (q, J = 7.2 Hz, 1H), 3.84 (s, 3H), 1.49 ppm (d, J = 7.2 Hz, 3H), [acid proton not visible due to fast exchange].

^{13}C NMR (126 MHz, CDCl_3) δ = 156.78, 128.54, 128.16, 121.04, 110.92, 77.41, 76.91, 55.68, 39.10, 16.94 ppm.

HRMS (GC–EI) m/z calculated for $\text{C}_{10}\text{H}_{12}\text{O}_3$ [M–H]: 180.0781; found 180.0781.

2-(*m*-chlorophenyl)propanoic acid (32i)



Prepared according to general procedure **A** using 4-Chlorophenylacetic acid (5.0 g, 29.3 mmol) and obtained as a colorless solid (3.54 g, 19.2 mmol, 65% yield).

¹H NMR (501 MHz, CDCl₃) δ = 7.32 (s, 1H), 7.28–7.24 (m, 3H), 7.23–7.18 (m, 1H), 3.72 (q, J = 7.2 Hz, 1H), 1.52 ppm (d, J = 7.2 Hz, 3H).

¹³C NMR (126 MHz, CDCl₃) δ = 179.00, 141.57, 134.50, 129.92, 127.85, 127.65, 125.87, 44.89, 18.05 ppm.

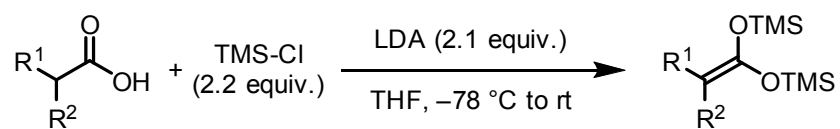
HRMS (GC–EI) m/z calculated for C₉H₉O₂ClNa [M–Na]: 207.0183; found 207.0183.

7.2.2 Synthesis and Characterization of *bis*-Silyl Ketene Acetals

Preparation of lithium diisopropyl amine (LDA) solution: To a stirring solution of freshly distilled diisopropyl amine (DPA; 50 mmol, 7.0 mL, 1.0 equiv.) in THF (21 mL, 1 M) under an atmosphere of argon, *n*-BuLi (2.45 M solution in hexane, 52.5 mmol, 24.5 mL, 1.05 equiv.) was added dropwise at –78 °C and the resulting reaction mixture was stirred for additional 30 min at this temperature.

Note. *n*-BuLi was freshly titrated.

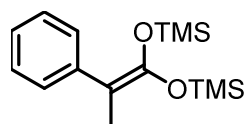
General Procedure B



A stirring solution of acid (30.0 mmol, 1.0 equiv.) and Me₃SiCl (4.6 mL, 33.0 mmol, 2.2 equiv.) in THF (12 mL) under an atmosphere of argon was cooled to –78 °C. The LDA solution (2.1 equiv.) was added *via* cannula. The cooling bath was removed after complete addition and the reaction solution was stirred for 1 hour at room temperature. The reaction mixture was concentrated *in vacuo*, and then hexane (50 mL) was added to the residue and was filtered under an atmosphere of argon. After concentration under reduced pressure, the crude product was purified by

distillation under reduced pressure to afford the disilyl ketene acetal as colorless liquids, which were stored in Schlenk flasks under an atmosphere of argon at 4 °C.

2-Methyl-2-phenyl-1,1-bis(trimethylsilyloxy)ethane (31a)



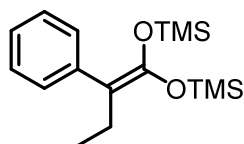
Prepared according to general procedure **B** using 2-phenylpropionic acid (6.0 g, 40.0 mmol) and obtained after distillation (bp = 65 °C at 5×10^{-2} mbar) as colorless liquid (8.6 g, 29.0 mmol, 73% yield).

^1H NMR (501 MHz, CD_2Cl_2) δ = 7.39–7.34 (m, 2H), 7.26–7.19 (m, 2H), 7.11–7.03 (m, 1H), 1.89 (s, 3H), 0.27 (s, 9H), –0.05 ppm (s, 9H).

^{13}C NMR (126 MHz, CD_2Cl_2) δ = 148.17, 142.51, 129.34, 129.34, 128.27, 128.27, 125.44, 95.09, 17.13, 0.90, 0.53 ppm.

HRMS (ESI) m/z calculated for $\text{C}_{15}\text{H}_{26}\text{O}_2\text{Si}_2$ $[\text{M}+\text{H}]^+$: 295.1544; found 295.1544.

3-Ethyl-2-phenyl-1,1-bis(trimethylsilyloxy)ethane (31b)



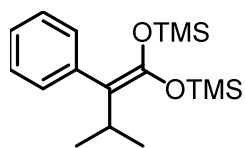
Prepared according to general procedure **B** using 2-phenylbutanonic acid (5.0 g, 30.5 mmol) and obtained after distillation (bp = 71 °C at 5×10^{-2} mbar) as a colorless liquid (7.2 g, 23.0 mmol, 76% yield).

^1H NMR (501 MHz, CD_2Cl_2) δ = 7.34–7.26 (m, 2H), 7.23 (dd, J = 8.5, 6.9 Hz, 2H), 7.13–7.05 (m, 1H), 2.37 (q, J = 7.5 Hz, 2H), 0.90 (t, J = 7.4 Hz, 3H), 0.28 (s, 9H), –0.09 ppm (s, 9H).

^{13}C NMR (126 MHz, CD_2Cl_2) δ = 147.20, 140.78, 129.71, 129.71, 127.81, 127.81, 125.14, 101.66, 23.85, 13.59, 0.15, –0.04 ppm.

HRMS (ESIpos) m/z calculated for $\text{C}_{16}\text{H}_{28}\text{O}_2\text{Si}_2$ $[\text{M}+\text{H}]^+$: 309.1701; found 309.1702.

3-Isopropyl-2-phenyl-1,1-bis(trimethylsilyloxy)ethane (31c)



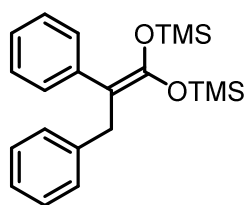
Prepared according to general procedure **B** using 3-methyl-2-phenylbutyric acid (4.0 g, 22.4 mmol) and obtained after distillation (bp = 86 °C at 5×10^{-2} mbar) as a colorless liquid (5.0 g, 15.5 mmol, 69% yield).

$^1\text{H NMR}$ (501 MHz, CD_2Cl_2) δ = 7.27–7.21 (m, 2H), 7.21–7.10 (m, 3H), 2.91 (hept, J = 7.0 Hz, 1H), 0.94 (d, J = 7.0 Hz, 6H), 0.27 (s, 9H), –0.15 ppm (s, 9H).

$^{13}\text{C NMR}$ (126 MHz, CD_2Cl_2) δ = 146.68, 139.45, 132.08, 132.08, 127.90, 127.90, 126.13, 106.27, 29.28, 22.32, 22.32, 0.64, 0.16 ppm.

HRMS (ESI) m/z calculated for $\text{C}_{17}\text{H}_{30}\text{O}_2\text{Si}_2$ $[\text{M}+\text{H}]^+$: 323.1857; found 323.1857.

3-Benzyl-2-phenyl-1,1-bis(trimethylsilyloxy)ethane (31d)



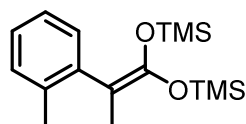
Prepared according to general procedure **B** using 2,3-diphenylpropionic acid (4.0 g, 17.7 mmol) and obtained after distillation (bp = 110 °C at 5×10^{-2} mbar) as a colorless liquid (5.3 g, 14.3 mmol, 43% yield).

$^1\text{H NMR}$ (501 MHz, CD_2Cl_2) δ = 7.30–7.25 (m, 2H), 7.23–7.14 (m, 6H), 7.13–7.07 (m, 1H), 7.07–7.01 (m, 1H), 3.72 (s, 2H), 0.24 (s, 9H), –0.04 (s, 9H) ppm.

$^{13}\text{C NMR}$ (126 MHz, CD_2Cl_2) δ = 149.60, 142.62, 141.18, 129.85, 129.85, 128.95, 128.95, 128.52, 128.52, 128.09, 128.09, 125.93, 125.46, 98.65, 37.09, 0.75, 0.38 ppm.

HRMS (ESI) m/z calculated for $\text{C}_{21}\text{H}_{30}\text{O}_2\text{Si}_2$ $[\text{M}+\text{H}]^+$: 371.1857; found 371.1858.

2-(2-methylphenyl)-2-methyl-1,1-bis(trimethylsilyloxy)ethane (31e)



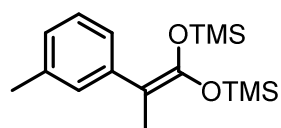
Prepared according to general procedure **B** using 2-(*o*-tolyl)propanoic acid (1.8 g, 10.7 mmol) and obtained after distillation (bp = 68 °C at 5×10^{-2} mbar) as a colorless liquid (2.2 g, 7.1 mmol, 67% yield).

¹H NMR (501 MHz, CD₂Cl₂) δ = 7.21–6.98 (m, 4H), 2.24 (s, 3H), 1.80 (s, 3H), 0.27 (s, 9H), 0.16 (s, 9H) ppm.

¹³C NMR (126 MHz, CD₂Cl₂) δ = 146.54, 141.69, 137.60, 130.69, 130.19, 126.35, 125.60, 94.00, 20.30, 18.02, 0.80, 0.13 ppm.

HRMS (GC–Cl) m/z calculated for C₁₆H₂₈O₂Si₂[M]: 308.1622; found 308.1619.

2-*m*-Tolyl-2-methyl-1,1-bis(trimethylsilyloxy)ethane (31f)



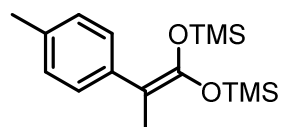
Prepared according to general procedure **B** using 2-(*m*-tolyl)propanoic acid (1.3 g, 7.6 mmol) and obtained after distillation (bp = 65 °C at 5 x 10⁻² mbar) as a colorless liquid (1.5 g, 4.8 mmol, 64% yield).

¹H NMR (501 MHz, CD₂Cl₂) δ = 7.21 (d, J = 1.8, 1H), 7.18–7.06 (m, 2H), 6.94–6.81 (m, 1H), 2.30 (s, 3H), 1.87 (s, 3H), 0.27 (s, 9H), –0.04 (s, 9H) ppm.

¹³C NMR (126 MHz, CD₂Cl₂) δ = 147.56, 141.80, 137.11, 129.62, 127.65, 125.74, 125.64, 94.53, 21.47, 16.66 ppm.

HRMS (GC–Cl) m/z calculated for C₁₆H₂₈O₂Si₂ [M]: 308.1622; found 308.1620.

2-*p*-Tolyl-2-methyl-1,1-bis(trimethylsilyloxy)ethane (31g)



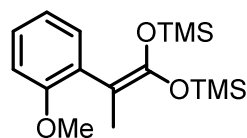
Prepared according to general procedure **B** using 2-(*p*-tolyl)propanoic acid (1.5 g, 9.4 mmol) and obtained after distillation (bp = 67 °C at 5 x 10⁻² mbar) as a colorless liquid (2.0 g, 6.5 mmol, 68% yield).

¹H NMR (501 MHz, CD₂Cl₂) δ = 7.28–7.22 (m, 2H), 7.09–7.02 (m, 2H), 2.29 (s, 3H), 1.86 (s, 3H), 0.27 (s, 9H), –0.07 (s, 9H) ppm.

¹³C NMR (126 MHz, CD₂Cl₂) δ = 147.63, 139.13, 134.67, 128.87, 128.87, 128.70, 128.70, 94.63, 21.28, 16.93, 0.66, 0.34 ppm.

HRMS (GC–Cl) m/z calculated for C₁₆H₂₈O₂Si₂ [M]: 308.1622; found 308.1619.

2-*o*-Methoxyphenyl-2-methyl-1,1-bis(trimethylsilyloxy)ethane (31m)



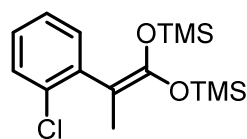
Prepared according to general procedure **B** using 2-(*o*-methoxyphenyl)propanoic acid (1.7 g, 10.6 mmol) and obtained after distillation (bp = 98 °C at 5×10^{-2} mbar) as a colorless liquid (1.5 g, 4.6 mmol, 43% yield).

^1H NMR (501 MHz, CD_2Cl_2) δ = 7.17–7.09 (m, 2H), 6.87–6.81 (m, 2H), 3.77 (s, 3H), 1.77 (s, 3H), 0.27 (s, 9H), –0.14 ppm (s, 9H).

^{13}C NMR (126 MHz, CD_2Cl_2) δ = 158.50, 147.40, 132.69, 127.87, 120.80, 111.52, 92.84, 55.95, 17.20, 0.90, 0.35 ppm.

HRMS (GC–Cl) m/z calculated for $\text{C}_{16}\text{H}_{28}\text{O}_3\text{Si}_2$ [M]: 324.1566; found 324.1572.

2-*o*-Chlorophenyl-2-methyl-1,1-bis(trimethylsilyloxy)ethane (31h)



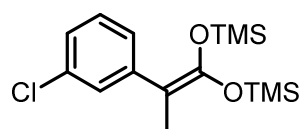
Prepared according to general procedure **B** using 2-(2-chlorophenyl)propanoic acid (2.1 g, 11.3 mmol) and obtained after distillation (bp = 91 °C at 5×10^{-2} mbar) as a colorless liquid (1.2 g, 3.6 mmol, 33% yield).

^1H NMR (501 MHz, CD_2Cl_2) δ = 7.34 (dd, J = 7.9, 1.4 Hz, 1H), 7.24 (dd, J = 7.5, 1.9 Hz, 1H), 7.19 (td, J = 7.4, 1.4 Hz, 1H), 7.13 (ddd, J = 7.8, 7.2, 1.9 Hz, 1H), 1.83 (s, 3H), 0.30 (s, 9H), –0.09 ppm (s, 9H).

^{13}C NMR (126 MHz, CD_2Cl_2) δ = 141.86, 135.68, 133.75, 130.51, 128.55, 127.56, 125.25, 94.18, 17.74, 1.48, 0.90 ppm.

HRMS (GC–Cl) m/z calculated for $\text{C}_{15}\text{H}_{25}\text{O}_2\text{Cl}_1\text{Si}_2$ [M]: 328.1076; found 328.1079.

2-*m*-Chlorophenyl-2-methyl-1,1-bis(trimethylsilyloxy)ethane (31i)



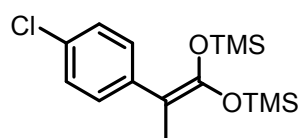
Prepared according to general procedure **B** using 2-(3-chlorophenyl)propanoic acid (1.5 g, 7.9 mmol) and obtained after distillation (bp = 82 °C at 5×10^{-2} mbar) as a colorless liquid (1.2 g, 3.6 mmol, 46% yield).

¹H NMR (501 MHz, CD₂Cl₂) δ = 7.44 (t, *J* = 1.9 Hz, 1H), 7.27 (ddd, *J* = 7.9, 1.7, 1.1 Hz, 1H), 7.18 (m, 1H), 7.05 (ddd, *J* = 8.0, 2.2, 1.1 Hz, 1H), 1.88 (s, 3H), 0.28 (s, 9H), 0.00 ppm (s, 9H).

¹³C NMR (126 MHz, CD₂Cl₂) δ = 149.38, 144.84, 134.30, 129.91, 129.60, 127.50, 125.51, 94.45, 17.05, 1.23, 0.90 ppm.

HRMS (GC–Cl) *m/z* calculated for C₁₅H₂₅O₂Cl₁Si₂ [M]: 328.1076; found 328.1072.

2-*p*-Chlorophenyl-2-methyl-1,1-bis(trimethylsilyloxy)ethane (31j)



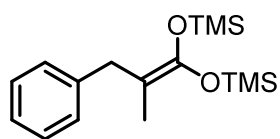
Prepared according to general procedure **B** using 2-(2-chlorophenyl)propanoic acid (3.5 g, 19.2 mmol) and obtained after distillation (bp 86 °C at 5 × 10⁻² mbar) as a colorless liquid (3.9 g, 11.9 mmol, 62%).

¹H NMR (501 MHz, CD₂Cl₂) δ = 7.37–7.29 (m, 2H), 7.24–7.14 (m, 2H), 1.87 (s, 3H), 0.27 (s, 9H), –0.02 ppm (s, 9H).

¹³C NMR (126 MHz, CD₂Cl₂) δ = 148.97, 141.45, 130.94, 130.89, 129.05, 128.61, 128.46, 94.46, 17.18, 1.21, 0.90 ppm.

HRMS (GC–Cl) *m/z* calculated for C₁₅H₂₅O₂Cl₁Si₂ [M]: 328.1076; found 328.1072.

3-Benzyl-2-methyl-1,1-bis(trimethylsilyloxy)ethane (31k)



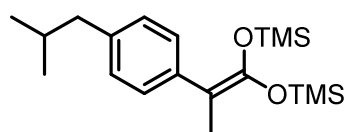
Prepared according to general procedure **B** using 2-methyl-3-phenylpropionic acid (5.0 g, 30.5 mmol) and obtained after distillation (bp = 72 °C at 5 × 10⁻² mbar) as a colorless liquid (4.5 g, 14.6 mmol, 48% yield).

¹H NMR (501 MHz, CD₂Cl₂) δ = 7.30–7.20 (m, 2H), 7.19–7.10 (m, 3H), 3.27 (s, 2H), 1.40 (s, 3H), 0.20 ppm (d, *J* = 1.4 Hz, 18H).

¹³C NMR (126 MHz, CD₂Cl₂) δ = 146.89, 142.45, 129.08, 129.08, 128.57, 128.57, 126.00, 92.02, 37.81, 15.14, 0.90, 0.88 ppm.

HRMS (ESI) *m/z* calculated for C₁₆H₂₈O₂ [M+H]⁺: 309.1701; found 309.1701.

2-*p*-isobutylphenyl-2-methyl-1,1-bis(trimethylsilyloxy)ethane (31o)



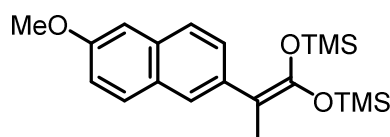
Prepared according to general procedure **B** using 2-(4-isobutylphenyl)propanoic acid (5.0 g, 24.2 mmol) and obtained after distillation (bp = 105 °C at 5×10^{-2} mbar) as a colorless liquid (6.5 g, 18.5 mmol, 77% yield).

^1H NMR (501 MHz, CD_2Cl_2) δ = 7.28–7.23 (m, 2H), 7.04–6.99 (m, 2H), 2.42 (d, J = 7.2 Hz, 2H), 1.87 (s, 3H), 1.84–1.77 (m, 1H), 0.88 (d, J = 6.6 Hz, 6H), 0.26 (s, 9H), –0.06 ppm (s, 9H).

^{13}C NMR (126 MHz, CD_2Cl_2) δ = 147.89, 139.70, 138.92, 129.06, 129.06, 129.02, 129.02, 94.98, 45.80, 31.15, 22.88, 17.17, 0.90, 0.56 ppm.

HRMS (ESI) m/z calculated for $\text{C}_{19}\text{H}_{35}\text{O}_2\text{Si}_2$ $[\text{M}+\text{H}]^+$: 351.2171; found 351.2170.

2-(6-methoxynaphthalen-2-yl)-2-methyl-1,1-bis(trimethylsilyloxy)ethane (31l)



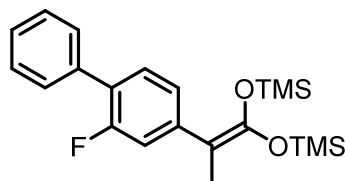
Prepared according to general procedure **B** using 2-(6-methoxynaphthalen-2-yl)propanoic acid (4.0 g, 17.4 mmol) and obtained after sublimation (sp = 150 °C at 5×10^{-2} mbar) as a colorless solid (4.0 g, 10.8 mmol, 62% yield).

^1H NMR (501 MHz, CD_2Cl_2) δ = 7.70–7.69 (m, 1H), 7.67–7.64 (m, 1H), 7.63–7.56 (m, 2H), 7.10 (d, J = 2.6 Hz, 1H), 7.07 (dd, J = 8.8, 2.6 Hz, 1H), 3.90 (s, 3H), 1.98 (s, 3H), 0.30 (s, 9H), –0.06 ppm (s, 9H).

^{13}C NMR (126 MHz, CD_2Cl_2) δ = 137.60, 132.88, 129.53, 129.53, 128.90, 126.64, 126.03, 118.74, 118.74, 106.02, 106.02, 94.76, 55.77, 16.92, 0.69, 0.34 ppm.

HRMS (ESI) m/z calculated for $\text{C}_{20}\text{H}_{30}\text{O}_3\text{Si}_2\text{Na}$ $[\text{M}+\text{Na}]^+$: 397.1629; found 397.1626.

2-(3-fluoro-4-phenyl-phenyl)-2-methyl-1,1-bis(trimethylsilyloxy)ethane (31p)



Prepared according to general procedure **B** using 2-(3-fluoro-4-phenyl-phenyl)propanoic acid (4.0 g, 16.4 mmol) and obtained after distillation (bp = 145 °C at 5×10^{-2} mbar)

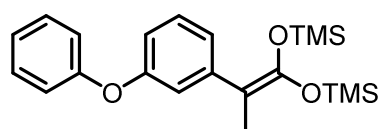
as a colorless liquid (4.0 g, 10.3 mmol, 63% yield).

¹H NMR (501 MHz, CD₂Cl₂) δ = 7.58–7.54 (m, 2H), 7.46–7.40 (m, 2H), 7.37–7.31 (m, 2H), 7.30–7.25 (m, 2H), 1.92 (s, 3H), 0.29 (d, *J* = 1.0 Hz, 9H), 0.06 ppm (s, 9H).

¹³C NMR (75 MHz, CD₂Cl₂) δ = 160.43 (d, *J* = 244.6 Hz), 149.12, 143.73 (d, *J* = 8.6 Hz), 136.74, 130.00 (d, *J* = 4.3 Hz), 129.41 (d, *J* = 3.2 Hz), 128.94, 127.81, 124.73 (d, *J* = 3.0 Hz), 116.07 (d, *J* = 23.7 Hz), 93.87, 16.43, 0.72, 0.45 ppm.

HRMS (ESI) *m/z* calculated for C₂₁H₃₀O₂F₁Si₂ [M+H]⁺: 389.1764; found 389.1763.

2-*m*-phenoxyphenyl-2-methyl-1,1-bis(trimethylsilyloxy)ethane (31n)



Prepared according to general procedure **B** using 2-(3-phenoxyphenyl)propanoic acid (2.0 g, 8.3 mmol) and obtained after distillation (bp = 135 °C at 5 x10⁻² mbar)

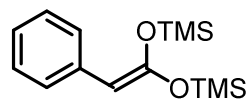
as a colorless liquid (1.3 g, 3.4 mmol, 41% yield).

¹H NMR (501 MHz, CD₂Cl₂) δ = 7.35–7.29 (m, 2H), 7.25–7.20 (m, 1H), 7.17 (d, *J* = 7.8, 1H), 7.11 (dd, *J* = 2.5, 1.7 Hz, 1H), 7.07 (tt, *J* = 7.4, 1.1 Hz, 1H), 7.01–6.96 (m, 2H), 6.73 (ddd, *J* = 7.9, 2.5, 1.2 Hz, 1H), 1.88 (s, 3H), 0.27 (s, 9H), 0.00 ppm (s, 9H).

¹³C NMR (126 MHz, CD₂Cl₂) δ = 158.51, 156.85, 148.37, 144.34, 130.15, 129.18, 124.44, 123.19, 120.17, 118.76, 116.05, 94.39, 16.76, 0.64, 0.36 ppm.

HRMS (ESI) *m/z* calculated for C₂₁H₃₁O₂Si₂ [M+H]⁺: 387.1807; found 387.1806.

4-benzylidene-2,2,6,6-tetramethyl-3,5-dioxa-2,6-disilaheptane (31r)

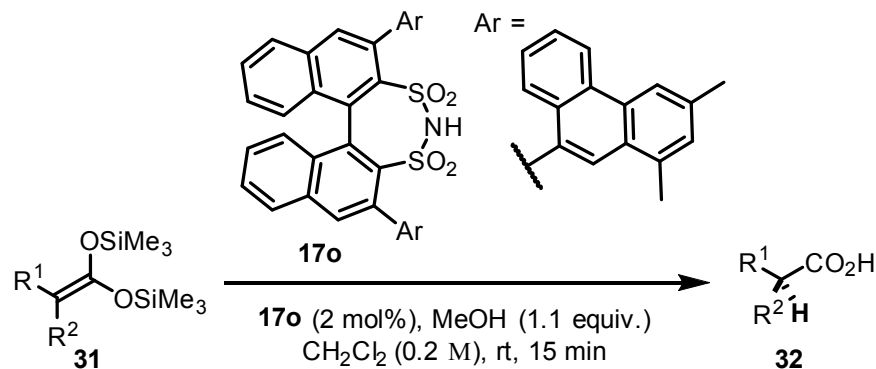


Prepared according to general procedure **B** using phenylacetic acid (5.0 g, 36.7 mmol) and obtained after distillation (bp = 59 °C at 5 x10⁻² mbar) as a colorless liquid (7.6 g, 27.0 mmol, 74%) yield.

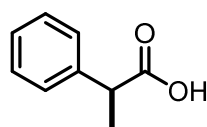
¹H NMR (501 MHz, CD₂Cl₂) δ = 7.40–7.34 (m, 2H), 7.22–7.16 (m, 2H), 6.98 (tt, *J* = 7.1, 1.3 Hz, 1H), 4.61 (s, 1H), 0.33 (s, 9H), 0.30 ppm (s, 9H).

¹³C NMR (126 MHz, CD₂Cl₂) δ = 152.73, 138.11, 128.52, 128.52, 126.74, 126.74, 123.92, 85.58, 0.84, 0.16 ppm.

HRMS (GC–Cl) *m/z* calculated for C₁₄H₂₄O₂Si₂ [M]: 280.13053; found 280.13094.

7.2.3 General procedure for the asymmetric protonation of *bis*-SKAs

An oven dry 2 ml vial was charged with disulfonamide **17o** (4.0 μmol , 3.2 mg, 2 mol%), a magnetic stir bar and, under argon atmosphere, dry CH_2Cl_2 (0.5 mL) and *bis*-silyl ketene acetal **31** (0.2 mmol, 1.0 equiv.) were added. Then MeOH (9.0 μL , 1.1 equiv.) in CH_2Cl_2 (2% solution, v/v) was added over 15 min *via* Hamilton syringe using a syringe pump (33 $\mu\text{L}/\text{min}$). Afterwards, the reaction mixture was diluted with water, stirred for 5 min and the organic phase was extracted with aq. NaOH (1M). The organic phase was acidified with HCl (6M) for 5 min, extracted with CH_2Cl_2 (3x5 mL), and the solvent was removed under reduced pressure to fully recycle catalyst **17o**. The aqueous phase was acidified with HCl (1M) and extracted with Et_2O (3x3 mL). The combined organic phase was dried over MgSO_4 and the solvent was removed under reduced pressure to yield the targeted product **32** as a colorless solid in >99% purity (analyzed by $^1\text{H-NMR}$). The obtained product was dissolved in HPLC grade Heptane:*i*PrOH (1:1, v/v) and directly used for the determination of the enantiomeric ratio.

(S)-2-phenylpropanoic acid (32a)

Prepared according to the general procedure using 2-methyl-2-phenyl-1,1-*bis*(trimethylsilyloxy)ethane (**31a**) (59 mg, 59 μL , 0.2 mmol) and obtained after extraction as a colorless liquid (22 mg, 0.15 mmol, 73% yield, 95.5:4.5 er).

^1H NMR (501 MHz, CDCl_3) δ = 7.38–7.30 (m, 4H), 7.28 (ddd, J = 6.3, 3.1, 1.8 Hz, 1H), 3.74 (q, J = 7.1 Hz, 1H), 1.52 ppm (d, J = 7.2 Hz, 3H), [acid proton not visible due to fast exchange].

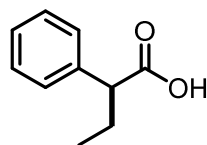
^{13}C NMR (126 MHz, CDCl_3) δ = 180.36, 139.75, 128.69, 127.60, 127.40, 45.31, 18.11 ppm.

HRMS (GC–EI) m/z calculated for $\text{C}_9\text{H}_{10}\text{O}_2$ [M]: 150.0678; found 150.0675.

The enantiomeric ratio was determined by HPLC analysis using Daicel Chiralpak OD-3, *n*-Heptane/*i*PrOH/TFA = 97.9:2:0.1 (v/v/v), flow rate = 1 mL/min, 25 °C, λ = 210 nm, t_{R} = 6.57 min (minor) and t_{R} = 7.62 min (major).

$[\alpha]_{\text{D}}^{25}$ = 69.2 (c 1.0, CHCl_3). Lit $[\alpha]_{\text{D}}^{20}$ = 75.0 (c 1.6, CHCl_3). (obtained from Sigma-Aldrich)

(S)-2-phenylbutanoic acid (32b)



Prepared according to general procedure using 3-Ethyl-2-phenyl-1,1-bis(trimethylsilyloxy)ethane (**31b**) (62 mg, 60 μL , 0.2 mmol) and obtained after extraction as a colorless solid (26 mg, 0.16 mmol, 82% yield, 95:5 er).

^1H NMR (501 MHz, CDCl_3) δ = 7.36–7.26 (m, 5H), 3.47 (t, J = 7.7 Hz, 1H), 2.11 (m, 1H), 1.82 (m, 1H), 0.92 ppm (t, J = 7.4 Hz, 3H), [acid proton not visible due to fast exchange].

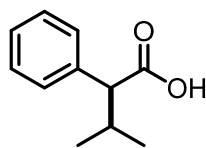
^{13}C NMR (126 MHz, CDCl_3) δ = 180.00, 138.38, 128.63, 128.07, 127.43, 53.18, 26.31, 12.09 ppm.

HRMS (GC–EI) m/z calculated for $\text{C}_{10}\text{H}_{12}\text{O}_2$ [M]: 164.0834; found 164.0832.

The enantiomeric ratio was determined by HPLC analysis using Daicel Chiralpak OD-3, *n*-Heptane/*i*PrOH/TFA = 97.9:2:0.1 (v/v/v), flow rate = 1 mL/min, 25 °C, λ = 210 nm, t_{R} = 5.68 min (minor) and t_{R} = 7.54 min (major).

$[\alpha]_{\text{D}}^{20}$ = 32.5 (c 1.1, CHCl_3). Lit^[10a]

(S)-3-methyl-2-phenylbutanoic acid (32c)



Prepared according to general procedure using 3-isopropyl-2-phenyl-1,1-bis(trimethylsilyloxy)ethane (**31c**) (65 mg, 59 μ L, 0.2 mmol) and obtained after extraction as a colorless solid (32 mg, 0.18 mmol, 89% yield, 70.5:29.5 er).

$^1\text{H NMR}$ (501 MHz, CDCl_3) δ = 7.35–7.29 (m, 4H), 7.30–7.23 (m, 1H), 3.15 (d, J = 10.5 Hz, 1H), 2.33 (dp, J = 10.6, 6.6 Hz, 1H), 1.08 (d, J = 6.5 Hz, 3H), 0.71 ppm (d, J = 6.7 Hz, 3H), [acid proton not visible due to fast exchange].

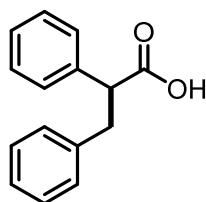
$^{13}\text{C NMR}$ (126 MHz, CDCl_3) δ = 179.85, 137.73, 128.59, 128.54, 127.46, 59.95, 59.91, 31.56, 21.47, 20.11 ppm.

HRMS (GC–EI) m/z calculated for $\text{C}_{11}\text{H}_{14}\text{O}_2$ [M]: 178.0990; found 178.0988.

The enantiomeric ratio was determined by HPLC analysis using Daicel Chiralpak OD-3, *n*-Heptane/*i*PrOH/TFA = 97.9:2:0.1 (v/v/v), flow rate = 1 mL/min, 25 $^\circ\text{C}$, λ = 210 nm, t_{R} = 5.09 min (minor) and t_{R} = 6.88 min (major).

$[\alpha]_{\text{D}}^{25}$ = 23.4 (c 0.95, CHCl_3). Lit^[156]

(S)-2,3-diphenylpropanoic acid (31d)



Prepared according to general procedure using 3-benzyl-2-phenyl-1,1-bis(trimethylsilyloxy)ethane (**32d**) (74 mg, 68 μ L, 0.2 mmol) and obtained after extraction as a colorless solid (43 mg, 0.19 mmol, 96% yield, 95:5 er).

$^1\text{H NMR}$ (501 MHz, CDCl_3) δ = 7.42–7.15 (m, 8H), 7.14–7.08 (m, 2H), 3.87 (dd, J = 8.4, 7.0 Hz, 1H), 3.42 (dd, J = 13.8, 8.4 Hz, 1H), 3.05 ppm (dd, J = 13.8, 7.0 Hz, 1H), [acid proton not visible due to fast exchange].

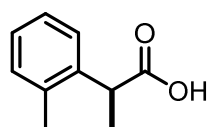
$^{13}\text{C NMR}$ (126 MHz, CDCl_3) δ = 178.77, 138.80, 138.05, 129.05, 128.85, 128.51, 128.23, 127.77, 126.61, 53.52, 39.42 ppm.

HRMS (GC–EI) m/z calculated for $\text{C}_{15}\text{H}_{14}\text{O}_2$ [M]: 226.0990; found 226.0988.

The enantiomeric ratio was determined by HPLC analysis using Daicel Chiralpak OD-3, *n*-Heptane/*i*PrOH/TFA = 97.9:2:0.1 (v/v/v), flow rate = 1 mL/min, 25 °C, λ = 210 nm, t_R = 8.08 min (minor) and t_R = 9.97 min (major).

$[\alpha]_D^{25}$ = 56.0 (c 1.1, CHCl₃). Lit^[156]

(S)-2-(*o*-tolyl)propanoic acid (32e)



Prepared according to general procedure using 2-*o*-tolyl-2-methyl-1,1-*bis*(trimethylsilyloxy)ethane (**31e**) (62 mg, 56 μ L, 0.2 mmol) and obtained after extraction as a colorless solid (3 mg, 0.18 mmol, 91% yield, 96.5:3.5 er).

¹H NMR (501 MHz, CDCl₃) δ = 7.29 (d, J = 7.2 Hz, 1H), 7.23–7.14 (m, 3H), 3.99 (q, J = 7.1 Hz, 1H), 2.38 (s, 3H), 1.50 ppm (d, J = 7.1 Hz, 3H), [acid proton not visible due to fast exchange].

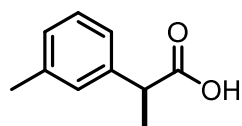
¹³C NMR (126 MHz, CDCl₃) δ 179.59, 138.33, 135.88, 130.56, 127.21, 126.55, 126.47, 40.95, 19.63, 17.56 ppm.

HRMS (GC–EI) m/z calculated for C₁₀H₁₂O₂ [M]: 164.0834; found 164.0832.

The enantiomeric ratio was determined by HPLC analysis using Daicel Chiralpak OD-3, *n*-Heptane/*i*PrOH/TFA = 97.9:2:0.1 (v/v/v), flow rate = 1 mL/min, 25 °C, λ = 210 nm, t_R = 7.05 min (minor) and t_R = 8.06 min (major).

$[\alpha]_D^{25}$ = 50.9 (c 1.05, CHCl₃). Lit^[157]

(S)-3-(*o*-tolyl)propanoic acid (32f)



Prepared according to general procedure using 2-*m*-tolyl-2-methyl-1,1-*bis*(trimethylsilyloxy)ethane (**31f**) (62 mg, 57 μ L, 0.2 mmol) and obtained after extraction as a colorless solid (29 mg, 0.19 mmol,

97% yield, 92.5:7.5 er).

¹H NMR (501 MHz, CDCl₃) δ = 7.25–7.19 (m, 1H), 7.16–7.03 (m, 3H), 3.72 (q, J = 7.2 Hz, 1H), 2.35 (s, 3H), 1.51 ppm (d, J = 7.2 Hz, 3H), [acid proton not visible due to fast exchange].

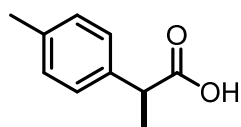
^{13}C NMR (126 MHz, CDCl_3) δ = 167.33, 139.72, 138.38, 128.59, 128.28, 128.16, 124.58, 45.05, 21.41, 18.16 ppm.

HRMS (GC–EI) m/z calculated for $\text{C}_{10}\text{H}_{12}\text{O}_2$ [M]: 164.0834; found 164.0832.

The enantiomeric ratio was determined by HPLC analysis using Daicel Chiralpak OD-3, *n*-Heptane/*i*PrOH/TFA = 97.9:2:0.1 (v/v/v), flow rate = 1 mL/min, 25 °C, λ = 210 nm, t_{R} = 6.0 min (minor) and t_{R} = 7.64 min (major).

$[\alpha]_{\text{D}}^{25}$ = 33.3 (c 0.75, CHCl_3). Lit^[157]

(S)-2-(*p*-Tolyl)propanoic acid (32g)



Prepared according to general procedure using 2-*p*-Tolyl-2-methyl-1,1-*bis*(trimethylsilyloxy)ethane (**31g**) (63 mg, 60 μL , 0.2 mmol) and obtained after extraction as a colorless solid (29 mg,

0.18 mmol, 88% yield, 95.5:4.5 er).

^1H NMR (501 MHz, CDCl_3) δ = 11.38 (s, 1H), 7.20 (d, J = 8.1, 2H), 7.13 (d, J = 8.1, 2H), 3.68 (q, J = 7.1, 1H), 1.47 ppm (d, J = 7.1, 3H).

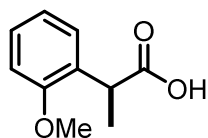
^{13}C NMR (126 MHz, CDCl_3) δ = 181.14, 137.04, 136.75, 129.33, 127.43, 44.94, 21.01, 18.05 ppm.

HRMS (GC–EI) m/z calculated for $\text{C}_{10}\text{H}_{12}\text{O}_2$ [M]: 164.0835; found 164.0832.

The enantiomeric ratio was determined by HPLC analysis using Daicel Chiralpak OD-3, *n*-Heptane/*i*PrOH/TFA = 97.9:2:0.1 (v/v/v), flow rate = 1 mL/min, 25 °C, λ = 210 nm, t_{R} = 6.25 min (minor) and t_{R} = 9.95 min (major).

$[\alpha]_{\text{D}}^{25}$ = 42.3 (c 0.6, CHCl_3).

(S)-2-(2-methoxyphenyl)propanoic acid (32m)



Prepared according to general procedure using 2-*o*-methoxyphenyl-2-methyl-1,1-*bis*(trimethylsilyloxy)ethane (**31m**) (73 mg, 65 μL , 0.2 mmol) and obtained after extraction as a colorless solid (33 g, 0.18

mmol, 92% yield, 95:5 er).

¹H NMR (501 MHz, CDCl₃) δ = 7.29–7.22 (m, 2H), 6.96 (dt J = 7.5, 1.1 Hz, 1H), 6.89 (dd, J = 8.7, 1.1 Hz, 1H), 4.09 (q, J = 7.2 Hz, 1H), 3.84 (s, 3H), 1.49 ppm (d, J = 7.2 Hz, 3H), [acid proton not visible due to fast exchange].

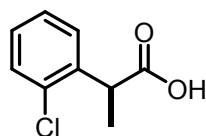
¹³C NMR (126 MHz, CDCl₃) δ = 156.63, 128.65, 128.65, 128.39, 128.01, 120.89, 110.77, 55.53, 38.95, 16.79 ppm.

HRMS (GC–EI) m/z calculated for C₁₀H₁₂O₃ [M]: 180.0781; found 180.0781.

The enantiomeric ratio was determined by HPLC analysis using Daicel Chiralpak OD-3, *n*-Heptane/*i*PrOH/TFA = 97.9:2:0.1 (v/v/v), flow rate = 1 mL/min, 25 °C, λ = 210 nm, t_R = 15.3 min (minor) and t_R = 16.5 min (major).

$[\alpha]_D^{25}$ = 69.5 (c 1.1, CHCl₃). Lit^[158]

(S)-2-(2-chlorophenyl)propanoic acid (32h)



Prepared according to general procedure using 2-*o*-chlorophenyl-2-methyl-1,1-*bis*(trimethylsilyloxy)ethane (**31h**) (73 mg, 70 μ L, 0.2 mmol) and obtained after extraction as a colorless solid (35 mg, 0.19 mmol, 95% yield, 95:5 er).

¹H NMR (501 MHz, CDCl₃) δ = 7.37 (ddd, J = 17.1, 7.8, 1.6 Hz, 2H), 7.26 (td, J = 7.6, 1.5 Hz, 1H), 7.21 (td, J = 7.6, 1.8 Hz, 1H), 4.28 (q, J = 7.2 Hz, 1H), 1.53 ppm (d, J = 7.3 Hz, 3H), [acid proton not visible due to fast exchange].

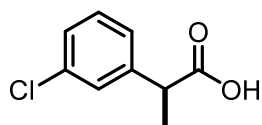
¹³C NMR (126 MHz, CDCl₃) δ = 178.76, 137.66, 129.70, 128.53, 128.45, 127.20, 41.80, 17.31 ppm.

HRMS (ESI) m/z calculated for C₉H₈ClO₂ [M–H]: 183.0218; found 183.0218.

The enantiomeric ratio was determined by HPLC analysis using Daicel Chiralpak OJ-3, *n*-Heptane/*i*PrOH/TFA = 97.9:2:0.1 (v/v/v), flow rate = 1 mL/min, 25 °C, λ = 210 nm, t_R = 32.2 min (minor) and t_R = 35.1 min (major).

$[\alpha]_D^{25}$ = 46.2 (c 0.6, CHCl₃). Lit^[158]

(S)-2-(3-chlorophenyl)propanoic acid (32i)



Prepared according to general procedure using 2-*m*-chlorophenyl-2-methyl-1,1-*bis*(trimethylsilyloxy)ethane (**31i**) (73

mg, 69 μ L, 0.2 mmol) and obtained after extraction as a colorless solid (32 mg, 0.17 mmol, 87% yield, 93:7 er).

^1H NMR (501 MHz, CDCl_3) δ = 7.32 (bs, 1H), 7.30–7.22 (m, 2H), 7.23–7.18 (m, 1H), 3.72 (q, J = 7.2 Hz, 1H), 1.52 ppm (d, J = 7.2 Hz, 3H), [acid proton not visible due to fast exchange].

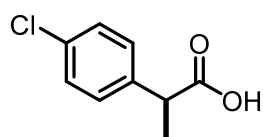
^{13}C NMR (126 MHz, CDCl_3) δ = 179.00, 141.57, 134.50, 129.92, 127.85, 127.65, 125.87, 44.89, 18.05 ppm.

HRMS (ESI) m/z calculated for $\text{C}_9\text{H}_8\text{Cl}_1\text{O}_2\text{Na}_1$ $[\text{M}+\text{Na}]^+$: 207.0183; found 207.0183.

The enantiomeric ratio was determined by HPLC analysis using Daicel Chiralpak OJ-3, *n*-Heptane/*i*PrOH/TFA = 97.9:2:0.1 (v/v/v), flow rate = 1 mL/min, 25 $^\circ\text{C}$, λ = 210 nm, t_{R} = 27.3 min (minor) and t_{R} = 31.5 min (major).

$[\alpha]_{\text{D}}^{25}$ = 32.9 (c 0.85, CHCl_3). Lit^[158]

(S)-2-(4-chlorophenyl)propanoic acid (**32j**)



Prepared according to general procedure using 2-*p*-chlorophenyl-2-methyl-1,1-*bis*(trimethylsilyloxy)ethane (**31j**) (73 mg, 70 μ L, 0.2 mmol) and obtained after extraction as a colorless

solid (29 mg, 0,16 mmol, 79% yield, 95:5 er).

^1H NMR (501 MHz, CDCl_3) δ = 7.30 (d, J = 8.1 Hz, 2H), 7.24 (d, J = 8.3 Hz, 2H), 3.71 (q, J = 6.6 Hz, 1H), 1.49 ppm (d, J = 7.2 Hz, 3H), [acid proton not visible due to fast exchange].

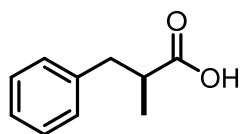
^{13}C NMR (126 MHz, CDCl_3) δ = 180.14, 138.58, 133.18, 129.29, 129.29, 129.05, 129.05, 45.09, 18.49 ppm. z

HRMS (ESI) m/z calculated for $\text{C}_9\text{H}_8\text{Cl}_1\text{O}_2\text{Na}_1$ $[\text{M}+\text{Na}]^+$: 207.0183; found 207.0183.

The enantiomeric ratio was determined by HPLC analysis using Daicel Chiralpak OD-3, *n*-Heptane/*i*PrOH/TFA = 97.9:2:0.1 (v/v/v), flow rate = 1 mL/min, 25 $^\circ\text{C}$, λ = 210 nm, t_{R} = 13.8 min (minor) and t_{R} = 16.38 min (major).

$[\alpha]_{\text{D}}^{25}$ = 36.2 (c 0.80, CHCl_3). Lit^[158].

(S)-2-methyl-3-phenylpropanoic acid (32k)



Prepared according to general procedure using 3-benzyl-2-methyl-1,1-bis(trimethylsilyloxy)ethane (**31k**) (62 mg, 60 μ L, 0.2 mmol) and obtained after extraction as a colorless solid (29 mg, 0.18 mmol, 89% yield, 51:49 er).

^1H NMR (501 MHz, CDCl_3) δ = 7.30–7.26 (m, 2H), 7.23–7.17 (m, 3H), 3.08 (dd, J = 13.8, 6.6 Hz, 1H), 2.80–2.73 (m, 1H), 2.67 (dd, J = 13.8, 8.4 Hz, 1H), 1.17 ppm (d, J = 7.2 Hz, 3H), [acid proton not visible due to fast exchange].

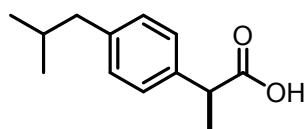
^{13}C NMR (126 MHz, CDCl_3) δ = 182.2, 139.2, 129.1, 128.5, 126.5, 41.3, 39.4, 16.6 ppm.

HRMS (GC-EI) m/z calculated for $\text{C}_{10}\text{H}_{12}\text{O}_2$ [M]: 164.0835; found 164.0832.

The enantiomeric ratio was determined by HPLC analysis using Daicel Chiralpak OJ-3, *n*-Heptane/*i*PrOH/TFA = 97.9:2:0.1 (v/v/v), flow rate = 1 mL/min, 25 $^\circ\text{C}$, λ = 210 nm, t_{R} = 7.58 min (minor) and t_{R} = 8.55 min (major).

$[\alpha]_{\text{D}}^{25}$ = -0.0 (c 0.75, CHCl_3).

(S)-Ibuprofen (32o)



Prepared according to general procedure using 2-*p*-isobutylphenyl-2-methyl-1,1-bis(trimethylsilyloxy)ethane (**31o**) (70 mg, 62 μ L, 0.2 mmol) and obtained after extraction as a colorless solid (38 mg, 0.18 mmol, 92% yield, 96.5:3.5 er).

^1H NMR (501 MHz, CDCl_3) δ = 7.24–7.18 (m, 2H), 7.14–7.06 (m, 2H), 3.71 (q, J = 7.2 Hz, 1H), 2.45 (d, J = 7.2 Hz, 2H), 1.84–1.77 (m, 1H), 1.50 (d, J = 7.2 Hz, 3H), 0.90 ppm (d, J = 6.6 Hz, 6H), [acid proton not visible due to fast exchange].

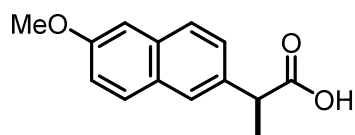
^{13}C NMR (126 MHz, CDCl_3) δ = 180.79, 140.86, 136.96, 129.39, 127.27, 45.05, 44.94, 30.17, 22.40, 18.11 ppm.

HRMS (GC-EI) m/z calculated for $\text{C}_{13}\text{H}_{18}\text{O}_2$ [M]: 206.1307; found 206.1309.

The enantiomeric ratio was determined by HPLC analysis using Daicel Chiralpak OD-3, *n*-Heptane/*i*PrOH/TFA = 97.9:2:0.1 (v/v/v), flow rate = 1 mL/min, 25 $^\circ\text{C}$, λ = 210 nm, t_{R} = 5.37 min (minor) and t_{R} = 6.11 min (major).

$[\alpha]_D^{25} = 39.1$ (c 1.0, CHCl₃). Lit^[158]

(S)-Naproxen (32I)



Prepared according to general procedure using 2-(6-methoxynaphthalen-2-yl)-2-methyl-1,1-bis(trimethylsilyloxy)ethane (**31I**) (75 mg, 0.2 mmol) and

obtained after extraction as a colorless solid (41 mg, 0.18 mmol, 90% yield, 93:7).

¹H NMR (501 MHz, CDCl₃) $\delta = 7.74$ – 7.64 (m, 3H), 7.41 (dd, $J = 8.5, 1.9$ Hz, 1H), 7.18– 7.07 (m, 2H), 3.91 (s, 3H), 3.87 (q, $J = 7.3$ Hz, 1H), 1.59 ppm (d, $J = 7.2$ Hz, 3H), [acid proton not visible due to fast exchange].

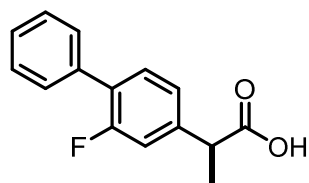
¹³C NMR (126 MHz, CDCl₃) $\delta = 179.66, 157.72, 134.87, 133.82, 129.30, 128.89, 127.24, 126.13, 119.05, 105.60, 55.31, 45.12, 18.17$ ppm.

HRMS (GC-EI) m/z calculated for C₁₄H₁₄O₂ [M]: 230.0930; found 230.0928.

The enantiomeric ratio was determined by HPLC analysis using Daicel Chiralpak OD-3, *n*-Heptane/*i*PrOH/TFA = 97.9:2:0.1 (v/v/v), flow rate = 1 mL/min, 25 °C, $\lambda = 210$ nm, $t_R = 14.9$ min (minor) and $t_R = 17.8$ min (major).

$[\alpha]_D^{25} = 41.2$ (c 0.90, CHCl₃). Lit^[158]

(S)-Flurbiprofen (32p)



Prepared according to general procedure using 2-(3-fluoro-4-phenyl-phenyl)-2-methyl-1,1-bis(trimethylsilyloxy)ethane (**31p**) (70 mg, 0.2 mmol) and obtained after extraction as a colorless solid (43 mg, 0.18 mmol, 89% yield, 95:5 er).

¹H NMR (501 MHz, CDCl₃) $\delta = 7.53$ (m, 2H), 7.48– 7.31 (m, 4H), 7.22– 7.11 (m, 2H), 3.80 (q, $J = 7.2$ Hz, 1H), 1.57 ppm (d, $J = 7.2$ Hz, 3H), [acid proton not visible due to fast exchange].

¹³C NMR (126 MHz, CDCl₃) $\delta = 178.71, 159.69$ (d, $J = 248.5$ Hz), 140.95 (d, $J = 7.6$ Hz), 135.40, 130.91 (d, $J = 4.1$ Hz), 128.96, 128.94, 128.45, 128.45, 128.21 (d, $J = 13.5$ Hz), 127.71, 123.66 (d, $J = 3.6$ Hz), 115.46 (d, $J = 23.6$ Hz), 44.64, 18.06 ppm.

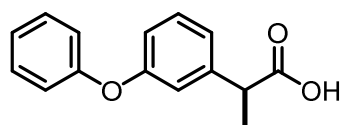
¹⁹F NMR (471 MHz, CDCl₃) $\delta = -117.39$.

HRMS (GC-EI) m/z calculated for C₁₅H₁₃FO₂ [M]: 244.0900; found 244.0895.

The enantiomeric ratio was determined by HPLC analysis using Daicel Chiralpak OD-3, *n*-Heptane/*i*PrOH/TFA = 97.9:2:0.1 (v/v/v), flow rate = 1 mL/min, 25 °C, λ = 210 nm, t_R = 8.46 min (minor) and t_R = 9.47 min (major).

$[\alpha]_D^{25}$ = 29.2 (c 0.95, CHCl₃). Lit^[158]

(S)-Fenopropfen (32n)



Prepared according to general procedure using 2-*m*-phenoxyphenyl-2-methyl-1,1-*bis*(trimethylsilyloxy)ethane (**31n**) (68 mg, 59 μ L, 0.2 mmol) and obtained after extraction as a colorless solid (35 mg, 0.16 mmol, 76%, 92:8 er).

¹H NMR (501 MHz, CDCl₃) δ = 7.36–7.30 (m, 2H), 7.30–7.26 (m, 1H), 7.13–7.08 (m, 1H), 7.08–7.04 (m, 1H), 7.03–6.97 (m, 3H), 6.88 (ddd, J = 8.1, 2.5, 0.9 Hz, 1H), 3.71 (q, J = 7.2 Hz, 1H), 1.50 ppm (d, J = 7.2 Hz, 3H), [acid proton not visible due to fast exchange].

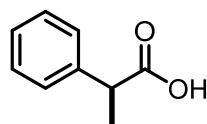
¹³C NMR (126 MHz, CDCl₃) δ = 179.56, 157.49, 156.92, 141.68, 129.88, 129.76, 123.38, 122.35, 118.98, 118.98, 118.22, 117.50, 77.27, 77.01, 76.76, 45.09, 18.09 ppm.

HRMS (GC-EI) m/z calculated for C₁₅H₁₄O₃ [M]: 242.0943; found 242.0946.

The enantiomeric ratio was determined by HPLC analysis using Daicel Chiralpak OD-3, *n*-Heptane/*i*PrOH/TFA = 97.9:2:0.1 (v/v/v), flow rate = 1 mL/min, 25 °C, λ = 210 nm, t_R = 15 min (minor) and t_R = 17.8 min (major).

$[\alpha]_D^{25}$ = 39.1 (c 1.05, CHCl₃). Lit^[158]

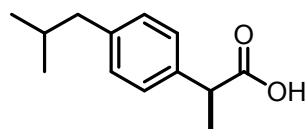
(S)-2-phenylpropanoic acid (32a)



Prepared according to the general procedure using water as the proton source (6 μ L, 0.11 mmol, 0.55 equiv.) in CH₂Cl₂ (2% solution, v%) and 2-methyl-2-phenyl-1,1-*bis*(trimethylsilyloxy)ethane (**31a**) (59 mg, 59 μ L, 0.2 mmol). The product was obtained after extraction as a colorless liquid (27 mg, 0.18 mmol, 82% yield, 95:5 er).

Analytcs matched compound **31a**.

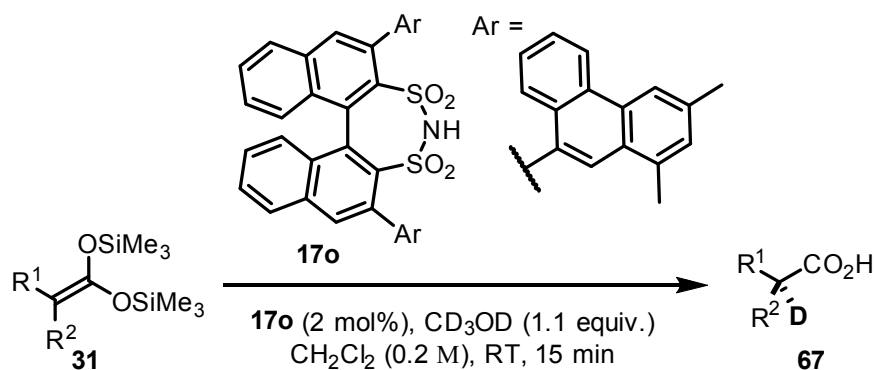
(S)-Ibuprofen (32o)



Prepared according to the general procedure using water as the proton source (6 μL , 0.11 mmol, 0.55 equiv.) in CH_2Cl_2 (2% solution, v%) and 2-*p*-isobutylphenyl-2-methyl-1,1-*bis*(trimethylsilyloxy)ethane (**31o**) (70 mg, 62 μL , 0.2 mmol) and obtained after extraction as a colorless solid (33 mg, 0.17 mmol, 82% yield, 95.5:4.5 er).

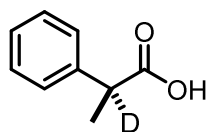
Analytically matched compound **31o**.

7.2.4 General Procedure for the Asymmetric Deuteration of *Bis*-SKAs



An oven dried 2 mL vial was charged with disulfonamide **17o** (4.0 μmol , 3.2 mg, 2 mol%), a magnetic stir bar and, under argon atmosphere, dry CH_2Cl_2 (0.5 mL) and *bis*-silyl ketene acetal **31** (0.2 mmol, 1 equiv.) were added. Then CD_3OD (9 μL , 0.22 mmol, 1.1 equiv.) in CH_2Cl_2 (2% solution, v%) was added over 15 min *via* Hamilton syringe using a syringe pump (33 $\mu\text{L}/\text{min}$). Afterwards, the reaction mixture was acidified with HCl (1M) and extracted with Et_2O (3x3 mL), and the combined organic phase was dried over MgSO_4 and purified by column chromatography (CH_2Cl_2 :MeOH, 98:2, v/v). The obtained product (**67**) was dissolved in HPLC grade Hept:*i*PrOH (1:1, v/v) and directly used for the determination of the enantiomeric ratio.

(S)-2-phenylpropanoic acid (67a)



Prepared according to general procedure using 2-methyl-2-phenyl-1,1-bis(trimethylsilyloxy)ethane (**31a**) (59 mg, 59 μ L, 0.2 mmol) and obtained after extraction as a colorless liquid (25 mg, 0.16 mmol,

77% yield, 95.5:4.5 er)

^1H NMR (501 MHz, CDCl_3) δ = 7.41–7.28 (m, 4H), 7.27–7.21 (m, 1H), 1.50 ppm (s, 3H).

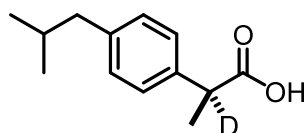
^{13}C NMR (126 MHz, CDCl_3) δ = 180.68, 139.77, 139.72, 128.68, 127.61, 127.59, 127.39, 45.00 (J = 19.2 Hz), 18.01 ppm.

HRMS (GC-Cl) m/z calculated for $\text{C}_9\text{H}_9\text{DO}_2$: 151.07436; found 151.07435.

The enantiomeric ratio was determined by HPLC analysis using Daicel Chiralpak OD-3, *n*-Heptane/*i*PrOH/TFA = 97.9:2:0.1 (v/v/v), flow rate = 1 mL/min, 25 °C, λ = 210 nm, t_R = 6.57 min (minor) and t_R = 7.62 min (major)

$[\alpha]_D^{25}$ = 35.1 (c 1.05, CHCl_3). Lit^[159]

(S)-Ibuprofen-d (67b)



Prepared according to general procedure using 2-*p*-isobutylphenyl-2-methyl-1,1-bis(trimethylsilyloxy)ethane (**31o**) (70 mg, 62 μ L, 0.2 mmol) and obtained after extraction as a

colorless solid (40 mg, 0.19 mmol, 94% yield, 95:5 er).

^1H NMR (501 MHz, CD_2Cl_2) δ = 7.29–7.17 (m, 2H), 7.15–7.05 (m, 2H), 2.45 (d, J = 7.2 Hz, 2H), 1.85 (dhept, J = 13.6, 6.8 Hz, 1H), 1.46 (s, 3H), 0.90 ppm (d, J = 6.6 Hz, 6H).

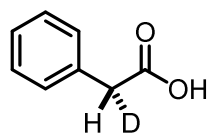
^{13}C NMR (126 MHz, CDCl_3) δ = 178.25, 141.28, 138.43, 129.86, 129.86, 127.77, 127.77, 49.77 (t [1:1:1], J = 19.9 Hz), 45.50, 30.81, 22.67, 22.67, 18.67 ppm.

HRMS (GC-Cl) m/z calculated for $\text{C}_{13}\text{H}_{17}\text{DO}_2$: 207.1367; found 207.1368.

The enantiomeric ratio was determined by HPLC analysis using Daicel Chiralpak OD-3, *n*-Heptane/*i*PrOH/TFA = 97.9:2:0.1 (v/v/v), flow rate = 1 mL/min, 25 °C, λ = 210 nm, t_R = 5.37 min (minor) and t_R = 6.11 min (major)

$[\alpha]_D^{25}$ = 37.9 (c 0.95, CHCl_3). Lit^[158]

(R)-2-phenylacetic-2-d acid (67c)



Prepared according to general procedure using 2-(3-fluoro-4-phenyl-phenyl)-2-methyl-1,1-bis(trimethylsilyloxy)ethane (**31r**) (70 mg, 79 μ L, 0.2 mmol) and obtained after extraction as a clear liquid (43 mg,

0.18 mmol, 89% yield, 81:19 er).

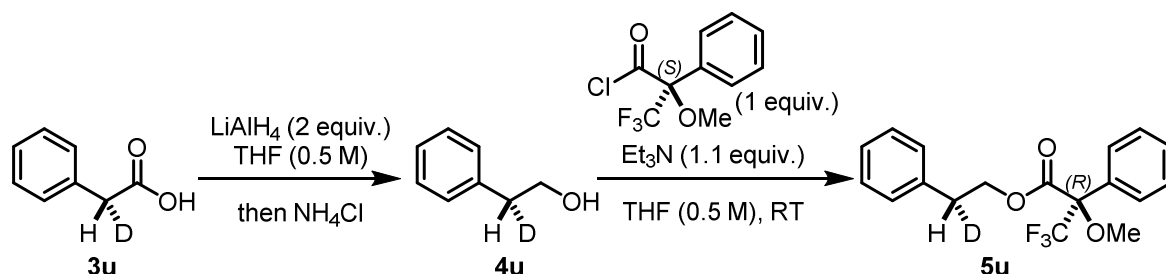
$^1\text{H NMR}$ (501 MHz, CDCl_3) δ = 7.37–7.31 (m, 2H), 7.31–7.27 (m, 3H), 3.64 ppm (t [1:1:1], J = 2.2 Hz, 1H).

$^{13}\text{C NMR}$ (126 MHz, CDCl_3) δ = 176.97, 133.21, 129.36, 129.34, 128.66, 128.66, 127.36, 40.64 ppm (t [1:1:1], J = 2.2 Hz,).

HRMS (GC-Cl) m/z calculated for $\text{C}_8\text{H}_7\text{DO}_2$: 137.0587; found 137.0586.

The enantiomeric ratio was determined by $^1\text{H NMR}$ analysis upon derivatization to the corresponding Mosher ester (Scheme 1), following the reported procedure for the derivatization and the diastereomeric ratio determination.^[122]

$[\alpha]_D^{25}$ = 0.6 (c 0.60, CHCl_3). $\text{Lit}^{[158]}$



Scheme 1. Derivatization sequence for the determination of the enantiomeric ratio.

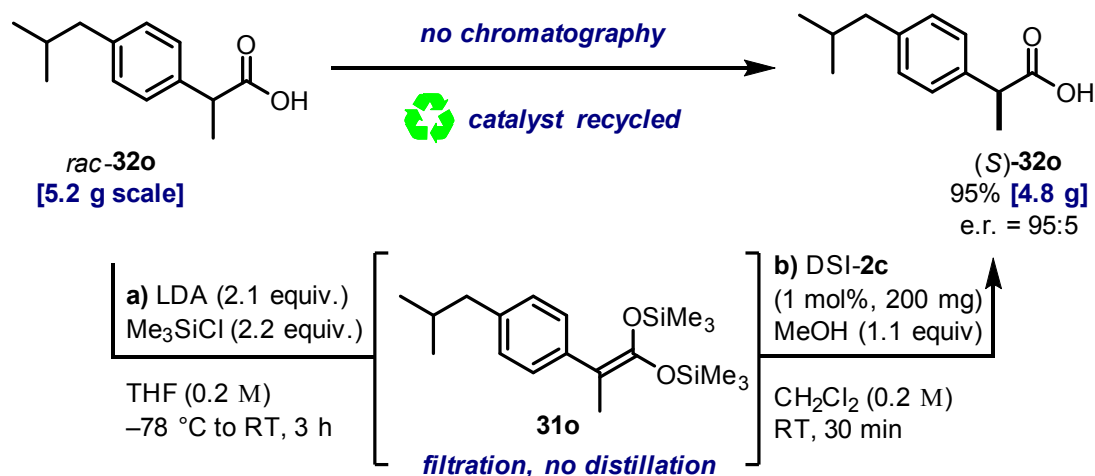
(R)-2-phenylethan-2-d-1-ol (4u)

$^1\text{H NMR}$ (501 MHz, CDCl_3) δ = 7.36–7.28 (m, 2H), 7.28–7.20 (m, 3H), 3.87 (dt, J = 6.6, 0.9 Hz, 2H), 2.86 (ddt, J = 6.6, 4.1, 2.1 Hz, 1H), 1.43 ppm (bs, 1 H).

(R)-2-phenylethyl-2-d (R)-3,3,3-trifluoro-2-methoxy-2-phenylpropanoate (5u)

$^1\text{H NMR}$ (500 MHz, CD_2Cl_2) δ = 7.44–7.39 (m, 3H), 7.39–7.34 (m, 2H), 7.31–7.25 (m, 2H), 7.25–7.20 (m, 1H), 7.20–7.16 (m, 2H), 4.61–4.44 (m, 2H), 3.44 (s, 3H), 2.99 ppm (dtt, J = 13.9, 7.1, 1.9 Hz, 1H).

7.2.5 Gram Scale Reaction

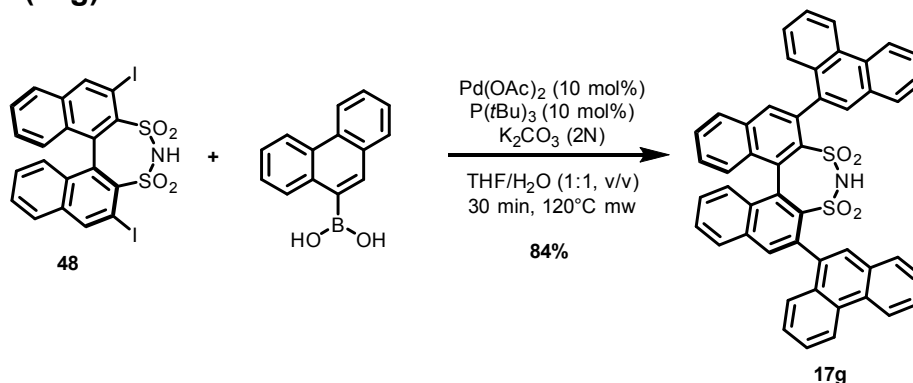


A stirring solution of acid *rac-32o* (5.2 g, 24.7 mmol, 1.0 equiv.) and Me₃SiCl (6.9 mL, 54.3 mmol, 2.2 equiv.) in THF (200 mL) under an atmosphere of dry argon was cooled to -78 °C. The freshly prepared LDA solution (54.3 mmol, 1 M, 55 mL 2.2 equiv.) was added dropwise at -78 °C via canula. The ice bath was removed upon complete addition and the reaction solution was stirred for 1 hour at room temperature. The reaction mixture was concentrated *in vacuo*. Hexane (50 mL) was added to the residue and the organic layer was filtered under argon. After concentration under reduced pressure, the crude product (**31o**) was dissolved in dry CH₂Cl₂ (60 mL) and a solution of catalyst **17o** (200 mg, 1 mol%) in CH₂Cl₂ (40 mL) was added at room temperature. A solution of MeOH (1.1 mL, 32 mmol, 1.1 equiv.) in CH₂Cl₂ (19 mL) was added *via* syringe pump (0.66 mL/min) in 30 min. The reaction mixture was diluted with HCl (1 M, 2 mL), stirred for 5 min, and the organic phase was concentrated *in vacuo* and diluted with Et₂O (50 mL). The crude mixture was extracted with aq. NaOH (1 M, 3x30 mL). The organic phase was acidified HCl (6 M) for 5 min, extracted with CH₂Cl₂ (3x50 mL), and the solvent was removed under reduced pressure to fully recycle catalyst **17o**. The aqueous phase was acidified with HCl (1 M, 50 mL) and extracted with Et₂O (3x50 mL). The combined organic phase was dried over MgSO₄ and the solvent was removed under reduced pressure to yield the desired product **32o** as a colorless solid (4.81 g, 23.3 mmol, 95% yield, 95:5 er).

7.2.6 Synthesis and Characterization of DSI Catalysts

Compound **48** and **17g** were synthesized following the reported procedure ^[160]

2,6-di(phenanthren-9-yl)-4*H*-dinaphtho[2,1-*d*:1',2'-*f*][1,3,2]dithiazepine 3,3,5,5-tetraoxide (**17g**)



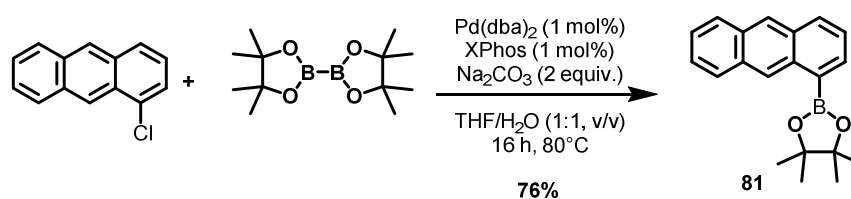
In an oven dried microwave vial (5 mL) (*S*)-3,3'-diiododisulfonimide (**48**, 100 mg, 0.15 mmol, 1 equiv.), 9-phenanthracenyl boronic acid (137 mg, 0.45 mmol, 3 equiv.), K_2CO_3 (85 mg, 0.6 mmol, 4 equiv.), Palladium(II)-acetate (3.5 mg, 0.015 mmol, 10 mol%) were suspended in THF/water (4 mL, 1:1, v/v) under an atmosphere of dry argon. Tri-*tert*-butylphosphine (1 M, dioxane solution) (0.1 mL, 81 mg, 0.1 mmol) was added and the vial was sealed and heated for 30 min at 120 °C in a microwave reactor. The reaction was poured into HCl (1 N, 5 mL) and extracted with CH_2Cl_2 (3x10mL), and the combined organic layers were washed with water (10 mL) and brine (2x10 mL). The organic layer was dried over MgSO_4 , and the product was purified by flash column chromatography ($\text{CH}_2\text{Cl}_2/\text{MeOH}$ = 100:0 to 98:2). The purified product was dissolved in CH_2Cl_2 (30 mL), acidified with HCl (6 M, 20 mL) and the solvent was removed in vacuo to obtain the targeted product **17g** as pale yellow solid (96 mg, 84% yield).

Note: Upon acidification, catalyst **17g** equilibrates to an unseparable mixture of 3 rotamers

¹H NMR (501 MHz, CDCl₃) δ = 8.87–8.71 (m, 4H), 8.34–8.17 (m, 2H), 8.17–8.02 (m, 2H), 8.02–7.92 (m, 2H), 7.92–7.85 (m, 2H), 7.85–7.76 (m, 2H), 7.76–7.35 (m, 14H), 1.53 ppm (bs, 1H).

¹³C NMR (126 MHz, CDCl₃) δ = 138.30, 138.25, 138.06, 136.04, 135.48, 135.35, 135.27, 135.11, 134.88, 134.86, 134.77, 134.75, 134.29, 134.24, 133.91, 133.75, 133.47, 133.04, 132.98, 132.44, 132.42, 132.28, 132.22, 132.16, 132.07, 131.34, 131.29, 131.17, 131.13, 130.41, 130.39, 130.36, 130.34, 129.93, 129.81, 129.79, 128.85, 128.74, 128.68, 128.61, 128.53, 128.48, 128.40, 128.26, 128.24, 127.92, 127.45, 127.43, 127.14, 127.03, 126.98, 126.94, 126.92, 126.90, 126.88, 126.81, 126.78, 126.53, 126.50, 126.46, 126.09, 126.01, 123.11, 122.90, 122.87, 122.72, 122.69 ppm.

2-(anthracen-1-yl)-4,4,5,5-tetramethyl-1,3,2-dioxaborolane (81)



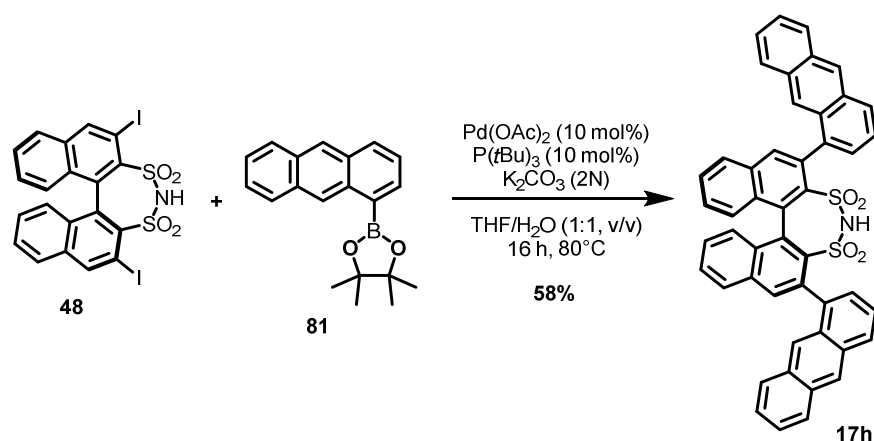
In a vial with stir bar was charged with 1-chloro-anthracene (500 mg, 2.4 mmol, 1.0 equiv.), anhydrous NaOAc (385 mg, 4.7 mmol, 2.0 equiv.), B₂Pin₂ (627 mg, 2.5 mmol, 1.05 equiv.), Pd(dba)₂ (13.5 mg, 0.02 mmol, 1 mol%), XPhos (11.2 mg, 0.02 mmol, 1 mol%). The vial was transferred to a preheated oil bath (110 °C). After 16 h, the reaction mixture was cooled, dissolved in CH₂Cl₂–H₂O mixture (1:1, v/v), the organic phase separated, the solvent evaporated under vacuum and the product isolated by flash chromatography on silica gel by elution with hexanes/CH₂Cl₂ (9:1 to 7:3), to obtain **81** (535 mg, 1.8 mmol, 76% yield).

¹H NMR (501 MHz, CDCl₃) δ = 9.35 (s, 1H), 8.42 (s, 1H), 8.17–8.05 (m, 3H), 8.04–7.94 (m, 1H), 7.56–7.36 (m, 3H), 1.48 ppm (s, 12H).

^{13}C NMR (126 MHz, CDCl_3) δ = 135.98, 134.31, 132.02, 131.98, 131.98, 131.58, 131.24, 128.97, 127.87, 127.30, 126.61, 125.30, 125.10, 124.54, 83.82, 83.82, 25.04, 25.04, 25.04, 25.04 ppm.

HRMS (EI) m/z calculated for $\text{C}_{20}\text{H}_{21}\text{O}_2\text{B}_1$ [M]: 304.1635; found 304.1637.

2,6-di(anthracen-1-yl)-4H-dinaphtho[2,1-d:1',2'-f][1,3,2]dithiazepine 3,3,5,5-tetraoxide (17h)



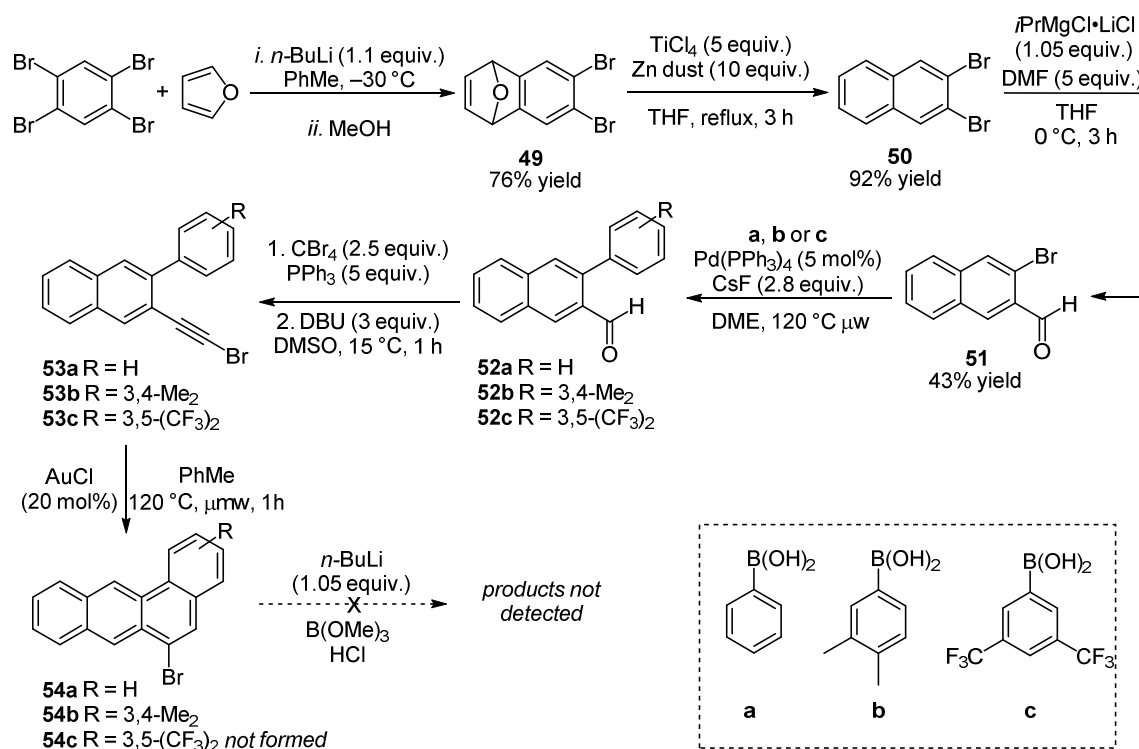
In a 25 mL Schlenk flask were placed (S)-**48** (387 mg, 0.6 mmol, 1 equiv.), aryl boronic ester **81** (545 mg, 1.8 mmol, 3 equiv.), $\text{Pd}(\text{OAc})_2$ (10.5 mg, 0.05 mmol, 8 mol%), 6 mL of THF and 2 M aqueous K_2CO_3 (6 mL). The reaction flask was evacuated and filled with Ar for three times with stirring. $\text{P}(\text{tBu})_3$ (94 μl , 0.09 mmol, 15 mol%) was then added. The reaction mixture was heated at 80°C until the consumption of the starting material (16 h). After the reaction was completed, the resulting mixture was acidified with 1 N HCl and extracted with CHCl_3 for three times. The combined organic phase was dried over MgSO_4 followed by filtration and evaporation. The crude product was purified by column chromatography (DCM:MeOH, 98:2) to give the coupled compound **17h** as a solid.

¹H NMR (501 MHz, CDCl₃) δ = 8.42 (s, 1H), 8.23 (d, *J* = 0.8 Hz, 1H), 8.10–8.00 (m, 3H), 7.93–7.88 (m, 1H), 7.76 (ddd, *J* = 8.2, 6.8, 1.2 Hz, 1H), 7.69–7.62 (m, 2H), 7.57 (dd, *J* = 8.5, 6.7 Hz, 1H), 7.52 (ddd, *J* = 8.2, 6.9, 1.3 Hz, 1H), 7.44 (dq, *J* = 8.7, 0.9 Hz, 1H), 7.32 (ddd, *J* = 8.3, 6.5, 1.2 Hz, 1H), 7.17 ppm (ddd, *J* = 8.1, 6.5, 1.2 Hz, 1H).

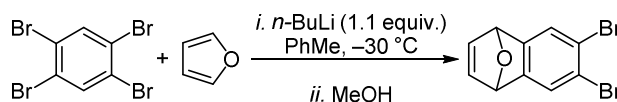
¹³C NMR (126 MHz, CDCl₃) δ = 138.49, 136.99, 135.64, 134.97, 134.13, 133.59, 132.09, 131.83, 131.75, 131.48, 131.09, 130.00, 128.69, 128.64, 128.61, 128.37, 128.36, 127.70, 126.47, 125.87, 125.59, 125.50, 125.14, 124.42 ppm.

HRMS (ESI) *m/z* calculated for C₄₈H₂₈N₁O₄S₂ [M–H][−]: 746.1465; found 746.1470.

Synthesis of Tetraphene Derivatives



6,7-dibromo-1,4,4a,8a-tetrahydro-1,4-epoxynaphthalene (49)

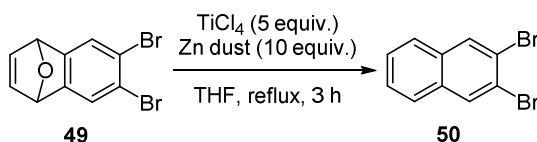


Under inert conditions 1,2,4,5-tetrabromobenzene (8.0 g, 20.5 mmol, 1.0 equiv.) was dissolved in dry toluene (200 mL). Dry furan (10 mL, 137 mmol, 6.8 equiv) was added and the solution was cooled down to $-30\text{ }^{\circ}\text{C}$, which led to the precipitation of starting compound. *n*-Butyl lithium (9 mL, 2.4M in hexane, 22.6 mmol) was added dropwise during 20 minutes. Following an additional 15 min stirring at $-30\text{ }^{\circ}\text{C}$, the mixture was warmed to $25\text{ }^{\circ}\text{C}$ and MeOH (1 ml) was added. The solution was washed with water (30 mL) and brine (30 mL), the organic layer was dried with MgSO_4 and all solvents were evaporated under vacuum. The brownish raw product was applied onto silica gel via dichloromethane and subjected to column chromatography (hexanes/EtOAc, 10:1) to yield a yellowish oil, which upon cooling crystallized to give a colourless solid (4.1 g, 66%).

$^1\text{H NMR}$ (501 MHz, CDCl_3) δ = 7.48 (s, 2H), 7.03–6.97 (m, 2H), 5.68–5.65 ppm (m, 2H).

$^{13}\text{C NMR}$ (126 MHz, CDCl_3) δ = 150.2, 150.2, 142.7, 142.7, 125.5, 125.5, 120.7, 120.7, 81.8 81.8 ppm.

2,3-dibromonaphthalene (50)



TiCl_4 (8.5 mL, 75 mmol) was added dropwise to a stirred suspension of Zn-dust (8.5 g, 125 mmol) in THF (150 mL) at $0\text{ }^{\circ}\text{C}$ under Ar carefully. (Caution: Violent reaction)

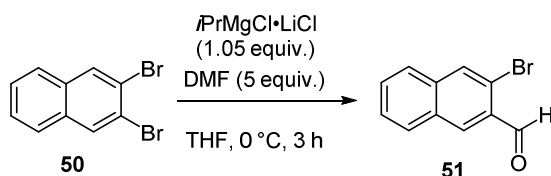
The resulting mixture was heated to reflux for 5 min then cooled to 0 °C again. Compound **49** (4 g, 13.2 mmol, 1 equiv.) was added in THF solution (15 mL) and the mixture was heated at reflux for an additional 3 h. After cooling to 25 °C, it was poured on ice cold aqueous HCl (0.1 M, 300 mL), followed by extraction with CH₂Cl₂. The organic phase was washed with water (30 mL) and brine (30 mL), dried, MgSO₄ and filtered. After removal of the solvent under reduced pressure, purification by column chromatography (hexanes) gave **50** as white crystals (3.5 g, 92% yield).

¹H NMR (500 MHz, CDCl₃) δ = 8.14 (s, 2H), 7.73 (dd, *J* = 6.2, 3.2, 2H), 7.51 ppm (dd, *J* = 6.3, 3.2, 2H).

¹³C NMR (125 MHz, CDCl₃) δ = 133.0, 132.2, 132.2, 127.2, 127.2, 126.9, 126.9, 122.0, 122.0 ppm.

In agreement with literature data.^[161]

3-bromo-2-naphthaldehyde (**51**)



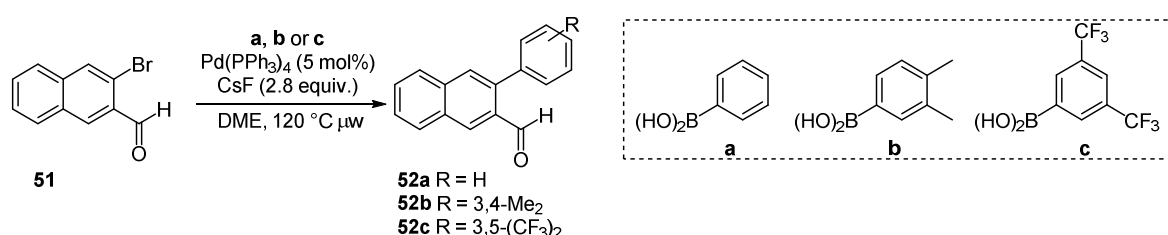
*i*PrMgCl·LiCl (1.3M in THF, 5.0 mL, 6.8 mmol, 1.0 equiv.) was added dropwise to a solution of compound **50** (1.86 g, 1.75 mmol) in THF (50 mL) at 0 °C under Ar in 10 min. After stirring for 90 min at 0 °C, DMF (3 mL, 38.7 mmol, 6 equiv.) was added and the mixture stirred for an additional 15 min at 0 °C. The mixture was treated with water (100 mL) and the aqueous mixture extracted with EtOAc. The organic phase was washed with water (50 mL) and brine (30 mL), dried over MgSO₄ and filtered. The solvent was removed under reduced pressure, and the crude product was purified by column chromatography (hexanes/EtOAc, 20:1) giving **51** as a colorless solid (692 mg, 45% yield).

^1H NMR (500 MHz, CDCl_3) δ = 10.51 (s, 1H), 8.47 (s, 1H), 8.13 (s, 1H), 8.00–7.94 (m, 2H), 7.82–7.78 (m, 1H), 7.64 (ddd, J = 8.2, 6.8, 1.3 Hz, 1H), 7.58 ppm (ddd, J = 8.2, 6.8, 1.3 Hz, 1H).

^{13}C NMR (125 MHz, CDCl_3) δ = 192.1, 137.1, 132.7, 132.1, 131.7, 130.7, 130.2, 130.1, 127.6, 127.6, 127.1, 120.7 ppm.

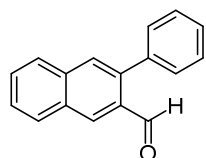
In agreement with literature data.^[162]

Synthesis of 3-Aryl-2-naphthaldehyde Derivatives (**52a–52c**)



In an oven dried microwave vial (5 mL) **51** (1 equiv.), boronic acid (1.2 equiv.), CsF (2.8 equiv.), tetrakis(triphenylphosphine)palladium(0) (5 mol%) were suspended in DME (0.5 M) under an atmosphere of dry argon. The vial was sealed and heated for 1 h at 120 °C in a microwave reactor. The reaction was poured into water (5 mL) and extracted with EtOAc (3x10mL), and the combined organic layers were washed with brine (2x10 mL). The organic layer was dried over MgSO_4 , and the product was purified by flash column chromatography (hexanes/EtOAc = 100:0 to 80:20). The targeted product as a colorless solid.

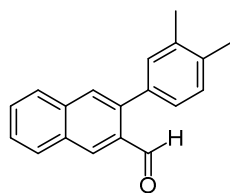
3-phenyl-2-naphthaldehyde (**52a**)



Prepared according to general procedure for 3-aryl-2-naphthaldehyde derivatives using 3-bromo-2-naphthaldehyde (**51**) (70 mg, 0.3 mmol) and obtained after extraction as a colorless solid (63 mg, 0.28 mmol, 96% yield).

¹H NMR (500 MHz, CDCl₃) δ = 10.13 (s, 1H), 8.58 (s, 1H), 8.07–8.01 (m, 1H), 7.93–7.89 (m, 1H), 7.88 (s, 1H), 7.65 (ddd, J = 8.1, 6.8, 1.3 Hz, 1H), 7.58 (ddd, J = 8.2, 6.9, 1.3 Hz, 1H), 7.54–7.43 ppm (m, 6H).

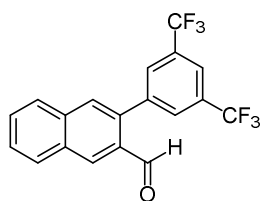
3-(3,4-dimethylphenyl)-2-naphthaldehyde (52b)



Prepared according to general procedure for 3-aryl-2-naphthaldehyde derivatives using 3-bromo-2-naphthaldehyde (**51**) (70 mg, 0.3 mmol) and obtained after extraction as a colorless solid (70 mg, 0.28 mmol, 90% yield).

¹H NMR (501 MHz, CDCl₃) δ = 10.07 (s, 1H), 8.49 (s, 1H), 7.96 (dd, J = 8.2, 1.1 Hz, 1H), 7.82 (dd, J = 8.4, 1.0 Hz, 1H), 7.79 (s, 1H), 7.56 (ddd, J = 8.2, 6.9, 1.3 Hz, 1H), 7.49 (ddd, J = 8.2, 6.9, 1.3 Hz, 1H), 7.42–7.37 (m, 1H), 7.22–7.16 (m, 1H), 7.13 (dd, J = 7.7, 2.1 Hz, 1H), 2.32–2.27 ppm (m, 6H).

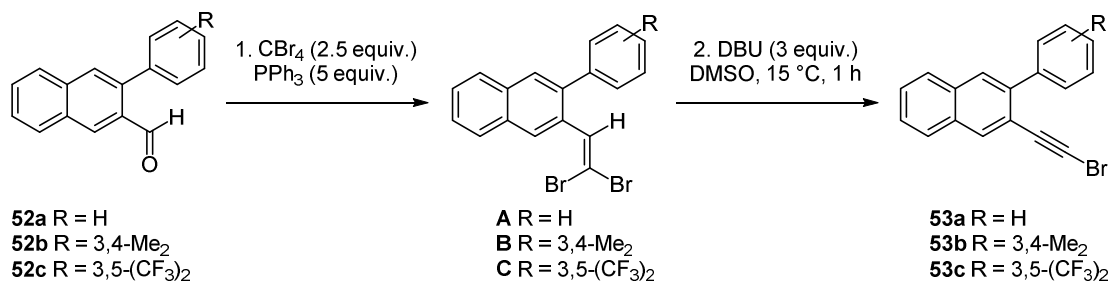
3-(3,5-bis(trifluoromethyl)phenyl)-2-naphthaldehyde (52c)



Prepared according to general procedure for 3-aryl-2-naphthaldehyde derivatives using 3-bromo-2-naphthaldehyde (**51**) (70 mg, 0.3 mmol) and obtained after extraction as a colorless solid (76 mg, 0.20 mmol, 69% yield).

¹H NMR (501 MHz, CDCl₃) δ = 10.10 (s, 1H), 8.57 (s, 1H), 8.14–8.05 (m, 1H), 7.98–7.92 (m, 2H), 7.90 (d, J = 1.6 Hz, 2H), 7.84 (s, 1H), 7.72 (ddd, J = 8.2, 6.9, 1.3 Hz, 1H), 7.67 ppm (ddd, J = 8.1, 6.9, 1.3 Hz, 1H).

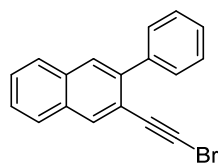
Synthesis of 2-(Bromoethynyl)-3-arylnaphthalene Derivatives (**53a–53c**)



Step 1: CBr₄ (2.5 equiv.) was added to a solution of PPh₃ (5 equiv.) in DCM (6 ml) and the resulting mixture was stirred for 10 min at 0 °C. A solution of 3-aryl-2-naphthaldehyde (**52a–52c**) (1 equiv.) in DCM (4 ml) was slowly introduced and stirring was continued for 1 h at 0 °C. The reaction was then quenched with brine (20 mL), the aqueous layer was repeatedly extracted with DCM (3x 20 mL), and the combined organic layer were dried with MgSO₄ and evaporated. The residue was purified with chromatography (hexanes/EtOAc, 95:5). The intermediate dibromocompound (**A–C**) was directly subjected to the following synthetic step.

Step 2: A solution of DBU (58 μl) in DMSO (2 ml) was added to a cooled solution of dibromide (**A–C**) (50 mg) in DMSO (20 ml) at such rate to maintain the internal temperature below 15 °C. The resulting mixture was stirred for 1 h before the reaction was quenched with aq HCl at 0 °C.

2-(bromoethynyl)-3-phenylnaphthalene (**53a**)

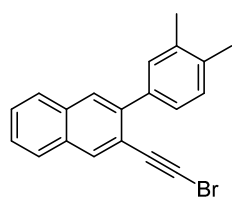


Prepared according to general procedure for 2-(bromoethynyl)-3-arylnaphthalene derivatives using 3-phenyl-2-naphthaldehyde (**52a**) (38 mg, 0.16 mmol) and obtained after two steps as a pale yellow solid (38 mg, 0.12 mmol, 75% yield).

Intermediate A: ¹H NMR (501 MHz, CDCl₃) δ = 8.16 (s, 1H), 7.93 – 7.88 (m, 1H), 7.88 – 7.83 (m, 1H), 7.82 (s, 1H), 7.56 – 7.39 (m, 6H), 7.31 ppm (d, J = 1.0 Hz, 1H).

¹H NMR (501 MHz, CDCl₃) δ = 8.11 (s, 1H), 7.85 – 7.77 (m, 3H), 7.69 – 7.61 (m, 2H), 7.54–7.43 (m, 4H), 7.44–7.37 ppm (m, 1H).

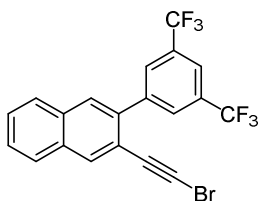
2-(bromoethynyl)-3-(3,4-dimethylphenyl)naphthalene (53b)



Prepared according to general procedure for 2-(bromoethynyl)-3-arylnaphthalene derivatives using 3-(3,4-dimethylphenyl)-2-naphthaldehyde (**52b**) (26 mg, 0.10 mmol) and obtained after two steps as a pale yellow solid (38 mg, 0.07 mmol, 75% yield).

¹H NMR (501 MHz, CDCl₃) δ = 8.10 (d, *J* = 0.8 Hz, 1H), 7.85–7.77 (m, 3H), 7.52–7.43 (m, 3H), 7.41 (dd, *J* = 7.7, 2.0 Hz, 1H), 7.23 (d, *J* = 7.7 Hz, 1H), 2.36 (s, 3H), 2.34 ppm (s, 3H).

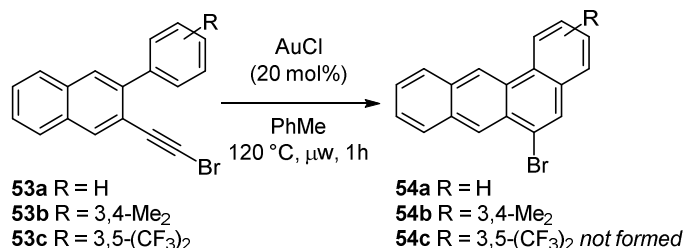
2-(3,5-bis(trifluoromethyl)phenyl)-3-(bromoethynyl)naphthalene (53c)



Prepared according to general procedure for 2-(bromoethynyl)-3-arylnaphthalene derivatives using 3-(3,5-bis(trifluoromethyl)phenyl)-2-naphthaldehyde (**52c**) (36 mg, 0.10 mmol) and obtained after two steps as a pale yellow solid (38 mg, 0.12 mmol, 69% yield).

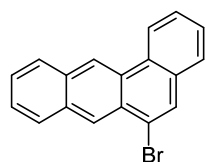
¹H NMR (501 MHz, CDCl₃) δ = 8.17–8.15 (m, 1H), 8.15–8.12 (m, 2H), 7.94–7.90 (m, 1H), 7.90–7.83 (m, 3H), 7.61–7.53 ppm (m, 2H).

Synthesis of 6-Bromo-tetraphene Derivatives (**54a–54c**)



In an oven dried microwave vial (5 mL) 2-(bromoethynyl)-3-arylnaphthalene derivatives (**53a–52c**) (1 equiv.) and AuCl (20 mol%) were dissolved in toluene (0.5 M) under an atmosphere of dry argon. The vial was sealed and heated for 1 h at 120 °C in a microwave reactor. The reaction was directly concentrated under reduced pressure and the crude reaction mixture was purified by flash column chromatography (hexanes/EtOAc = 100:0 to 95:5). The targeted product as pale yellow solid.

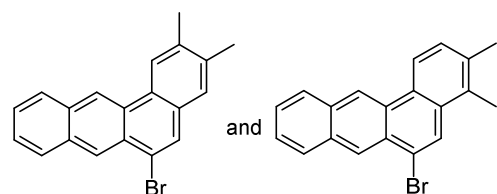
6-bromo-tetraphene (**54a**)



Prepared according to general procedure for 6-bromo-tetraphene derivatives (**54a–54c**) using 2-(bromoethynyl)-3-phenylnaphthalene (**53a**) (31 mg, 0.10 mmol) and obtained after column chromatography as a pale yellow solid (20 mg, 0.1 mmol, 65% yield).

¹H NMR (501 MHz, CDCl₃) δ = 9.18 (s, 1H), 8.86 (s, 1H), 8.81 (d, *J* = 8.2 Hz, 1H), 8.19–8.11 (m, 2H), 8.04 (s, 1H), 7.79–7.74 (m, 1H), 7.71 (ddd, *J* = 8.4, 7.1, 1.4 Hz, 1H), 7.66–7.58 ppm (m, 3H).

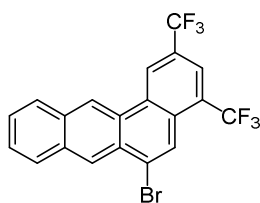
6-bromo-2,3-*bis*-methyl-tetraphene and 6-bromo-3,4-dimethyl-tetraphene (**54b**)



Prepared according to general procedure for 6-bromo-tetraphene derivatives (**54a–54c**) using 2-(bromoethynyl)-3-(3,4-dimethylphenyl)naphthalene (**53b**) (32 mg, 0.10 mmol). The desired regioisomers could not be separated by column chromatography.

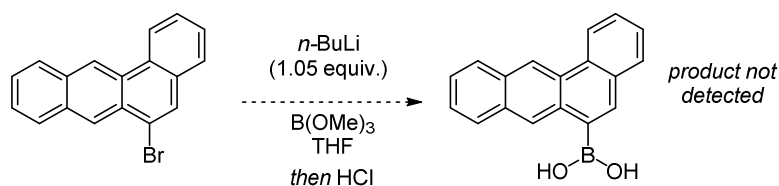
After repeated attempts to purify the compounds, the final products could not be recovered as they fully decomposed (the compounds are unstable in the presence of oxygen and light).

2,4-bis-trifluoromethyl-6-bromo-tetraphene (**54c**)



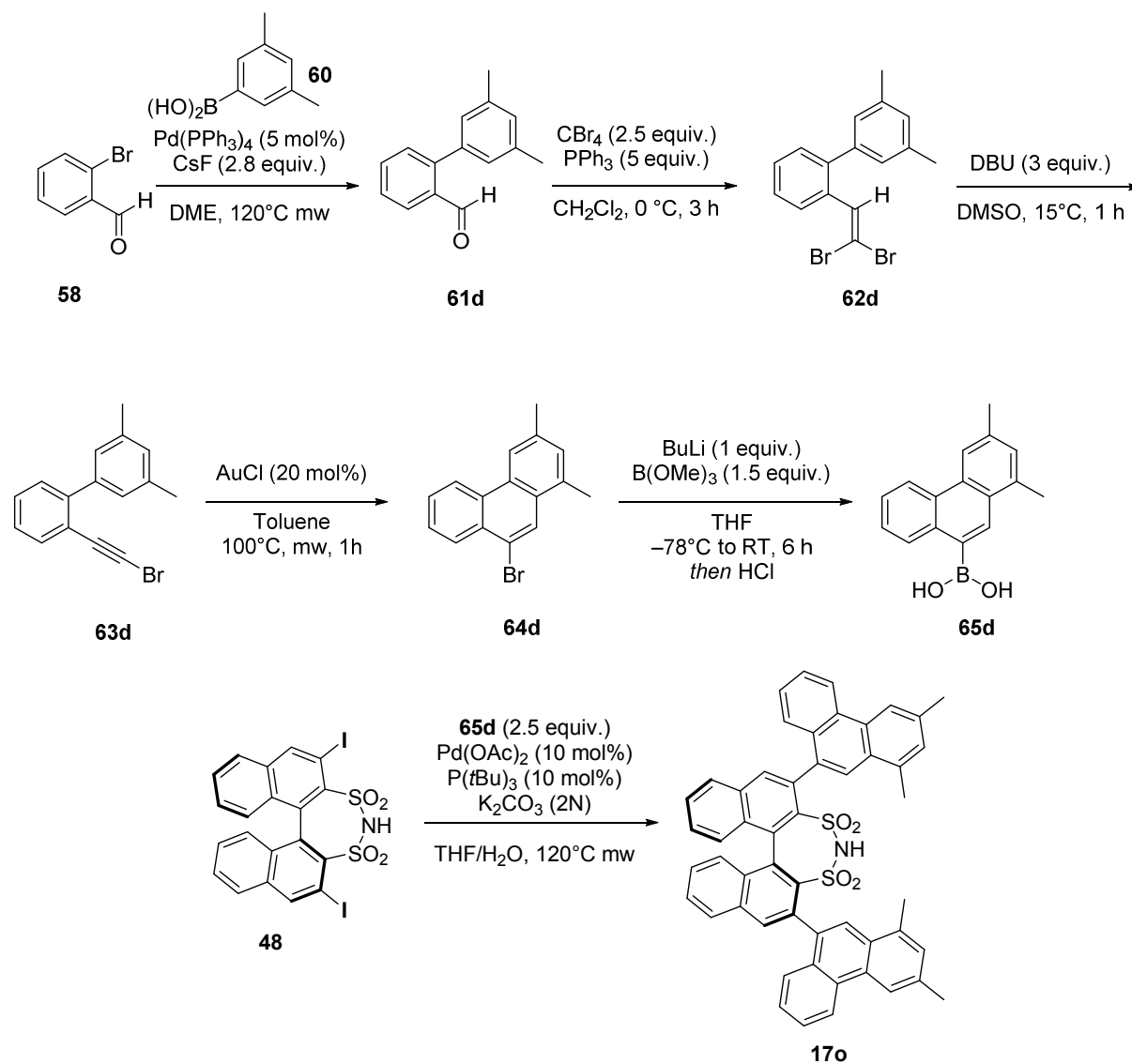
The desired product was not formed and only starting material was recovered. Increasing the AuCl catalyst loading, the reaction time or the temperature led to decomposition to undefined by-products.

Boronic acid **82**



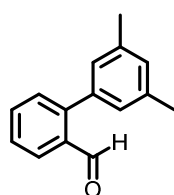
A two-necked 25 mL flask was charged with 6-bromo-tetraphene (**54a**) (20 mg, 0.1 mmol) under argon. Dry THF (3 mL) was added, and the solution was cooled to $-78\text{ }^{\circ}\text{C}$. To this solution was added *n*-butyllithium (40 μL , 2.5 M, 0.1 mmol) dropwise. The solution was stirred at $-78\text{ }^{\circ}\text{C}$ for 2 h whereupon trimethyl borate (16 μg , 0.15 mmol) dissolved in 1 mL of dry THF was added dropwise through the second dropping funnel. The solution was allowed to warm to room temperature overnight. The crude reaction was checked via $^1\text{H-NMR}$, however the desired compound was not identified and exclusively highly insoluble solids were obtained.

Synthesis of DSI 17o



Compound **64d** was synthesized following a modification of the reported procedure.^[163]

2-(3,5-dimethylphenyl)benzaldehyde (61d)



In a oven dried 20 mL microwave vial under an atmosphere of dry argon 2-bromobenzaldehyde **58** (1.0 g, 5.4 mmol, 1 equiv.), 3,5-dimethylphenyl boronic acid **60** (0.97 g, 6.5 mmol, 1.2 equiv.), cesium fluoride (2.3 g, 15.1 mmol, 2.8 equiv.) and

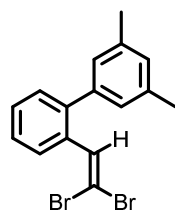
tetrakis(triphenylphosphine)palladium(0) (0.313 g, 0.27 mmol, 5 mol%) were added and suspended in degassed 1,2-DME (10 mL). The vial was sealed and heated at 120 °C for 1 hour in a microwave reactor. The reaction mixture was diluted with EtOAc (30 mL) and water (30 mL) and extracted with EtOAc (3×20 mL). The combined organic layers were dried over MgSO₄, concentrated under reduced pressure and the crude product was purified by flash column chromatography (Hexanes/EtOAc = 100:0 to 95:5) to obtain **61d** as a colorless solid (1.06 g, 5.0 mmol, 93% yield).

¹H NMR (501 MHz, CDCl₃) δ = 9.99 (d, *J* = 0.8 Hz, 1H), 8.01 (dd, *J* = 7.8, 1.5 Hz, 1H), 7.62 (td, *J* = 7.5, 1.5 Hz, 1H), 7.47 (tt, *J* = 7.6, 1.1 Hz, 1H), 7.44 (dd, *J* = 7.7, 1.2 Hz, 1H), 7.08 (s, 1H), 7.00 (s, 2H), 2.46–2.31 ppm (m, 6H).

¹³C NMR (126 MHz, CDCl₃) δ 192.89, 146.49, 138.16, 137.80, 133.90, 133.59, 130.83, 129.86, 128.19, 127.68, 127.51, 21.45 ppm.

HRMS (GC–EI) *m/z* calculated for C₁₅H₁₄O [M]: 210.1041; found 210.1039.

2-(2,2-dibromovinyl)-3',5'-dimethyl-1,1'-biphenyl (**62d**)



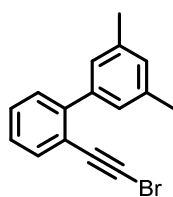
CBr₄ (4.20 g, 12.6 mmol, 2.5 equiv.) was added portion wise to a solution of PPh₃ (6.7 g, 25.0 mmol, 5.0 equiv.) in CH₂Cl₂ (20 mL) and the resulting yellow mixture was stirred for 10 min at 0 °C. A solution of 2-(3,5-dimethylphenyl)benzaldehyde (**61d**; 1.06 g, 5.0 mmol, 1.0 equiv.) in CH₂Cl₂ (20 mL) was added dropwise and stirring was continued for an additional 1 h at 0 °C. The reaction was then quenched with brine and the aqueous layer was extracted with CH₂Cl₂ (3×20 mL). The combined organic layers were dried over MgSO₄, concentrated under reduced pressure and the crude product was purified by flash column chromatography (Hexanes/EtOAc = 100:0 to 95:5) to obtain **62d** as a colorless solid (1.60 g, 88% yield)

¹H NMR (501 MHz, CDCl₃) δ = 7.73–7.65 (m, 1H), 7.43–7.32 (m, 3H), 7.23 (s, 1H), 7.02 (s, 1H), 6.95 (s, 2H), 2.38 ppm (s, 6H).

^{13}C NMR (126 MHz, CDCl_3) δ = 141.17, 139.87, 137.62, 137.59, 132.86, 132.03, 131.80, 129.62, 129.04, 128.97, 128.43, 128.33, 127.29, 126.78, 90.23, 21.25 ppm.

HRMS (GC–EI) m/z calculated for $\text{C}_{16}\text{H}_{14}\text{Br}_2$ [M]: 363.9460; found 363.9457.

2-(bromoethynyl)-3',5'-dimethyl-1,1'-biphenyl (**63d**)

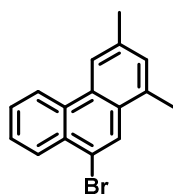


A solution of DBU (1.4 mL, 9.8 mmol, 3.0 equiv.) in DMSO (20 mL) was added to a cooled solution of **62d** (1.2 g, 3.3 mmol, 1.0 equiv.) in DMSO (30 mL) at such rate to maintain the internal temperature below 15 °C. The resulting mixture was stirred at 15 °C for 1 h before the reaction was quenched with aq. HCl (1M) at 0°C. The aqueous layer was extracted with CH_2Cl_2 (3 x 20 mL) and the combined organic layers were washed with sat. aq. NaHCO_3 solution (20 mL), water (10 mL) and brine (2x10 mL). Afterwards, the organic layer was dried over MgSO_4 , the solvent was removed under reduced pressure to obtain **63d** the as colorless solid (703 mg, 75% yield) without further purification.

^1H NMR (501 MHz, CDCl_3) δ = 7.55 (dt, J = 7.6, 1.0 Hz, 1H), 7.38 (dd, J = 3.9, 0.9 Hz, 2H), 7.31–7.23 (m, 1H), 7.23–7.18 (m, 2H), 7.02 (m, 1H), 2.41–2.35 ppm (m, 6H).

HRMS (GC–EI) m/z calculated for $\text{C}_{15}\text{H}_{13}\text{Br}$ [M]: 284.0197; found 284.0195.

9-Bromo-1,3-dimethyl-phenanthrene (**64d**)



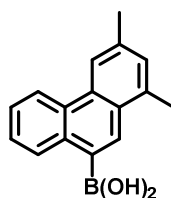
In an oven-dried 5 mL microwave vial under an atmosphere of dry argon, AuCl (102 mg, 0.44 mmol, 20 mol%) and **63d** (630 mg, 2.2 mmol, 1.0 equiv.) in toluene (3 mL) were heated at 100°C for 1 h. The mixture was then adsorbed on silica gel and purified by flash chromatography (Hexanes/EtOAc = 9:1 to 8:2) to obtain **64d** as a colorless solid (576 mg, 91% yield).

¹H NMR (501 MHz, CDCl₃) δ = 8.73–8.64 (m, 1H), 8.39–8.29 (m, 2H), 8.26 (s, 1H), 7.73–7.62 (m, 2H), 7.29 (s, 1H), 2.69 (s, 3H), 2.57 ppm (s, 3H).

¹³C NMR (126 MHz, CDCl₃) δ = 136.41, 134.03, 131.40, 130.22, 130.17, 130.05, 129.17, 127.97, 127.23, 127.16, 126.85, 123.10, 120.75, 120.62, 22.10, 19.69 ppm.

HRMS (GC–EI) m/z calculated for C₁₆H₁₃Br [M]: 284.0201; found 284.0195.

1,3-dimethyl-phenanthren-9-yl boronic acid (**65d**)



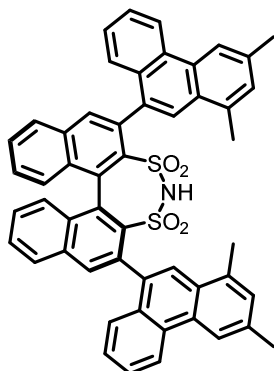
An oven dried two-necked 100 mL flask was charged with **64d** (570 mg, 2.0 mmol, 1.0 equiv.) under an atmosphere of dry argon. Dry THF (20 mL) was added and the resulting solution was cooled to –78 °C and *n*-butyllithium (0.8 mL, 2.6 M in hexane, 2 mmol, 1.0 equiv.) was added dropwise. The reaction mixture was stirred at –78 °C for 1 h and a solution of trimethyl borate (0.34 mL, 312 mg, 3 mmol, 1.5 equiv.) in dry THF (10 mL) was added dropwise. The solution was allowed to warm to room temperature overnight. The reaction was quenched with aq. HCl (1 M, 5 mL), concentrated under reduced pressure to 50% of its original volume and poured into H₂O. The resulted biphasic solution was extracted with Et₂O (2 x 50 mL). The ethereal solution was washed twice with H₂O and concentrated under reduced pressure. The targeted product **65d** was obtained after filtration as a colorless solid (375 mg, 76% yield).

¹H NMR (501 MHz, d₈-THF) δ = 8.64 (ddd, J = 19.4, 8.2, 1.5 Hz, 2H), 8.34 (m, 2H), 7.47 (m, 2H), 7.22 (s, 1H), 2.68 (s, 3H), 2.49 ppm (s, 3H), [acid proton not visible due to fast exchange].

¹³C NMR (126 MHz, d₈-THF) δ = 135.98, 134.86, 134.40, 131.35, 130.20, 129.97, 129.48, 129.07, 127.88, 125.56, 125.35, 122.52, 120.11, 21.19, 18.94 ppm.

HRMS (ESI) m/z calculated for C₁₆H₁₄BO₂ [M–H][–]: 249.1092; found 249.1096.

2,6-bis(1,3-dimethylphenanthren-9-yl)-4H-dinaphtho[2,1-d':1',2'-f][1,3,2]dithiazepine 3,3,5,5-tetraoxide (17o)



In an oven dried microwave vial (5 mL) (S)-3,3'-diiododisulfonimide **48** (320 mg, 0.5 mmol, 1 equiv.), **65d** (330 mg, 1.5 mmol, 3 equiv.), K₂CO₃ (273 mg, 2.0 mmol, 4 equiv.), Palladium(II)-acetate (11 mg, 0.05 mmol, 0.1 equiv, 10 mol%.) were suspended in THF/water (4 mL, 1:1, v/v) under an atmosphere of dry argon. Tri-*tert*-butylphosphine (1M, dioxane solution) (0.1 mL, 81 mg, 0.1 mmol) was added and the vial was sealed and heated for 30 min at 120 °C in a microwave reactor.

The reaction was poured into HCl (1N, 5 mL) and extracted with CH₂Cl₂ (3 x 10mL), and the combined organic layers were washed with water (10 mL) and brine (2x10 mL). The organic layer was dried over MgSO₄, and the product was purified by flash column chromatography (CH₂Cl₂/MeOH = 100:0 to 98:2). The purified product was dissolved in CH₂Cl₂ (30 mL), acidified with HCl (6 M, 20 mL) and the solvent removed in vacuo to obtain the targeted product as pale yellow solid (365 mg, 91% yield).

Note: Upon acidification, catalyst **17o** equilibrates to an unseperable mixture of 3 rotamers (1.7:49:3.4).

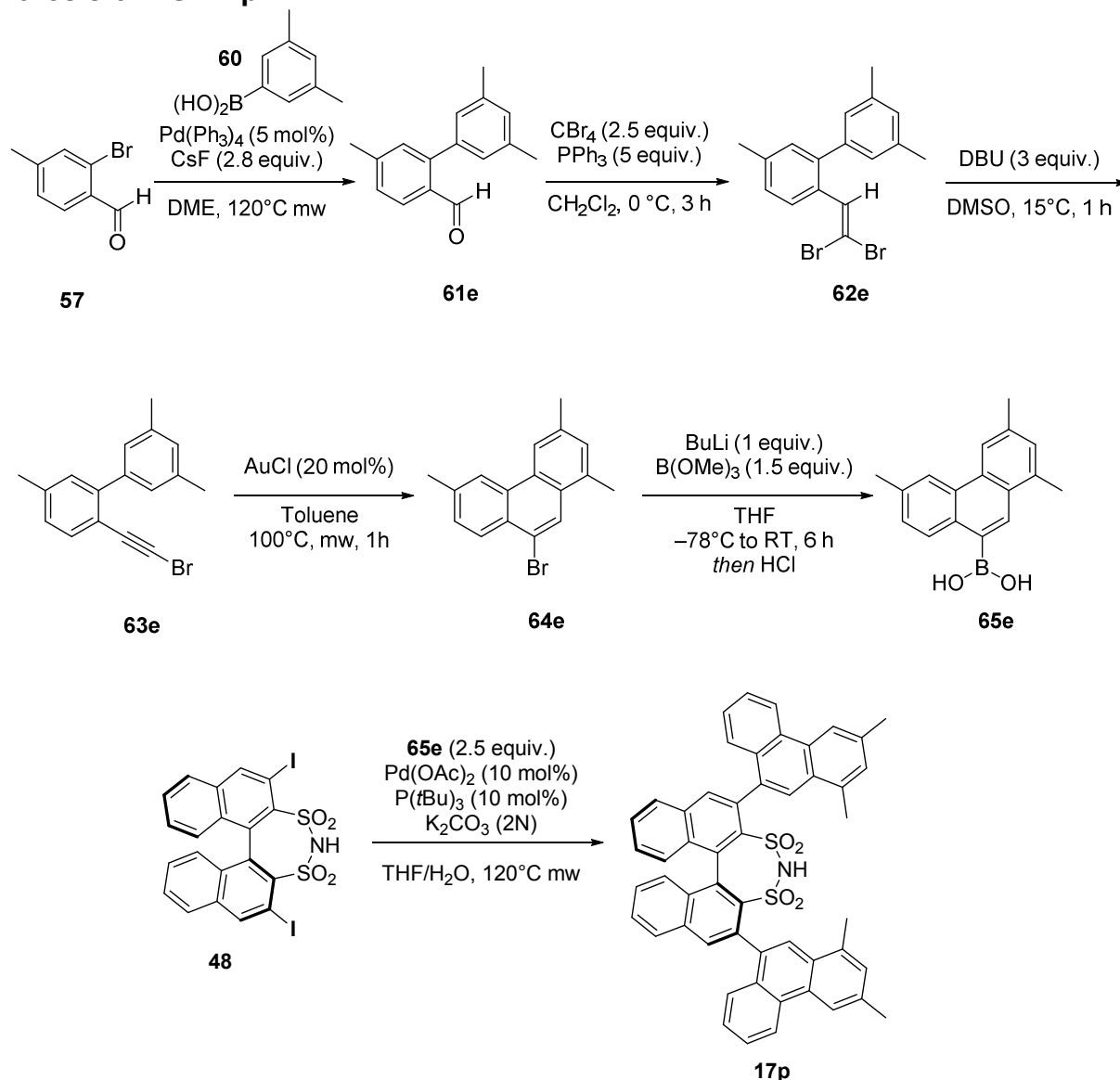
¹H NMR (501 MHz, CDCl₃) δ = 8.82–8.72 (m, 2H), 8.41 (d, *J* = 4.4 Hz, 2H), 8.28–8.17 (m, 2H), 8.10–7.98 (m, 4H), 7.80–7.69 (m, 2H), 7.69–7.46 (m, 8H), 7.46–7.28 (m, 6H), 2.80–2.68 (m, 6H), 2.64–2.54 ppm (m, 6H).

¹³C NMR (126 MHz, CDCl₃) δ 138.28, 138.25, 138.04, 137.98, 136.21, 136.06, 136.04, 135.98, 135.87, 135.45, 135.40, 135.12, 135.08, 135.00, 134.81, 134.76, 134.74, 134.39, 134.37, 134.35, 134.32, 134.21, 134.06, 133.87, 133.54, 133.34, 132.71, 132.62, 132.23, 132.17, 132.13, 132.01, 130.62, 130.59, 130.55, 130.01, 129.98, 129.95, 129.90, 129.86, 129.83, 129.81, 128.61, 128.59, 128.56, 128.53, 128.51, 128.39, 128.30, 128.24, 128.22, 128.12, 128.08, 127.94, 127.91, 126.95, 126.68, 126.66, 126.49, 126.44, 126.25, 126.21, 126.16, 125.84, 125.70, 123.88,

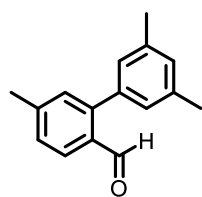
123.86, 123.58, 123.50, 123.39, 123.37, 123.14, 123.11, 120.61, 120.58, 22.12, 22.11, 19.94, 19.91 ppm.

HRMS (ESI) m/z calculated for $C_{52}H_{36}N_1O_4S_2$ $[M-H]^-$: 802.2102; found 802.2091.

Synthesis of DSI-17p



2-(3,5-dimethylphenyl)-4-methylbenzaldehyde (61e)



In a oven dried 20 mL microwave vial under an atmosphere of dry argon 2-bromo-4-methylbenzaldehyde **57** (1.0 g, 5.4 mmol, 1 equiv.), 3,5-dimethylphenyl boronic acid **60** (0.97 g, 6.5 mmol, 1.2 equiv.),

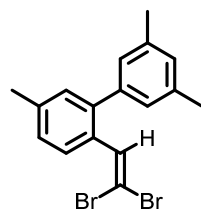
cesium fluoride (2.3 g, 15.1 mmol, 2.8 equiv.) and tetrakis(triphenylphosphine)palladium(0) (0.313 g, 0.27 mmol, 5 mol%) were added and suspended in degassed 1,2-DME (10 mL). The vial was sealed and heated at 120 °C for 1 hour in a microwave reactor. The reaction mixture was diluted with EtOAc (30 mL) and water (30 mL) and extracted with EtOAc (3×20 mL). The combined organic layers were dried over MgSO₄, concentrated under reduced pressure and the crude product was purified by flash column chromatography (Hexanes/EtOAc = 100:0 to 95:5) to obtain **61e** as a colorless solid (1.13 g, 5.0 mmol, 93% yield).

¹H NMR (501 MHz, CDCl₃) δ = 9.96 (s, 1H), 7.95 (d, *J* = 7.9 Hz, 1H), 7.33–7.22 (m, 3H), 7.09 (s, 1H), 7.01 (s, 2H), 2.47 (s, 3H), 2.40 ppm (s, 6H).

¹³C NMR (126 MHz, CDCl₃) δ = 192.43, 144.40, 137.93, 133.29, 131.27, 129.61, 128.45, 127.97, 127.97, 127.49, 77.27, 77.01, 76.76, 21.82, 21.35, 21.30 ppm.

HRMS (GC–EI) *m/z* calculated for C₁₅H₁₄O [M]: 224.1201; found 224.1203.

2-(2,2-dibromovinyl)-3',5,5'-trimethyl-1,1'-biphenyl (**62e**)

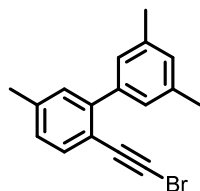


CBr₄ (4.18 g, 12.6 mmol, 2.5 equiv.) was added portion wise to a solution of PPh₃ (6.7 g, 25.0 mmol, 5.0 equiv.) in CH₂Cl₂ (20 mL) and the resulting yellow mixture was stirred for 10 min at 0 °C. A solution of 2-(3,5-dimethylphenyl)-4-methylbenzaldehyde (**61e**; 1.06 g, 5.0 mmol, 1.0 equiv.) in CH₂Cl₂ (20 mL) was added dropwise and stirring was continued for an additional 1 h at 0 °C. The reaction was then quenched with brine and the aqueous layer was extracted with CH₂Cl₂ (3×20 mL). The combined organic layers were dried over MgSO₄, concentrated under reduced pressure and the crude product was purified by flash column chromatography (Hexanes/EtOAc = 100:0 to 95:5) to obtain **62e** as a colorless solid (1.83 g, 95% yield)

¹H NMR (501 MHz, CDCl₃) δ = 7.63 – 7.57 (m, 1H), 7.22 – 7.13 (m, 3H), 7.01 (s, 1H), 6.94 (s, 2H), 2.38 (s, 3H), 2.37 (s, 6H).

¹³C NMR (126 MHz, CDCl₃) δ = 141.17, 139.87, 137.62, 137.59, 132.86, 132.03, 131.80, 129.62, 129.04, 128.97, 128.43, 128.33, 127.29, 126.78, 90.23, 21.25 ppm.

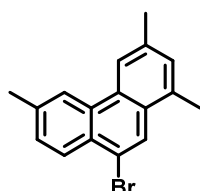
2-(bromoethynyl)-3',5,5'-trimethyl-1,1'-biphenyl (**63e**)



A solution of DBU (1.0 mL, 14.4 mmol, 3.0 equiv.) in DMSO (30 mL) was added to a cooled solution of **62e** (1.8 g, 3.3 mmol, 4.8 equiv.) in DMSO (30 mL) at such rate to maintain the internal temperature below 15 °C. The resulting mixture was stirred at 15 °C for 1 h before the reaction was quenched with aq. HCl (1M) at 0°C. The aqueous layer was extracted with CH₂Cl₂ (3 x 20 mL) and the combined organic layers were washed with sat. aq. NaHCO₃ solution (20 mL), water (10 mL) and brine (2x10 mL). Afterwards, the organic layer was dried over MgSO₄, the solvent was removed under reduced pressure to obtain **63e** the as colorless solid (850 mg, 59% yield) without further purification.

¹H NMR (501 MHz, CDCl₃) δ = 7.44 (d, *J* = 7.8 Hz, 1H), 7.21–7.18 (m, 3H), 7.08 (ddd, *J* = 7.9, 1.8, 0.8 Hz, 1H), 7.03–6.99 (m, 1H), 2.61 (s, 3H), 2.38 ppm (s, 6H).

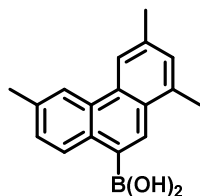
9-Bromo-1,3,6-trimethyl-phenanthrene (**64e**)



In an oven-dried 5 mL microwave vial under an atmosphere of dry argon, AuCl (217 mg, 0.94 mmol, 20 mol%) and **63e** (1400 mg, 4.7 mmol, 1.0 equiv.) in toluene (5 mL) were heated at 100°C for 1 h. The mixture was then adsorbed on silica gel and purified by flash chromatography (Hexanes/EtOAc = 9:1 to 8:2) to obtain **64e** as a colorless solid (600 mg, 43% yield).

¹H NMR (501 MHz, CDCl₃) δ = 8.47 (s, 1H), 8.33–8.30 (m, 1H), 8.23 (d, *J* = 8.4 Hz, 1H), 8.18 (d, *J* = 0.8 Hz, 1H), 7.52–7.48 (m, 1H), 7.28 (s, 1H), 2.68 (s, 3H), 2.64 (s, 3H), 2.56 ppm (s, 3H).

1,3,6-trimethyl-phenanthren-9-yl boronic acid (65e)

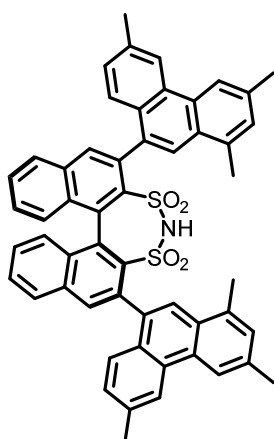


An oven dried two-necked 100 mL flask was charged with **64e** (500 mg, 1.7 mmol, 1.0 equiv.) under an atmosphere of dry argon. Dry THF (20 mL) was added and the resulting solution was cooled to $-78\text{ }^{\circ}\text{C}$ and *n*-butyllithium (0.7 mL, 2.4 M in hexane, 1.7 mmol, 1.0 equiv.) was added dropwise. The reaction mixture was stirred at $-78\text{ }^{\circ}\text{C}$ for 1 h and a solution of trimethyl borate (0.28 mL, 260 mg, 2.5 mmol, 1.5 equiv.) in dry THF (10 mL) was added dropwise. The solution was allowed to warm to room temperature overnight. The reaction was quenched with aq. HCl (1 M, 5 mL), concentrated under reduced pressure to 50% of its original volume and poured into H₂O. The resulted biphasic solution was extracted with Et₂O (2 x 50 mL). The ethereal solution was washed twice with H₂O and concentrated under reduced pressure. The targeted product **65e** was obtained after filtration as a colorless solid (320 mg, 75% yield).

¹H NMR (501 MHz, CDCl₃) δ = 8.56–8.48 (m, 1H), 8.42–8.31 (m, 1H), 8.28 – 8.18 (m, 1H), 7.72 – 7.62 (m, 1H), 7.52–7.41 (m, 1H), 7.36–7.28 (m, 1H), 7.18 (d, *J* = 11.1 Hz, 1H), 2.78–2.67 (m, 3H), 2.67–2.51 (m, 6H).

The product is highly insoluble in CHCl₃, therefore ¹³C-NMR spectra was not informative.

2,6-bis(1,3,6-trimethylphenanthren-9-yl)-4H-dinaphtho[2,1-d:1',2'-f][1,3,2]dithiazepine 3,3,5,5-tetraoxide (17p)



In an oven dried microwave vial (5 mL) (*S*)-3,3'-diiododisulfonimide **48** (69 mg, 0.1 mmol, 1 equiv.), **65e** (112 mg, 0.4 mmol, 3 equiv.), K₂CO₃ (58 mg, 0.4 mmol, 4 equiv.), Palladium(II)-acetate (2.4 mg, 0.01 mmol, 0.1 equiv, 10 mol%) were suspended in THF/water (4 mL, 1:1, v/v) under an atmosphere of dry argon. Tri-*tert*-butylphosphine (1M, dioxane solution) (0.02 mL, 21 mg, 0.1 mmol) was added and the vial

was sealed and heated for 30 min at 120 °C in a microwave reactor. The reaction was poured into HCl (1N, 5 mL) and extracted with CH₂Cl₂ (3 x 10mL), and the combined organic layers were washed with water (10 mL) and brine (2x10 mL). The organic layer was dried over MgSO₄, and the product was purified by flash column chromatography (CH₂Cl₂/MeOH = 100:0 to 98:2). The purified product was dissolved in CH₂Cl₂ (30 mL), acidified with HCl (6 M, 20 mL) and the solvent removed in vacuo to obtain the targeted product as pale yellow solid (69 mg, 78% yield).

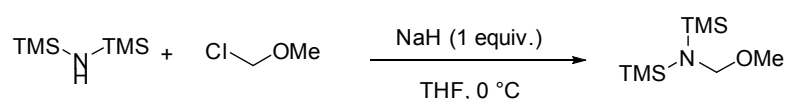
Note: Upon acidification, catalyst **17p** equilibrates to an unseperable mixture of 3 rotamers.

¹H NMR (501 MHz, CDCl₃) δ = 8.58–8.50 (m, 2H), 8.39 (d, J = 5.5 Hz, 2H), 8.24 (d, J = 7.7 Hz, 2H), 8.18 (d, J = 2.2 Hz, 2H), 8.06 (d, J = 8.1 Hz, 2H), 8.05–8.00 (m, 2H), 7.97–7.90 (m, 2H), 7.80–7.68 (m, 2H), 7.59–7.45 (m, 4H), 7.40 (q, J = 7.7, 6.9 Hz, 3H), 7.35–7.27 (m, 3H), 7.23–7.18 (m, 1H), 2.79–2.64 (m, 6H), 2.66–2.47 (m, 12H).

7.3 Asymmetric α -Aminomethylation for the Direct Synthesis of Unprotected β -Amino Acids

7.3.1 Synthesis of Aminomethylating Reagents

N-(methoxymethyl)-1,1,1-trimethyl-*N*-(trimethylsilyl)silanamine (**38**)

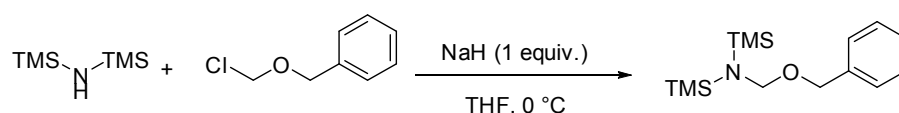


A solution of *n*-BuLi (4.8 mL, 2.2 M, 10.5 mmol, 1.05 equiv.) was added dropwise at 0 °C to a stirred solution of hexamethyldisilazane (2.1 mL, 10 mmol, 1.0 equiv.) in THF (200 mL) under argon atmosphere and the mixture was stirred for 30 min. Chloromethyl methyl ether (0.8 mL, 10 mmol, 1 equiv.) was added dropwise to the cooled and stirred mixture, and stirring was continued for 2 h at 0 °C. The solvent was removed by evaporation and the resulting residue was filtered to remove the lithium chloride, which was rinsed by *n*-hexane. After removal of the solvent, distillation of the liquid residue gave pure **38** (1.8 g, 8.6 mmol, 89% yield), bp 67-68 °C (50 mBar).

¹H NMR (501 MHz, CD₂Cl₂) δ = 4.27 (s, 2H), 3.14 (s, 3H), 0.13 ppm (s, 18H).

¹³C NMR (126 MHz, CD₂Cl₂) δ = 81.23, 53.77, (6x) 2.08 ppm.

N-((benzyloxy)methyl)-1,1,1-trimethyl-*N*-(trimethylsilyl)silanamine (**80**)



A solution of *n*-BuLi (4.8 mL, 2.2 M, 10.5 mmol, 1.05 equiv.) was added dropwise at 0 °C to a stirred solution of hexamethyldisilazane (2.1 mL, 10 mmol, 1.0 equiv.) in

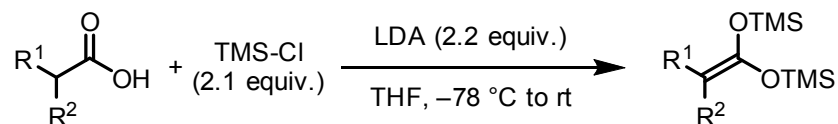
THF (200 mL) under argon atmosphere and the mixture was stirred for 30 min. Chloromethyl benzyl ether (10 mmol, 1 equiv.) was added dropwise to the cooled and stirred mixture, and stirring was continued for 2 h at 0 °C. The solvent was removed by evaporation and the resulting residue was filtered to remove the lithium chloride, which was rinsed by *n*-hexane. After removal of the solvent, distillation of the liquid residue gave pure **80**, bp 39–42 °C (4.5 x 10⁻² mBar).

¹H NMR (501 MHz, CD₂Cl₂) δ = 7.29–7.23 (m, 2H), 7.17–7.12 (m, 2H), 7.08–7.03 (m, 1H), 4.33 (s, 2H), 4.24 (s, 2H), 0.19 ppm (s, 18H).

¹³C NMR (126 MHz, CD₂Cl₂) δ = 139.42, 129.15, 128.42, 128.22, 127.58, 127.40, 79.54, 68.57, (6x) 2.00 ppm.

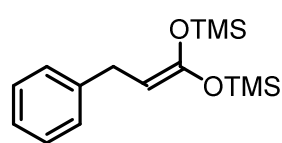
7.3.2 Synthesis and Characterization of *bis*-Silyl Ketene Acetals

General Procedure B:



A stirring solution of acid (1.0 equiv.) and Me₃SiCl (2.1 equiv.) in THF (0.5 M) under an atmosphere of argon was cooled to –78 °C. The LDA solution (2.2) was added via cannula. The cooling bath was removed after complete addition and the reaction solution was stirred for 1 hour at room temperature. The reaction mixture was concentrated *in vacuo*, and then hexane (50 mL) was added to the residue and was filtered under an atmosphere of argon. After concentration under reduced pressure, the crude product was purified by distillation under reduced pressure to afford the *bis*-silyl ketene acetals as colorless liquids, which were stored in Schlenk flasks under an atmosphere of argon at 4 °C.

2,2,6,6-tetramethyl-4-(2-phenylethylidene)-3,5-dioxa-2,6-disilaheptane (31q)

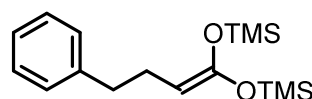


Prepared according to general procedure **B** using 3-phenylpropanoic acid (1.5 g, 10 mmol) and obtained after distillation (bp = 69–70 °C at 1.0×10^{-2} mBar) as colorless liquid (1.5 g, 5.0 mmol, 50 % yield).

$^1\text{H NMR}$ (501 MHz, CD_2Cl_2) δ = 7.28–7.22 (m, 2H), 7.22–7.17 (m, 2H), 7.17–7.10 (m, 1H), 3.76 (t, J = 7.3 Hz, 1H), 3.27 (d, J = 7.3 Hz, 2H), 0.23 (s, 9H), 0.20 (s, 9H).

$^{13}\text{C NMR}$ (126 MHz, CD_2Cl_2) δ = 151.92, 143.94, 129.03, 128.67, 128.66, 128.37, 125.93, 82.32, 31.92, 0.75, 0.14 ppm.

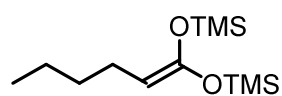
2,2,6,6-tetramethyl-4-(3-phenylpropylidene)-3,5-dioxa-2,6-disilaheptane (31s)



Prepared according to general procedure **B** using 4-phenylbutanoic acid (3.9 g, 20.0 mmol) and obtained after distillation (bp = 86–88 °C at 7.8×10^{-2} mbar) as colorless liquid.

$^1\text{H NMR}$ (501 MHz, CD_2Cl_2) δ = 7.15–7.04 (m, 2H), 7.04–6.92 (m, 3H), 3.38 (t, J = 7.1 Hz, 1H), 2.49–2.31 (m, 2H), 2.10–1.95 (m, 2H), 0.02 (s, 9H), 0.00 (s, 9H).

2,2,6,6-tetramethyl-4-pentylidene-3,5-dioxa-2,6-disilaheptane (31t)

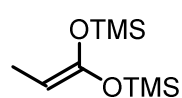


Prepared according to general procedure **B** using hexanoic acid (2.3 g, 20.0 mmol) and obtained after distillation (bp = 41–42 °C at 5.7×10^{-2} mbar) as colorless liquid.

$^1\text{H NMR}$ (501 MHz, CD_2Cl_2) δ = 3.53 (t, J = 7.1 Hz, 1H), 1.89 (q, J = 7.1 Hz, 2H), 1.36–1.17 (m, 4H), 0.95–0.84 (m, 3H), 0.21 (s, 9H), 0.18 ppm (s, 9H).

$^{13}\text{C NMR}$ (126 MHz, CD_2Cl_2) δ = 150.83, 83.87, 33.45, 25.24, 22.78, 14.35, 0.66, 0.06 ppm.

4-ethylidene-2,2,6,6-tetramethyl-3,5-dioxa-2,6-disilaheptane (31u)

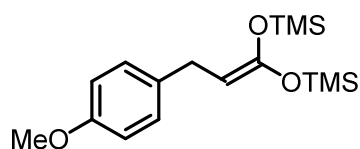


Prepared according to general procedure **B** using propanoic acid (1.0 g, 13.5 mmol) and obtained after distillation (bp = 65-68 °C at 20 mBar) as colorless liquid (2.3 g, 13.4 mmol, 79 % yield).

¹H NMR (501 MHz, CD₂Cl₂) δ = 3.36 (q, *J* = 6.5 Hz, 1H), 1.25 (d, *J* = 6.5 Hz, 3H), 0.02 (s, 9H), 0.00 (s, 9H).

¹³C NMR (126 MHz, CD₂Cl₂) δ = 151.33, 77.42, 10.38, 0.69, 0.08 ppm.

4-(2-(4-methoxyphenyl)ethylidene)-2,2,6,6-tetramethyl-3,5-dioxa-2,6-disilaheptane (31v)

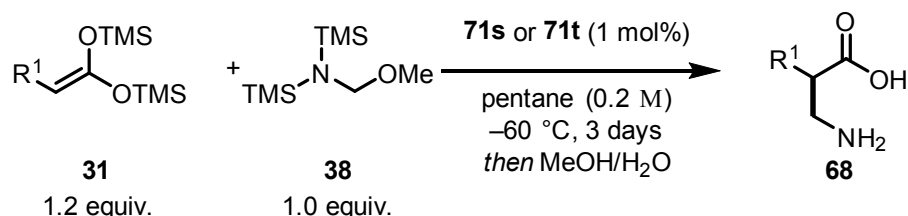


Prepared according to general procedure **B** using 3-(4-methoxyphenyl)propanoic acid (3.6 g, 20 mmol) and obtained after distillation (bp = 108–110 °C at 4.8 *10⁻² mBar) as colorless liquid.

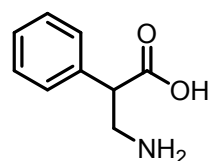
¹H NMR (501 MHz, CD₂Cl₂) δ = 7.20–7.03 (m, 2H), 6.86–6.75 (m, 2H), 3.83–3.70 (m, 4H), 3.20 (d, *J* = 7.3 Hz, 2H), 0.23 (s, 9H), 0.21 (s, 9H).

7.3.3 General procedure for the α -Aminomethylation of *bis*-SKAs

General Procedure C



An oven dry 2 ml vial was charged with imidodiphosphate **71s** or **71t** as the catalyst (0.2 μ mol, 0.5 mg, 1 mol%), a magnetic stir bar and, under argon atmosphere, dry pentane (0.1 mL) and *bis*-silyl ketene acetal **31** (0.024 mmol, 1.2 equiv.) were added. The reaction mixture was cooled down to the desired temperature, and then *N*-(methoxymethyl)-1,1,1-trimethyl-*N*-(trimethylsilyl)silanamine **38** (0.02 μ L, 1.0 equiv.) was added. After 3 days, the targeted product **68** was precipitated with water (0.1 mL) and directly dissolved with water/MeOH (0.5 mL, 1:1, v/v). The aqueous phase was extracted with Et₂O (2x 1 mL) in order to remove the catalyst. The water was evaporated under reduced pressure to obtain the desired product as a colorless solid in >99% purity (analyzed by ¹H-NMR). The obtained product was dissolved in HPLC grade water:MeCN (1:1, v/v) and directly used for the determination of the enantiomeric ratio.

3-amino-2-phenylpropanoic acid (68r)

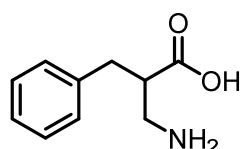
Prepared according to general procedure **C** using 2,2,6,6-tetramethyl-4-(2-phenylethylidene)-3,5-dioxo-2,6-disilaheptane (**31r**) (5.5 mg, 0.02 mmol) using catalyst **71s** and obtained after extraction as a colorless solid (91% yield, 91:9 er).

¹H NMR (501 MHz, CDCl₃) δ = 7.26–7.15 (m, 3H), 7.14–7.10 (m, 2H), 3.86 (t, *J* = 7.5 Hz, 1H), 3.37 (dd, *J* = 13.1, 7.6 Hz, 1H), 3.13 ppm (dd, *J* = 13.1, 7.4 Hz, 1H).

¹³C NMR (126 MHz, CDCl₃) δ = 174.6, 134.3, 129.6, 128.9, 128.9, 128.3, 128.3, 48.5, 41.1 ppm.

The enantiomeric ratio was determined by HPLC analysis using Daicel Chirobiotic T2, water:methanol = 50:50 (v/v), flow rate = 1 mL/min, 25 °C, λ = 210 nm, t_R = 11.1 min (minor) and t_R = 17.1 min (major).

3-amino-2-benzylpropanoic acid (68q)



Prepared according to the general procedure using 2,2,6,6-tetramethyl-4-(2-phenylethylidene)-3,5-dioxo-2,6-disilaheptane (31q) (5.6 mg, 0.02 mmol) using catalyst 71s and obtained after

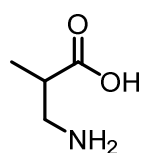
precipitation as a colorless solid (5.0 mg, 0.019 mmol, 95 % yield, 96:4 er).

¹H NMR (501 MHz, D₂O) δ = 7.45 – 7.34 (m, 2H), 7.35 – 7.27 (m, 3H), 3.16 – 3.06 (m, 1H), 3.06 – 2.98 (m, 2H), 2.94 – 2.80 (m, 2H).

¹³C NMR (126 MHz, D₂O) δ = 179.52, 138.48, 128.96, 128.96, 128.69, 128.69, 126.75, 46.90, 40.63, 36.15 ppm.

The enantiomeric ratio was determined by HPLC analysis using Daicel Chirobiotic T2, water:methanol = 50:50 (v/v), flow rate = 1 mL/min, 25 °C, λ = 210 nm, t_R = 6.3 min (minor) and t_R = 7.9 min (major)

3-amino-2-phenylpropanoic acid (68w)



Prepared according to the general procedure using 4-ethylidene-2,2,6,6-tetramethyl-3,5-dioxo-2,6-disilaheptane (31w) (4.1 mg, 0.02 mmol) using catalyst 71t and obtained after precipitation as a colorless solid (95% NMR

yield, 82.5:17.5 er).

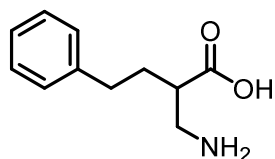
¹H NMR (501 MHz, D₂O) δ = 3.17 (ddd, J = 14.0, 6.9, 1.1 Hz, 1H), 2.66 (dd, J = 14.0, 7.6 Hz, 1H), 2.40 (h, J = 7.3 Hz, 1H), 0.9 ppm (d, J = 7.1 Hz, 3H).

¹³C NMR (126 MHz, D₂O) δ = 181.67, 42.37, 39.25, 15.13 ppm.

The enantiomeric ratio was determined by HPLC analysis after derivatization of the obtained product to the corresponding

HPLC analysis using Chiralpak ID-3, *n*-heptane:*i*-PrOH = 80:20 (v/v), flow rate = 1 mL/min, 25 °C, λ = 210 nm, t_R = 4.5 min (major) and t_R = 4.9 min (minor)

3-amino-2-phenylpropanoic acid (**68s**)



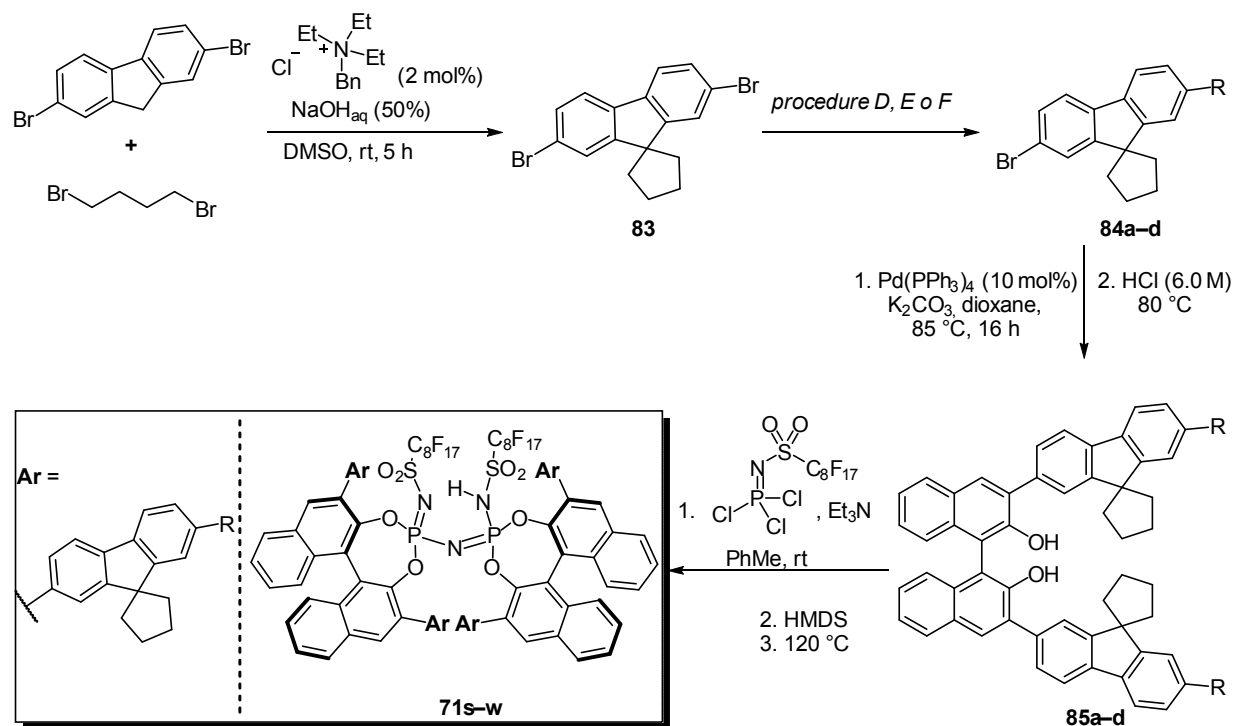
Prepared according to the general procedure using 2,2,6,6-tetramethyl-4-(3-phenylpropylidene)-3,5-dioxo-2,6-disilaheptane (**31s**) (6.1 mg, 0.02 mmol) using catalyst **71s** and obtained after extraction as a colorless solid (91% NMR yield, 95.5:4.5 er).

¹H NMR (501 MHz, CDCl₃) δ = 7.35–7.27 (m, 2H), 7.27–7.19 (m, 3H), 3.14–3.05 (m, 1H), 3.05–2.96 (m, 1H), 2.67–2.52 (m, 2H), 2.52–2.44 (m, 1H), 1.92–1.81 (m, 1H), 1.80–1.70 ppm (m, 1H).

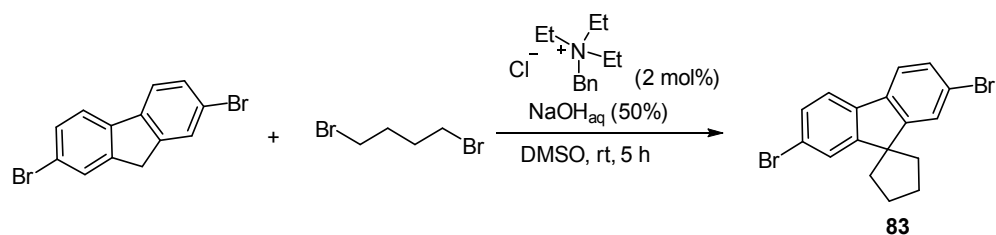
¹³C NMR (126 MHz, CDCl₃) δ = 180.47, 141.87, 128.69, 128.51, 126.21, 45.03, 41.07, 32.50, 31.89 ppm.

The enantiomeric ratio was determined by HPLC analysis using Daicel Chirobiotic T2, water:methanol = 50:50 (v/v), flow rate = 1 mL/min, 25 °C, λ = 210 nm, t_R = 8.0 min (minor) and t_R = 10.2 min (major).

7.3.4 Synthesis and Characterization of IDP*i* Catalysts



7.3.4.1 Procedure for derivatization of 2,7-dibromo-9H-fluorene



2',7'-dibromospiro[cyclopentane-1,9'-fluorene] (**83**)

Aq. NaOH (50%, 110 mmol, 5.5 equiv.) was added dropwise to the mixture of 2,7-dibromo-9H-fluorene (6.5 g, 20 mmol, 1.0 equiv.) and benzyltriethylammonium chloride (91.1 mg, 0.4 mmol, 2 mol%) in DMSO (10 mL) under argon at rt (NOTE:

rapid color change from yellow to red). After the subsequent addition of 1,4-dibromobutane (2.4 mL, 20 mmol, 1.0 equiv.) (NOTE: color change from red to beige), the reaction was stirred for 5 hours at rt. Then, water (30 mL) and toluene (30 mL) were added and the organic layer was separated, dried over MgSO₄ and concentrated under reduced pressure. The crude product was purified by column chromatography (hexanes) to yield 2',7'-dibromospiro[cyclopentane-1,9'-fluorene] **83** as a light yellow solid (5.4 g, 14.2 mmol, 71%).

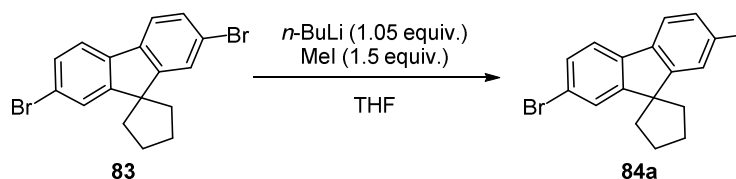
¹H NMR (501 MHz, CDCl₃) δ = 7.55–7.50 (m, 4H), 7.44 (dd, *J* = 8.1, 1.8 Hz, 2H), 2.18–2.10 (m, 4H), 2.10–2.00 ppm (m, 4H).

¹³C NMR (126 MHz, CDCl₃) δ = 156.01, 156.01, 137.44, 137.44, 130.01, 130.01, 126.31, 126.31, 121.57, 121.57, 120.99, 120.99, 57.90, 39.65, 39.65, 26.92, 26.92 ppm.

7.3.4.1 Derivatization of 2',7'-Dibromospiro[cyclopentane-1,9'-fluorene]

Procedure D

2'-bromo-7'-methylspiro[cyclopentane-1,9'-fluorene] (**84a**)



n-BuLi (2.54 M in hexanes, 2.1 equiv.) was added dropwise to a solution of 2',7'-dibromospiro[cyclopentane-1,9'-fluorene] **83** (1.0 equiv.) in THF (0.2 M) at –78 °C and the reaction mixture was allowed to stir at this temperature for 15 min. Methyl iodide (1.0 equiv., neat) was added to the reaction mixture dropwise over 10 min. The reaction was allowed to stir and warm to room temperature overnight. The reaction was quenched with sat. NH₄Cl_(aq) solution. After 5 min, the reaction mixture

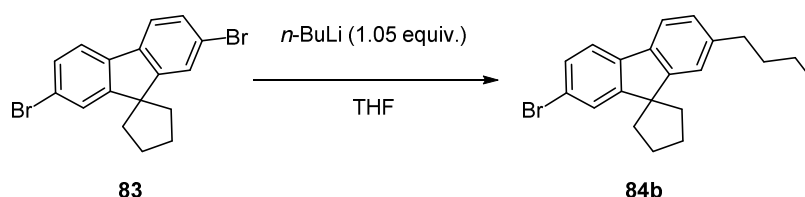
was diluted with diethyl ether. The aqueous layer was extracted with diethyl ether (x3). The combined organic layers were washed with sat. $\text{Na}_2\text{S}_2\text{O}_4(\text{aq})$ solution until the organic phase turn to transparent, then washed with brine, dried with magnesium sulfate, concentrated under reduced pressure, and the solid residue was purified by flash column chromatography (SiO_2 , dichloromethane/methanol = 95:5).

^1H NMR (501 MHz, CDCl_3) δ = 7.57–7.48 (m, 3H), 7.42 (dd, J = 8.0, 1.8 Hz, 1H), 7.24–7.20 (m, 1H), 7.17–7.11 (m, 1H), 2.42 (s, 3H), 2.25–1.91 ppm (m, 8H).

^{13}C NMR (126 MHz, CDCl_3) δ = 156.51, 154.34, 138.73, 137.97, 135.96, 129.81, 127.87, 126.34, 123.74, 120.72, 120.67, 119.53, 57.77, 39.91, 27.11, 22.00 ppm.

Procedure E

2'-bromo-7'-butylspiro[cyclopentane-1,9'-fluorene] (84b)



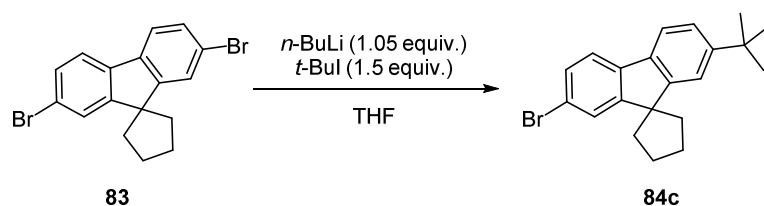
$n\text{-BuLi}$ (2.54 M in hexanes, 2.1 equiv.) was added dropwise to a solution of acid (1.0 equiv.) in THF (0.2 M) at -78 °C and the reaction mixture was allowed to stir at room temperature overnight. The reaction was quenched with sat. $\text{NH}_4\text{Cl}(\text{aq})$ solution. After 5 min, the reaction mixture was diluted with diethyl ether. The aqueous layer was extracted with diethyl ether (x3). The combined organic layers were washed with sat. $\text{Na}_2\text{S}_2\text{O}_4(\text{aq})$ solution until the organic phase turn to transparent, then washed with brine, dried with magnesium sulfate, concentrated under reduced pressure, and the solid residue was purified by flash column chromatography (SiO_2 , dichloromethane/methanol = 95:5).

^1H NMR (501 MHz, CDCl_3) δ = 7.67–7.46 (m, 3H), 7.41 (dd, J = 7.8, 1.8 Hz, 1H), 7.21 (d, J = 1.5 Hz, 1H), 7.14 (dd, J = 7.7, 1.5 Hz, 1H), 2.66 (td, J = 8.0, 3.1 Hz, 2H),

2.19–2.01 (m, 8H), 1.70–1.58 (m, 2H), 1.44–1.34 (m, 2H), 0.95 ppm (t, $J = 7.3$ Hz, 3H).

Procedure D

2'-bromo-7'-(tert-butyl)spiro[cyclopentane-1,9'-fluorene] (84c)

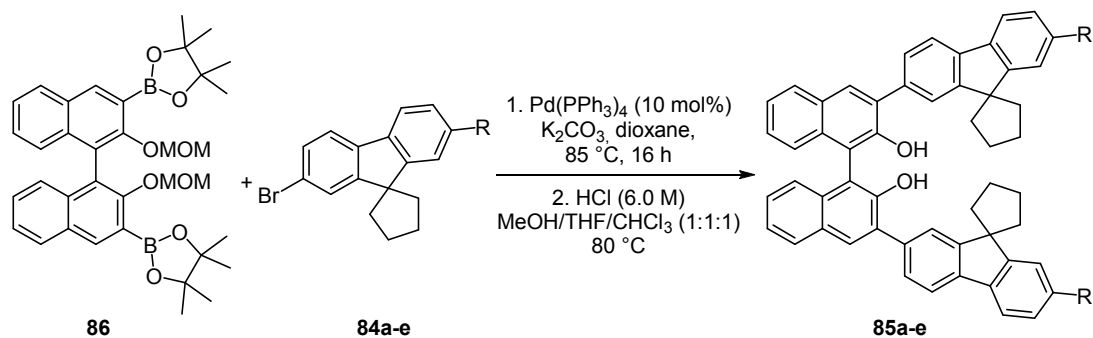


$n\text{-BuLi}$ (2.54 M in hexanes, 2.1 equiv.) was added dropwise to a solution of acid (1.0 equiv.) in THF (0.2 M) at -78 °C and the reaction mixture was allowed to stir at this temperature for 15 min. *tert*-Butyl iodide (1.0 equiv., neat) was added to the reaction mixture dropwise over 10 min. The reaction was allowed to stir and warm to room temperature overnight. The reaction was quenched with sat. $\text{NH}_4\text{Cl}_{(\text{aq})}$ solution. After 5 min, the reaction mixture was diluted with diethyl ether. The aqueous layer was extracted with diethyl ether (x3). The combined organic layers were washed with sat. $\text{Na}_2\text{S}_2\text{O}_4_{(\text{aq})}$ solution until the organic phase turn to transparent, then washed with brine, dried with magnesium sulfate, concentrated under reduced pressure, and the solid residue was purified by flash column chromatography (SiO_2 , dichloromethane/methanol = 95:5).

$^1\text{H NMR}$ (501 MHz, CDCl_3) $\delta = 7.51$ (d, $J = 7.9$ Hz, 1H), 7.46–7.42 (m, 2H), 7.37–7.32 (m, 2H), 7.30 (dd, $J = 8.0, 1.8$ Hz, 1H), 2.13–1.92 (m, 8H), 1.30 ppm (s, 9H).

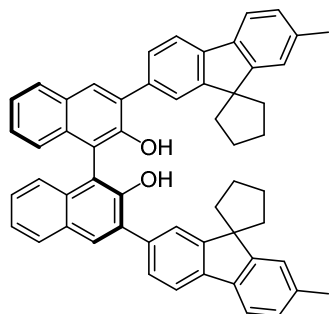
$^{13}\text{C NMR}$ (126 MHz, CDCl_3) $\delta = 156.61, 153.66, 151.33, 138.49, 135.86, 129.64, 126.18, 124.10, 120.63, 120.54, 119.53, 119.09, 64.39, 57.84, 39.78, 26.91, 25.35, 14.19, 14.19, 14.19$ ppm.

7.3.4.2 Suzuki Coupling of 2-Bromo-7-alkyl-9H-fluorene and MOM-protected (S,S)-BINOL



To a flame dried two-neck round-bottom flask with a condenser was added (S)-2,2'-(2,2'-bis(methoxymethoxy)-1,1'-binaphthyl-3,3'-diyl)bis(4,4',5,5'-tetramethyl-1,3,2-dioxaborolane) **86** (0.5 mmol, 1.0 equiv), 2-bromo fluorenyl derivative **84a-e** (1.1 mmol, 2.2 equiv) and tetrakis(triphenylphosphine)palladium (0.05 mmol, 0.1 equiv). After degassing the reaction mixture with argon for 20 min, toluene/ethanol/methanol (3:2:1, v/v/v, 0.15 M) and K₂CO₃ (3 mmol, 6 equiv.) were sequentially added. The mixture was then heated to 110 °C and stirred at that temperature for 16 h. After cooling the reaction to room temperature, the reaction mixture was extracted with EtOAc (3x), the combined organic phase was dried over MgSO₄ and concentrated under reduced pressure. Subsequently, the solid was dissolved in dioxane and HCl in dioxane was added. This mixture was stirred at room temperature until the starting material was consumed (as monitored by TLC analysis). The reaction was then evaporated under reduced pressure. The resulting residue was purified by column chromatography (EtOAc:hexanes = 1:5) to afford the targeted compound **85a-e** as a colorless solid.

(S)-3,3'-bis(2'-methylspiro[cyclopentane-1,9'-fluoren]-7'-yl)-[1,1'-binaphthalene]-2,2'-diol (85a)

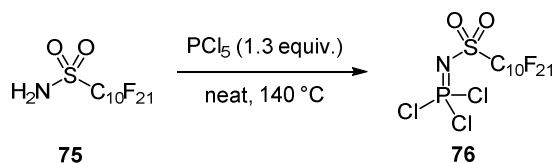


Prepared according to the representative procedure on a 0.5 mmol scale for (S)-2,2'-(2,2'-bis(methoxymethoxy)-1,1'-binaphthyl-3,3'-diyl)bis(4,4',5,5'-tetramethyl-1,3,2-dioxaborolane) **86** with 2'-bromo-7'-methylspiro[cyclopentane-1,9'-fluorene] (**84a**) (345.0 mg, 1.1 mmol) to give the title compound **85a** as an off-white solid.

¹H NMR (501 MHz, CDCl₃) δ = 8.08 (s, 2H), 7.98–7.93 (m, 2H), 7.81–7.75 (m, 4H), 7.69 (dd, *J* = 7.8, 1.6 Hz, 2H), 7.63 (d, *J* = 7.6 Hz, 2H), 7.41 (ddd, *J* = 8.1, 6.7, 1.4 Hz, 2H), 7.34 (ddd, *J* = 8.1, 6.7, 1.3 Hz, 2H), 7.30–7.27 (m, 1H), 7.20–7.13 (m, 2H), 2.45 (s, 6H), 2.24–2.05 (m, 16H).

¹³C NMR (126 MHz, CDCl₃) δ = 154.94, 154.94, 154.52, 154.52, 150.16, 150.16, 139.35, 139.35, 137.52, 137.52, 136.48, 136.48, 135.97, 135.97, 132.97, 132.97, 131.16, 131.16, 131.13, 131.13, 129.52, 129.52, 128.40, 128.40, 128.23, 128.23, 127.62, 127.62, 127.19, 127.19, 124.42, 124.42, 124.28, 124.28, 124.14, 124.14, 123.67, 123.67, 119.52, 119.52, 119.29, 119.29, 112.71, 112.71, 57.64, 57.64, 39.92, 39.92, 39.87, 39.87, 27.03, 27.03, 27.03, 27.03, 21.88, 21.88 ppm.

((Perfluoro-*n*-decyl)sulfonyl)phosphorimidoyl trichloride (76)



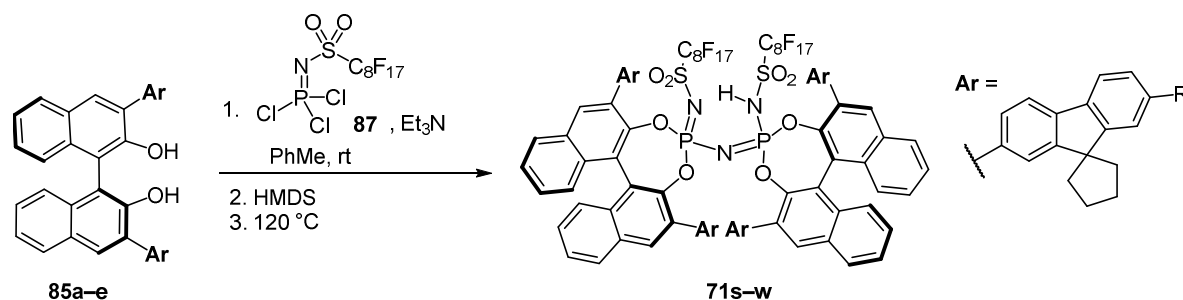
In a Schlenk flask under Argon equipped with a magnetic stirring bar connected to a two-neck flask containing NaOH pellets and a vacuum pump in this order, a mixture of sulfonamide **75** (600.0 mg, 1 mmol, 1.0 equiv) and PCl₅ (270.0 mg, 1.3 mmol, 1.3 equiv) was heated to 140 °C under Argon for 2 h. The reaction was monitored by ¹H,

^{19}F , and ^{31}P NMR to ensure full consumption of sulfonamide. Removal of the excess amount of PCl_5 by prolonged evacuation in vacuum afforded the title compound **76** in quantitative yield as colorless solid, which was stored in a Schlenk flask under argon.

^{19}F NMR (471 MHz, CD_2Cl_2) δ = -81.10, -112.32, -120.23, -121.65, -121.82, -121.82, -121.82, -122.04, -122.86, -126.30 ppm.

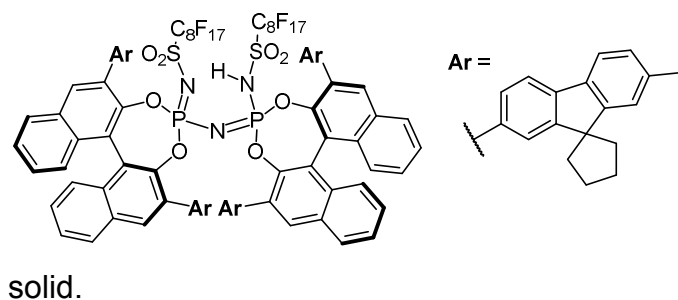
^{31}P NMR (203 MHz, CD_2Cl_2) δ = 16.89 ppm.

7.3.4.3 General Procedure for IDP*i* synthesis



In a Schlenk tube under argon, a suspension of 3,3'-substituted (S,S)-BINOL (1.05 mmol, 2.1 equiv.) in toluene (2.5 mL) was treated with phosphorimidoyl trichloride **87** (1.05 mmol, 2.1 equiv.) and then NEt₃ (1.12 mL, 8.0 mmol, 16 equiv.). The reaction mixture was stirred for 15 min at r.t., until neat hexamethyldisilazane (HMDS, 104 μ L, 0.5 mmol, 1 equiv.) was added dropwise. The reaction mixture was stirred for additional 15 min at r.t., the Schlenk tube was subsequently sealed and heated to 120 °C for 3 days. After cooling to r.t., aq. HCl (10%) was added and the mixture was extracted with DCM or Et₂O. The combined organic layers were washed with brine, dried over MgSO₄ and concentrated under reduced pressure. The crude material was purified by column chromatography on silica gel (hexane/MTBE 90:10→80:20→70:30→60:40→50:50 and/or 0.5–5% EtOAc in DCM) to afford the desired product as a salt. The corresponding IDP*i* Brønsted acids (S,S)-**71s-w** were obtained after acidification in DCM or Et₂O with aq. HCl (6 M) and evaporation of the solvent followed by drying under high vacuum as typically off-white solids.

(S,S)-(71s)



Prepared according to the general procedure on a 0.1 mmol scale (with respect to HMDS) and purified by column chromatography (hexane/EtOAc, 95:5). Colorless

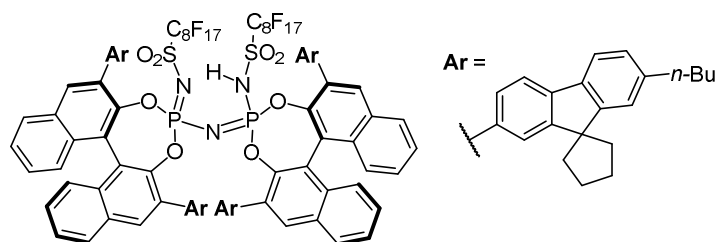
solid.

¹H NMR (501 MHz, CDCl₃) δ = 8.02 (d, J = 7.9 Hz, 4H), 7.95 (d, J = 8.3 Hz, 2H), 7.85 – 7.79 (m, 2H), 7.76 (d, J = 8.5 Hz, 2H), 7.67 – 7.61 (m, 2H), 7.58 – 7.52 (m, 2H), 7.49 – 7.46 (m, 2H), 7.40 (d, J = 7.8 Hz, 2H), 7.37 – 7.29 (m, 6H), 7.22 – 7.15 (m, 6H), 7.10 (s, 2H), 7.00 – 6.93 (m, 6H), 6.58 (d, J = 8.1 Hz, 2H), 6.53 (d, J = 8.0 Hz, 2H), 6.42 (dd, J = 8.1, 1.6 Hz, 2H), 2.33 (d, J = 3.0 Hz, 12H), 2.23 – 1.86 (m, 22H), 1.77 (dd, J = 12.8, 6.9 Hz, 2H), 1.35 – 1.14 ppm (m, 12H).

¹⁹F NMR (471 MHz, CDCl₃) δ = -80.78, -110.28 – -112.60 (m), -120.00 (d, J = 53.4 Hz), -121.48, -122.01 (d, J = 58.6 Hz), -122.79 (d, J = 17.9 Hz), -126.18 ppm (d, J = 15.4 Hz).

³¹P NMR (203 MHz, CDCl₃) δ = -16.67 ppm.

(S,S)-(71v)



Prepared according to the general procedure on a 0.1 mmol scale (with respect to HMDS) and purified by column chromatography (hexane/EtOAc, 95:5). Colorless solid.

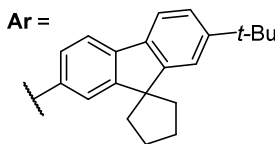
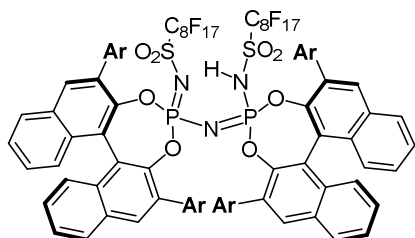
95:5). Colorless solid.

¹H NMR (501 MHz, CDCl₃) δ = 7.93 (s, 2H), 7.89 – 7.79 (m, 1H), 7.76 – 7.61 (m, 2H), 7.59 – 7.50 (m, 1H), 7.46 (dd, J = 8.1, 3.6 Hz, 2H), 7.41 (d, J = 1.6 Hz, 1H), 7.34 (d, J = 7.8 Hz, 2H), 7.32 – 7.28 (m, 3H), 7.26 – 7.20 (m, 6H), 7.17 – 7.11 (m, 6H), 7.09 (s, 2H), 7.02 (d, J = 1.6 Hz, 2H), 6.93 – 6.82 (m, 6H), 6.39 (d, J = 7.9 Hz, 2H), 2.50 (td, J = 7.5, 5.5 Hz, 8H), 2.27 – 1.75 (m, 22H), 1.63 – 1.39 (m, 16H), 1.31 – 1.14 (m, 12H), 0.83 (t, J = 7.3 Hz, 6H), 0.77 ppm (t, J = 7.3 Hz, 6H).

¹⁹F NMR (471 MHz, CDCl₃) δ = -80.79, -109.52 – -112.99 (m), -119.95 (dt, J = 31.1, 13.7 Hz), -121.39, -121.94 (d, J = 33.4 Hz), -122.72, -126.15 ppm (d, J = 14.4 Hz).

³¹P NMR (203 MHz, CDCl₃) δ = -16.65 ppm.

(S,S)-(71t)



Prepared according to the general procedure on a 0.1 mmol scale (with respect to HMDS) and purified by column chromatography (hexane/EtOAc,

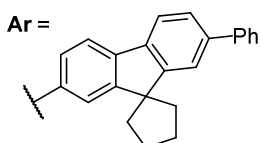
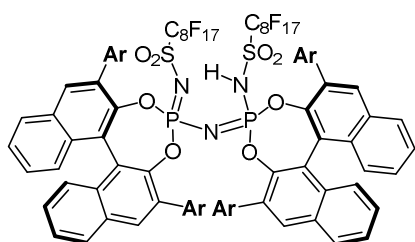
95:5). Colorless solid.

¹H NMR (501 MHz, CDCl₃) δ = 8.08–7.99 (m, 4H), 7.96 (d, *J* = 8.3 Hz, 2H), 7.85–7.79 (m, 2H), 7.76 (d, *J* = 8.5 Hz, 2H), 7.64 (ddd, *J* = 8.5, 6.7, 1.4 Hz, 2H), 7.55 (ddd, *J* = 8.2, 5.8, 2.2 Hz, 2H), 7.49 (d, *J* = 1.6 Hz, 2H), 7.46–7.38 (m, 3H), 7.37–7.29 (m, 8H), 7.23–7.13 (m, 8H), 6.97 (s, 2H), 6.62 (d, *J* = 8.0 Hz, 1H), 6.54–6.44 (m, 3H), 2.25–2.01 (m, 22H), 1.83–1.58 (m, 4H), 1.29 ppm (d, *J* = 1.3 Hz, 36H).

¹⁹F NMR (471 MHz, CDCl₃) δ = -80.79, -109.52 – -112.99 (m), -119.95 (dt, *J* = 31.1, 13.7 Hz), -121.39, -121.94 (d, *J* = 33.4 Hz), -122.72, -126.15 ppm (d, *J* = 14.4 Hz).

³¹P NMR (203 MHz, CDCl₃) δ = -16.69 ppm.

(S,S)-(71w)



Prepared according to the general procedure on a 0.1 mmol scale (with respect to HMDS) and purified by column chromatography (hexane/EtOAc,

95:5). Colorless solid.

¹H NMR (501 MHz, CDCl₃) δ = 8.04 (d, *J* = 9.3 Hz, 4H), 7.98 (d, *J* = 8.2 Hz, 2H), 7.87–7.82 (m, 2H), 7.80 (d, *J* = 8.5 Hz, 2H), 7.71–7.65 (m, 2H), 7.64 – 7.50 (m, 18H), 7.50–7.27 (m, 28H), 7.01 (s, 2H), 6.72 (d, *J* = 8.0 Hz, 2H), 6.63 (d, *J* = 7.9 Hz, 2H), 6.53 (dd, *J* = 7.9, 1.5 Hz, 2H), 2.23 (dd, *J* = 12.6, 6.0 Hz, 2H), 2.19 – 1.92 (m, 22H), 1.88 – 1.74 (m, 6H).

¹⁹F NMR (471 MHz, CDCl₃) δ = -80.81 (t, J = 9.9 Hz), -110.41 – -112.49 (m), -119.95 (d, J = 56.1 Hz), -121.44, -121.96 (d, J = 56.1 Hz), -122.74, -126.18 ppm (d, J = 15.3 Hz).

³¹P NMR (203 MHz, CDCl₃) δ = -16.46 ppm.

8 Bibliography

- [1] S. Patai, *Carboxylic Acids and Esters*, Interscience Publishers: New York, **1969**.
- [2] M. A. Ogliaruso, J. F. Wolfe, *Synthesis of Carboxylic Acids, Esters and Their Derivatives*, S. Patai ed., Wiley-Interscience: New York, **1991**.
- [3] N. Rodríguez, L. J. Goossen, *Chemical Society Reviews* **2011**, *40*, 5030-5048.
- [4] a) J. Cornella, J. T. Edwards, T. Qin, S. Kawamura, J. Wang, C.-M. Pan, R. Gianatassio, M. Schmidt, M. D. Eastgate, P. S. Baran, *Journal of the American Chemical Society* **2016**, *138*, 2174-2177; b) T. Qin, J. Cornella, C. Li, L. R. Malins, J. T. Edwards, S. Kawamura, B. D. Maxwell, M. D. Eastgate, P. S. Baran, *Science* **2016**, *352*, 801; c) J. Wang, T. Qin, T.-G. Chen, L. Wimmer, J. T. Edwards, J. Cornella, B. Vokits, S. A. Shaw, P. S. Baran, *Angewandte Chemie International Edition* **2016**, *55*, 9676-9679; d) F. Toriyama, J. Cornella, L. Wimmer, T.-G. Chen, D. D. Dixon, G. Creech, P. S. Baran, *Journal of the American Chemical Society* **2016**, *138*, 11132-11135.
- [5] J. March, *Advanced organic chemistry*, Wiley-Interscience: New York, **1992**.
- [6] a) D. A. Evans, M. D. Ennis, D. J. Mathre, *Journal of the American Chemical Society* **1982**, *104*, 1737-1739; b) D. A. Evans, F. Urpi, T. C. Somers, J. S. Clark, M. T. Bilodeau, *Journal of the American Chemical Society* **1990**, *112*, 8215-8216; c) A. G. Myers, B. H. Yang, H. Chen, J. L. Gleason, *Journal of the American Chemical Society* **1994**, *116*, 9361-9362; d) A. I. Meyers, G. Knaus, K. Kamata, M. E. Ford, *Journal of the American Chemical Society* **1976**, *98*, 567-576; e) A. G. Myers, B. H. Yang, H. Chen, L. McKinstry, D. J. Kopecky, J. L. Gleason, *Journal of the American Chemical Society* **1997**, *119*, 6496-6511; f) P. E. Sonnet, R. R. Heath, *The Journal of Organic Chemistry* **1980**, *45*, 3137-3139; g) D. A. Evans, J. M. Takacs, *Tetrahedron Letters* **1980**, *21*, 4233-4236; h) Y. Kawanami, Y. Ito, T. Kitagawa, Y. Taniguchi, T. Katsuki, M. Yamaguchi, *Tetrahedron Letters* **1984**, *25*, 857-860; i) W. Oppolzer, R. Moretti, S. Thomi, *Tetrahedron Letters* **1989**, *30*, 5603-5606; j) A. Abiko, O. Moriya, S. A. Filla, S. Masamune, *Angewandte Chemie International Edition in English* **1995**, *34*, 793-795; k) J. Lin, W. H. Chan, A. W. M. Lee, W. Y. Wong, *Tetrahedron* **1999**, *55*, 13983-13998.
- [7] Y. Xue, S. Wu, Q. Xu, S. Huang, W. Li, J. Yang, (Ed.: L. JIANGSU ZHONGBANG PHARMACEUTICAL CO.), **2019**.
- [8] A. Ando, T. Shioiri, *Journal of the Chemical Society, Chemical Communications* **1987**, 656-658.
- [9] J.-i. Matsuo, K. Koga, *CHEMICAL & PHARMACEUTICAL BULLETIN* **1997**, *45*, 2122-2124.
- [10] a) C. E. Stivala, A. Zakarian, *Journal of the American Chemical Society* **2011**, *133*, 11936-11939; b) Y. Ma, C. E. Stivala, A. M. Wright, T. Hayton, J. Liang, I. Keresztes, E. Lobkovsky, D. B. Collum, A. Zakarian, *Journal of the American Chemical Society* **2013**, *135*, 16853-16864; c) P. Lu, J. J. Jackson, J. A. Eickhoff, A. Zakarian, *Journal of the American Chemical Society* **2015**, *137*, 656-659; d) K. Yu, P. Lu, J. J. Jackson,

-
- T.-A. D. Nguyen, J. Alvarado, C. E. Stivala, Y. Ma, K. A. Mack, T. W. Hayton, D. B. Collum, A. Zakarian, *Journal of the American Chemical Society* **2017**, *139*, 527-533; e) K. Yu, B. Miao, W. Wang, A. Zakarian, *Organic Letters* **2019**, *21*, 1930-1934.
- [11] W. P. G. T, *Greene's Protective Groups in Organic Synthesis*, John Wiley & Sons, Inc., **2006**.
- [12] a) B. List, L. Schreyer, R. Properzi, *Angewandte Chemie International Edition* **2019**; b) T. James, M. van Gemmeren, B. List, *Chemical Reviews* **2015**, *115*, 9388-9409.
- [13] a) S. Nakamura, M. Kaneeda, K. Ishihara, H. Yamamoto, *Journal of the American Chemical Society* **2000**, *122*, 8120-8130; b) D. Uraguchi, N. Kinoshita, T. Ooi, *Journal of the American Chemical Society* **2010**, *132*, 12240-12242; c) D. Uraguchi, T. Kizu, Y. Ohira, T. Ooi, *Chem Commun (Camb)* **2014**, *50*, 13489-13491.
- [14] L. Horner, H. Siegel, H. Büthe, *Angewandte Chemie* **1968**, *80*, 1034-1035.
- [15] W. S. Knowles, M. J. Sabacky, *Chemical Communications (London)* **1968**, 1445-1446.
- [16] T. P. Dang, H. B. Kagan, *Journal of the Chemical Society D: Chemical Communications* **1971**, 481-481.
- [17] H. Nozaki, H. Takaya, S. Moriuti, R. Noyori, *Tetrahedron* **1968**, *24*, 3655-3669.
- [18] a) K. B. Sharpless, D. W. Patrick, L. K. Truesdale, S. A. Biller, *Journal of the American Chemical Society* **1975**, *97*, 2305-2307; b) T. Katsuki, K. B. Sharpless, *Journal of the American Chemical Society* **1980**, *102*, 5974-5976; c) E. N. Jacobsen, I. Marko, W. S. Mungall, G. Schroeder, K. B. Sharpless, *Journal of the American Chemical Society* **1988**, *110*, 1968-1970.
- [19] W. S. Knowles, *Journal of Chemical Education* **1986**, *63*, 222.
- [20] a) A. KrÁMli, J. HorvÁTh, *Nature* **1948**, *162*, 619-619; b) F. S. Sariaslani, J. P. N. Rosazza, *Enzyme and Microbial Technology* **1984**, *6*, 242-253.
- [21] C. Wandrey, A. Liese, D. Kihumbu, *Organic Process Research & Development* **2000**, *4*, 286-290.
- [22] P. S. Fiske, G. Bredig, *Biochem. Z.* **1912**, *687*, 7-23.
- [23] H. Pracejus, *Justus Liebigs Annalen der Chemie* **1960**, *634*, 9-22.
- [24] Z. G. Hajos, D. R. Parrish, *The Journal of Organic Chemistry* **1974**, *39*, 1615-1621.
- [25] U. Eder, G. Sauer, R. Wiechert, *Angewandte Chemie International Edition in English* **1971**, *10*, 496-497.
- [26] A. Berkessel, H. Gröger, *Asymmetric Organocatalysis* **2005**, 1-8.
- [27] B. List, R. A. Lerner, C. F. Barbas, *Journal of the American Chemical Society* **2000**, *122*, 2395-2396.
- [28] K. A. Ahrendt, C. J. Borths, D. W. C. MacMillan, *Journal of the American Chemical Society* **2000**, *122*, 4243-4244.
- [29] L. Hoang, S. Bahmanyar, K. N. Houk, B. List, *Journal of the American Chemical Society* **2003**, *125*, 16-17.
- [30] a) B. List, J. W. Yang, **2006**, *313*, 1584-1586; b) D. W. C. MacMillan, *Nature* **2008**, *455*, 304.
- [31] J. Seayad, B. List, *Organic & Biomolecular Chemistry* **2005**, *3*, 719-724.
- [32] B. List, *Accounts of Chemical Research* **2004**, *37*, 548-557.
- [33] A. Erkkilä, I. Majander, P. M. Pihko, *Chemical Reviews* **2007**, *107*, 5416-5470.
- [34] M. r. Mec'iarova', P. Tisovsky', R. S'ebesta, *New Journal of Chemistry* **2016**, *40*.
-

-
- [35] D. M. Flanigan, F. Romanov-Michailidis, N. A. White, T. Rovis, *Chemical Reviews* **2015**, *115*, 9307-9387.
- [36] J. N. Brønsted, *Recl. Trav. Chim. Pays-Bas*. **1923**, *42*, 718-728.
- [37] T. M. Lowry, *Journal of the Society of Chemical Industry* **1923**, *42*, 43-47.
- [38] G. N. Lewis, *Valence and the structure of atoms and molecules*, J. J. Little & Ives Company, New York, U.S.A., **1923**.
- [39] M. S. Sigman, E. N. Jacobsen, *Journal of the American Chemical Society* **1998**, *120*, 4901-4902.
- [40] Y. Huang, A. K. Unni, A. N. Thadani, V. H. Rawal, *Nature* **2003**, *424*, 146-146.
- [41] S. Harada, S. Kuwano, Y. Yamaoka, K.-i. Yamada, K. Takasu, *Angewandte Chemie International Edition* **2013**, *52*, 10227-10230.
- [42] X.-H. Chen, X.-Y. Xu, H. Liu, L.-F. Cun, L.-Z. Gong, *Journal of the American Chemical Society* **2006**, *128*, 14802-14803.
- [43] a) G. B. Rowland, H. Zhang, E. B. Rowland, S. Chennamadhavuni, Y. Wang, J. C. Antilla, *Journal of the American Chemical Society* **2005**, *127*, 15696-15697; b) K. Mori, K. Ehara, K. Kurihara, T. Akiyama, *Journal of the American Chemical Society* **2011**, *133*, 6166-6169.
- [44] a) F. Xu, D. Huang, C. Han, W. Shen, X. Lin, Y. Wang, *The Journal of Organic Chemistry* **2010**, *75*, 8677-8680; b) I. Čorić, S. Müller, B. List, *Journal of the American Chemical Society* **2010**, *132*, 17370-17373.
- [45] a) Q.-S. Guo, D.-M. Du, J. Xu, *Angewandte Chemie International Edition* **2008**, *47*, 759-762; b) X.-H. Chen, W.-Q. Zhang, L.-Z. Gong, *Journal of the American Chemical Society* **2008**, *130*, 5652-5653; c) N. Momiyama, T. Konno, Y. Furiya, T. Iwamoto, M. Terada, *Journal of the American Chemical Society* **2011**, *133*, 19294-19297; d) N. Momiyama, K. Funayama, H. Noda, M. Yamanaka, N. Akasaka, S. Ishida, T. Iwamoto, M. Terada, *ACS Catalysis* **2016**, *6*, 949-956.
- [46] a) I. Čorić, B. List, *Nature* **2012**, *483*, 315; b) P. S. J. Kaib, L. Schreyer, S. Lee, R. Properzi, B. List, *Angewandte Chemie International Edition* **2016**, *55*, 13200-13203.
- [47] T. Hashimoto, K. Maruoka, *Chemical Reviews* **2007**, *107*, 5656-5682.
- [48] M. Mahlau, B. List, *Angewandte Chemie International Edition* **2013**, *52*, 518-533.
- [49] S. Mayer, B. List, *Angewandte Chemie International Edition* **2006**, *45*, 4193-4195.
- [50] J. Lacour, D. Linder, *Science* **2007**, *317*, 462.
- [51] T. Akiyama, J. Itoh, K. Yokota, K. Fuchibe, *Angewandte Chemie International Edition* **2004**, *43*, 1566-1568.
- [52] D. Uraguchi, M. Terada, *Journal of the American Chemical Society* **2004**, *126*, 5356-5357.
- [53] a) M. Hatano, K. Moriyama, T. Maki, K. Ishihara, *Angewandte Chemie International Edition* **2010**, *49*, 3823-3826; b) M. Klusmann, L. Ratjen, S. Hoffmann, V. Wakchaure, R. Goddard, B. List, *Synlett* **2010**, *2010*, 2189-2192.
- [54] D. Parmar, E. Sugiono, S. Raja, M. Rueping, *Chemical Reviews* **2014**, *114*, 9047-9153.
- [55] a) S. Hoffmann, A. M. Seayad, B. List, *Angewandte Chemie International Edition* **2005**, *44*, 7424-7427; b) J. Seayad, A. M. Seayad, B. List, *Journal of the American Chemical Society* **2006**, *128*, 1086-1087; c) J. Zhou, B. List, *Journal of the American Chemical Society* **2007**, *129*, 7498-7499; d) G. Adair, S. Mukherjee, B. List,
-

-
- Aldrichimica ACTA* **2008**, *41*, 31-39; e) J. Tiago Menezes Correia, *Synlett* **2015**, *26*, 416-417.
- [56] a) M. Rueping, B. J. Nachtsheim, W. Ieawsuwan, I. Atodiresei, *Angewandte Chemie International Edition* **2011**, *50*, 6706-6720; b) C. H. Cheon, H. Yamamoto, *Chemical Communications* **2011**, *47*, 3043-3056; c) D. Nakashima, H. Yamamoto, *Journal of the American Chemical Society* **2006**, *128*, 9626-9627; d) C. H. Cheon, H. Yamamoto, *Journal of the American Chemical Society* **2008**, *130*, 9246-9247; e) M. Sai, H. Yamamoto, *Journal of the American Chemical Society* **2015**, *137*, 7091-7094; f) K. Kaupmees, N. Tolstoluzhsky, S. Raja, M. Rueping, I. Leito, *Angewandte Chemie International Edition* **2013**, *52*, 11569-11572.
- [57] L. M. Yagupolskii, V. N. Petrik, N. V. Kondratenko, L. Sooväli, I. Kaljurand, I. Leito, I. A. Koppel, *Journal of the Chemical Society, Perkin Transactions 2* **2002**, 1950-1955.
- [58] a) V. N. Wakchaure, B. List, *Angewandte Chemie International Edition* **2010**, *49*, 4136-4139; b) S. Vellalath, I. Čorić, B. List, *Angewandte Chemie International Edition* **2010**, *49*, 9749-9752.
- [59] P. S. J. Kaib, B. List, *Synlett* **2016**, *27*, 156-158.
- [60] a) P. García-García, F. Lay, P. García-García, C. Rabalakos, B. List, *Angewandte Chemie International Edition* **2009**, *48*, 4363-4366; b) M. Treskow, J. Neudörfl, R. Giernoth, *European Journal of Organic Chemistry* **2009**, *2009*, 3693-3697.
- [61] L.-Y. Chen, H. He, W.-H. Chan, A. W. M. Lee, *The Journal of Organic Chemistry* **2011**, *76*, 7141-7147.
- [62] S. Prévost, N. Dupré, M. Leutzsch, Q. Wang, V. Wakchaure, B. List, *Angewandte Chemie International Edition* **2014**, *53*, 8770-8773.
- [63] A. Berkessel, P. Christ, N. Leconte, J.-M. Neudörfl, M. Schäfer, *European Journal of Organic Chemistry* **2010**, *2010*, 5165-5170.
- [64] a) W. L. F. Armarego, E. E. Turner, *Journal of the Chemical Society (Resumed)* **1957**, 13-22; b) S. C. Pan, B. List, *Chemistry – An Asian Journal* **2008**, *3*, 430-437; c) D. Kampen, A. Ladépêche, G. Claßen, B. List, *Advanced Synthesis & Catalysis* **2008**, *350*, 962-966.
- [65] M. Hatano, T. Maki, K. Moriyama, M. Arinobe, K. Ishihara, *Journal of the American Chemical Society* **2008**, *130*, 16858-16860.
- [66] M. Hatano, K. Ishihara, *Asian Journal of Organic Chemistry* **2014**, *3*, 352-365.
- [67] Z. Sun, G. A. Winschel, A. Borovika, P. Nagorny, *Journal of the American Chemical Society* **2012**, *134*, 8074-8077.
- [68] a) S. Liao, I. Čorić, Q. Wang, B. List, *Journal of the American Chemical Society* **2012**, *134*, 10765-10768; b) J. H. Kim, I. Čorić, S. Vellalath, B. List, *Angewandte Chemie International Edition* **2013**, *52*, 4474-4477; c) G. C. Tsui, L. Liu, B. List, *Angewandte Chemie International Edition* **2015**, *54*, 7703-7706.
- [69] L. Liu, P. S. J. Kaib, A. Tap, B. List, *Journal of the American Chemical Society* **2016**, *138*, 10822-10825.
- [70] L. Liu, H. Kim, Y. Xie, C. Farès, P. S. J. Kaib, R. Goddard, B. List, *Journal of the American Chemical Society* **2017**, *139*, 13656-13659.
- [71] Y. Xie, G.-J. Cheng, S. Lee, P. S. J. Kaib, W. Thiel, B. List, *Journal of the American Chemical Society* **2016**, *138*, 14538-14541.
-

-
- [72] J. Ouyang, J. L. Kennemur, C. K. De, C. Farès, B. List, *Journal of the American Chemical Society* **2019**, *141*, 3414-3418.
- [73] N. Tsuji, J. L. Kennemur, T. Buyck, S. Lee, S. Prévost, P. S. J. Kaib, D. Bykov, C. Farès, B. List, *Science* **2018**, *359*, 1501.
- [74] a) M. Johannsen, K. A. Jørgensen, G. Helmchen, *Journal of the American Chemical Society* **1998**, *120*, 7637-7638; b) G. A. Olah, G. Rasul, G. K. S. Prakash, *Journal of the American Chemical Society* **1999**, *121*, 9615-9617.
- [75] a) A. D. Dilman, S. L. Ioffe, *Chemical Reviews* **2003**, *103*, 733-772; b) J. Gawronski, N. Wascinska, J. Gajewy, *Chemical Reviews* **2008**, *108*, 5227-5252.
- [76] a) M. Schmeißer, P. Sartori, B. Lippsmeier, *Chemische Berichte* **1970**, *103*, 868-879; b) H. W. Roesky, H. H. Giere, *Zeitschrift für Naturforschung* **1970**, *25 b*, 773-776.
- [77] H. Vorbrüggen, K. Krolkiewicz, *Angewandte Chemie International Edition in English* **1975**, *14*, 421-422.
- [78] T. Tsunoda, M. Suzuki, R. Noyori, *Tetrahedron Letters* **1980**, *21*, 71-74.
- [79] E. M. Carreira, R. A. Singer, *Tetrahedron Letters* **1994**, *35*, 4323-4326.
- [80] L. Ratjen, P. García-García, F. Lay, M. E. Beck, B. List, *Angewandte Chemie International Edition* **2011**, *50*, 754-758.
- [81] A. Tap, A. Blond, V. N. Wakchaure, B. List, *Angewandte Chemie International Edition* **2016**, *55*, 8962-8965.
- [82] J. Guin, C. Rabalakos, B. List, *Angewandte Chemie International Edition* **2012**, *51*, 8859-8863.
- [83] Q. Wang, M. Leutzsch, M. van Gemmeren, B. List, *Journal of the American Chemical Society* **2013**, *135*, 15334-15337.
- [84] Q. Wang, M. van Gemmeren, B. List, *Angewandte Chemie International Edition* **2014**, *53*, 13592-13595.
- [85] Z. Zhang, H. Y. Bae, J. Guin, C. Rabalakos, M. van Gemmeren, M. Leutzsch, M. Klussmann, B. List, *Nature Communications* **2016**, *7*, 12478.
- [86] J. Guin, Q. Wang, M. van Gemmeren, B. List, *Angewandte Chemie International Edition* **2015**, *54*, 355-358.
- [87] M. Mahlau, P. García-García, B. List, *Chemistry - A European Journal* **2012**, *18*, 16283-16287.
- [88] H. Mayr, T. Bug, M. F. Gotta, N. Hering, B. Irrgang, B. Janker, B. Kempf, R. Loos, A. R. Ofial, G. Remennikov, H. Schimmel, *Journal of the American Chemical Society* **2001**, *123*, 9500-9512.
- [89] J. Ammer, C. Nolte, H. Mayr, *Journal of the American Chemical Society* **2012**, *134*, 13902-13911.
- [90] S. Gandhi, B. List, *Angewandte Chemie International Edition* **2013**, *52*, 2573-2576.
- [91] H. Y. Bae, D. Höfler, P. S. J. Kaib, P. Kasaplar, C. K. De, A. Döhring, S. Lee, K. Kaupmees, I. Leito, B. List, *Nature Chemistry* **2018**, *10*, 888-894.
- [92] T. Gatzenmeier, P. S. J. Kaib, J. B. Lingnau, R. Goddard, B. List, *Angewandte Chemie International Edition* **2018**, *57*, 2464-2468.
- [93] T. Gatzenmeier, M. Turberg, D. Yepes, Y. Xie, F. Neese, G. Bistoni, B. List, *Journal of the American Chemical Society* **2018**, *140*, 12671-12676.
-

-
- [94] a) S. Lee, P. S. J. Kaib, B. List, *Journal of the American Chemical Society* **2017**, *139*, 2156-2159; b) S. Lee, H. Y. Bae, B. List, *Angewandte Chemie International Edition* **2018**, *57*, 12162-12166.
- [95] L. Schreyer, P. S. J. Kaib, V. N. Wakchaure, C. Obradors, R. Properzi, S. Lee, B. List, *Science* **2018**, *362*, 216.
- [96] C. Ainsworth, Y.-N. Kuo, *Journal of Organometallic Chemistry* **1972**, *46*, 73-87.
- [97] A. D. Dilman, H. Mayr, *European Journal of Organic Chemistry* **2005**, *2005*, 1760-1764.
- [98] W. J. Middleton, E. M. Bingham, *Journal of the American Chemical Society* **1980**, *102*, 4845-4846.
- [99] S. T. Purrington, D. L. Woodard, *The Journal of Organic Chemistry* **1990**, *55*, 3423-3424.
- [100] K. Okano, T. Morimoto, M. Sekiya, *CHEMICAL & PHARMACEUTICAL BULLETIN* **1985**, *33*, 2228-2234.
- [101] G. M. Rubottom, R. Marrero, *The Journal of Organic Chemistry* **1975**, *40*, 3783-3784.
- [102] M. T. Reetz, K. Schwellnus, F. Hübner, W. Massa, R. E. Schmidt, *Chemische Berichte* **1983**, *116*, 3708-3724.
- [103] Y. Nishimoto, T. Saito, M. Yasuda, A. Baba, *Tetrahedron* **2009**, *65*, 5462-5471.
- [104] R. Mounné, B. Denise, A. Parlier, S. Lavielle, H. Rudler, P. Karoyan, *Tetrahedron Letters* **2007**, *48*, 8277-8280.
- [105] A. Wissner, *Synthesis* **1979**, *1979*, 27-28.
- [106] J.-E. Dubois, G. Axiotis, E. Bertounesque, *Tetrahedron Letters* **1984**, *25*, 4655-4658.
- [107] T. Hvidt, O. R. Martin, W. A. Szarek, *Tetrahedron Letters* **1986**, *27*, 3807-3810.
- [108] N. Lensen, S. Mouelhi, M. Bellassoued, *Synthetic Communications* **2001**, *31*, 1007-1011.
- [109] H. Rudler, V. Comte, E. Garrier, M. Bellassoued, E. Chelain, J. Vaissermann, *Journal of Organometallic Chemistry* **2001**, *621*, 284-298.
- [110] H. Rudler, T. Durand-Réville, *Journal of Organometallic Chemistry* **2001**, *617-618*, 571-587.
- [111] H. Rudler, A. Parlier, F. Cantagrel, P. Harris, M. Bellassoued, *Chemical Communications* **2000**, 771-772.
- [112] K. Ishihara, M. Kaneeda, H. Yamamoto, *Journal of the American Chemical Society* **1994**, *116*, 11179-11180.
- [113] a) K. Ishihara, S. Nakamura, M. Kaneeda, H. Yamamoto, *Journal of the American Chemical Society* **1996**, *118*, 12854-12855; b) C. H. Cheon, O. Kanno, F. D. Toste, *J Am Chem Soc* **2011**, *133*, 13248-13251.
- [114] a) C. Fehr, J. Galindo, *Journal of the American Chemical Society* **1988**, *110*, 6909-6911; b) T. Yasukata, K. Koga, *Tetrahedron: Asymmetry* **1993**, *4*, 35-38; c) A. Yanagisawa, T. Kuribayashi, T. Kikuchi, H. Yamamoto, *Angewandte Chemie International Edition in English* **1994**, *33*, 107-109; d) E. Vedejs, N. Lee, S. T. Sakata, *Journal of the American Chemical Society* **1994**, *116*, 2175-2176.
- [115] a) C. Fehr, J. Galindo, *Angewandte Chemie International Edition in English* **1994**, *33*, 1888-1889; b) A. Yanagisawa, T. Kikuchi, T. Watanabe, T. Kuribayashi, H. Yamamoto, *Synlett* **1995**, *1995*, 372-374; c) P. Riviere, K. Koga, *Tetrahedron Letters* **1997**, *38*, 7589-7592; d) E. Vedejs, A. W. Kruger, *The Journal of Organic Chemistry* **1998**, *63*, 2792-2793.
-

-
- [116] a) T. Poisson, V. Dalla, F. Marsais, G. Dupas, S. Oudeyer, V. Levacher, *Angew Chem Int Ed Engl* **2007**, *46*, 7090-7093; b) M. Morita, L. Drouin, R. Motoki, Y. Kimura, I. Fujimori, M. Kanai, M. Shibasaki, *Journal of the American Chemical Society* **2009**, *131*, 3858-3859.
- [117] a) M. Amere, M.-C. Lasne, J. Rouden, *Organic Letters* **2007**, *9*, 2621-2624; b) H. Brunner, P. Schmidt, *European Journal of Organic Chemistry* **2000**, *2000*, 2119-2133.
- [118] S. L. Wiskur, G. C. Fu, *Journal of the American Chemical Society* **2005**, *127*, 6176-6177.
- [119] D. Leow, S. Lin, S. K. Chittimalla, X. Fu, C.-H. Tan, *Angewandte Chemie International Edition* **2008**, *47*, 5641-5645.
- [120] a) C. Fehr, *Angewandte Chemie International Edition in English* **1996**, *35*, 2566-2587; b) J. Eames, N. Weerasooriya, *Tetrahedron: Asymmetry* **2001**, *12*, 1-24; c) L. Duhamel, P. Duhamel, J.-C. Plaquevent, *Tetrahedron: Asymmetry* **2004**, *15*, 3653-3691; d) J. T. Mohr, A. Y. Hong, B. M. Stoltz, *Nature Chemistry* **2009**, *1*, 359.
- [121] K. Matsumoto, S. Tsutsumi, T. Ihori, H. Ohta, *Journal of the American Chemical Society* **1990**, *112*, 9614-9619.
- [122] K. Matoishi, S. Hanzawa, H. Kakidani, M. Suzuki, T. Sugai, H. Ohta, *Chemical Communications* **2000**, 1519-1520.
- [123] a) H. Yamamoto, K. Futatsugi, *Angewandte Chemie International Edition* **2005**, *44*, 1924-1942; b) H. Yamamoto, *Proceedings of the Japan Academy, Series B* **2008**, *84*, 134-146.
- [124] H. Ishibashi, K. Ishihara, H. Yamamoto, *The Chemical Record* **2002**, *2*, 177-188.
- [125] C. H. Cheon, T. Imahori, H. Yamamoto, *Chem Commun (Camb)* **2010**, *46*, 6980-6982.
- [126] a) T. Poisson, S. Oudeyer, V. Dalla, F. Marsais, V. Levacher, *Synlett* **2008**, *2008*, 2447-2450; b) T. Poisson, V. Gembus, V. Dalla, S. Oudeyer, V. Levacher, *The Journal of Organic Chemistry* **2010**, *75*, 7704-7716; c) A. Claraz, G. Landelle, S. Oudeyer, V. Levacher, *European Journal of Organic Chemistry* **2013**, *2013*, 7693-7696.
- [127] J. Li, S. An, C. Yuan, P. Li, *Synlett* **2019**, *30*, 1317-1320.
- [128] J. Guin, G. Varseev, B. List, *J Am Chem Soc* **2013**, *135*, 2100-2103.
- [129] J.-W. Lee, B. List, *Journal of the American Chemical Society* **2012**, *134*, 18245-18248.
- [130] K. Ishihara, D. Nakashima, Y. Hiraiwa, H. Yamamoto, *Journal of the American Chemical Society* **2003**, *125*, 24-25.
- [131] S. Takeuchi, Y. Nakamura, Y. Ohgo, D. P. Curran, *Tetrahedron Letters* **1998**, *39*, 8691-8694.
- [132] a) D. Seebach, A. K. Beck, S. Capone, G. Deniau, U. Grošelj, E. Zass, *Synthesis* **2009**, *2009*, 1-32; b) G. Lelais, D. Seebach, *Peptide Science* **2004**, *76*, 206-243.
- [133] J. H. Smitrovich, G. N. Boice, C. Qu, L. DiMichele, T. D. Nelson, M. A. Huffman, J. Murry, J. McNamara, P. J. Reider, *Org. Lett.* **2002**, *4*, 1963.
- [134] D. L. Steer, R. A. Lew, P. Perlmutter, A. Ian Smith, M.-I. Aguilar, *Letters in Peptide Science* **2001**, *8*, 241-246.
- [135] D. Seebach, J. L. Matthews, *Chemical Communications* **1997**, 2015-2022.
- [136] T. E. Horstmann, D. J. Guerin, S. J. Miller, *Angewandte Chemie International Edition* **2000**, *39*, 3635-3638.
-

-
- [137] J. W. Yang, M. Stadler, B. List, *Angewandte Chemie International Edition* **2007**, *46*, 609-611.
- [138] Y. Chi, S. H. Gellman, *Journal of the American Chemical Society* **2006**, *128*, 6804-6805.
- [139] B. List, *Journal of the American Chemical Society* **2000**, *122*, 9336-9337.
- [140] A. Córdova, S.-i. Watanabe, F. Tanaka, W. Notz, C. F. Barbas, *Journal of the American Chemical Society* **2002**, *124*, 1866-1867.
- [141] S. Mitsumori, H. Zhang, P. Ha-Yeon Cheong, K. N. Houk, F. Tanaka, C. F. Barbas, *Journal of the American Chemical Society* **2006**, *128*, 1040-1041.
- [142] F. Zhou, H. Yamamoto, *Angewandte Chemie International Edition* **2016**, *55*, 8970-8974.
- [143] a) A. Kubo, H. Kubota, M. Takahashi, K.-i. Nunami, *The Journal of Organic Chemistry* **1997**, *62*, 5830-5837; b) J. F. Bower, R. Jumnah, A. C. Williams, J. M. J. Williams, *Journal of the Chemical Society, Perkin Transactions 1* **1997**, 1411-1420.
- [144] H. M. L. Davies, C. Venkataramani, *Angewandte Chemie International Edition* **2002**, *41*, 2197-2199.
- [145] C. Mannich, W. Krösche, *Archiv der Pharmazie* **1912**, *250*, 647-667.
- [146] a) C. Mannich, *Archiv der Pharmazie* **1917**, *255*, 261-276; b) C. Mannich, E. Ganz, *Berichte der deutschen chemischen Gesellschaft (A and B Series)* **1922**, *55*, 3486-3504.
- [147] A. G. Wenzel, E. N. Jacobsen, *Journal of the American Chemical Society* **2002**, *124*, 12964-12965.
- [148] a) N. Sakai, A. Sato, T. Konakahara, *Synlett* **2009**, *2009*, 1449-1452; b) D. Enders, D. Ward, J. Adam, G. Raabe, *Angewandte Chemie International Edition in English* **1996**, *35*, 981-984; c) S. Rehn, A. R. Ofial, H. Mayr, *Synthesis* **2003**, *2003*, 1790-1796.
- [149] C. E. Stivala, A. Zakarian, *J. Am. Chem. Soc.* **2008**, *130*, 3774.
- [150] E. J. Corey, A. W. Gross, *Tetrahedron Letters* **1984**, *25*, 495-498.
- [151] H. Hart, A. Bashir-Hashemi, J. Luo, M. A. Meador, *Tetrahedron* **1986**, *42*, 1641-1654.
- [152] F. Kopp, S. Wunderlich, P. Knochel, *Chemical Communications* **2007**, 2075-2077.
- [153] F. Gallou, R. Haenggi, H. Hirt, W. Marterer, F. Schaefer, M. Seeger-Weibel, *Tetrahedron Letters* **2008**, *49*, 5024-5027.
- [154] a) E. J. Corey, P. L. Fuchs, *Tetrahedron Letters* **1972**, *13*, 3769-3772; b) V. Ratovelomanana, Y. Rollin, C. Gébéhenne, C. Gosmini, J. Périchon, *Tetrahedron Letters* **1994**, *35*, 4777-4780.
- [155] V. Mamane, P. Hannen, A. Furstner, *Chemistry* **2004**, *10*, 4556-4575.
- [156] H.-Y. Hsieh, H.-C. Chuang, F.-H. Shen, K. Detroja, L.-W. Hsin, C.-S. Chen, *European Journal of Medicinal Chemistry* **2017**, *140*, 42-51.
- [157] C. H. Senanayake, T. J. Bill, R. D. Larsen, J. Leazer, P. J. Reider, *Tetrahedron Letters* **1992**, *33*, 5901-5904.
- [158] Z.-L. Wu, Z.-Y. Li, *Tetrahedron: Asymmetry* **2001**, *12*, 3305-3312.
- [159] E. Coulbeck, M. Dingjan, J. Eames, *Chirality* **2010**, *22*, 193-205.
- [160] H. He, L.-Y. Chen, W.-Y. Wong, W.-H. Chan, A. W. M. Lee, *European Journal of Organic Chemistry* **2010**, *2010*, 4181-4184.
- [161] T. K. Wood, W. E. Piers, B. A. Keay, M. Parvez, *Chemistry – A European Journal* **2010**, *16*, 12199-12206.
-

Appendix

- [162] T. K. Wood, W. E. Piers, B. A. Keay, M. Parvez, *Chemistry - A European Journal* **2010**, *16*, 12199-12206.
- [163] A. Fürstner, V. Mamane, *The Journal of Organic Chemistry* **2002**, *67*, 6264-6267.

9 Appendix

9.1 Erklärung/Declaration

“Ich versichere, dass ich die von mir vorgelegte Dissertation selbständig angefertigt, die benutzten Quellen und Hilfsmittel vollständig angegeben und die Stellen der Arbeit – einschließlich Tabellen, Karten und Abbildungen – , die anderen Werken im Wortlaut oder dem Sinn nach entnommen sind, in jedem Einzelfall als Entlehnung kenntlich gemacht habe; dass diese Dissertation noch keiner anderen Fakultät oder Universität zur Prüfung vorgelegen hat; dass sie – abgesehen von unten angegebenen Teilpublikationen – noch nicht veröffentlicht worden ist sowie, dass ich eine solche Veröffentlichung vor Abschluss des Promotionsverfahrens nicht vornehmen werde. Die Bestimmungen der Promotionsordnung sind mir bekannt. Die von mir vorgelegte Dissertation ist von Herrn Professor Dr. Benjamin List betreut worden.”

Mülheim an der Ruhr, November 2019

Bisher ist folgende Teilpublikation veröffentlicht worden:

“Deracemizing α -Branched Carboxylic Acids by Catalytic Asymmetric Protonation of *Bis*-Silyl Ketene Acetals with Water or Methanol” F. Mandrelli, A. Blond, T. James, H. Kim, B. List, *Angew. Chem. Int. Ed.* **2019**, *58*, 11479–11482.

9.2 Lebenslauf/CV

Francesca Mandrelli

Geboren am 11. März 1990 in Sansepolcro/Italien

Staatsangehörigkeit: Italienisch

Akademischer Werdegang

Promotion

01.2016–11.2019 Dissertation im Arbeitskreis von Prof. Dr. Benjamin List

Max-Planck-Institut für Kohlenforschung, Mülheim an der Ruhr

Title: *“Organocatalytic Asymmetric α -Functionalization of bis-Silyl Ketene Acetals”*

Hochschulstudium

09.2009–02.2015 M.Sc. im Arbeitskreis von Dr. Francesco Venturoni, Dr. Antimo Gioiello

Chimica e Tecnologia Farmaceutiche, Università degli studi di Perugia

Title: *“Development of Thiourea Organocatalysts as Enabling Tools for Asymmetric Michael Addition”*

Schulbildung

09.2004–07.2009 Liceo Piero della Francesca, naturwissenschaftliches Gymnasium,
Sansepolcro, Italien

09.2001–07.2004 Leonardo da Vinci, Sekundarschule, Selci–Lama, Italien

09.1996–07.2001 Don Lorenzo Milani, Grundschule, Lama, Italien

